Protein-Protein Interactions Underlying Damage Checkpoint Activation in *S. pombe*

Christopher Wardlaw

Submitted for the Degree of Doctor of Philosophy

University of Sussex

September 2013

Declaration

I hereby declare that this thesis has not been and will not be, submitted in whole or in part to another University for the award of any other degree.

Signature:.....

Acknowledgements

I would like to thank Tony Carr for the opportunity to undertake my PhD in his laboratory, and for his great supervision, help and advice throughout the process. I would also like to thank Jo Murray for her helpful input, ideas and discussion, and thank my second supervisor Alessandro Bianchi.

Many thanks to all of the Carr and Murray lab members, past and present, for their help and input over the past four years, and for creating such a wonderful working environment. Special thanks to Valerie Garcia for her supervision and support, and Adam Watson for his never ending technical help and patience. I am also very thankful to Stephanie Schalbetter and Yasu Daigaku for their advice and discussion, Chieh-Ju Lee for her microscope expertise, Charly Chawan for alignments and project ideas and Hung Quang Dang for his fusion PCR help. Many thanks to Su-Jiun Lin for her advice regarding the AAD project at the beginning of my PhD. Thank you to our collaborators Li Lin Du, Laurence Pearl and Tony Oliver for all of their contribution, discussion and work, and for including me in such a great project.

I would like to thank the entire Brighton Bunch for their great friendship and support during my PhD, and for making it a very enjoyable time. Special thanks to Ann-Sophie, Carol, Diana, Iga, Sophie, Marcel, Michal, Ted and Yari. Thanks to all of my other friends from Brighton, London, Manchester and York for their support and continued friendship. A big thank you to all of my family, particularly my parents for everything they have done for me during my PhD and before.

I would never have made it to this stage without all of the above people, thank you!

UNIVERSITY OF SUSSEX

Christopher Wardlaw

A thesis submitted for the degree of Doctor of Philosophy

Protein-Protein Interactions Underlying Damage Checkpoint Activation in *S. pombe*

DNA damage can lead to the accumulation of mutations and diseases such as cancer. It is therefore integral for cells to identify this damaged DNA and promote its repair. To carry out this function eukaryotic cells have evolved signal transduction pathways known as the DNA structure checkpoints. Much of the molecular mechanism underlying these pathways is still far from understood. The work in this thesis uses the model organism *Schizosaccharomyces pombe* to investigate these mechanisms, with a particular focus on the TopBP1 homolog Rad4.

TopBP1 plays an essential scaffolding role in the initiation of DNA replication, but is also a key protein in the DNA structure checkpoints. It has previously been shown in metazoans and budding yeast to stimulate the kinase activity of ATR, via its ATR Activation Domain (AAD), an early event in checkpoint activation. The work presented in here, along with initial work carried by previous members of the Carr Laboratory; Su-Jiun Lin and Valerie Garcia, shows that the $Rad4^{TopBP1}$ AAD acts in a chromatin dependent pathway to amplify the checkpoint signal in G1/S-phase, where DNA resection is limited. A second AAD is also identified in the checkpoint clamp protein Rad9, which acts redundantly with the Rad4 AAD.

As well as its AAD function, Rad4 also plays a scaffolding role in the DNA structure checkpoint pathways. The work in this thesis, in collaboration with the Laurence Pearl and Li Lin Du laboratories, identifies the molecular mechanism of the interaction between Rad4 and the mediator protein $Crb2^{53BP1}$. It is shown that sequential phosphorylation of Crb2 by $Cdc2^{CDK}$ is required for the interaction with BRCT domains 1 and 2 of Rad4 and checkpoint activation. It is also shown that Rad4 most likely does not interact with Mrc1 or Slx4 in the *S. pombe* checkpoint pathways.

Contents

List of Tables

List of Figures

Chapter 1
Introduction

1.0 General Introduction

An organism's genetic information is stored as Deoxyribonucleic acid (DNA) within its cells and this genome encodes all of the information required for life. For cells to proliferate, its DNA is replicated and segregated into daughter cells in a tightly controlled process known as the cell cycle. It is therefore important for the cell to prevent changes or mutations to its DNA, either from endogenous or exogenous sources, which may impact on the integrity of the genome.

In this chapter, the cell cycle, the way in which it is controlled and the checkpoints that are in place to prevent cell cycle progression and maintain genomic integrity in the event of DNA damage, will be introduced. The recent findings relating to the particular checkpoint protein of interest, TopBP1, will be described in more detail. The model organism used for this work is *Schizosaccharomyces pombe,* an overview of *S. pombe* and its use as a model organism, is given. Due to the complexity of the gene/ protein names in different organisms and to ensure that it is clear which organism and protein is being discussed, in some cases, references shall be made to human proteins with an *h*, Xenopus with an *x*, *Schizosaccharomyces pombe* with *sp and Saccharomyces cerevisiae* with *sc.* A table of homologs is included (Table1-1).

1.1 *Schizosaccharomyces pombe*; an overview

S. pombe is a unicellular eukaryotic organism from the family of Schizosacchascomycetaceae fungi and is one of three main species within the *Schizosaccharomyces* genus (Sipiczki, 2000). It is as diverged from the other main yeast model organism *S. cerevisiae* as it is human cells. *S. pombe* diverged from *S. cerevisiae* approximately 420-330 million years ago (Yoshioka et al., 1997, Sipiczki, 2000).

Table 1-1

	Human	*S.pombe*	*S.cerevisiae*
PIKK	ATR	Rad3	Mec1
	ATM	Tel1	Tel1
PIKK Partner	ATIRP	Rad26	Ddc2
Checkpoint Clamp	Rad9	Rad9	Ddc1
	Hus1	Hus1	Mec3
	Rad1	Rad1	Rad17
Clamp Loader	Rad17	Rad17	Rad24
Mediators	53BP1	Crb2	Rad9
	Mdc1/PTIP	Brc1	Rtt107
	Claspin	Mrc1	Mrc1
Scaffold	TopBP1	Rad4	Dpb11
MRN Complex	Mre11	Mre11/Rad32	Mre11
	Rad50	Rad50	Rad50
	Nbs1	Nbs1	Xrs2
Nucleases /Helicases	CtIP	Ctp1	Sae2
	Exo1	Exo1	Exo1
	DNA2	DNA2	DNA2
	BLM	Rqh1	Sgs1
CDK	CDK	Cdc2	Cdc28

Table 1-1. Table of homologs
Table shows the names of Human, *S. pombe* and *S. cerevisiae* homologous proteins that are discussed regularly in this thesis. Proteins are grouped together depending on their function or the complex of which they are a part.

S. pombe has three chromosomes consisting of 4940 reported genes and a genome size of 14mb, which was sequenced in 2002 by Wood et al., (2002). It is a haploid organism, unlike *S. cerevisiae* which is normally a diploid (Kuramae et al., 2006, Wood et al., 2002). A typical *S. pombe* cell at the time of division is 12-15µm long and 3-4µm wide. A single cell cycle takes between 2 and 4 hours, with the majority of that time spent in G2 phase. G2 is followed by M phase, a very short G1 phase, then S-phase which coincides with cell septation and cell division (Figure 1-1A). Paradoxically *S. cerevisiae* is mainly a G1 organism and has a very short G2 phase (Figure 1-1B). Furthermore, *S. cerevisiae* divides its cytoplasm by a budding process as opposed to the fission process that occurs in *S. pombe*. This leads to the two yeasts being known as budding yeast and fission yeast respectively (Figure 1-1AB). *S. pombe* was first used as a model organism in the 1940s and 1950s by U. Leupold and M. Mitchison, because it is cheap, easy and quick to grow, whilst allowing use of genetic techniques which may not be possible in higher eukaryotes. The standard strain used in research and in this study is derived from Leupolds original 972 strain. This was obtained in 1946 from a yeast culture deposited by A.Osterwalder in the yeast collection at Delft, The Netherlands (Nurse, 2002).

1.2 The Cell Cycle

1.2.1 Cell Cycle Overview

Cells undergo the mitotic cell cycle in order to proliferate, this cell cycle is made up of four main phases: G1, S, G2 and M (Mitosis). G1, S, G2 can be grouped together and termed interphase, as, during these phases the cells are preparing for cell division. G1 or Gap1 phase is between the previous M phase and the start of S phase. During G1 the cells are growing and preparing for DNA replication. In S phase, cells replicate their DNA, resulting in each chromosome consisting of two sister chromatids. Following S phase cells enter the second gap phase, G2, where they continue to grow, ensure DNA replication is complete and that they are ready to enter M phase. During M phase the cells undergo mitosis; the process of nuclear division, where the cells separate equally their two identical sets of sister chromatids into two separate nuclei (Nurse, 1997).

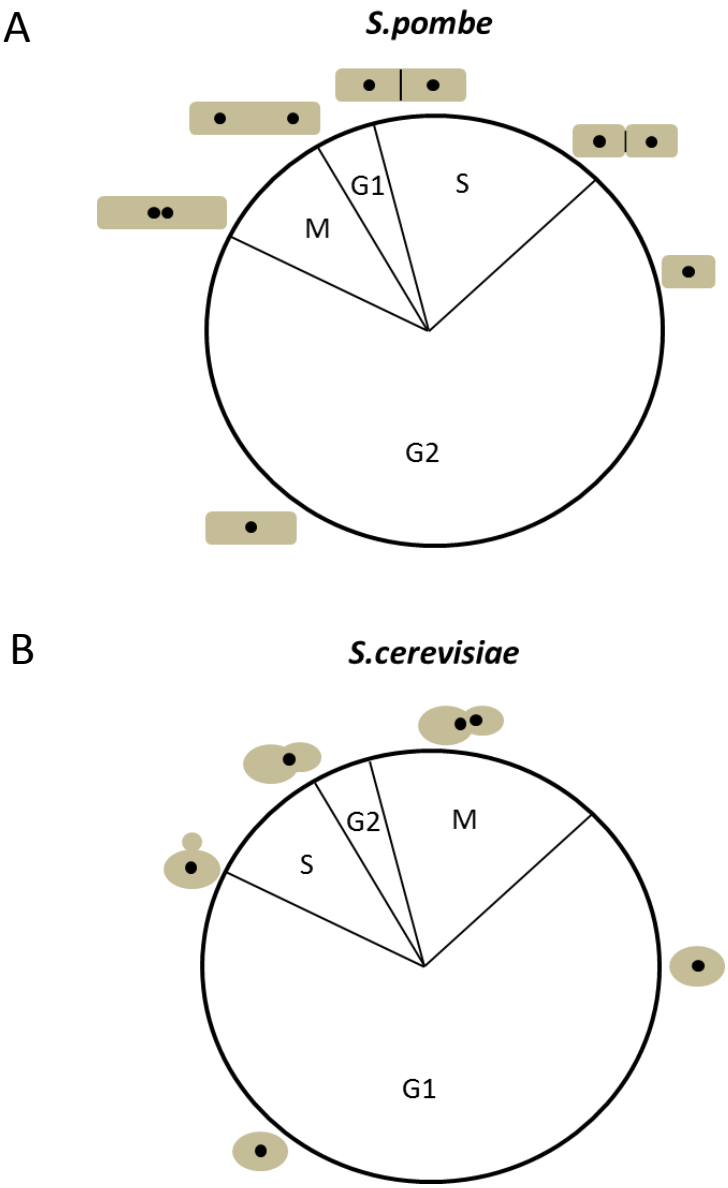

Figure 1-1. Overview of *S. pombe* and *S. cerevisiae* cell cycles.
A. Overview of the *S. pombe* cell cycle, with illustrations relating to the appearance of the *S. pombe* cells at various cell cycle stages. It can be seen that *S.pombe* cells spend ~70% of the cell cycle in G2 phase and have a very short G1. Also, septation (cytokinesis) occurs concurrently with S-phase. B. Overview of the *S. cerevisiae* cell cycle, with illustrations relating to the appearance of the *S. cerevisiae* cells at various cell cycle stages. *S. cerevisiae* cells spend the majority of time in G1 and have a very short G2 phase. The cells divide via a budding mechanism which is completed in M-phase. Adapted from Su-Jiun Lin (Carr lab)

In most higher eukaryotes nuclear division is followed directly by cytokineseis; cellular division, however in *S. pombe* this does not occur until later in the cell cycle during S phase. In fact cytokinesis or septation, as it is known in *S. pombe*, occurs concurrent with DNA replication (Mitchison and Creanor, 1971) (Figure 1-1A).

1.2.2 Regulation of Cell Cycle Progression

Progression through the cell cycle is tightly regulated in eukaryotic cells in order to ensure the correct duplication and separation of the genomic material. This regulation comes in the form of serine/ threonine protein kinases, known as Cyclin Dependent Kinases (CDKs). In both budding and fission yeasts there is only one main cell cycle CDK, CDC28 and CDC2 respectively, however in human cells there are seven known CDKs; CDKs1-7. CDKs phosphorylate specific targets on K/R-S/T-P-X-K/R consensus sites at specific points within the cell cycle to allow progression through and transition between cell cycle phases (Lees, 1995). For this to occur the activity of CDKs fluctuate during the cell cycle; during G1 phase there is little CDK activity, thus allowing formation of the pre replication complex (Pre-RC) on the replication origins in a process known as licensing, the first step of DNA replication. At the G1-S transition, CDK activity increases allowing the licensed origins to fire, subsequent DNA replication and progression through S-phase. CDK activity remains high through G2, thus preventing relicensing and re-replication of the genome. At the G2-M transition there is a further increase in CDK activity resulting in the onset of mitosis. This activity rapidly decreases towards the end of mitosis at a point known as the metaphase-anaphase transition, where the two sets of chromatids separate. This resets the CDK activity to a level in which licensing can occur once again (Diffley, 2004, Kiang et al., 2009). The levels of the catalytic subunit of CDK stay constant throughout the cell cycle, therefore their changes in activity is regulated by interactions with other proteins and post translational modifications, such as phosphorylation. The main way in which CDKs are regulated is via interaction with cyclin, this is absolutely necessary for CDK activity (Nurse, 2002). Cyclins interact with CDKs via a highly conserved 100 amino acid motif within the cyclin protein, known as a cyclin-Box. This interaction causes a conformational change within CDK, exposing its kinase domain and therefore increasing its kinase activity 400,000 fold (Lees, 1995). There are two main categories

of cyclins; G1 cyclins which are required for the G1-S transition (in *S. pombe* these are Cig1 and Puc1) and G2 cyclins or B-type cyclins, required for progression through G2 into M,(in *S. pombe* these are Cig2 and Cdc13). *S. cerevisiae* has nine cyclins and human cells have four main subtypes (cyclins D, E, A and B), however, there is some redundancy between them (Kiang et al., 2009, Pines, 1994). Cyclin levels are controlled by transcription and degradation, it is these changes in cyclin levels through the cell cycle that regulates when CDK is active. Cell cycle mediated degradation plays an important role in the control of B-type cyclin levels: The Anaphase promoting complex (APC) ubiquitylates B-type cyclins leading to their proteolysis and their rapid degradation at the metaphase to anaphase transition (Diffley, 2004). G1 cyclin degradation is not regulated in the same way, however they do have a short half-life, maybe due to the presence of numerous PEST (Pro,Glu, Ser, Thr) sequences which are thought to be signal peptides that target proteins to the proteosome (Lees, 1995).

Cyclins are not the only way to control CDK activity, another level of regulation comes in the form of phosphorylation and dephosphorylation of CDK. For example, in humans CDK Activating Kinase, CAK, phosphorylates T160 on CDK2 increasing kinase activity further and maybe stabilising the cyclin-CDK complex. However, this is not a rate limiting step as the cell cycle still progresses even without this phosphorylation (Jeffrey et al., 1995). Another more complex example of how phosphorylation can affect CDK activity is that of the G2-M transition. In *S. pombe* CDC2-CDC13 remains inactive due to a phosphorylation on Tyr15 within the ATP binding loop of the kinase domain, a phosphorylation which is conserved up to the human protein (Gould and Nurse, 1989). This phosphorylation in fission yeast is carried out by Wee1 or a second kinase Mik1 (Figure1-2). Wee1Δ cells progress through the cell cycle more quickly and give rise to smaller cells (hence the name wee) as they enter mitosis, before fully growing (Russell and Nurse, 1987b). Wee1 activity itself is regulated throughout the cell cycle by phosphorylation in response to cell size. Its activity is high during interphase to prevent cells entering mitosis prematurely and low during early mitosis. The low activity of Wee1 in mitosis is mainly due to an inhibitory phosphorylation by Nim1 (Figure1-2) (Russell and Nurse, 1987a). Counteracting the Wee1/Mik1 phosphorylation of Cdc2 is the phosphatase Cdc25, which removes the Wee1/Mik1 inhibitory phosphorylation

from Cdc2 (Russell and Nurse, 1986). Again Cdc25 is tightly regulated and is only active once all DNA replication has been completed. Once activated a positive feedback loop comes into play where the active dephosphorylated Cdc2-Cdc13 phosphorylates Cdc25, increasing Cdc25 activity. This positive feedback loop allows a rapid switch- like mechanism of Cdc2-Cdc13 activation and subsequent entry into Mitosis (Figure 1-2) (Lu et al., 2012, Russell and Nurse, 1986).

There are yet further levels of CDK regulation, for example the mutation of Y15 (the site of the Wee1 inhibitory phosphorylation) does not lead to the initiation of mitosis before DNA replication is completed, even though cyclin levels have accumulated sufficiently at this point. This regulation comes in the form of CDK inhibitors (CDIs) that bind to and inhibit Cyclin-CDK complexes and may also prevent phosphorylation of the complex by CAKs (Pines, 1994). The *S. pombe* CDK inhibitor is spRum1 which binds to and inhibits Cdc13-Cdc2 (Figure1-2). Over expression of Rum1 leads to massive re-replication of the DNA, due to Cdc2 activity being lowered to that equivalent to a cell in G1-S, whilst it is actually in S or G2 (Correa-Bordes and Nurse, 1995, Moreno and Nurse, 1994). Another example of CDIs in mammalian cells is the p21 family of proteins. This family is made up of three proteins which mainly inhibit G1 cyclin-CDk complexes (Lees, 1995).

Overall a complex network of kinases, phosphatases and protein interactions regulating CDK activity controls much of the progression through the cell cycle. This network of control also allows cells to halt cell cycle progression in the event of DNA damage via a pathway known as the DNA damage checkpoint (Figure 1-2).

1.3 The DNA Damage and Replication Checkpoints

1.3.1 Overview of the DNA Damage and Replication Checkpoints

A cell's DNA is constantly undergoing insult from exogenous mutagens such as ultraviolet light (UV), ionising radiation (IR) or chemicals, and from endogenous sources such as reactive oxygen species or spontaneous damage that occurs during replication (Lindahl, 1993).

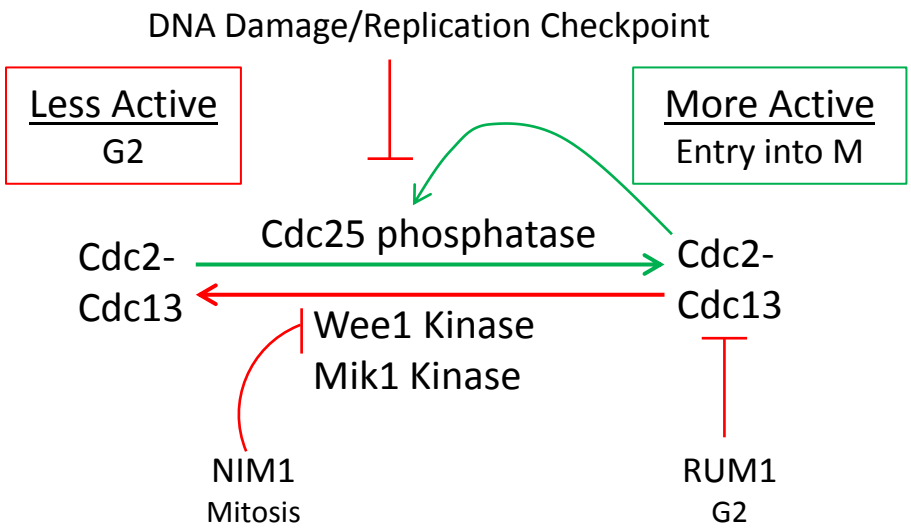

Figure 1-2. Summary of Cdc2 regulation at the G2/M transition in *S. pombe*
Cdc2-Cdc13 activity is kept low enough in G2 to prevent entry in M phase until the cell is large enough and is ready to divide. The Cdc2-Cdc13 activity is kept low via an inhibitory phosphorylation on Cdc2 -T15 by Wee1 and Mik1 and by Rum1 binding. The T15 phosphorylation is counteracted by Cdc25 phosphatase. Once Cdc2-Cdc13 activity increases it can phosphorylate Cdc2-Cdc13 increasing its phosphatase activity and thus leading to further Cdc2-Cdc13 activation. Once Cdc2-Cdc13 activity is high enough for cells to enter M-phase NIM1 can inhibit Wee1. The DNA damage and replication checkpoints can prevent entry into mitosis by phosphorylating and inhibiting Cdc25.

Eukaryotic cells have evolved checkpoints that monitor the integrity of the DNA and, in the event of a lesion, prevent progress from one phase of the cell cycle to the next through the CDK regulatory network described above. This allows time for repair of the damaged DNA, stabilisation of replication forks, slowing of DNA replication and in extreme cases can promote apoptosis (Nyberg et al., 2002). The idea of a DNA damage checkpoint was first proposed in the 1980s with the observation that Ataxia Telangiectasia (AT) patient cell lines experienced less radiation induced mitotic delay, compared to wild type (WT) cells, and little inhibition of DNA replication after X-ray damage. The sensitivity of AT cells to radiation was therefore assigned to a failure in delaying the cell cycle in order to allow DNA repair to occur, rather than a DNA damage repair defect per-se (Painter and Young, 1980). The term checkpoint was first coined by Weinert and Hartwell (1989) following studies into a *S. cerevisiae rad9* mutant, which showed no cell cycle delay after DNA damage. Cells continued to divide for a number of cell cycles before dying. If after DNA damage these cells were artificially delayed in G2 by the use of a mitotic spindle poison the cells would no longer subsequently die (Weinert and Hartwell, 1989, Weinert and Hartwell, 1988). These DNA checkpoints have now been split into two major categories; the DNA damage checkpoints and the DNA replication checkpoint (Weinert, 1992).

The DNA damage checkpoints respond to either DNA double strand breaks(DSBs) or single strand lesions and require double stranded DNA ends, single stranded DNA (ssDNA) or double strand single strand DNA junctions for activation (Cimprich and Cortez, 2008, Zou and Elledge, 2003). These DNA damage checkpoints can be sub-classified into the G1-S checkpoint which responds to damage in G1, the intra S phase checkpoint which responds to DNA damage during S phase and the G2-M checkpoint which prevents entry into mitosis after damage in G2 (Nyberg et al., 2002). The replication checkpoint monitors the fidelity of DNA replication and requires the presence of a replication fork and ssDNA for its activation. Hence, it is activated in the event of replication stress or fork stalling (Tercero et al., 2003, Lupardus et al., 2002). A stalled replication fork can be classified as a replication fork which has stopped progressing but still has the main replication proteins (replisome) associated with it,

this protects the DNA from inappropriate processing ; the DNA thus remains undamaged (Lambert and Carr, 2012). Therefore, the replication checkpoint responds to a lack of, or, imbalance of deoxyribonucleotides (dNTPS), a DNA lesion that cannot be replicated through such as bulky adducts or photoproducts, secondary DNA structures such as G-quadruplexed DNA (G4), nucleotide repeats or DNA bound proteins (Lambert and Carr, 2012). Although the DNA damage and replication checkpoints are classified as separate entities, there is some interplay between them. For example a stalled replication fork may collapse, a process in which the replisome becomes inappropriately associated with the fork, leaving the fork accessible to DNA processing. This may then lead to a hand over from the replication checkpoint to the intra-S phase damage checkpoint (Carr, 2002, Nyberg et al., 2002).

These checkpoints are elaborate networks of proteins that form complexes on, or in the vicinity of, the DNA lesion (Stucki and Jackson, 2006). These proteins are tightly regulated via protein interactions and post translational modifications and can be classified by the role they play within the checkpoint. Sensors are the main group of proteins that detect the DNA substrate and initiate the activation of the checkpoint. These sensors are often required to activate effector kinases, which when activated, phosphorylate the downstream targets involved in cell cycle arrest, inhibition of origin firing, replication fork stabilisation or the regulation of DNA repair. For the sensors to activate the effectors, “mediator” proteins are required. Mediator proteins bring the effector kinases into close proximity to the sensors on the DNA via specific protein interactions, thus allowing interaction between the sensors and effectors (Harrison and Haber, 2006). The use of a particular mediator protein will determine which effector kinase is recruited and therefore whether the damage or replication checkpoint is activated (Tanaka and Russell, 2001).

The DNA damage and replication checkpoints are very well conserved from yeasts to mammals (Rhind and Russell, 2000, Chen and Sanchez, 2004). They are important for maintaining genomic integrity and do so by helping to prevent mutations from occurring that can be passed onto daughter cells. Defects in a number of checkpoint proteins can lead to a mutator phenotype, this accumulation of mutations can lead to

various types of cancer and/or developmental diseases (Loeb, 1991, Bartkova et al., 2005, Kerzendorfer and O'Driscoll, 2009).

Each step of the activation of the DNA damage and replication checkpoints, and the proteins involved will now be described in more detail, focusing on the protein interactions and modifications that underpin their regulation.

1.3.2 The Phosphatidylinositol (PI) 3 Kinase like Kinases (PIKKs)

Ataxia Telangiectasia Mutated (ATM) and Ataxia and Rad3 Related (ATR) are the protein kinases at the top of the checkpoint cascade which, along with their binding partners, act as the DNA damage sensors and checkpoint activators. They are part of an atypical protein kinase family known as the PIKKs. They are known as PIKKs because their sequences are similar to PI3K lipid kinases which phosphorylate phosphoinositides. All PIKKs have a conserved kinase domain sequence and phosphorylate proteins on serine or threonine residues (Lempiainen and Halazonetis, 2009). ATR and ATM share a common consensus sequence of serine/threonine followed by glutamic acid (SQ/TQ motifs) and may preferentially phosphorylate SQ/TQ cluster domains (SCDs) (Kim et al., 1999, O'Neill et al., 2000). The PIKK family contains five sub families of proteins ATM, ATR, DNA-dependent protein kinase catalytic subunit (DNA-PKcs), Mammalian target of rapamycin (mTor) and suppressor of morphogenesis in genitalia (SMG-1). There is also a sixth subfamily known as transformation/transcription domain-associated protein (TRRAP), however this does not exhibit any protein kinase activity (Figure 1-3) (Abraham, 2001, Lempiainen and Halazonetis, 2009). The ATM, ATR, TOR and TRRAP subfamilies are highly conserved from yeast to humans, with many of the PIKKS being isolated, such as the scTor1, ATM, ATR genes and their homolog's, in the early to mid-1990s (Cafferkey et al., 1994, Savitsky et al., 1995, Cimprich et al., 1996, Jimenez et al., 1992, Weinert et al., 1994, Bentley et al., 1996). However, it is only the ATM and ATR kinases and their corresponding yeast homolog's Tel1 and spRad3/scMec1 respectively, that have a direct role in the activation of the checkpoint cascade (Nyberg et al., 2002).

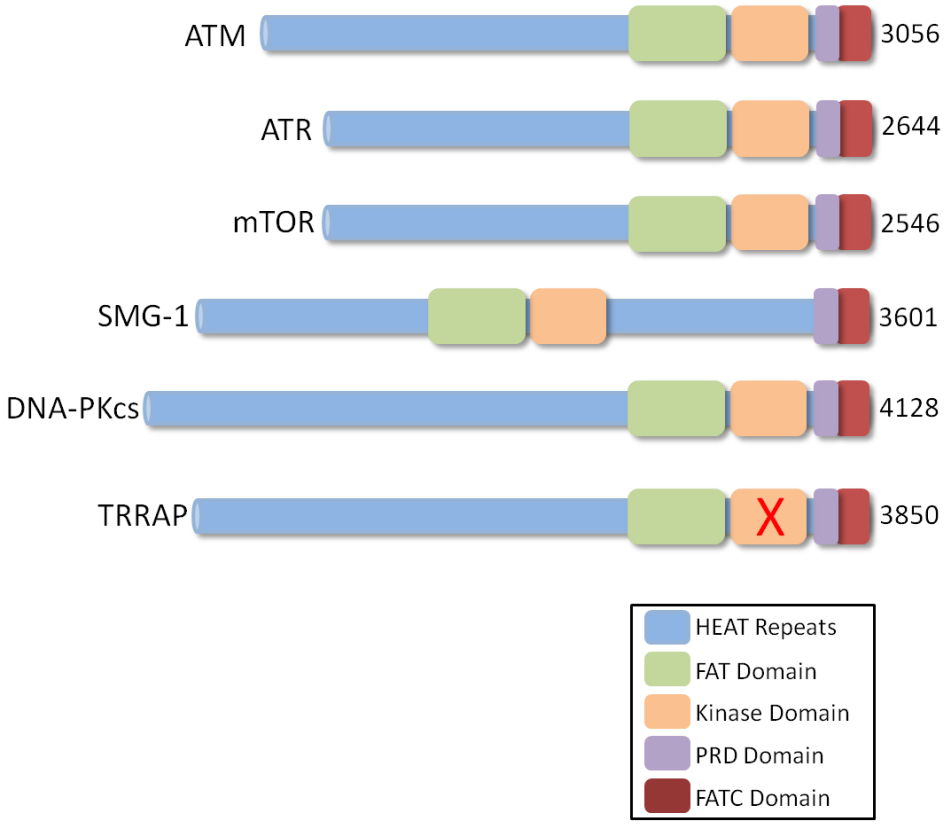

Figure 1-3. PIKKs share similar domain architecture
Schematic of the 6 human PIKKs all of which contain a FAT domain (green), Kinase domain (orange), PRD domain (purple) and FATC domain (red). The proteins vary in length due to differences in the number of N-terminal HEAT repeats (blue). Note TRAPP has an inactive kinase domain (red cross). SMG-1 has more N-terminal FAT and kinase domains compared to the other PIKKs which have a highly conserved C-terminal domain architecture. Adapted from Derheimer and Kastan, (2011)

The other PIKK family members have no significant role in the checkpoint with DNA-PKcs being involved in DNA repair, mTOR functioning in insulin/nutrient sensing and SMG-1 in RNA degradation pathways (Lempiainen and Halazonetis, 2009).

All of the PIKKs are very large proteins, for example the ATR protein is 2644 amino acids and its *S. pombe* homolog Rad3 is 2386 amino acids. Never the less, all PIKKs have a highly conserved domain structure with the C-terminus being the most highly conserved across not only the family members of a single organism, but also between organisms (Bosotti et al., 2000). This C-terminus consists of a FRAP-ATM-TRRAP (FAT) domain, a kinase domain and a FAT-C-terminal (FATC) domain. The with FAT and FATC domains are always found together, one either side of the kinase domain (Figure 1-3). This domain orientation maybe important in their role in regulating the proteins kinase activity (Bosotti et al., 2000). The regulation of the kinase domain by the FAT and FATC domains is most probably achieved by intermolecular and intramolecular interactions that cause conformational changes in the protein, regulating the availability of the kinase domain to phosphorylate its substrates. Indeed in ATM it was seen that the FAT domain interacts with the kinase domain to stabilise the C-terminus of the protein. A similar role has also been seen for the DNA-PKcs FAT domain via structural analysis (Leuther et al., 1999, Bakkenist and Kastan, 2003, Llorca et al., 2003, Sibanda et al., 2010).

The FATC domain has been shown to be essential for the regulation of the PIKKs kinase activity, with hydrophobic residues within this domain being of particular importance. For example mutation of W2545 in mTOR completely abolished its kinase activity and equivalent mutations in the FATC domains of other PIKKs show similar results (Takahashi et al., 2000, Mordes et al., 2008a, Morita et al., 2007). The importance of the FATC domain is due to its ability to interact with other proteins involved in the activation of the kinase activity. Deletion of the ATM FATC prevents interaction with one of its activating proteins, Tip60, and this may explain the loss of its kinase activity when the FATC is mutated (Discussed in “1.4.2 The Activation of ATM” section) (Bhatti et al., 2011, Sun et al., 2007). However, replacement of ATMs FATC with that of DNA-PKcs or TRRAP leads to no loss of kinase activity, suggesting a common domain architecture and mechanism of activation amongst PIKKs (Jiang et al., 2006).

More recently another domain within the C-terminus of PIKKs, which has previously being classified as part of the FATC, termed the PIKK Regulatory Domain (PRD), has been described (Figure 1-3) (Kumagai et al., 2006, Mordes et al., 2008a). The PRD is a small domain of 16-82 amino acids in size, positioned between the FATC and kinase domain and is not well conserved between PIKKs (Lovejoy and Cortez, 2009). Complete deletion of the PRD domain abolishes kinase activity, however small deletions in the N-terminus region of the domain have little effect, implicating the more highly conserved C-terminal portion of the PRD domain in having the key role (Mordes et al., 2008a). The PRD domain regulates the PIKK kinase activity through protein-protein interactions, such as that between TopBP1 and ATR (Discussed in "1.6.4 TopBP1 Dependent ATR Activation" and "1.5.5 Activation of ATR Checkpoint Pathway" sections) and post translational modifications, such as acetylation of ATMs PRD (Discussed in "1.5.4 The Activation of ATM" section) (Mordes et al., 2008a, Sun et al., 2007). Interestingly, replacement of ATRs PRD with that of ATM leads to ATR losing its kinase activity, but ATM is still functional when its PRD is replaced with that of ATR (Mordes et al., 2008a). This suggests that the PRD domain allows some specificity with regard to which PIKK is activated. Overall the studies so far point to the idea that PRD and FATC domains act synergistically to stimulate the PIKKs kinase activity by interacting with other proteins and/or via post translational modifications. These most likely cause conformational changes in the C-terminus exposing the kinase domain, allowing it to phosphorylate its targets (Lempiainen and Halazonetis, 2009). Furthermore, without these regulatory domains the PIKKs show only basal kinase activity if any at all.

The N-terminus of the PIKKs is not as well conserved and varies in length considerably between proteins, leading to the differences in their overall sizes (Figure 1-3). In all the PIKKs the N-terminus is made up of a series of alpha helices known as Huntingtin Elongation Factor 3 Alpha subunit and TOR1 (HEAT) repeats, this has been confirmed by a low resolution (6.6 Å) crystal structure of DNA-PKcs and cyro EM structures of ATM (Figure 1-3) (Leuther et al., 1999, Bakkenist and Kastan, 2003, Llorca et al., 2003, Perry and Kleckner, 2003, Sibanda et al., 2010). Following bioinformatics analysis of DNA-PKcs and other PIKKs, it has been suggested that some of these HEAT repeats may

in fact be classified as other similar types of helical repeats such as tetratricopeptide (TPR) and Armadillo (ARM) repeats (Brewerton et al., 2004). Due to the repetitive nature of the PIKKs N-terminus they are able to act as a scaffolding matrix for protein-protein interactions. For example, the N-terminus of ATM contains a NBS1 interaction motif, a substrate binding motif, a chromatin association domain, a nuclear localisation signal (NLS) and its first 30 amino acids are a Tel1/ATM N-terminal (TAN) motif, required for localisation to the telomere (Bhatti et al., 2011). The lower level of conservation between the N-terminus of PIKKs may allow for the specificity seen in the protein-protein interactions that they make, thus giving the proteins their specific functions within the cell, and giving specificity to the targets that they phosphorylate.

ATM, ATR and their homolog's are the key regulators of checkpoint activation and the subsequent downstream checkpoint events. Each of the two proteins, the cell cycle phases and pathways they act in, how they are recruited to the sites of damage, how they are activated, their downstream targets and the outcomes of their activation will now be described in more detail and compared this between organisms. The ATM pathway will be addressed first before a more detailed account of the ATR pathway, which is the more prevalent pathway in the yeasts

1.4 The ATM/Tel1 Checkpoint

1.4.1 ATM Background

ATM was identified in 1995 by Savitsky et al., (1995) using a positional cloning method (Savitsky et al., 1995). It is an inessential gene and can be knocked out in mice, as can the yeast homolog Tel1 (Greenwell et al., 1995, Morrow et al., 1995, Xu et al., 1996, Naito et al., 1998). However, as previously mentioned, ATM was found to be the gene mutated in the autosomal recessive disorder Ataxia Telangiectasia (AT), a developmental disease resulting in cerebella ataxia (leading to problems with co-ordination), telangiectasia (widened blood vessels in the skin), immune deficiency, sensitivity to ionising radiation (IR) and increased malignancy (Shiloh, 2003). These phenotypes are presumed to arise due to disruption of ATMs roles in; the DNA damage

checkpoint; maintenance of genome stability; the regulation of meiotic crossover and; the control of telomere length (Derheimer and Kastan, 2010).

ATM is activated mainly by double strand breaks (DSB), as in most cases its activation requires double strand DNA ends, which are caused by IR, a number of drugs such as radiomimetics or from breaks arising due to replication fork breakage(Banin et al., 1998, Canman et al., 1998). ATM can therefore activate the DNA damage checkpoint in G1, intra-S and G2. This can be seen from the phenotype of AT cells which exhibit IR insensitive replication, a process in which IR in G1/S does not prevent DNA replication or cell cycle progression through S-phase. AT cells also enter mitosis after IR in G2, demonstrating a lack of a G2 checkpoint (Painter and Young, 1980). In both the *S. pombe* and *S. cerevisiae* systems, Tel1 plays a much smaller role in checkpoint activation and its primary role is in telomere maintenance. Many of the checkpoint roles carried out by ATM in higher organisms are performed by the ATR homolog's spRad3 and scMec1 in yeasts (Greenwell et al., 1995, Morrow et al., 1995, Naito et al., 1998). This most probably reflects the fact that DSBs are transient in yeasts, as they are rapidly resected to ssDNA ends. In mammals however, resection is restricted and the primary DSBs thus exist for much longer.

1.4.2 The Activation of ATM

The ATM protein is always present in the cell and its levels do not change upon DNA damage. Its regulation is therefore completely dependent on protein-protein interaction and post translational modifications (Kurz and Lees-Miller, 2004). Normally, in the undamaged cell, ATM is present as an inactive dimer, however, the active form of ATM is a monomer (Bakkenist and Kastan, 2003). For ATM activation and monomerisation a number of factors and processes are required (Figure 1-4). One of the main prerequisites of ATM monomerisation and activation is autophosphorylation, which occurs within ATMs FAT domain on S1981 (Figure 1-4). Mutation of S1981 to alanine leads to a checkpoint defect and failure of ATM to phosphorylate its downstream substrates after IR. This suggests that autophosphorylation is required for ATM activation (Bakkenist and Kastan, 2003).

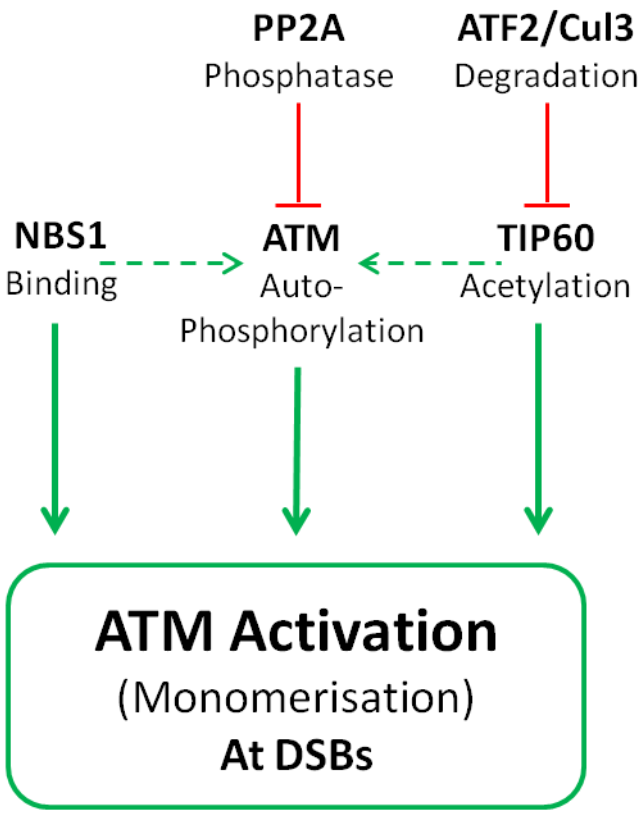

Figure 1-4. Numerous factors control activation of ATMs kinase activity. At a DSB ATM auto-phosphorylates leading to its monomerisation and activation. This auto phosphorylation can be promoted by NBS1 binding ATM at the damage site and acetylation of ATM by Tip60 (dotted green arrows). However, auto-phosphorylation is not sufficient for ATM activity. The binding of Nbs1, and the Tip60 dependent acetylation, also promote ATM activation via promoting conformational changes in the C-terminus of ATM. In the absence of DNA damage ATM auto-phosphorylation is counteracted by PP2A phosphatase, and ATM acetylation is prevented by ATF2/Cul3 dependent degradation of Tip60 (red lines).

Furthermore, the S1981A mutant cannot complement AT patient cell lines-adding to the notion that it is required for ATM activation (Iijima et al., 2008). However, in *vitro* this autophosphorylation site is not required for ATM monomerisation or for kinase activity (Lee and Paull, 2005). Interestingly, mutation of the equivalent site in mice does not result in any phenotype. This may-in part-be due to the presence of other auto phosphorylation sites in mouse ATM (Pellegrini et al., 2006). Indeed two more ATM autophosphorylation sites were later identified in human cells, one on S367 and the other on S1893. Although these phosphorylation sites have a less severe phenotype in human cells than S1981 and therefore seem to be less important, they are still unable to complement AT cells (Kozlov et al., 2006). This would suggest that ATM autophosphorylates on a number of sites and that in humans phosphorylation of S1981 is the most important in ATM activation.

It is important for cells to prevent ATM autophosphorylation in the absence of damage, as this may lead to inappropriate checkpoint activation. Within the cell a number of ATM-phosphatase complexes are found, which would prevent such a scenario, the most important being with PP2A. PP2A is constitutively bound to ATM in the absence of damage and dephosphorylates ATM should any phosphorylation occur. Consistent with this, expression of a dominant negative mutation in the PP2A catalytic domain leads to an increase in ATM S1981 phosphorylation in the absence of damage. After DNA damage, PP2A no longer interacts with ATM and is released, allowing ATM to autophosphorylate and become active. Interestingly, use of the phosphatase inhibitor Okadaic acid leads to an increase in ATM autophosphorylation in undamaged cells, but does not lead to phosphorylation of all of ATMs targets (Goodarzi et al., 2004). This suggests that ATM autophosphorylation is necessary but not sufficient for its activation.

For ATM to become fully active and phosphorylate its targets it also needs to be recruited to the site of damage. In most cases this may be achieved via ATM interacting with the MRE11-Rad50-NBS1 (MRN) complex (Uziel et al., 2003). This complex is a heterotrimer which binds to both ends of a DSB. It is therefore, along with ATM, a DNA damage sensor and bridges the two ends of the break (Williams et al., 2008). The MRN complex has a number of roles at the site of damage in checkpoint

activation, DNA processing and DNA repair (Bhatti et al., 2011). Within the complex, it is NBS1 which is important for both ATM recruitment and activation (Figure 1-4). NBS1 contains an FHA domain, two BRCT domains, an Mre11 binding domain and an ATM interaction motif (AIM) (Iijima et al., 2008). The NBS1 AIM is critical for ATM recruitment and is required for the full activation of ATM (Figure 1-4). NBS1 binds ATMs N-terminal HEAT repeats and the AIM domain interacts with ATMs FATC domain which, as already discussed, is important in regulating ATMs kinase activity. The interaction between NBS1 and ATM stimulates ATM phosphorylation of downstream targets such as Chk2 and p53, suggesting it is an activator of ATMs kinase activity (Falck et al., 2005, Lee and Paull, 2005, You et al., 2005).

Interestingly, mutations in Rad50 (of the MRN complex) also lead to inefficient activation of ATM, suggesting that the entire MRN complex is required for ATM recruitment and activation at sites of damage. (Lee and Paull, 2005, Gatei et al., 2011, He et al., 2012). A model proposed by You et al., (2005) predicts that, once activated by NBS1, ATM autophosphorylates and monomerises leading to its full activation and release from NBS1. This then may allow more ATM to be recruited and activated leading to an increase in the checkpoint signal (You et al., 2005). NBS1 acts both up and downstream of ATM activation; as well as recruiting and potentially activating ATM at sites of damage, NBS1 is also a substrate of the kinase. Active ATM phosphorylates NBS1 on S343 and S278 and these phosphorylations are essential for the intra-S checkpoint and telomere maintenance (Bhatti et al., 2011). Consistent with the MRN complex being important for ATM activation, a number of AT-like disease which harbour mutations in the complex have been described (Carney et al., 1998, Stewart et al., 1999, Waltes et al., 2009).

Deletion of the AIM domain within NBS1 reduces ATMs kinase activity but does not abolish it. Also, the requirement for MRN in checkpoint activation can be bypassed by the use of high doses of IR. Therefore, while MRN plays a role in stimulating ATM kinase activity, it is not the only mechanism for ATM activation (Figure1-4). Indeed, other mechanisms of ATM activation have been described and these may play significant roles in fully activating the kinase (Cerosaletti and Concannon, 2004, Bhatti et al., 2011). One such mechanism is via the histone acetyl transferase (HAT) Tip60

(Figure1-4). Tip60 is known to acetylate histone H2A and Histone H4 after IR and this is required for efficient DNA repair (Murr et al., 2006). Tip60 is also able to bind to ATMs FATC domain and acetylate ATM on S3016 within its PRD after DSB formation. This binding and acetylation is thought to cause a conformational change in ATM, leading to ATM dimer dissociation and full kinase activation. This acetylation occurs independently of ATMs kinase activity and is required for ATM to phosphorylate its downstream targets. An ATM K3016 mutant cannot rescue the IR sensitivity of AT cells, which together with the other data confirms Tip60 as a true ATM activator. Interestingly, the K3016 mutant still exhibits some ATM autophosphorylation but this does not lead to monomerisation (Sun et al., 2005, Jiang et al., 2006, Sun et al., 2007, Sun et al., 2010). It maybe that Tip60 works in tandem with other ATM activators such as NBS1. Indeed, Tip60 has been shown to associate with NBS1 via the kinase null PIKK; TRRAP (Chailleux et al., 2010).

It is thus also important to control Tip60 in order to prevent ATM acetylation in the absence of damage (as it is with the ATM autophosphorylation) (Figure 1-4). This control comes in the form of the ATF2, a transcription factor which is known to be part of the JNK/P38 stress pathway (Tsai et al., 1996). However, this function of ATF2 is independent of its transcription factor function in controlling Tip60 levels. ATF2 is always found bound to ATM-associated Tip60 in the absence of DNA damage. ATF2 also associates with the E3 ubiquitin ligase Cul3 and apparently promotes Cul3 dependent ubiquitylation and degradation of Tip60; knockdown of either ATF2 or Cul3 leads to stabilisation of Tip60 and over expression of ATF2 leads to a decrease in Tip60 levels. Thus both ATF2 and Cul3 negatively regulate Tip60 protein levels (Figure 1-4). This ATF2/Cul3 dependent degradation of Tip60 attenuates Tip60 acetylation and activation of ATM, ensuring that ATM is not activated in the absence of damage (Figure 1-4). Following DNA damage, the interaction between ATF2 decreases, allowing acetylation and activation of ATM (Bhoumik et al., 2008). Interestingly, ATF2 is also a target of active ATM. Following IR ATM phosphorylates ATF2 on S490 and S498, this phosphorylation leads to relocalisation of ATF2 to Ionising radiation induced foci (IRIF) on the chromatin surrounding the DSB. Recruitment of ATF2 to the chromatin is required for efficient MRN complex recruitment and contributes to the intra-S

checkpoint and DNA repair (Bhoumik et al., 2005). This has led to the model proposed by Bhoumik et al., (2008) whereby ATM-Tip60-ATF2 and Cul3 are in a complex under normal conditions, leading to Tip60 ubiquitylation and degradation. Upon IR ATF2 dissociates from Tip60 allowing ATM acetylation and activation. This coincides with ATM phosphorylation of ATF2 causing its relocalisation to IRIF, where it contributes to DNA repair and the intra-S checkpoint by aiding recruitment of the MRN complex. This, in turn, leads to further ATM activation (Figure 1-4) (Bhoumik et al., 2008).

Overall ATM can be activated after DNA DSB by a number of factors including protein-protein interactions and posttranslational modifications. This activation of ATM is tightly regulated to prevent activation when it is not required.

1.4.3 Mediators and the ATM Checkpoint Pathway

One of the first targets of active ATM is S139 on the histone variant H2AX, giving rise to γH2AX (Burma et al., 2001). γH2AX IRIF are therefore commonly used as a marker of DSBs and checkpoint activation, although γH2AX foci do form after other types of DNA damage that do not activate ATM. γH2AX is important for the recruitment of checkpoint mediator proteins and thus for phosphorylation of downstream ATM targets as well as for amplifying the checkpoint signal (Derheimer and Kastan, 2010). H2AX null mice are radiation sensitive, growth retarded and immune deficient, phenotypes associated with a defect in the DNA damage checkpoints and/or DNA repair (Celeste et al., 2002, Celeste et al., 2003). Consistent with this, a number of repair and checkpoint proteins fail to form IRIF at DSBs in H2AX deficient cells (Celeste et al., 2003).

One of the key mediator proteins to be recruited to γH2AX is MDC1. MDC1 is recruited via an interaction between its tandem BRCT domains and phosphorylated S139 on H2AX. Mutation of the BRCT domains within MDC1, knockdown of the protein using siRNA or knock out in mice cells leads to a phenotype very similar to that of the γH2AX S139A mutation. This implicates MDC1 as the main binding partner of γH2AX (Stewart et al., 2003, Stucki and Jackson, 2004, Lee et al., 2005, Stucki et al., 2005, Lou et al., 2006). Once recruited to the chromatin, MDC1 can then recruit a number of other proteins within the checkpoint and DNA repair pathways. Firstly MDC1 can recruit

activated ATM via an interaction between ATM S1981 and the FHA domain of MDC1. This leads to retention of ATM and thus ATM foci formation at the site of the break. This ATM MDC1 interaction brings ATM into close proximity of more H2AX, leading to more γH2AX and more MDC1 recruitment. This positive feedback loops results in γH2AX spreading for mega bases either side of the DSB site (Lou et al., 2006, Savic et al., 2009).

Interestingly, MDC1 also interacts with NBS1 of the MRN complex, via NBS1s FHA and BRCT domains. MDC1 is constitutively phosphorylated on CK2 sites. These phosphorylation events result in NBS1 foci that co-localise with MDC1 and γH2A (Chapman and Jackson, 2008, Melander et al., 2008, Spycher et al., 2008). This presence of NBS1 and most probably the other components of the MRN complex on the chromatin may be important for further activating ATM, recruiting ATM substrates and for DNA repair. As well as recruiting ATM to the chromatin, MDC1 is also phosphorylated by ATM. This phosphorylation is important for recruitment of the ring finger ubiquitin ligase RNF8 via its N-terminal FHA domain (Huen et al., 2007, Mailand et al., 2007). RNF8 ubiquitylates γH2AX, this ubiquitylation is required for the recruitment of mediator proteins 53BP1 and BRACA1, as well as for the recruitment of another ring finger ubiquitin ligase RNF168 (Doil et al., 2009, Huen et al., 2007, Mailand et al., 2007). Mutation of the ATM phosphorylation site on MDC1, the RNF8 FHA domain or the RNF8 ring finger domain (required for its ubiquitylation activity) all result in loss of 53BP1, BRCA1 and RNF168 IRIF, but not MDC1, ATM or NBS1 foci. This shows that γH2AX ubiquitylation is required for recruitment of these downstream proteins. Furthermore, an RNF8 knock-down leads to a G2-M checkpoint defect after IR confirming the importance of γH2AX ubiquitylation and its downstream effects in maintaining the checkpoint (Huen et al., 2007, Kolas et al., 2007, Mailand et al., 2007, Doil et al., 2009).

The recruitment of RNF168 by RNF8 ubiquitylated γH2AX leads to further ubiquitylation of γH2A. This ubiquitylation allows BRCA1 binding to the chromatin via a Rap80-Ubiquitin interaction (Sobhian et al., 2007, Doil et al., 2009). RNF8 ubiquitlyation of the nucleosome is also thought to expose H4K20me2, which allows 53BP1 to bind to the chromatin via an interaction between 53BP1s Tudor domain and

the methylated H4K20. (Wang et al., 2002, Ward et al., 2003, Huyen et al., 2004). Once recruited, BRCA1 and 53BP1 are both phosphorylated by ATM (Cortez et al., 1999, Xia et al., 2001). These phosphorylations are important for recruitment of repair proteins and of additional chromatin modifiers to the site of damage and therefore for efficient DNA repair (Thompson, 2012). The phosphorylation of 53BP1 is also thought to be important for the recruitment of the effector kinase Chk2, although the mechanism of this recruitment is not well understood. Once recruited, Chk2 is phosphorylated on T68 by ATM, leading to its activation and a full checkpoint response (Matsuoka et al., 1998, Matsuoka et al., 2000).

1.4.4 Downstream Cell Cycle targets of the ATM pathway

In S-phase, one of the main targets of ATM activated Chk2 in preventing cell cycle progression is CDC25A. Chk2 phosphorylation of CDC25A leads to its degradation and thus to an increase in inhibitory phosphorylations on CDK. This reduces CDK activity, resulting in the prevention of origin firing and slowing of S-phase (Falck et al., 2001). Chk2 acts in a similar manner after activation in G2, targeting CDC25 to prevent the G2-M transition (Matsuoka et al., 1998). The main target of ATM activation in G1 is the tumour suppressor p53 (Chehab et al., 1999). p53 is phosphorylated directly by ATM leading to p53 dependent trans-activation of genes such as the CDK inhibitor p21, thus preventing progression from G1-S phase (Lavin, 2008).

1.4.5 Role of the Yeast ATM Homolog, Tel1, in Checkpoint activation

As already mentioned, the ATM homolog (Tel1) in both budding and fission yeasts play a minor role in checkpoint activation compared with the metazoan counterpart. Tel1's most crucial role is in telomere maintenance. *tel1* in both yeast systems is not an essential gene and a *tel1Δ* has no effect on overall cell proliferation (Lustig and Petes, 1986, Greenwell et al., 1995, Morrow et al., 1995, Naito et al., 1998). Like ATM, Tel1 can bind to the MRN complex and this is via the C-terminus of *S. pombe* NBS1 or the *S. cerevisiae* homolog Xrs2. In budding yeast this interaction recruits Tel1 to DNA ends and has been shown, in *vitro*, to stimulate Tel1's kinase activity (Nakada et al., 2003, You et al., 2005, Fukunaga et al., 2011). Moreover, enhanced Tel1 kinase activity can be seen following induction of dirty ended DSB, where the MRX^{MRN}

complex remains bound to DNA ends for a longer period of time. This suggests MRX can also stimulate Tel1 activity in *vivo* (Dodson and Russell, 2011). However, in both *S. pombe* and *S. cerevisiae* a *tel1Δ* mutant cell is not sensitive to DNA damaging agents and Tel1 is not required for checkpoint activation in a wild type background (Willis and Rhind, 2010). Some data from budding yeast does suggest though that Tel1 can still function within the DNA damage checkpoint; over expression of Tel1 can partially rescue the damage sensitivity of a *mec1-1*^{ATR} temperature sensitive mutant. Furthermore a *tel1Δ* mutant is synergistically sensitive with a mec1-1 mutant to DNA damaging agents including radio mimetics (Morrow et al., 1995). This suggests that Tel1 can function in the DNA damage checkpoint but its role is masked by the scMec1 or spRad3 pathway.

The one situation where Tel1 is important for checkpoint activation in *S. pombe,* is when resection of a DSB is prevented. As discussed in "1.5.2 The Formation of ssDNA" section the Rad3^{ATR} checkpoint pathway requires the formation of ssDNA for activation (Limbo et al., 2011). If the formation of this ssDNA is prevented using a *ctp1Δ* mutant then Tel1 has a more significant role in checkpoint activation. A *ctp1Δ* strain partially restores the checkpoint defect in a rad3Δ background, as seen by the increased Chk1 phosphorylation after damage when compared with that of a *rad3Δ* cells alone. This increase is dependent on Tel1. The levels of Chk1 phosphorylation are still lower than in wild type cells suggesting that this Tel1 pathway, in the absence of resection, is not as efficient as the Rad3 pathway in checkpoint activation (Limbo et al., 2011). It maybe that the lack of Tel1 function in *S. pombe* checkpoint activation may not be due to the inability of Tel1 to act in the checkpoint pathway per-se, but may reflect the cell cycle differences between *S. pombe* and metazoans. The fact that *S. pombe* resides mostly in G2 phase means that most DSBs are processed to give ssDNA (as discussed in "1.5.2 The Formation of ssDNA" section). Thus, rapid activation of the Rad3 checkpoint pathway bypasses the requirement for Tel1. However, the same cannot be said for *S. cerevisiae* which is mainly a G1 organism, but depends on Mec1^{ATR} for checkpoint activation. Interestingly, expression of budding yeast Tel1 can partially complement human AT cells. Tel1 complements the telomere shortening phenotype but has no effect on p53 stability or phosphorylation and only partially complements the radio

sensitivity phenotype. This suggests it may only carry out some of the functions of ATM (Fritz et al., 2000).

1.5 ATR/Rad3/Mec1 Pathway of Checkpoint Activation

1.5.1 ATR/Rad3/Mec1 Background

S. pombe Rad3^{ATR} was first identified in 1992 by Jimenez at al., (1992) as a sequence complementing a radiation sensitive mutant. This mutant strain did not display cell cycle arrest in G2 after IR, and subsequently it entered mitosis without completing DNA replication(Jimenez et al., 1992). However, it was not until 1996 that the full *rad3* gene was cloned (Bentley et al., 1996). The *S. cerevisiae* homolog was identified by two independent groups; Weinert et al., (1994) identified Mec1^{ATR} in a screen for proteins required for cell cycle arrest in S and/or G2 phase after DNA damage (Weinert et al., 1994). Kato and Ogawa (1994) also identified *MEC1* in a screen for MMS sensitive mutants, naming it *ERS1* (Kato and Ogawa, 1994). The human homolog ATR was subsequently cloned by two independent groups (Cimprich et al., 1996, Bentley et al., 1996). ATR and its homologs are activated after a number of different DNA lesions that cause replication stress, such as DNA abducts, cross links and inhibition of DNA polymerase, as well as after DNA damage such as DSB (Zou, 2007). All of these lesions cause the formation of ssDNA, it is this ssDNA that is required for the activation of the ATR (and homologs) checkpoint (MacDougall et al., 2007). Due to this dependence on ssDNA, ATR can activate the intra S, replication and G2 checkpoints, but not the G1 checkpoint (see formation of ssDNA section). As already discussed, the ATR homologs scMec1 and spRad3 have a broad role in checkpoint activation because of the reduced role of the Tel1 pathway in comparison with that of ATM.

ATR is an essential gene, with disruption of the mouse ATR gene leads to chromosome fragmentation and embryonic death before E7.5 (Brown and Baltimore, 2000, de Klein et al., 2000). Budding yeast *MEC1* is also an essential gene, however fission yeast *rad3* is not essential and can be knocked out (Jimenez et al., 1992, Weinert et al., 1994). The

reason why *MEC1* is essential and *rad*3 is not is that *MEC1* has been shown to have a direct role in regulation of cellular dNTP pools. dNTP's are synthesised by the reduction of NDP's , a process which is catalysed by a mutlimeric protein complex called ribonuclease reductase (RNR) (Elledge et al., 1992). RNR activity in *S. cerevisiae* is controlled by a small inhibiting protein known as Sml1, which is normally found associated with RNR (Zhao et al., 1998). Sml1 has been shown to be phosphorylated by a downstream target of Mec1, the Dun1 kinase (Zhao et al., 2001, Zhao and Rothstein, 2002, Uchiki et al., 2004). This phosphorylation of Sml1 by Dun1 leads to Sml1 ubiquitylation and degradation, RNR activation and the production of dNTP's (Andreson et al., 2010). The control of RNR activity by Mec1 is important after replication stress caused by HU or DNA damage as dNTP's are required for the DNA repair and replication restart processes. However, this RNR regulation in budding yeast is also essential for unperturbed S-phase, as the lethality of a *mec1Δ* can be rescued by knocking out *SML1* (Zhao et al., 1998). In *S. pombe* Rad3 does not play a direct role in the regulation of dNTP pools in an unperturbed cell cycle; degradation of the RNR inhibitor (Spd1) is controlled via the signalosome (Liu et al., 2003a).

One reason why ATR is essential and *rad3* is not maybe due to the differences in the genome size between higher eukaryotes and *S. pombe*. The human genome for example is estimated to be 3,200 Mbp (Lander et al., 2001) whereas the *S. pombe* genome is only approximately 12.57 Mbp. The difference in size means that the human genome is much more susceptible to damage and replication errors during S-phase that would require the activation of the ATR checkpoint (Sonoda et al., 1998). Also higher eukaryotes contain much more repetitive DNA sequences which are difficult to replicate, these sequences often lead to replication fork stalling and thus require ATR activation (Lander et al., 2001, Caspari et al., 2002). This notion is backed up by the fact that conditional knock out of ATR in either human or mouse cells leads to cells progressing into mitosis with chromosome breaks which subsequently lead to cell death (Cortez et al., 2001, Brown and Baltimore, 2003). The fact that ATR is an essential gene means that ATR mutations are rare in the human population. However, heterozygous or hypomorphic mutations in ATR lead to a rare condition known as

Seckle Syndrome, a developmental disease resulting in growth retardation and microcephaly (O'Driscoll and Jeggo, 2003, O'Driscoll et al., 2003).

The steps required for the activation of the ATR/Rad3/Mec1 checkpoint pathways will now be considered, with an emphasis on the yeast pathways and especially that of *S. pombe,* as this is directly relevant to the work presented in the results chapters

1.5.2 The Formation of ssDNA

For ATR, or its homologs, to recognise a DNA lesion or a stalled replication fork , ssDNA needs to be formed. When a replication fork runs into a lesion it stalls. However, the helicase continues to unwind the DNA for a period after the fork stalling. This creates the single stranded DNA required for the ATR response (Byun et al., 2005, MacDougall et al., 2007). In the case of DSB's in G2, the ssDNA first needs to be formed by resection of one of the DNA strands. It is thought that, in part, this resection is carried out by the MRN complex (Figure 1-5) (Paull and Gellert, 1998, Trujillo et al., 1998). Although the entire MRN complex is required for resection, it is Mre11 which possesses the nuclease activity. In *vitro* Mre11 has been shown to have both endonuclease and exonuclease activity, which is dependent on four phosphodiesterase motifs at its N-terminus. Mre11 nuclease activity is increased when bound to Rad50 and NBS1. Rad50 is a member of the SMC family of proteins and like other SMC proteins it contains walker A and B domains at its N and C terminus respectively, and has a zinc hook in the centre of the protein. These three domains are joined by coiled coils allowing the walker domains to come together giving Rad50 ATPase activity. This Rad50 ATPase activity stimulates Mre11's nuclease activity via a conformational change (Williams et al., 2010a).

The Mre11 exonuclease activity was shown to be in the 3'-5' direction in *vitro*, but at a DSB in *vivo* resection in the 5'-3' direction is required to form the ssDNA. Furthermore both the endo and exo nuclease activity of Mre11 is poor in *vitro* (Furuse et al., 1998, Paull and Gellert, 1998).

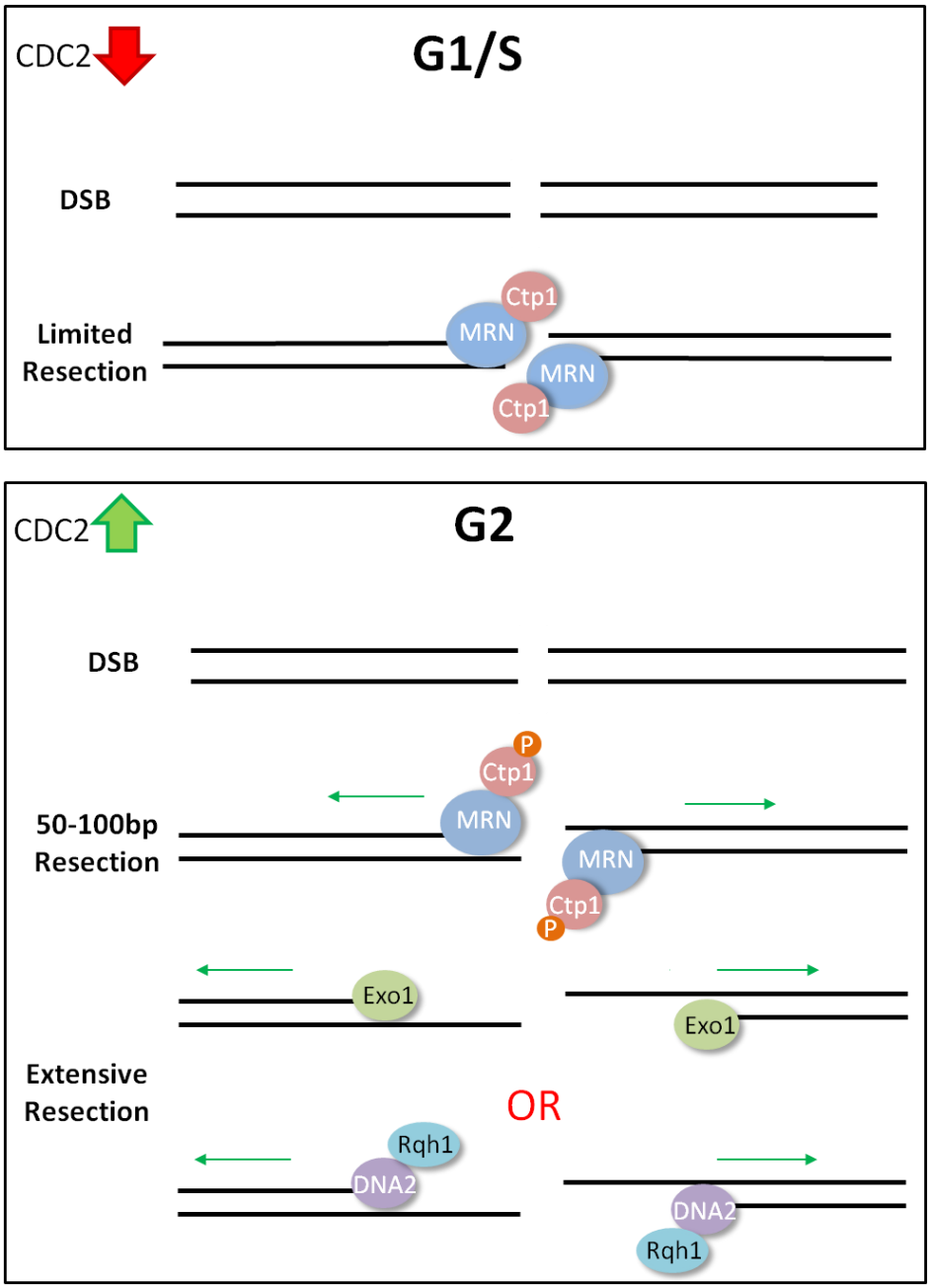

Figure 1-5. **Overview of DNA resection after DNA damage in *S. pombe***
Top panel. In G1 CDK (Cdc2) activity is very low. At a DNA DSB there is limited resection due to the lack of Ctp1 phosphorylation by Cdc2 and low Ctp1 expression. Bottom Panel. In G2 Cdc2 activity is higher leading to higher Ctp1 expression. Also at a DSB, Ctp1 is phosphorylated by Cdc2 leading to the initial resection of 50-100bp by MRN-Ctp1. Exo1 is then recruited, which leads to extensive resection of the DSB. In the absence of Exo1, DNA2 and the Rqh1 helicase can carry out the extensive DNA resection.

This suggested that accessory factors and other nucleases were acting to regulate the resection of DSB in *vivo*. Sae2 in budding yeast (CtIP in mammals and Ctp1 in *S. pombe*) was shown to associate with the chromatin bound MRX^{MRN} complex in *vivo* and a *sae2Δ* exhibits a similar phenotype to an *mre11* nuclease dead strain. This suggests that Sae2 regulates Mre11 nuclease activity and may also cooperate with Mre11 in resection, as it also exhibits nuclease activity (Figure 1-5) (McKee and Kleckner, 1997, Neale et al., 2005, Lengsfeld et al., 2007). However, Sae2 and Mre11 are only required for the initial resection of about 50bp-100bp Figure 1-5)(Mimitou and Symington, 2008). It is known that a 5'-3' exonuclease Exo1 then continues this initial resection giving large stretches of ssDNA (Figure 1-5). Indeed, in budding yeast an *mre11Δ*, *exo1Δ* strain resection is severely restricted but not abolished (Llorente and Symington, 2004, Nakada et al., 2004). This may be due to another nuclease, Dna2, along with the helicase Sgs1(hBLM), being functionally redundant with Exo1 in DNA end resection at DSB's (Figure 1-5)(Huertas, 2010).

This method of resection is only active in G2 when CDK activity is high (Figure 1-5). In yeast and human cells Sae2/CtIP are phosphorylated by CDK. This phosphorylation is required for the nuclease activity of the CtIP/Sae2 -MRN/X complex at DSB (Huertas et al., 2008, Huertas and Jackson, 2009). In G1, as mentioned earlier, CDK activity is low and CtIP is not phosphorylated, thus resection does not occur (Figure 1-5). In this case, in mammals, the checkpoint is ATM dependent rather than ATR dependent. Regulation of resection also determines the repair pathway; in G2 phase a sister chromatid is present allowing DSBs to be repaired by a homologous recombination (HR) pathway which is dependent on ssDNA. However, in G1 there is no sister chromatid therefore resection of the DSB is not desirable and the lesion is repaired via an end joining mechanism (Huertas et al., 2008, Mimitou and Symington, 2008). Interestingly, in humans ATM activity is also required for resection of a DSB, the subsequent formation of ssDNA and ATR dependent checkpoint activation. ATM, along with CDK activity, stimulates CTIP activation and this leads to the initial resection of the DSB. The MRN complex and associated ATM then dissociate from the DNA allowing the Exo1 or DNA2 dependent extensive resection. This subsequently leads to the ssDNA required for ATR recruitment, which gives a switch from the initial ATM activation to a ATR checkpoint

response in G2 (Shiotani and Zou, 2009). Overall extensive ssDNA formation is required for the full activation of the ATR pathway. This is most prominent in S/G2 phases and is formed by either the uncoupling of the DNA helicase and polymerase during replication, or processing of DNA lesions such as DSB's.

1.5.3 Recruitment of ATR to ssDNA

Once the ssDNA has been generated either by damage, resection or uncoupling of the replication fork, it is immediately coated by replication protein A (RPA) (Zou and Elledge, 2003, Fanning et al., 2006). It is this RPA coated ssDNA which is required for ATR to sense and be recruited to damage. In the cell, ATR is found in a complex with ATRIP. This is also the case in yeasts with *S. pombe* $Rad3^{ATR}$ being found in a complex with $Rad26^{ATRIP}$ and *S. cerevisiae* $Mec1^{ATR}$ in a complex with $Ddc2^{ATRIP}$ (Paciotti et al., 2000, Cortez et al., 2001, Edwards et al., 1999). The ATRIP-ATR interaction is mediated by a phosphorylation event dependent on NEK1, which physically interacts with the ATR-ATRIP heterodimer. This phosphorylation event is independent of DNA damage but is required for the stability of the ATR-ATRIP complex and its activity (Liu et al., 2013). ATRIP has an important role in ATR recruitment to the RPA coated single stranded DNA (Cortez et al., 2001). A conserved domain within $Ddc2^{ATRIP}$ that is not required for the Ddc2 and Mec1 interaction, is required for both Mec1 and Ddc2 recruitment to RPA. This domain forms an α- helix that specifically interacts with the large subunit of RPA (Zou and Elledge, 2003, Ball et al., 2007). In budding yeast the *ddc2Δ* mutant cells have the same phenotype as mec1Δ mutants and mutations in RPA lead to a reduction in Ddc2 foci formation after DNA damage (Paciotti et al., 2000, Zou and Elledge, 2003). Furthermore, deletion of ATRIP in metazoans leads to cell death by chromosomal fragmentation in the same way that an ATR knockout does. Mutations in ATRIP can also lead to Seckle Syndrome (Ogi et al., 2012). However, the effective recruitment of the heterodimer requires domains in both proteins. Mutation of the conserved FAT domain in Mec1 reduced both Mec1 and Ddc2 interaction with RPA, this FAT domain was also shown to interact with RPA in a two hybrid assay (Ball et al., 2005, Nakada et al., 2005). A model can therefore be envisaged in which ATRIP is required for ATR recruitment to RPA ssDNA and that ATR itself can further enhance this recruitment or stabilise its binding to RPA, once recruited.

1.5.4 The DNA Damage Sensor 9-1-1 is Required for the ATR Dependent Checkpoint

Although recruitment of ATR-ATRIP to sites of ssDNA is necessary for activation of the DNA damage checkpoint, it is not sufficient and a second DNA sensing complex is also required (MacDougall et al., 2007). This complex, known as the 9-1-1 complex, consists of three proteins; Rad9, Hus1 and Rad1, (or Ddc1, Mec3 and Rad17 in budding yeast). The first of these to be identified was the *S. pombe rad9* gene. Mutations in *rad9* caused cells to show sensitivity to both IR and UV, linking it with a role in the checkpoint response (Murray et al., 1991). Furthermore, deletion of mouse Rad9 leads to sensitivity to DNA damaging agents, spontaneous chromosome abrasions and embryonic lethality (Hopkins et al., 2004). The 9-1-1 proteins share sequence similarity to the proliferating cell nuclear antigen (PCNA), a homodimer replication clamp that forms a similar ring like structure (Venclovas and Thelen, 2000, Dore et al., 2009). Each of the 9-1-1 proteins contains a PCNA-like domain which consist of intra-domain loops (Xu et al., 2009). In PCNA these intra-domain loops act as binding surfaces for other proteins, and this may also be the case for the 9-1-1 complex. However, this is yet to be fully established (Maga and Hubscher, 2003). Importantly, the Rad9 protein within the complex differs from the other two proteins, as it contains a flexible C-terminal tail which is not required for the formation of the heterotrimeric complex. This tail most likely protrudes from the ring structure (Sohn and Cho, 2009). It also contains a nuclear localisation signal, which is required for the localisation of all three of the proteins in the nucleus (Hirai and Wang, 2002).The 9-1-1 complex is recruited to the 5' ss-dsDNA junction and depends on RPA to create the specificity for this 5'junction (Zou et al., 2003, Majka et al., 2006a, MacDougall et al., 2007). The recruitment and loading of the 9-1-1 complex at the 5' junction requires another complex of proteins, known as the checkpoint clamp loader, with loading occurring in a similar way to PCNA loading.

The checkpoint clamp loader consists of the Replication factors (RFC) 2-5, which are also required for PCNA loading, however, Rad17 (Rad24 in budding yeast) is required instead of Rfc1. It is Rad17 that interacts specifically with the Rad1 subunit of the heterotrimer and remains bound even after loading (Sohn and Cho, 2009, Lee and Dunphy, 2010). The loading of the 9-1-1 clamp onto the 5' junction requires ATP hydrolysis by Rad17 to open the ring, it is then thought to close the 9-1-1 complex

around the DNA, thereby encircling it (Bermudez et al., 2003, Ellison and Stillman, 2003). The interface at which the complex opens is still under debate, as Xu et al.,2009 and Dore et al., 2009 hypothesise it is the Rad9-Rad1 interface which opens, as this is the weakest interface between the proteins. However, Sohn and Cho (2009) believe it is the Hus1-Rad1 interface which is able to open and close as this most closely resembles the opening/closing interface of PCNA (Dore et al., 2009, Sohn and Cho, 2009, Xu et al., 2009). Interestingly, it is predicted that the C-terminus tail of Rad9 blocks access to the centre of the 9-1-1 ring and only moves out of the central "hole" of the ring upon interaction with RPA to allow the complex to load onto the DNA (Kemp and Sancar, 2009, Sohn and Cho, 2009). The recruitment and loading of the 9-1-1 complex has been shown to be independent of ATR-ATIP, therefore confirming the 9-1-1 complex as a true DNA damage sensor (Melo et al., 2001). For full checkpoint activation both the 9-1-1 complex and ATR-ATRIP need to be recruited to the damage site (Majka et al., 2006a, Parrilla-Castellar et al., 2004).

1.5.5 The Activation of the ATR Checkpoint Pathway

Once recruited to the site of damage, ATR and its homologs process a basal kinase activity that allows them to phosphorylate a number of early targets, but not the downstream targets such as the effector kinase. One of the first of these phosphorylation events is the phosphorylation of its binding partner ATRIP on S68 and S72. Mutation of these phosphorylation sites did not give any obvious phenotype, as downstream targets of ATR were still phosphorylated. They do, however, act as a good initial marker for ATR recruitment and its basal kinase activity, after damage (Itakura et al., 2004). Another phosphorylation event dependent solely on ATR's basal kinase activity but not its full activation, is an in *Trans* phosphorylation of ATR itself. After damage/replication stress, ATR becomes phosphorylated on a number of residues; S428, S435, possibly S436 and S437, and T1989 (Daub et al., 2008, Dephoure et al., 2008, Liu et al., 2011). The phosphorylation of T1989 is within the FAT domain of ATR and has been shown to be important for the full activation of ATR (via a mechanism described in "1.6.4 TopBP1 Dependent ATR Activation" section). T1989 phosphorylation depends on the recruitment of ATR-ATRIP complexes onto ssDNA, where multiple heterodimers will be in close proximity (Liu et al., 2011). In *S. pombe*

Rad3s basal kinase activity is also required to phosphorylate the Rad9 c-terminal tail on two residues T412 and S423, and this phosphorylation is important for the activation of the DNA damage checkpoint pathway (Figure 1-6) (Furuya et al., 2004).

In higher eukaryotes the Rad9 C-terminal tail is also phosphorylated, however this not ATR dependent. The phosphorylation of two sites; S341 and S387 is dependent on CK2 and are constitutively phosphorylated sites (St Onge et al., 2003, Takeishi et al., 2010, Ueda et al., 2012). There is an SQ/TQ site within the Rad9 C-terminal tail which is phosphorylated, however this did not give a phenotype after damage when mutated (Roos-Mattjus et al., 2003). The phosphorylated Rad9 C-terminal tail recruits a scaffold protein, TopBP1 in higher eukaryotes, (Rad4 in *S. pombe* or Dpb11 in *S. cerevisiae*) which is able to make contact with many of the proteins already described in this pathway (Figure 1-6) (Furuya et al., 2004, Puddu et al., 2008, Takeishi et al., 2010) (For more detail on this protein see TopBP1 review section). At this point, to phosphorylate its downstream targets ATR/Rad3/Mec1 needs to become fully active. The basal kinase activity is not adequate to phosphorylate these downstream proteins, this may be due to differences in the tertiary structure around the phosphorylation site, making it more difficult to phosphorylate.

In the budding yeast system it has been shown that the C-terminal tail of $Ddc1^{Rad9}$ is able to directly stimulate $Mec1^{ATR}$ kinase activity and activate the checkpoint. (Majka et al., 2006b, Bonilla et al., 2008, Navadgi-Patil and Burgers, 2009). Initially Majka et al., 2006b showed, in *vitro*, that the activation of Mec1 kinase activity required only the 9-1-1 clamp and specifically an interaction between Ddc1 and Mec1. However, the clamp needed to be loaded onto partially duplexed DNA in order to carry out this function. Subsequently Bonilla et al., 2008 showed that in *vivo* co-recruitment of Mec1-$Ddc2^{ATRIP}$ and Ddc1 to the DNA is sufficient for Mec1 activation. To do this they used a LacO system, first developed in human cells by Soutoglou and Misteli (2008), in which 256 repeats of LacO sequence are inserted into the genome (Soutoglou and Misteli, 2008). Ddc2 and Ddc1 were then tagged with LacI and expressed, this causes Ddc2 (with associated Mec1) and Ddc1 to be recruited to the chromatin independently of DNA damage.

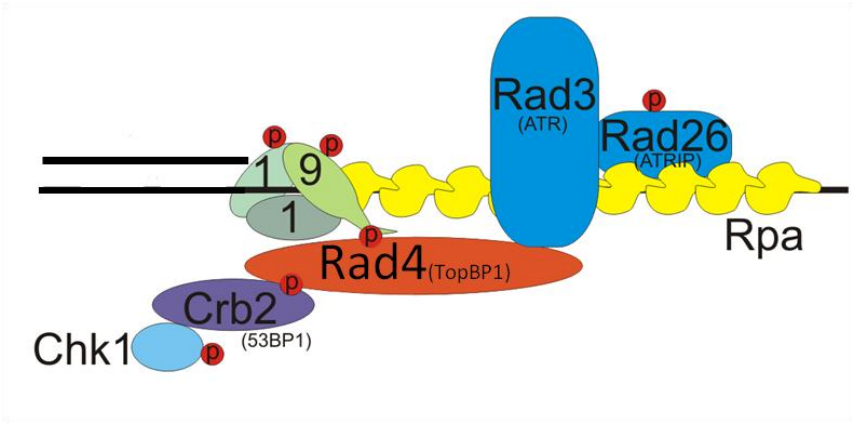

Figure 1-6. Overview of the activation of the *S.pombe* DNA damage checkpoint

Upon DNA damage, the DNA is processed (Figure 1-5) leading to large stretches of ssDNA. This is coated by RPA. The Rad3-Rad26 heterodimer is recruited to the RPA coated ssDNA and the 9-1-1 complex is loaded onto the ss-dsDNA junction. Rad3 then phosphorylates (amongst other targets) Rad26 and the C-terminal tail of Rad9. Rad4 is recruited to the phosphorylated Rad9 tail. Crb2 is recruited along with Rad4 via an interaction which is at least in part dependent on Cdc2 phosphorylation of T215 on Crb2. Rad3 then phosphorylates Crb2 leading to the recruitment of Chk1. Chk1 is then phosphorylated by Rad3 leading to Chk1 auto-phosphorylation, activation and release from the site of damage. Chk1 can now phosphorylate its downstream targets leading to a full checkpoint response. (See text for more detail). Adapted from Carr, (2002)

They observed Ddc1 dependent Mec1 dependent checkpoint activation, suggesting that Ddc1 alone can fully activate Mec1 (Bonilla et al., 2008).

More recently Navadgi-Patil and Burgers, 2009 identified the key residues within Ddc1 that were required for Mec1 activation. They showed that two tryptophan residues, W352 on the PCNA like domain and W544 within the unstructured C- terminal tail, were sufficient to activate Mec1 in both G1 and G2 of the cell cycle. Interestingly though, these residues were only essential for Mec1 activation in G1 (Navadgi-Patil and Burgers, 2009). The presence of ATR activation activity within the Ddc1 homologs has not been identified in any other organism to date, suggesting that there are other ways that ATR and its homologs can be activated. Indeed the Rad9 recruited TopBP1 has been shown to be able to stimulate ATR/Mec1 kinase activity and phosphorylation of its downstream targets (Discussed in "1.6.4 TopBP1 Dependent Activation of ATR" section) (Kumagai et al., 2006, Delacroix et al., 2007, Lee et al., 2007, Navadgi-Patil et al., 2011, Pfander and Diffley, 2011). Very recently it has been suggested that NBS1 of the MRN complex is able to directly activate ATR in *vitro* and *vivo*, as it is ATM, and that this is independent of the 9-1-1 complex and Mre11: Fusion of the NBS1 C-terminus onto the replication clamp PCNA in rad17 (9-1-1 clamp loader) null DT40 cells led to ATR activation. This potential activation appears to be independent of TopBP1, but both are required for a full checkpoint response (Kobayashi et al., 2013)

The recruitment of *S. pombe* Rad4^{TopBP1} by Rad9 brings the mediator protein Crb2 into the complex. In budding yeast Dpb11^{TopBP1} recruits the Crb2 homolog, scRad9 (not part of the 9-1-1 complex), and in higher eukaryotes an interaction between 53BP1 and TopBP1 has been described (Figure 1-6) (Saka et al., 1997, Mochida et al., 2004, Du et al., 2006, Pfander and Diffley, 2011). Crb2 was first identified as Rhp9 in 1997 and was shown to be required for the activation of the DNA damage checkpoint, but not the replication checkpoint (Willson et al., 1997). Crb2 contains a pair of BRCT domains and a Tudor domain at its C-terminus These BRCT domains along with the phosphorylation of S666 within the second BRCT domain are required for Crb2 dimerisation, a formation in which Crb2 is found even in the absence of DNA damage and is critical to its function (Kilkenny et al., 2008). It has also been reported that the *S. cerevisiae* homolog scRad9 also functions as homodimer (Watts and Brissett, 2010).

Crb2 is recruited to Rad4 in a manner involving a CDK phosphorylation on T215 (Figure 1-6). This is not DNA damage dependent, but as it is CDK dependent it can only occur when CDK activity is high in Late S-G2 phases. Mutation of the T215 site leads to mild DNA damage sensitivity and a checkpoint defect. This is not as severe as a *crb2Δ*, suggesting that Crb2 may also be recruited by other means (Du et al., 2003, Du et al., 2006). Once recruited, Crb2 is maintained at the damage site in a Rad1 and Rad3 dependent manner. However, the exact mechanism of this is not fully understood (Du et al., 2003).

Once stably associated at the site, Crb2 is phosphorylated by Rad3 on two SQ/TQ residues in its N-terminus; T73 and S80. These phosphorylated residues are required for recruitment of the effector kinase Chk1 and activation of the DNA damage checkpoint (Figure 1-6). Chk1 interacts with these two phosphorylated residues via its FHA domain, and mutation of these residues prevents the formation of Chk1 foci at the damage site. Furthermore, the requirement of Crb2 in the damage checkpoint can be bypassed by fusing a 19 amino acid peptide of Crb2 containing the phosphorylated residues to Rad4. This shows that the role of Crb2 in the checkpoint is grossly mediating Chk1 recruitment to DNA damage (Qu et al., 2012). A similar pathway is also present in budding yeast where Mec1 phosphorylates S390, an SQ site within the scRad9 SCD. However, there is some functional redundancy between the SQ/TQ sites within the SCD and mutation of S390 can, in part, be compensated for by the other SQ/TQs (Emili, 1998, Vialard et al., 1998, Schwartz et al., 2002). This interaction, as in *S. pombe,* is dependent on Rad53s FHA domain in *vitro* and in *vivo*, with both of Rad53s FHA domains being able to bind (Sun et al., 1998, Schwartz et al., 2002).

Once recruited, Chk1/Rad53 is phosphorylated by Rad3/ATR/Mec1 (Figure 1-6). In the mammalian system, Chk1 is phosphorylated by ATR on two SQ sites, S345 and S367, both of these phosphorylation events are required for Chk1 activation (Guo et al., 2000, Liu et al., 2000). In *S. pombe* both of these SQ sites are conserved, but only S345 is required for Chk1 and checkpoint activation (Lopez-Girona et al., 2001). The ATR phosphorylation of Chk1 induces Chk1 autophosphorylation on S296 which leads to dimerisation and full Chk1 (Schwartz et al., 2002, Lee et al., 2003, Okita et al., 2012). The phosphorylation of Chk1 (or $Rad53^{Chk2}$ in *S. cerevisiae*) is commonly used as a

marker of activation of the checkpoint in all organisms. Once activated, Chk1 dissociates from the site of damage and activated Chk1 is then soluble in the nucleus; it can therefore diffuse throughout the nucleus and phosphorylate its substrates (Smits et al., 2006). The downstream targets of *S. pombe* Chk1 include those proteins involved in regulating cell cycle progression and those involved in DNA repair.

1.5.6 ATR and the Replication Checkpoint

The DNA replication checkpoint, as has already been mentioned, is activated in response to stalled replication forks (Tercero et al., 2003). This pathway depends upon many of the same proteins as the ATR DNA damage pathway, with a number of important exceptions (Figure 1-7). Once ATR-ATRIP and the 9-1-1 complex are recruited to a stalled fork, ATR must be activated in much the same way as in the damage pathway. In budding yeast this activation of the ATR homolog Mec1 has been shown to be dependent on the nuclease-helicase DNA2 (Kumar and Burgers, 2013). DNA2 is already found at the replication fork in unperturbed S-phase as it is required for the processing of Okazaki fragments in lagging strand synthesis (Bae and Seo, 2000). Upon replication stress, the unstructured N-terminus of DNA2 can directly activate Mec1, this is dependent upon two key residues in DNA2; W128 and Y130. Mutation of these two residues reduced checkpoint activation, when combined with mutations that prevented recruitment of the other two known Mec1 activators ($Ddc1^{Rad9}$ and $Dpb11^{TopBP1}$), they abolished checkpoint activation (Kumar and Burgers, 2013). Dna2 has not been shown to activate ATR in any other organisms.

Once active, ATR and its homologs phosphorylate a mediator protein. However, this mediator protein is distinct from that used in the DNA damage pathway. In the replication checkpoint pathway a large scaffolding protein known as Mrc1 in the yeast systems, and Claspin in the metazoan systems, acts as the checkpoint mediator(Figure 1-7) (Kumagai and Dunphy, 2000, Alcasabas et al., 2001). Mrc1 was first identified in budding yeast and fission yeast by two independent groups in 2001 (Alcasabas et al., 2001, Tanaka and Russell, 2001).

It was identified in a screen for genes that showed sensitivity to HU whilst also displaying classical markers of a checkpoint defect (Alcasabas et al., 2001).

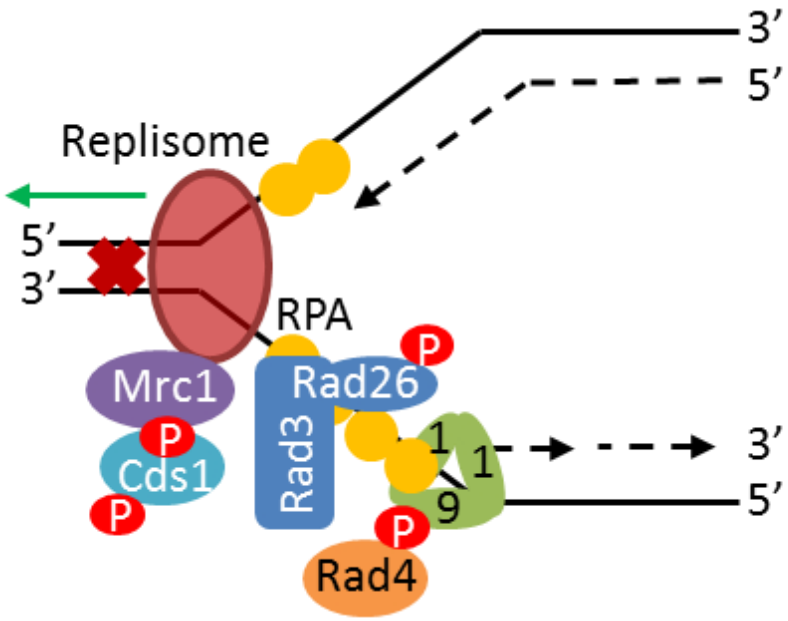

Figure 1-7. Overview of the Replication checkpoint in *S.pombe*
Upon encountering a lesion or protein DNA barrier (red X) the replication fork stalls and the helicase and polyermase become uncoupled, leading to the formation of ssDNA. RPA binds to the ssDNA and this leads to the recruitment of the Rad3-Rad26 heterodimer and the loading of the 9-1-1 complex on the ss-dsDNA junction. Rad3 phosphorylates Rad26 and Rad4 is recruited to phosphorylated Rad9. Rad3 also phosphorylates the mediator protein Mrc1 which is associated with the replisome. This Mrc1 phosphorylation leads to the recruitment of Cds1 which is subsequently phosphorylated by Rad3. Cds1 then auto phosphorylates leading to its full activation. (See text for further detail). Adapted from Carr, (2002)

It was shown that Mrc1 was required for the recruitment and activation of the effector kinase Cds1^{Chk2} in *S. pombe* and Rad53^{Chk2} in *S. cerevisiae*. This recruitment was dependent on Mrc1 phosphorylation, and the interaction was specific to S-phase (Figure 1-7). Mrc1 mRNA levels increased as cells entered S-phase, suggesting that Mrc1 is cell cycle controlled (Alcasabas et al., 2001, Tanaka and Russell, 2001). It was later shown that the phosphorylation of Mrc1 was dependent on spRad3^{ATR} and scMec1^{ATR}, in *S. pombe* these phosphorylation sites were identified as T645 and T653 (Zhao et al., 2003, Xu et al., 2006). These phosphorylation sites are required for the recruitment of the replication checkpoint effector kinase Cds1 to stalled replication forks, and this interaction was mediated by the FHA domain within Cds1 (Figure 1-7) (Xu et al., 2006). Indeed, in budding yeast, co-localisation of Mec1 and Mrc1 to the chromatin, using a LacO-LacI recruitment system, is sufficient for activation of the replication checkpoint. This suggests that no other mediator proteins are required (Berens and Toczyski, 2012). Interestingly, Alcasabas et al., (2001) also noted that *mrc1Δ* cells progressed through S-phase more slowly than WT and suggested that Mrc1 may also play a role in replication (Alcasabas et al., 2001). Consistent with this, Mrc1 has been shown in *S. pombe* to bind Swi1-Swi3 and is required for stabilising replication forks and for the maintenance of fork integrity; this implicates Mrc1 as being at the replication fork before activation of the checkpoint (Tanaka et al., 2010).

Once recruited by phosphorylated Mrc1, Cds1 is phosphorylated by Rad3 on T11 (Figure 1-7). This recruitment and phosphorylation of Cds1 promotes Cds1 dimerisation and subsequent in *Trans* autophosphorylation on T328 (Yue et al., 2011). Monomeric Cds1 is unable to autophosphorylate as the C-terminus of the protein prevents access to the phosphorylation site; this is thought to prevent unwanted activation of Cds1 (Xu and Kelly, 2009). Once autophosphorylation has occurred, Cds1 is fully active and can phosphorylate its downstream targets. Targets of Cds1 and its homologs include proteins that are involved in stabilising replication forks, processing of forks, origin firing and slowing of S-phase and cell cycle control. These include; Dna2, Rad60, Mus81 and Cdc25 (Zeng et al., 1998, Miyabe et al., 2009, Willis and Rhind, 2009, Hu et al., 2012).

A similar pathway of replication checkpoint activation has also been described in higher eukaryotes, initially in the Xenopus system. Claspin was discovered as a protein required for Chk1 phosphorylation and cell cycle arrest after replication stress. It was also shown to be bound to the Swi1-Swi3 homologs Timless-Tipin at the replication fork, suggesting a conserved pathway from yeast to higher eukaryotes (Kumagai and Dunphy, 2000, Kumagai et al., 2004, Errico et al., 2007). However, it would seem that the roles of the Chk1 and Chk2 homologs have swapped over time with the Chk2 homolog Cds1 being required in fission yeast for the replication checkpoint, whereas in higher eukaryotes, Chk1 functions in the replication checkpoint. Chk2, as already mentioned, acts in the damage checkpoint. In budding yeast it would seem that $Rad53^{Chk2}$ carries out most of the functions of both Chk1 and Chk2 and operates in both the damage and replication checkpoints (Rhind and Russell, 2000).

1.5.7 ATR Checkpoint Maintenance and Amplification

Once the checkpoint has been activated it is important to ensure the signal is strong enough to cause a full checkpoint response and that this response is maintained long enough to allow the DNA damage to be repaired. Once activated, ATR and its homologs phosphorylate the C-terminal tail of the histone H2A on S129, or in the case of the higher eukaryotes the histone variant H2AX, giving γH2A/γH2AX (Ward and Chen, 2001). This γH2AX spreads 1Mb in the case of metazoans and 50-100kb in the case of yeasts, along the chromatin from the DNA damage site (Rogakou et al., 1999, Shroff et al., 2004). Mutation in S129 in yeasts leads to mild checkpoint defects and a modest decrease in viability in the presence of DNA damaging agents (Redon et al., 2003, Nakamura et al., 2004). This checkpoint defect seems to be due to reduced checkpoint amplification and maintenance rather than a direct defect in checkpoint activation, as shown by the creation of a persistent HO induced DSB (Du et al., 2006). γH2A acts to recruit BRCT domain containing mediator proteins. In *S. pombe* these proteins include $Crb2^{53BP1}$ and Brc1. Crb2 binds γH2A via its 2^{nd} BRCT domain. Two point mutations in this domain, K617E and K619E, reduce Crb2 binding to the histone. These mutations cause defects in the repair of IR induced DSBs (Kilkenny et al., 2008).

A second histone modification also plays a part in Crb2 foci formation and recruitment to γH2A, this modification comes in the form of H4-K20me. This methylation event is dependent on the methyltransferase Set9 in *S. pombe*, and a tudor domain within Crb2 is required for the interaction with H4-K20me. Mutation of this tudor domain reduced Crb2 foci at the chromatin and gave a mild sensitivity to ionising radiation that was not increased in a *set9Δ* background (Du et al., 2006). Crb2 can then recruit Chk1, this leads to increased checkpoint activation and maintenance of the checkpoint during DNA repair where RPA is lost from ssDNA (Sofueva et al., 2010).

Brc1, a six BRCT domain containing protein which is similar to mammalian MDC1 and PTIP, and budding yeast Rtt109, also interacts with γH2A. The interaction between γH2A and Brc1 depends on the 5th and 6th BRCT domains of Brc1, point mutations within these domains prevent damage induced Brc1 foci formation (Williams et al., 2010b). Interestingly, it appears that Brc1 chromatin foci are most prevalent after hydroxy urea (HU) treatment, which causes replication fork stalling. This coincides with reports that show Brc1 is required for survival after DNA damaging agents that have their effect in S-phase (Sheedy et al., 2005, Dovey and Russell, 2007). Brc1 also plays a role in the unperturbed S-phase, as *brc1Δ* mutant cells show a significant increase in Rad52 foci (a protein required for DNA repair), even without the addition of genotoxic agents. Therefore, it could be that Brc1 may play a role in maintaining the checkpoint in S-phase, whereas Crb2 has more of a role after IR radiation in G2. However, Brc1 foci can still be seen after IR and other DNA damaging agents not specific to S-phase and the *brc1Δ crb2Δ* double mutant is more sensitive to IR than *crb2Δ* alone (Williams et al., 2010b).

1.6 TopBP1; a Review

The work presented in this thesis mainly focuses on the TopBP1 homolog Rad4. Therefore a detailed review of what is already known about Rad4 and its homologs is included. TopBp1 and its homologs have been the subject of much research since the last time it was compressively reviewed in 2005 (Garcia et al., 2005). The review will therefore go on to focus on this more recent work.

1.6.1 Identification of TopBP1 and its Homologs

TopBP1 was first discovered in *S. pombe* in two independent screens. The first identified it as *rad4* in a screen for mutants that were sensitive to UV (Schupbach, 1971). The second identified it as having a "CUT" (Cell untimely torn) phenotype, in which cytokinesis occurs in the presence of unsegregated chromatids (Hirano et al., 1986). *cut5* and *rad4* were later shown to be the same gene (Saka and Yanagida, 1993). Although these screens showed that *rad4* most likely had a role in the checkpoint, they also identified the *rad4* mutant as being inviable at 36˚C, suggesting an essential role in another cellular pathway. It was later shown that *rad4* has an essential role in the initiation of DNA replication as well as functioning in the G1, S-phase and G2 checkpoints (Garcia et al., 2005). This essential role in replication was further confirmed with the identification of the *S. cerevisiae* homolog *DPB11,* which was identified in a screen for multicopy suppressors of temperature sensitive mutants in the Polε subunit *DPB2* (Araki et al., 1995). TopBP1 was later identified in Human cells in a two hybrid screen to find factors that interact with Topoisomerase IIβ (although the importance of this interaction is yet to be shown in *vivo*). Disruption of TopBP1 in multi cellular model organisms such as drosophila and mouse lead to larval/ early embryonic lethality, thus confirming the essential role of Rad4 is conserved (Yamamoto et al., 2000, Jeon et al., 2011).

1.6.2 TopBP1 Domain Architecture

Rad4/Dpb11/TopBP1 are all scaffolding proteins which are able to make protein-protein interactions with many other proteins via their BRCT domains. BRCT domains often come in the form of Tandem repeats and the interactions that the BRCT domains make are normally phospho-specific, allowing regulation over when they interact with their binding partners (Yu et al., 2003). These BRCT domains are therefore essential in TopBP1/Rad4/Dpb11s role in bringing proteins together into complexes under defined cellular processes such as DNA replication initiation and checkpoint activation. However, the number of BRCT domains varies considerably between the homologs (Figure 1-8).

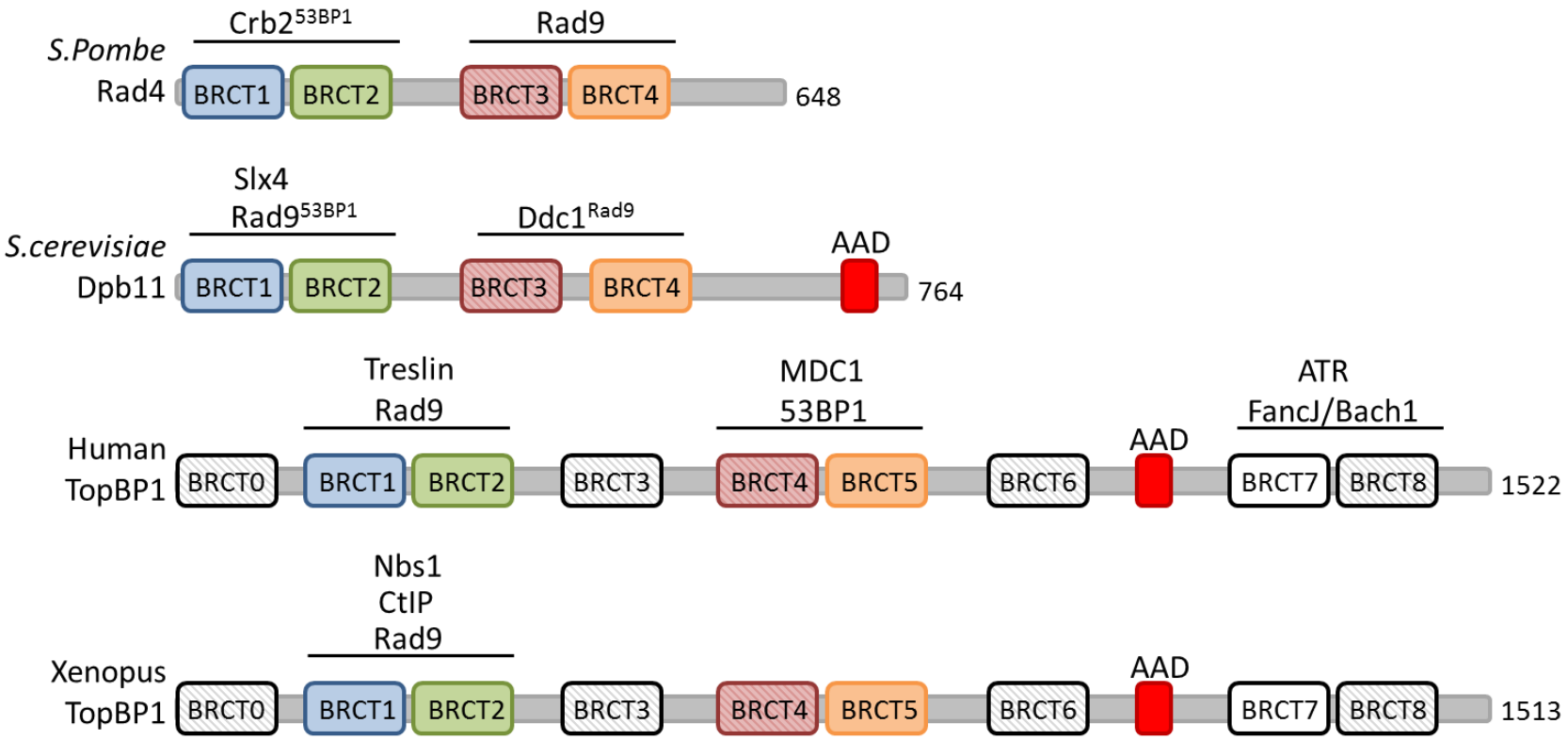
Crb2^53BP1
Rad9
S.Pombe
Rad4
BRCT1
BRCT2
BRCT3
BRCT4
648
Slx4
Rad9^53BP1
Ddc1^Rad9
AAD
S.cerevisiae
Dpb11
BRCT1
BRCT2
BRCT3
BRCT4
764
Treslin
Rad9
MDC1
53BP1
ATR
FancJ/Bach1
AAD
Human
TopBP1
BRCT0
BRCT1
BRCT2
BRCT3
BRCT4
BRCT5
BRCT6
BRCT7
BRCT8
1522
Nbs1
CtIP
Rad9
AAD
Xenopus
TopBP1
BRCT0
BRCT1
BRCT2
BRCT3
BRCT4
BRCT5
BRCT6
BRCT7
BRCT8
1513

Figure 1-8. Domain architecture of *S. pombe* Rad4 and its homologs Dpb11 and TopBP1
Diagrams of *s. pombe* Rad4, *S.cerevisiae* Dpb11, Human and Xenopus TopBP1, showing the position of the BRCT domains and the reported ATR activation domains (AAD). BRCT domains in Dpb11 and TopBP1 that are homologous to those in *S. pombe* Rad4 are represented by the same colours. BRCT domains containing diagonal lines have no phospho binding ability. The proteins which a BRCT domain is reported to bind to in the DNA damage or replication checkpoint are labelled above the appropriate domain for each organism. Modified from Garcia et al., (2005).

Both *S. pombe* Rad4^{TopBP1} and *S. cerevisiae* Dpb11^{TopBp1} contain four BRCT domains, two tandem BRCT repeats, and share 38% sequence similarity and 24% identity (Figure 1-8) (Garcia et al., 2005). Both human and Xenopus TopBP1 were originally shown to contain 8 BRCT domains, with BRCTs 1+2, 4+5 and 7+8 coming in the form of tandem repeats. Later a 9th BRCT domain at the extreme N-terminus was identified and termed BRCT0 (Figure 1-8) (Garcia et al., 2005, Rappas et al., 2011). Not all of these BRCT domains are predicted to have phospho-binding potential. In the human protein, crystal structures and structural predictions have shown that only BRCT1, 2, 3, 5 and 7 are likely to bind phosphorylated peptides. In yeast BRCT3 (which is homologous to BRCT4 in humans) is predicted to not contain a phospho binding pocket (Figure 1-8) (Leung et al., 2010, Leung et al., 2011, Rappas et al., 2011). Although Rad4/Dpb11 and TopBP1 act within the same cellular pathways, the similarity between the proteins is weak, with theTopBP1 protein being over twice the size of its yeast counter parts. However, the four BRCT domains of the yeast proteins are most similar to BRCTs 1+2 and 4+5 of TopBP1 (Figure 1-8). The *C.elegan*s and Drosophilia homologs have 6 and 7 BRCT domains respectively, suggesting TopBP1 has acquired additional functions in multicellular organisms which require the extra domains (Garcia et al., 2005). However, the core 1+2 and 4+5 pairs are conserved in all orthologs (human nomenclature) (Figure 1-8).

Interestingly xTopbp1, hTopbp1 and Dpb11 have all been shown to also contain an ATR Activation Domain (AAD) in their C-terminus, although no obvious sequence conservation between the TopBP1 and Dpb11 AADs has been observed (Figure 1-8)(Mordes et al., 2008b). In both Xenopus and human, this AAD is located between BRCTs 6 and 7. In budding yeast it is found at the extreme C-terminus after BRCT4 (Figure 1-8) (Kumagai et al., 2006, Mordes et al., 2008a, Mordes et al., 2008b). This domain gives another function to TopBP1 in addition to its scaffolding role.

1.6.3 TopBP1 as a Scaffold in the DNA Checkpoints.

As described briefly in the “1.5.1 The Activation of the ATR Checkpoint” section, TopBP1 is recruited to the sites of damage and replication stress, and this can be seen

by foci formation (Makiniemi et al., 2001). After damage TopBP1 and its homologs are recruited to the DNA lesion by either damage induced (in the case of yeasts) or constitutively (in the case of humans and Xenopus) phosphorylated Rad9 (scDdc1). This puts TopBP1 downstream of ATR-ATRIP and Rad9 recruitment and phosphorylation, but before the recruitment of the mediator proteins (Harris et al., 2003). The specific nature of the TopBP1-Rad9 interaction was first seen in *S. pombe*, where BRCT domains 3+4 of Rad4 were shown to interact with phosphorylated Rad9 T412 and S423. Furthermore, this interaction was required for the activation of the Chk1 damage checkpoint and was needed for the recruitment of Crb2 to the site of damage (Furuya et al., 2004). This was later confirmed by Taricani and Wang (2006), who showed Rad4 BRCT3+4 were required for checkpoint activation (Taricani and Wang, 2006).

A similar mechanism for $Dpb11^{TopBP1}$ recruitment to $Ddc1^{Rad9}$ has been seen in *S.cereviae,* where Dpb11 foci after damage in G1, S and G2 are dependent on the C-terminus of Dpb11 and components of the 9-1-1 complex (Figure 1-8) (Germann et al., 2011). This interaction is mediated by a $Mec1^{ATR}$ dependent phosphorylation on T602 on the C-terminal tail of Ddc1. This interaction is also required for the subsequent recruitment of the mediator protein $Rad9^{53BP1}$ and $Rad53^{Chk2}$ activation (Puddu et al., 2008, Pfander and Diffley, 2011). In higher eukaryotes, the fact that Rad9 is constitutively phosphorylated may mean the interaction between TopBP1 and Rad9 is not damage dependent. In line with this, TopBp1 and Rad9 co-immunoprecipitate even in the absence of DNA damage (Greer et al., 2003). In human cells the interaction is between phosphorylated S387 on Rad9 and BRCTs 1+2 of TopBP1 (Figure 1-8). Mutation of human TopBP1 BRCT1 results in a big reduction in the binding affinity between Rad9 and TopBP1, whereas the corresponding mutation in BRCT2 has little effect. However, mutation of BRCT2 in a protein already harbouring a BRCT1 mutation has an even lower affinity for the phosphorylated Rad9 tail than the BRCT1 mutation alone. This suggests that BRCT2 does play a role in the interaction (Rappas et al., 2011). Curiously it would therefore seem that the Rad9 binding ability of TopBP1 has switched from the second BRCT tandem repeat in yeast, to the first BRCT tandem repeat in human cells during evolution. A recently characterised protein Rhino is also

able to bind both Rad9 and TopBP1 in human cells, although it is unclear whether this is a TopBP1 BRCT domain dependent interaction. This interaction is important for checkpoint activation but the exact role it is playing is uncertain. It may stabilise the Rad9 TopBP1 interaction, retain TopBP1 at the site of damage after the initial recruitment, or even cause a conformational change in TopBP1, which could be important for full checkpoint activation (Cotta-Ramusino et al., 2011).

Xenopus TopBP1 can be recruited to sites of DNA damage independently of Rad9. Duursma et al., (2013) showed using ss-dsDNA-Junctions as ATR-dependent checkpoint activation structures in Xenopus egg extracts, that the MRN complex can recruit TopBP1. This was necessary for ATR to phosphorylate Chk1, although the 9-1-1 complex was still required for the phosphorylation (Duursma et al., 2013). The interaction between MRN and TopBP1 is also dependent on BRCT1+2 of TopBP1 and these make contact with the BRCT domains of NBS1 (Figure 1-8) (Yoo et al., 2009). Furthermore, a reduced level of TopBP1 can be seen at damage sites after depletion of the MRN complex (Lee and Dunphy, 2013). Recruitment of TopBP1 to the MRN complex is required for ATM dependent phosphorylation of TopBP1 on S1131 which is then required for the full activation of the ATR checkpoint (Yoo et al., 2007). Intriguingly, TopBP1 can also bind CtIP when it's in a complex with MRN, and this is dependent on two ATR/ATM phosphorylation sites in the N-terminus of CtIP and BRCT1+2 of TopBP1 (Figure 1-8) (Ramirez-Lugo et al., 2011). This suggests that TopBP1 can interact with different proteins that bind the MRN complex and these interactions may be regulated by phosphorylation under different circumstances.

It is yet to be seen if TopBP1 can interact with the MRN complex or CtIP in any other organism, but it is possible that this could be important for a hand over from the ATM dependent checkpoint to the ATR checkpoint in all higher eukaryotes. TopBP1 might have yet another binding partner in the activation of the replication checkpoint. For the initiation of replication TopBP1 binds Treslin (see "1.6.6 TopBP1 and the Initiation of Replication" section), and this is dependent on a CDK phosphorylation event on Treslin. This phosphorylation of Treslin and its subsequent interaction with TopBP1 BRCT1 and 2 has recently been shown, using a Treslin LacI-LacO tethering system, to be required for Chk1 activation (Figure 1-8) (Hassan et al., 2013).

It is not just BRCT1+2 in higher eukaryotes that are important for TopBP1 foci formation, BRCT5 has also been shown to be important for TopBP1 recruitment to sites of DNA damage and replication stress (Yamane et al., 2002). Indeed, BRCT5, has been shown to bind the SDT repeat of the mediator protein Mdc1 after replication stress, implicating TopBP1 in the γH2AX Mdc1 signal cascade, possibly to amplify the checkpoint signal (Figure 1-8) (Wang et al., 2011, Leung et al., 2013). Furthermore, recruitment of TopBP1 to sites of damage in G1 requires not only BRCT1+2 (Rad9 interaction),but also BRCT4+5. BRCT4 and 5 interact with 53BP1, and this interaction is required for a full G1 checkpoint response (Figure 1-8) (Yamane et al., 2002, Cescutti et al., 2010). The yeast Rad4/Dpb11^{TopBP1} proteins also interact with the 53BP1 homologs. *S. pombe* Rad4 interacts with Crb2^{53BP1} via BRCTs 1+2 in a two hybrid assay, this interaction maybe mediated at least in part by a CDK dependent phosphorylation of Crb2 on T215 (Saka et al., 1997, Du et al., 2006)(See "1.5.1 The Activation of the ATR Checkpoint Pathway" section). A similar mechanism is seen in *S. cerevisiae,* with Dpb11 interacting with scRad9^{53BP1}. Dpb11 BRCT1+2 interact with 2 CDK phosphorylation sites, S461 and T474, on scRad9. This interaction between Dpb11 and scRad9 is required for the subsequent recruitment of the effector kinase Rad53^{Chk2} (Figure 1-8) (Pfander and Diffley, 2011). This again suggests the first two tandem BRCT repeats of Rad4/Dpb11 and TopBP1 have swapped during evolution, although the function of the protein has remained consistent (Figure 1-8). Interestingly, Dpb11 has also been shown to bind Slx4, a DNA repair scaffold which is a subunit of a structure specific endonuclease required to resolve holiday junctions during homologous recombination (Fekairi et al., 2009, Svendsen et al., 2009). This interaction is mediated by SQ/TQ phosphorylations and more importantly, a CDK phosphorylation (S486) on Slx4 and Dpb11 BRCT1+2 (Figure 1-8). This binding to Slx4 therefore competes with the binding to Rad9 and is thought to attenuate Rad53 activation at stalled replication forks. This may be important for a local Mec1 dependent checkpoint response that allows DNA repair/fork restart without the full Rad53 dependent cell cycle arrest. This pathway has therefore been termed DAMP (dampens checkpoint adaptor-mediated phospho-signalling) (Ohouo et al., 2010, Ohouo et al., 2013).

The extra Tandem BRCT repeats, BRCT7+8, seen in higher eukaryotes but not in yeast, are also important for making protein-protein interactions during the checkpoint response, since removal of these domains leads to a checkpoint defect in Xenopus extracts (Yan et al., 2006). Cescutti et al., (2010) showed that BRCT7+ 8 as well as BRCT1+2 are important for checkpoint activation after replication stress and Yan et al., showed they were critical for Chk1 activation (Cescutti et al., 2010, Yan and Willis, 2013). Furthermore, TopBP1 BRCT7+8 bind to the Falconi Amenia helicase Bach1/FancJ, the crystal structure of this interaction has been solved, showing it is also a phospho-specific interaction (Figure 1-8). This interaction occurs after replication stress as the Bach1 phosphorylation is specific to S-phase. This Bach1 phosphorylation and subsequent TopBP1 interaction is required for the extension of RPA coated ssDNA and therefore the subsequent activation of the checkpoint (Gong et al., 2010, Leung et al., 2011). Also, BRCT7+8 have been shown to directly bind ATR (Figure 1-8). As described in the "1.5.5 The Activation of the ATR checkpoint pathway" section, ATR autophosphorylates once recruited to the RPA-ssDNA on T1989. TopBP1 BRCT7+8 binds to this phosphorylation site, and this is important for the full activation of ATR via TopBP1, the subsequent phosphorylation of downstream targets and checkpoint activation (Liu et al., 2011).

1.6.4 TopBP1 Dependent ATR Activation

As well as bringing DNA damage sensors, mediators and effectors together at sites of DNA damage, TopBP1 can also directly stimulate ATRs kinase activity. The ATR activation properties of TopBP1 were first seen by Kumagai et al., (2006). They showed that recombinant TopBP1 stimulates the kinase activity of both human and Xenopus ATR. The segment of TopBP1 responsible for this was narrowed down to a small region between BRCT domains 6 and 7 which was later termed the ATR Activation Domain (AAD). Expression of this fragment in human cells, or addition to Xenopus egg extracts, lead to ectopic ATR activation as seen by Chk1 phosphorylation. Expression of the AAD domain harbouring a point mutation at W1138 did not lead to this ectopic ATR activation. Furthermore the W1138 mutation lead to a checkpoint defect after Aphidicolin treatment of Xenopus egg extracts, where wild type TopBP1 had been ablated and replaced with recombinant mutant protein (Kumagai et al., 2006).

Following on from this, fusion of the TopBP1 AAD domain to either PCNA or histone H2B was shown to be sufficient for ATR activation in DT40 chicken cells, even if the 9-1-1 clamp loader (Rad17) was knocked out (Delacroix et al., 2007). As mentioned in "1.3.2 The Phosphatidylinositol (PI) 3 Kinase like Kinases (PIKKs)" section, the TopBP1 AAD domain contacts ATR in a region next to the FATC and kinase domains (now termed the PRD). The PRD domain is not required for ATRs basal kinase activity, but it is required for full ATR activity both in *vitro* and in *vivo*. Expression of ATR with a mutation in this domain in ATR $^{flox/-}$ cell lines, where ATR can be conditional knocked out, leads to loss of checkpoint signalling after replication stress and loss of viability. This suggests that the PRD domain is crucial for ATR activation in the replication checkpoint and ATR activation is required for cell viability (Mordes et al., 2008a). Furthermore, tethering LacI-TopBP1 to LacO arrays, either in vito or in *vivo*, leads to Chk1 phosphorylation. This phosphorylation is further enhanced when Claspin is also recruited, further implicating the TopBP1 AAD in ATR activation in the replication checkpoint (Lindsey-Boltz and Sancar, 2011). Interestingly, TopBP1 also needs to contact ATRs binding partner, ATRIP, to activate ATR. Mutation of the TopBP1 interacting domain within ATRIP confers sensitivity to HU, leads to reduced viability and causes a G2/M checkpoint defect. The TopBP1 interacting domain within ATRIP is conserved in budding yeast suggesting a similar mode of binding in lower eukaryotes (Mordes et al., 2008a). Furthermore, using an in *vitro* system to reconstitute the ATR checkpoint Choi et al., (2010) show that it is the N-terminus of TopBP1 that interacts with ATRIP (Choi et al., 2010). However, the molecular mechanism of this interaction is yet to be seen.

The phosphorylation of TopBP1 adjacent to the AAD by ATR/ATM is also important for TopBP1s ability to activate ATR (Kumagai et al., 2006, Yoo et al., 2007, Burrows and Elledge, 2008, Mordes et al., 2008b). A model of how TopBp1 activates ATR could now be envisaged: Replication fork stalling recruits ATR-ATRIP and the 9-1-1 complex with associated TopBP1. ATR auto-phosphorylates and phosphorylates ATRIP, the N-terminus of TopBP1 interacts with ATRIP via an unknown mechanism, this brings TopBP1 into close proximity to ATR. TopBP1 stably binds to the auto-phosphorylation site (T1989) on ATR and activates it via an interaction between its AAD and ATRs PRD.

ATR then phosphorylates TopBP1, leading to further stimulation of ATRs kinase activity by TopBP1. ATR can now phosphorylate its downstream targets leading to full checkpoint activation. (Burrows and Elledge, 2008, Liu et al., 2011). It is not yet clear whether TopBP1 can stimulate ATR kinase activity at any other stage of the cell cycle or after DNA damage such as DSBs. A recent study in mouse has shown that the TopBP1 AAD is essential for embryonic development. Deletion of the AAD shows an embryonic lethality phenotype similar to that of an ATR knockout, suggesting this is the main way in which ATR is activated, in the early stages of embryogenesis at least (Zhou et al., 2013).

S. cerevisiae Dpb11^{TopBP1} has also been shown to activate Mec1^{ATR}. Mordes et al., (2008b) showed Dpb11 interacts with Mec1-Ddc2 and activates Mec1s-kinase activity, this activation was dependent on Ddc2. Analogous with the higher eukaryotes, Mec1 is then able to phosphorylate Dpb11 on T731 further stimulating Dpb11s ability to activate Mec1 (Mordes et al., 2008b). It was also shown that the C-terminus of Dpb11 is the region required to stimulate the kinase activity of Mec1 and that Dpb11 was able to do this in *vitro*, even in the absence of ssDNA (Mordes et al., 2008b). Interestingly, Dpb11 and Ddc1^{Rad9} act synergistically to stimulate Mec1s kinase activity, suggesting both proteins are able to activate Mec1 independently of each other's AAD activity (Navadgi-Patil and Burgers, 2008)(see "1.5.5 The Activation of the ATR Checkpoint Pathway" section).

Cell cycle studies originally showed that Dpb11 activated Mec1 in S phase and G2, but was dispensable for Mec1 activation in G1, whilst Ddc1 activated Mec1 in G1 and also in G2 (Mordes et al., 2008b, Navadgi-Patil and Burgers, 2009). However, the S-phase activation of Mec1 by Dpb11 turned out to be an artefact of the mutation used. The Dpb11-1 allele has a mutation adjacent to the C-terminal end of BRCT4. This even at permissive temperature causes a replication initiation defect leading to less replication forks. Therefore, after treatment with HU there is less fork stalling compared to WT and hence, less Rad53 activation due to the reduced number of replication forks, rather than an inability to activate Mec1 directly (Navadgi-Patil et al., 2011). Identification of the residues within Dpb11, Y735 and W700, which are required for Dpb11s AAD activity, and a truncation mutant, Dpb11-601 (which does not interfere

with the BRCT domains within Dpb11) showed that Dpb11 only plays a relatively small role in Mec1 activation in G2 phase of the cell cycle, acting with partial redundancy with the Ddc1 AAD (Navadgi-Patil et al., 2011, Pfander and Diffley, 2011). Interestingly, the two residues required in Dpb11 for Mec1 activation are either side of the Mec1 phosphorylation site which, when phosphorylated, leads to an increase in Dpb11s ability to stimulate Mec1s kinase activity. This suggests that this phosphorylation may lead to a conformational change or a stronger interaction between the AAD and Mec1 (Mordes et al., 2008b, Navadgi-Patil et al., 2011).

Overall it would seem that the AAD within TopBP1 is more important for ATR activation than that in Dpb11 and also acts, a least in part, in a different cell cycle stage. However, many of the molecular interactions and mechanisms underlying the way in which TopBP1 and Dpb11 activate ATR/Mec1 are conserved.

1.6.5 TopBP1 and DNA Repair

In budding yeast, Dpb11^{TopBP1} has also been shown to play a role in the repair of DNA damage that is independent of its role in checkpoint activation. This was first seen in the *dpb11-1* temperature sensitive mutant: at the permissive temperature *dpb11-1* showed a defect in the repair of MMS induced damage, but not in the activation of the checkpoint. The repair defect is within the homologous recombination pathway as *dpb11-1* mutants were epistatic with *rad51* and *rad52* (genes required for the strand invasion step of HR) mutants after MMS but not HU. Furthermore, Dpb11 associates with the HO break site and the HML locus during mating type switching and is required for homologous recombination between the MAT locus and the HML locus (Ogiwara et al., 2006). Further confirmation of this was acquired through the identification of a Dpb11 separation of function mutant known as Dpb11-PF (P3A, F4A). This mutant is proficient in checkpoint activation and the initiation of DNA replication, but has altered levels of recombination at heteroallelic repeats and direct repeats. Dpb11-PF shows increased levels of heteroallelic recombination and reduced direct repeat recombination, suggesting a shift from sister chromatid to interhomolog repair. This is most likely to be due to slow repair kinetics. As with *dpb11-1*, *dpb11-PF* is sensitive to DNA damage, but the mutant protein is still able to form foci at the damage site which

co-localise with the Rad52 HR repair factor. Also, the *dpb11-PF* mutant as with the *dpb11-1* mutant has delayed kinetics in mating type switching due delayed extension of the invading strand (Germann et al., 2011). This delay in extension of the invading strand is due to a defect in the initiation of repair DNA synthesis (Hicks et al., 2011). Interestingly, other proteins required for the initiation of DNA replication such as MCM2-7, GINS, Cdc45 and Polε are not required for initiation of repair DNA synthesis (Hicks et al., 2011).

Importantly, it has been reported that hTopBP1 is also required for homologous recombination. Depletion of TopBp1 leads to an increase in inter sister chromatid exchange and a reduced level of DSB-induced HR, as seen in an I-SceI break system. Cells depleted of TopBP1 also exhibit sensitivity to DSB forming agents, such as IR and mitomycin C (Morishima et al., 2007). This suggests a conserved role for TopBP1 in homologous recombination. However, more work is required to understand the full mechanism. The role for TopBp1 in DNA repair may also extend to the repair of broken replication forks. Dpb11 has been shown to bind to Mec1 phosphorylated repair scaffold proteins Slx4 and RTT107, and this may be important for bringing repair proteins to the fork. Mutation of the Mec1 phosphorylation sites on Slx4 disrupts its interaction with Dpb11 and sensitises cells to MMS but not to HU or CPT, suggesting a role for Dpb11 in repair of broken forks (Ohouo et al., 2010).

1.6.6 TopBP1 and the Initiation of DNA Replication

As already mentioned, the essential function of TopBP1 and its homologs is in initiating DNA replication (Masumoto et al., 2000, Hashimoto and Takisawa, 2003). An early study by Araki et al (1995) showed *dpb11*^{TopBP1} genetically interacted with DNA polymerase II (pol epsilon), suggesting Dpb11 had a role in DNA replication (Araki et al., 1995). However, xTopBP1 is not required for the formation of the pre-replication complex (Pre-RC) which includes ORC, MCM, Cdc6 and Cdt1 (Hashimoto and Takisawa, 2003). Two independent screens gave insight into how Dpb11 functions in the initiation of DNA replication. Kamimura et al., (1998) carried out a synthetic lethal with Dpb11 (SLD) screen and identified a number of genes that encoded proteins which acted within the Dpb11 pathway, including Sld1 (Pol episilon), Cdc45, Sld3, Sld2 and

Sld5 (a member of the GINS complex) (Kamimura et al., 1998). Sld2 was also identified in a screen for dosage-dependent suppressors of the temperature sensitive mutant *dpb11-1* (Wang and Elledge, 1999). The data from these screens was backed up biochemically and showed that Sld2 interacted with Dpb11 and that this interaction was required for replication initiation (Kamimura et al., 1998, Wang and Elledge, 1999).

The interaction between Sld2 and Dpb11 is a CDK dependent interaction, with phosphorylation of a number of canonical CDK sites first being required for the phosphorylation of a non-canonical site, T84. This suggests that a threshold of CDK activity is required for replication initiation (Masumoto et al., 2002, Tak et al., 2006). Furthermore, this phosphorylated Sld2 interacts with Dpb11s BRCT domains 3 and 4 (Tak et al., 2006). Sld2 was also shown to bind to Pol epsilon and associated GINS complex (a complex of four proteins important for the helicase activity of MCM 2-7) (Moyer et al., 2006). The CDK-dependent interaction between Dpb11 and Sld2 therefore brings Dpb11-Sld2-Polε and GINS into a complex known as the Pre-Loading Complex (Pre-LC) (Figure 1-9B)(Araki, 2011). GINS has also recently been shown to interact with Dpb11 itself and interacts with the 100 amino acid inter BRCT1 and 2 region. This interaction is required for normal cell growth, and mutation leads to replication defects (Tanaka et al., 2013). The interaction between Dpb11 and GINS may therefore be important for stabilising the Pre-LC complex (Figure 1-9B).

Importantly, two studies showed that Sld3 is also phosphorylated by CDK (Tanaka et al., 2007, Zegerman and Diffley, 2007). Sld3 is known to bind to the pre-RC, along with Cdc45 in a DDK phosphorylation dependent manner (Figure 1-9A, B) (Yabuuchi et al., 2006, Heller et al., 2011). The Cdc45-Sld3 complex is also essential for replication initiation (Figure 1-9B) (Tercero et al., 2000, Kamimura et al., 2001). CDK phosphorylation of two sites on Sld3 is required for an interaction with Dpb11 (Figure 1-9B) (Tanaka et al., 2007, Zegerman and Diffley, 2007). A fusion between Sld3 and Dpb11 bypassed the requirement of both of these CDK phosphorylation sites and of BRCT's 1 and 2 of Dpb11, for replication initiation. If this fusion is combined with a phospho mimetic allele of Sld2, CDK activity is no longer required for replication initiation.

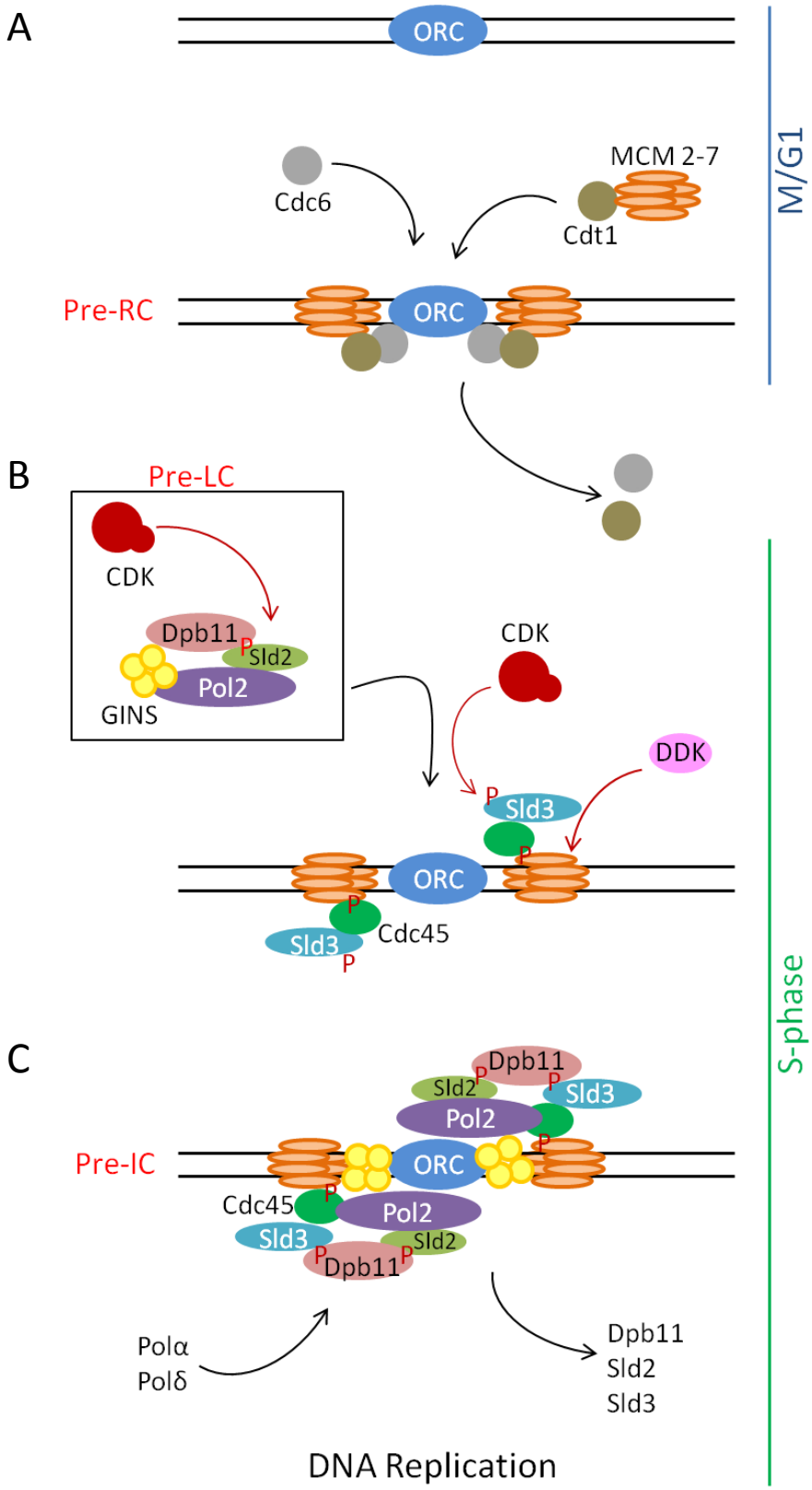
A
ORC
MCM 2-7
Cdc6
Cdt1
Pre-RC
ORC
M/G1
B
Pre-LC
CDK
Dpb11
Sld2
Pol2
GINS
CDK
DDK
Sld3
ORC
Cdc45
Sld3
S-phase
C
Dpb11
Sld2
Sld3
Pol2
Pre-IC
ORC
Cdc45
Pol2
Sld3
Sld2
Dpb11
Polα
Polδ
Dpb11
Sld2
Sld3
DNA Replication

Figure 1-9. Overview of the initiation of DNA replication.
Diagram showing each step of the initiation of DNA replication in *S. cerevisiae*. The *S. cerevisiae* pathway is shown as it has been most extensively studied. A. In late M phase ORC associates with the origins of replication. In Late M/G1 Cdc6 binds to ORC and this leads to the recruitment of Cdt1 and the associated MCM 2-7 helicase. This complex, at the origin of replication, is known as the pre-replication complex (Pre-RC). Cdc6 and Cdt1 subsequently dissociate from the origin B. As cells enter S-phase CDK activity increases and CDK phosphorylates Sld2. Dpb11 binds the phosphorylated Sld2, which is in complex with Pol2 and GINS. Dpb11 also makes contact with GINS and this Dpb11-Sld2-Pol2-GINS complex is known as the Pre-loading complex (Pre-LC). At the same time DDK phosphorylates the MCM complex leading to the recruitment of Cdc45 and the associated Sld3. CDK phosphorylates Sld3. C. The phosphorylation on Sld3 recruits the Pre-LC via an interaction with Dpb11 leading to the formation of the pre-initiation complex (Pre-IC). MCM-Cdc45-GINS now form an active helicase complex known as the CMG. Polα and Polδ are recruited, and Dpb11, Sld2 and Sld3 dissociate. DNA replication now initiates. Adapted from Araki, (2011)

Therefore, the minimal requirements of CDK in initiation of DNA replication in budding yeast is the phosphorylation of Sld2 and 3 to enable their interaction with Dpb11 (Zegerman and Diffley, 2007). Phosphorylation of Sld3 therefore bring the Pre-LC to the origin and promotes replication by bringing GINs-Polε and Cdc45 together (Figure 1-9C). GINS and Cdc45 can now interact with the MCM complex, creating the active helicase complex known as the CMG. Pol α and Pol δ are then recruited and DNA replication can initiate (Figure 1-9C) (Moyer et al., 2006, Araki, 2011). Interestingly Dpb11-Sld2-Sld3 dissociate from the origin once the CMG complex forms and do not travel with the replication fork (Figure 1-9C) (Masumoto et al., 2002, Bruck et al., 2011, Bruck and Kaplan, 2011).

A similar role for *S. pombe* $Rad4^{TopBP1}$ in the initiation of replication has also been shown: Sld2 is phosphorylated on T111 by CDK and interacts with BRCT3 and 4 of Rad4, whilst CDK phosphorylated Sld3 binds to BRCT1 and 2. Both these interactions are required for replication initiation. Furthermore, a 3 hybrid analysis between Sld2-Rad4-Sld3 showed the CDK-dependent association of Sld2-Rad4 enhanced the Sld3-Rad4 interaction. This gives a possible mechanism by which Rad4 bound to Sld2 is more likely to bind the origin associated Sld3 (Fukuura et al., 2011). As with Dpb11, Rad4 does not travel with the replication fork (Taylor et al., 2011).

In higher eukaryotes, TopBP1 is also essential for replication initiation but not elongation. However, the mechanisms for this are not so clear (Makiniemi et al., 2001, Hashimoto and Takisawa, 2003). The Sld2 and Sld3 homologs have been identified as RecQ4 and Treslin/TICCR, respectively (Matsuno et al., 2006, Kumagai et al., 2010, Sansam et al., 2010). Treslin is phosphorylated on S1000 and S976 by CDK2 Cyclin E in Xenopus, and mutation of these sites, as in yeast, leads to a deficiency in DNA replication (Kumagai et al., 2011). Furthermore, in human cells, the CDK phosphorylated Treslin binds TopBP1 BRCTs 1 and 2 in a similar way to how Sld3 binds BRCT3 and 4 of Dpb11 (Boos et al., 2011). Again, this adds to the notion that the first two tandem BRCT repeats in TopBP1 have switched around compared to those in yeasts. However, it was reported in HeLa cells that depletion of TopBP1 does not significantly reduce CMG formation, an event that does require CDK and RecQ4 (Im et al., 2009). It is worth noting though, that only a low level of TopBP1 is required for

initiation of replication and it maybe that the depletion was not efficient enough to prevent it. Furthermore, in Xenopus it appears that RecQ4 does not undergo the same CDK-dependent phosphorylation as its yeast counter parts (Matsuno et al., 2006). However, RecQ4 does co-IP with TopBP1, this is dependent on the N-terminus of RecQ4, and this N-terminal fragment can rescue the replication defect of RecQ4 depleted extracts (Matsuno et al., 2006). Overall, more work is required to understand the roles of TopBP1 in regards to RecQ4 in higher eukaryotes. BRCT6 of TopBP1 was also reported to be required for replication in Xenopus and in Human cells (Makiniemi et al., 2001, Schmidt et al., 2008). However, a truncation of TopBP1 which removes BRCT6, 7, 8 has also been reported to have no replication defects (Yan et al., 2006). It will therefore be interesting to see which BRCT domains in higher eukaryotes are required for DNA replication.

Upon DNA damage in S-phase the firing of unfired, or "late" origins is prevented (Santocanale and Diffley, 1998, Shirahige et al., 1998, Larner et al., 1999). This is due to the disruption of the critical interactions between TopBP1/Dpb11/Rad4 and Sld3/Treslin. In budding yeast, $Rad53^{Chk2}$ phosphorylates Dbf4 (DDK) and Sld3 after S-phase damage. The phosphorylation of Sld3 disrupts the interaction with Cdc45 and with Dpb11 (Lopez-Mosqueda et al., 2010, Zegerman and Diffley, 2010). This has also been shown to be the case in human cells, where Chk1 phosphorylation of Treslin prevents interaction with TopBP1 BRCT1 and 2 (Boos et al., 2011). A second mechanism by which the activation of the checkpoint may prevent origin firing is by $scDdc1^{Rad9}$ competing with Sld2 for binding to Dpb11 BRCT3/4. Over expression of Ddc1 in a Sld2 mutant leads to inviability (Wang and Elledge, 2002). It maybe that phosphorylation of Ddc1 after DNA damage out-competes Sld2 for binding to Dpb11, therefore preventing one of the interactions required for replication initiation.

1.6.7 TopBP1 and the Regulation of Transcription.

As well as its more established roles in the initiation of replication and the activation of the DNA structure dependent checkpoints,TopBP1 is emerging as having an important role in the regulation of transcription. hTopBP1 has been shown to have a transcription activation domain between amino acids 460 and 500, this maps to a

region including part of BRCT4. This region of TopBP1 was shown to up-regulate transcription using a Gal4 controlled luciferase reporter system (Wright et al., 2006). In the same study TopBP1 was also shown to have two transcription repressor domains which map to BRCT2 and BRCT5. These are thought to repress transcription by actively recruiting transcriptional repressor complexes to the promoter (Wright et al., 2006). BRCT6 of TopBP1 is also important for the regulation of transcription and has been reported to be involved in regulating the expression of a number of different genes, possibly by interacting with transcription factors or regulators of transcription.

TopBP1 has been shown to interact with E2F-1, a member of the E2F family of transcription factors involved in the regulation of the cell cycle. E2F-1 also has an additional role not seen for other E2F's in the regulation of apoptosis (Qin et al., 1994, Wu and Levine, 1994, Field et al., 1996). By interacting with E2F-1, TopBP1 represses EF2-1s transcriptional activity. It is thought to do this by facilitating the interaction between E2F1 and BRG1/BRM1 (SWI/SNF) chromatin remodelers. TopBP1 is therefore responsible for bringing BRG1/BRM1 to E2F-1 responsive promoters and the subsequent formation of a repressive chromatin, the formation of which, in turn, prevents apoptosis by repressing the transcription of apoptosis inducing genes. Indeed si-RNA of TopBP1 leads to an increase in apoptosis (Liu et al., 2004). TopBP1 interacts with E2F-1 at the G1-S boundary, presumably to prevent apoptosis during DNA replication. Furthermore TopBP1 is induced by E2F-1 at the G1-S transition, therefore leading to a feedback regulation mechanism in preventing apoptosis during DNA replication (Liu et al., 2004).

TopBP1 has also been shown to interact with E2F-1 after DNA damage, this is dependent on ATR/ATM phosphorylation of E2F-1 on S31 and TopBP1s BRCT6 (Lin et al., 2001). This interaction, again, represses the transcriptional activity of E2F-1, and in this case, prevents entry into S-phase. This presumably is to prevent cells from replicating damage DNA. It also prevents apoptosis (Liu et al., 2003b). A second phosphorylation event is also required for the interaction between TopBP1 and E2F-1 and this comes in the form of an AKT-dependent phosphorylation of TopBP1. AKT phosphorylates TopBP1 in *vitro* and in *vivo* on S1159. This phosphorylation leads to the oligomerisation of TopBP1 via BRCTs 7/8, binding to E2F-1 and the subsequent

repression of E2F-1 mediated apoptosis. Indeed, truncation of TopBP1 BRCT7/8 prevents interaction with E2F-1 and leads to an increase in apoptosis. Interestingly, phosphorylation by AKT and subsequent oligomerisation seems to be important in enabling TopBP1 to interact with most of the known transcription regulators it binds to, such as Miz1, SPBP and HPV16-E2 (discussed below) and seems to be a common theme in TopBP1s regulation of transcription (Liu et al., 2006).

Also, in the regulation of apoptosis, TopBP1 has been reported to bind to, and represses, the tumour suppressor p53. This report suggests, BRCTs 7/8 bind to the p53 DNA binding domain (DBD) and prevent p53 from binding promoter sequences. TopBp1 deletion up regulate p53 targets involved in cell cycle arrest and apoptosis and an increase in apoptosis after damage can be seen. Although, more work needs to be done to follow up this initial study (Liu et al., 2009).

TopBP1 also acts as a transcriptional co-repressor regulating expression of cell cycle genes via inhibiting the Myc-associated zinc finger protein Miz1. Miz1 is known to activate transcription of p21 (see “Regulation of the Cell Cycle” section) after UV damage, leading to cell cycle arrest (Adhikary and Eilers, 2005). TopBP1 associates with Miz1 in unstressed cells and dissociates following UV damage, leading to the induction of p21 (Herold et al., 2002). Depletion of TopBP1 has been shown to lead to p21 expression and inhibition of cyclinE/CDK2 in the absence of checkpoint activation and p53, showing that TopBP1 may indeed have a role in regulating cell cycle progression in the absence of damage (Jeon et al., 2007). The dissociation of TopBP1 from Miz1 after DNA damage may be due to the ribosyltransferase PARP1. PARP1 interacts with BRCT6 of TopBP1 in *vitro* and co-IPs in *vivo*. Furthermore, TopBP1 is ribosylated by PARP1 within BRCT6 and this impairs the interaction with Miz1 after UV damage, therefore giving insight into the mechanism of how p21 is expressed and the cell cycle is halted after UV damage (Wollmann et al., 2007). BRCT6 of TopBP1 also binds to the Stromelysin-1 PDGF response element binding protein (SPBP). SPBP is a transcriptional co-regulator and the interaction between TopBP1 BRCT6 and SPBPs ePHD domain leads to a co-operative stimulation of ETS1 regulated promotes such as c-Myc, PIP2 and MMP3 (Sjottem et al., 2007).

Finally, TopBP1 also plays a role in the regulation of viral transcription. Human Papilloma virus (HPV) transcription/replication factor E2 regulates the transcription and replication of the viral genome. Initially a two hybrid analysis for interacters of HPV16-E2 found TopBP1 which was shown to bind E2 in *vitro* and in *vivo*. This required the 3 most c-terminal BRCT domains (BRCTs 6/7/8) of TopBP1 (Boner and Morgan, 2002, Boner et al., 2002). TopBP1 acts as a transcriptional co-activator but also enhances viral replication, a process dependent on TopBP1s BRCTs 1 and 2. However, TopBp1 is not essential for either the transcription or replication processes, and the mechanism and roles for these interactions are not yet fully understood (Boner et al., 2002).

Overall there is an emerging picture of TopBP1 having a role in the regulation of transcription both as a co-activator and co-repressor, many of the process that it regulates seem to play a role in cell cycle progression and/or apoptosis.

1.6.8 TopBP1 and Disease

TopBP1 has been linked to breast cancer amongst other cancer types. However, there have been some contradictory reports on how important changes in TopBP1 are in predisposition and progression of cancer. A number of studies have implicated aberrant expression of TopBP1 in breast cancer. A histopathological study of breast carcinoma tissue showed that TopBP1, which is normally a nuclear protein, was expressed in both the nucleus and the cytoplasm or in just the cytoplasm, in 24 out of 61 samples tested. This compared to zero out of 12 normal tissues. Two of the 61 breast carcinoma tissue samples saw no TopBP1 expression at all (Going et al., 2007). Furthermore, a RT-Q-PCR study of 127 breast cancer samples from a number of different breast cancer types and tumour grades saw reduced expression of TopBP1 in hereditary breast cancers. However, the TopBP1 protein appeared to be more stable. The same study, in compliance with Going et al., (2007), also saw more cytoplasmic TopBP1 in breast cancer cells and this increased with increasing histological grade of the cancer (Forma et al., 2012). Slightly contradictorily to the results showing no TopBP1 expression in some breast cancer tissue samples, Liu et al., (2009) showed TopBP1 was over expressed in 46 of the 79 primary breast cancer tissues analysed, this

higher expression correlated with higher tumour grade and a shorter survival time for the patient. These effects of higher TopBP1 expression were suggested to be due to the increased levels of TopBP1 perturbing p53 function (see "1.6.7 TopBP1 and the Regulation of Transcription" section) (Liu et al., 2009). Over expression of TopBP1 has also been reported in Giloblastoma and the increased levels of TopBP1 expression in radioresistant non-small cell lung cancer cell lines correlated with reduced patient survival and brain metastasis (Seol et al., 2011a, Seol et al., 2011b).

A heterozygous polymorphism of TopBP1 between BRCTs 2 and 3 leading to Arg309Cys was found to be linked to an increased risk of breast and/or ovarian cancer in a screen of 125 Finnish cancer families (15.2% of cancer families had it compared to 7.0% of controls) (Karppinen et al., 2006). However, a larger screen of 1064 German breast cancer patients and 1014 population controls showed that Arg309cys did not show any elevated risk of breast cancer (Blaut et al., 2010). Another study of the haplotypes of BRCA1 and BRCA2 mutation carriers showed TopBP1 to have no association with ovarian cancer in BRACA1/2 mutant carriers (Rebbeck et al., 2009). It is therefore still unclear if polymorphisms in TopBP1 are associated with cancer risk and whether any mutations in TopBP1 are commonly found in cancer cells. Changes in TopBP1 expression do seem to be linked to breast cancer, the aggressiveness of the tumour and the radioresistance of other cancer types. However, more work needs to be done in this area of research to get a clearer picture.

1.7 Aims of this Work

The aim of this work is to try and further understand the molecular mechanisms and pathways in which TopBP1 (Rad4) acts, using *S. pombe* as a model organism. The role of the Rad4AAD in checkpoint activation and the pathway in which it is important, are identified using a LacO recruitment system and time course experiments. It is demonstrated that the Rad9 AAD domain is conserved from budding yeast and insights are made into the relative roles and importance of the Rad4 and Rad9 AAD's at different cell cycle phases. The phospho dependent interaction between Rad4 and the mediator protein Crb2 in the activation of the DNA damage checkpoint

are further characterised. Additionally, we cannot find evidence for an interaction between Rad4 and Slx4 in *S. pombe.* Finally, it is shown that Rad4, most likely, does not interact with a potential Rad4 interaction motif in Mrc1 during the activation of the replication checkpoint.

Chapter 2
Materials and Methods

2.1 Media

2.1.1 Yeast Media

Yeast Extract (YE), Rich Media

5 g/l	Yeast extract
30 g/l	Glucose
0.2 g/l	Adenine
0.1 g/l	Leucine
0.1 g/l	Uracil
0.1 g/l	Histidine
0.1 g/l	Arginine
(20 g/l	Peptone, for elutriation cultures)

YE Agar (YEA Plates)

As YE plus:

12.5 g/l	Difco Bacto Agar

Yeast Nitrogen Base (YNB), Minimal Media

1.9 g/l	Formedium YNB
5 g/l	Ammonium Sulphate
20 g/l	Glucose

Yeast Nitrogen Base Agar (YNBA Plates)

As YNB plus:

0.2 ml/l	10M NaOH
25 g/l	Difco Bacto Agar

YNB and YNBA were supplemented with adenine hydrochloride, histidine, leucine, uracil and lysine hydrochloride at a final concentration of 10 g/l depending on strain genotype

Extremely Low Nitrogen (ELN Plates; for *S. pombe* crosses)

27.3 g/l	Formedium EMM Broth (w/o Nitrogen)
0.05 g/l	Ammonium Chloride
0.2 g/l	Adenine
0.1 g/l	Leucine
0.1 g/l	Uracil
0.1 g/l	Histidine
0.1 g/l	Arginine
25 g/l	Agar

2.1.2 Bacteria Media

Luria-Bertani (LB)

10 g/l	Tryptone
5 g/l	Yeast Extract
5 g/l	Sodium Chloride

Luria-Bertani Agar (LA/LB plates)

As LB plus:

12 g/l	Agar

2.1.3 Chemicals and Drugs used for Selection

The following drugs and chemicals were added to the appropriate media in order to select for the cells containing the appropriate genetic marker (table 2-1).

Table 2-1

Drug/Chemical	Media added to	Concentration	Supplier
5-Fluorootic acid (5FOA)	YEA	0.1% (w/v)	Melford, F5001
Geneticin disulphite (G4-18)	YEA	200 µ/ml	Melford, G0175
Nourseothricin sulphate (NAT)	YEA	100 µg/ml	Sigma, 74667
Kanamycin monosulphate	LA	50 µg/ml	Melford, K0126
Ampicilin sodium salt	LA	100 µg/ml	Sigma, A9518

Table 2-1. **List of drugs and chemicals used for selection of *S. pombe* and *E. coli* strains**

2.2 General Molecular Techniques

2.2.1 DNA Restriction Digests

Restriction digests were carried out using New England Biolabs (NEB) restriction enzymes according to the manufacturers recommended conditions.

Restriction digested plasmid DNA fragments were gel purified using agarose gel electrophoresis and a Nucleospin clean up kit (Macherey Nagel, 740609.10)

2.2.2 Plasmid DNA Ligations

Restricted insert DNA was incubated with 50 ng of restricted vector DNA at a ratio of 2:1 and ligated using the Rapid Ligation Kit (Fermentas, K1422) according to manufacturer's guidelines.

2.2.3 PCR for Molecular Cloning

To PCR amplify genomic DNA for cloning KOD DNA Polymerase was used, due to its high fidelity. The standard reaction set up was as follows; 5 µl of 10x KOD Buffer, 3 µl of 25 mM $MgSO_4$, 5 µl of 2 mM (each) dNTPs, 1.5 µl of 10 µM forward primer, 1.5 µl of 10 µM reverse primer, 100-200 ng of *S. pombe* genomic DNA, in a total volume of 50 µl. The $MgSO_4$ concentration was optimised for some reactions in the range of 1.5-2.5 mM. The standard cycling conditions for the PCR reaction were as follows; 1x 95˚C for

2 minutes, 29x 95˚C for 20 seconds, 55˚C for 10 seconds, 70˚C for 20seconds/kb. The annealing temperature was often adjusted between 50˚C and 58˚C depending on the primers used.

PCR products were then purified using a Nucleospin clean up kit (Macherey Nagel, 740609.10)

2.2.4 Fusion PCR

Fusion PCR can be used to join two overlapping PCR fragments together. It was performed using the same KOD polymerase reaction setup as above, except with equal molar ratio of the two PCR fragments that were to be fused. The cycling conditions were as follows: 1x 95˚C for 30 seconds, 8x 95˚C 10 seconds, 50˚C for 1 minute, 70˚C for 25 seconds/kb. Followed by 29x 95˚C for 10 seconds, 53˚C for 30 seconds, 70˚C for 25 seconds/kb and a final elongation step of 1x 70˚C for 10 minutes. The initial eight cycles at the lower annealing temperature helps promote the annealing of the two PCR fragments, which can then be amplified more specifically in the following 29 cycles. The annealing temperatures can be adjusted depending on the Tm of the primers and the overlap between the two fragments.

2.2.5 Site Directed Mutagenesis (SDM)

Site directed mutagenesis was used to insert point mutants into a gene of interest, which had been cloned into the pAW8 vector for insertion into the genome by Recombination Mediated Cassette Exchange (RMCE). Overlapping forward and reverse primers of 30-45 bp containing a point mutation, were designed and used in the SDM PCR reaction. The PCR reaction was as follows: 1 µl (50 ng) of plasmid DNA, 5 µl of 10x PFU Turbo Buffer, 5 µl of dNTPs at 2 mM each, 1 µl of PFU Turbo polymerase, 1 µl (125 ng) of forward primer, 1 µl (125 ng) of reverse primer , 36 µl of dH_2O. The standard cycling conditions for the SDM PCR were: 1x 94˚C for 3 minutes, 20x 94 for 30 seconds, 58˚C for 1 minute,68˚C for 16.5 minutes. Followed by a final elongation step of 1 x 68˚C for 7 minutes. The annealing temperature may have been altered depending on the Tm of the primers and the elongation time was adjusted in accordance with the size of the plasmid.

The template DNA was then digested using 1 µl of Dpn1 (NEB) for 1 hour at 37˚C. The reaction was then cleaned up using a Nucleospin clean up kit (Macherey Nagel, 740609.10). All of the reaction was transformed into high competency DH5α cells.

2.2.6 E. coli Transformation

Competent DH5α *E. coli* cells were thawed on ice. Plasmid DNA was mixed with the thawed cells and incubated on ice for 30 minutes. The DNA-cell mixture was heat shocked at 42˚C for 90 seconds and placed back on ice for 15 minutes. 1 ml of LB was added and in the case of plasmids containing the Ampicilin marker, cells were plated straight on to LB-ampicilin plates. For plasmids containing the Kanamycin marker the LB-cell mix was incubated for 60 minutes at 37˚C before being plated on to LB-Kanamycin plates. Plates were then incubated at 37˚C overnight.

2.2.7 Extraction of Plasmid DNA from *E. coli*

For miniprep: A single colony of *E. coli* cells was inoculated in 5 ml of LB containing Amplicilin at 100 µg/ml or Kanamycin at 50 µg/ml, and incubated over night at 37˚C. Cells were then pelleted at 4,600 rpm for 10 minutes at room temperature. The plasmid DNA was then extracted using a Qiagen Miniprep Kit (27104) according to the manufactures instructions. The Plasmid DNA was resuspended in 50 µl of dH_2O and the concentration measured on a Nanodrop ND-1000 spectrophotometer.

For midiprep: A single colony of *E. coli* cells was inoculated in 50 ml of LB containing Ampicilin or Kanamycin and incubated at 37˚C over night. Cells were pelleted at 4,600 rpm for 10 minutes at room temperature. The plasmid DNA was then extracted using a Qiagen Midiprep Kit (12145) according to the manufacturer's recommendations. The plasmid DNA was resuspended in 200 µl of dH_2O and the concentration measured on a Nanodrop ND-1000 spectrophotometer.

2.3 General *S. pombe* Techniques

2.3.1 Genetic Cross and Random Spore analysis

h+ and h- cells were mixed together in a small patch on an ELN plate using 5 µl of H_2O. The plate was incubated at 25˚C for 2 days and the crossing efficiency checked by

microscopy. A loop of the crossed cells was resuspended in 1 ml of H_2O and 2 µl of Helix Promatia Juice (Biosepra, 213472) was added. The spores were incubated on a rotating wheel over night at room temperature. The digestion efficiency was then checked by microscopy and the spores counted using a Haemocytometer. The spores were serial diluted to $1x10^4$ and 500-1000 spores plated onto YEA. The plates were incubated for 5 days at 30˚C

2.3.2 *S. pombe* Transformation

$1x10^8$ mid-logarithmically growing *S. pombe* cells (10 ml of $1x10^7$ cells/ml) were used for each transformation. Cells were pelleted and washed once in 5 ml dH_2O and once in 1 ml of LiAc-TE (0.1 M LiAc, 10 mM Tris-HCL, 1 mM EDTA, pH7.5). They were then resuspended in 100 µl LiAc-TE. 2 µl of single stranded carrier DNA (Salmon Sperm DNA, In*vitro*gen, VX15632011) and 1 µg (1-10 µl) of plasmid DNA or up to 10 µg of PCR product were added. This was incubated at room temperature for 10 minutes. 260 µl of 40% PEG-4000/LiAc-TE was added and the cell suspensions incubated for 30-60 minutes at 30˚C. 43 µl of Dimethyl sulfoxide (DMSO) was added and the cells heat shocked at 42˚C for 5 minutes. Cells were then washed in 1 ml of dH_20 and resuspended in 200 µl dH_2O. 100 µl of cell suspension was plated onto YNB with the appropriate amino acid supplements to select for the transformants. The plates were incubated at 30˚C for 4-5 days until colonies had formed.

2.3.4 Extraction of Genomic DNA from *S. pombe*

Cells were grown in 10 ml of YE over night at 30˚C, pelleted and resuspended in 1 ml of SP1 buffer (1.2M sorbitol, 50mM citric acid, 50 mM Na_2HPO_4, 40 mM EDTA, pH5,6) containing 1 mg/ml Lyticase (Sigma, L2524). Cells were incubated for 15-30 minutes at 37˚C. Digestion efficiency was checked by spheroblasting under the microscope (5 µl of cells was mixed with 5 µl of 10% SDS on a slide).Once 95% digestion had occurred the digested cells were spun at 3000 rpm for 5 minutes and resuspended in 450 µl of 5X TE (5 mM EDTA, 50 mM Tris-HCL pH 7.5). 50 µl of 10% SDS was added and the cells incubated at room temperature for 5 minutes. 150 µl of 5M potassium acetate (KAc) was added to the samples and incubated on ice for 10 minutes. The DNA was then separated from the rest of the cell debris by centrifugation

at 13000 rpm for 10 minutes. The supernatant was transferred to a new tube and one volume of isopropanol added to precipitate the DNA. This was spun at 15000 rpm for 10 minutes at 4˚C, and the supernatant was removed. The pellet was then washed with 500 µl of 70% ethanol and dried. If the genomic DNA was to be used for PCR it was resuspended in 200 µl dH_20 and 5 µl of 10 mg/ml RibonucleaseA (RNase).

If the genomic DNA was to be used for southern blot, further purification steps were performed. The pellet was resuspended in 250 µl of 5x TE, 5 µl of 10 mg/ml RNase and incubated at 37˚C for 20 minutes. 2 µl of 10% SDS and 10µl of 5 mg/ml Proteinase K (Sigma, P2308) were added, and the DNA incubated at 55˚C for 60 minutes. The DNA was then phenol chloroform extracted twice by adding 500 µl of Phenol:chloroform:isoamyl alcohol (25:24:1, Sigma, 77617), spinning at 13000 rpm for 5 minutes and the upper phase (containing the DNA) being transferred to a new tube. Following the second extraction the DNA was precipitated by adding 1/20 volume of 3M NaAc, 1 volume isopropanol and incubating on ice for 10 minutes. The samples were then spun at 13000 rpm for 15 minutes at 4˚C and washed in 500 µl of 70% ethanol. The DNA was resuspended in 30 µl of dH_2O.

2.3.5 *S. pombe* Colony PCR

Colony PCR was used to quickly check the genome type of strains after a cross where the allele of interest does not have a selective marker. For example, it was used to test for the presence of *chk1-HA* or the lox sites in strains made by RMCE. A full tip of freshly patched yeast cells was resuspended in 5 µl of dH_2O and heated at 95˚C for 5 minutes in a PCR machine (Biometra T3 Thermocycler). 20 µl of reaction mix was added, containing; 2.5 µl of 10x Buffer IV, 2.5 µl of 25mM $MgCl_2$, 2.5 µl of 2mM (each) dNTPs, 0.05 µl of 100 µM forward primer, 0.05 µl of 100 µM reverse primer, 0.125 µl of 5U/µl Taq DNA Polymerase (Thermo Fisher Scientific, AB-0192/B) and dH_2O up to a final volume of 20 µl per reaction. Cells were briefly spun in a minifuge and the following PCR reaction carried out; 29 cycles of 95˚C for 30 seconds, 50-55˚C for 30 seconds, 72˚C for 1 minute. The 12 µl of the PCR product was then directly run on an agarose gel.

2.4 Creation of *S. pombe* Strains

2.4.1 Recombination Mediated Cassette Exchange (RMCE)

To allow the rapid integration of mutant alleles in to the *S. pombe* genome a recombination mediated cassette exchange system was used (Watson et al., 2008). In this system a base strain is first constructed. For an essential gene, this involves placing a loxP site upstream of the gene of interest and the ura4+-loxM3 sequence downstream, thereby retaining the gene ORF and promoter. For a non-essential gene, the loxP-ura4-loxM3 cassette is integrated at the gene locus of interest replacing the gene promoter and ORF, resulting in a knockout strain.

Once the base strain has been constructed, the gene promoter and ORF are cloned into the Cre expression plasmid pAW8 and this sequence can then be mutated using site directed mutagenesis (see above). After transformation of the pAW8 plasmid containing the mutant gene into the relevant base strain, cells are grown in YE media. Cre expression promotes the specific recombination between the loxP and loxM sites in the plasmid, with the loxP and loxM sites in the genome. This leads to the insertion of the mutant gene into its endogenous locus. This event can be screened for by determining the loss of the ura4 marker, by plating the cells onto media containing 5-flororotic acid (5-FOA). 5-FOA specifically kills uracil prototrophic cells as it is converted to 5-fluorouracil, a substance toxic to cells, during uracil de novo synthesis. Therefore, only cells that have undergone cassette exchange and contain the mutant gene of interest grow, and this can be confirmed by sequencing.

2.4.2 Creation of *rad4* Mutant Strains by RMCE

The *rad4* base strain was previously constructed in the laboratory, as was the pAW8-rad4 plasmid (Table 2-6) (Watson et al., 2008). Therefore, these were used to construct all of the *rad4* mutants used in this study. For mutagenesis primers see the list of oligos (Table 2-7)

2.4.3 Creation of the *rad9* Base Stain and Mutants by RMCE

To create the *rad9* base strain, the loxP site was inserted 183 bp upstream of the *rad9* ATG and the loxM3 site was inserted 33bp downstream of Rad9. To do this, the loxP-ura4-loxM cassette was PCR amplified from the pAW1 vector using long primers, rad9-S1F and rad9-S1R (Table2-7), with homology to the rad9 up and down stream sequences (Watson et al., 2008). This fragment was then used to transform AMC 501, and its integration selected for on YNBA plates lacking uracil. Correct interegration was confirmed by sequencing. This base strain is based on a previous base strain created by Thomas Caspari (University of Bangor).

The *rad9* sequence was amplified using rad9-S6 and rad9-S5.1 and cloned into pAW8 as a *Spe1/Sph1* fragment. The *rad9* mutants were made using the primers listed in Table 2-7

2.4.4 Creation of the *crb2* Base Strain and Mutants by RMCE

To create the *crb2* base strain, the loxP site was inserted 296 bp up stream of the ATG and the loxM3 1 bp downstream of the stop site. The primers used to amplify the loxP-ura4-loxM sequence from pAW1 were Crb2 lox-ura-lox-primer-F and R. However, the integration of the fragment into AMC 501 did not work, therefore this fragment was further amplified to increase its homology to the genomic DNA using Crb2_increase_homology_F and R primers (Table 2-7). This increased the efficiency of the integration and transformants were now obtained from the YNBA plates lacking uracil. Correct integration was confirmed by sequencing.

The *crb2* sequence was amplified using Crb2-clone-F and R primers and cloned into pAW8 as an *Spe1/Sph1* fragment (Tables 2-6 and 2-7). The *crb2* gene sequence was then mutated by SDM using the primers indicated in Table 2-7

2.4.5 Creation of *mrc1*-T32A Mutant by Fusion PCR

As only one mutant of the *mrc1* gene was needed, a base strain was not required. Instead the *mrc1-T32A* strain was constructed using fusion PCR. Fusion PCR consists of 3 reactions; reaction A amplified the upstream *mrc1* sequence to the point

mutation using primers MRC1-408-upstream-F and MRC1-T32-Fusion-R, with the reverse primer incorporating the T to C base change. Reaction B amplified from the base change to the *mrc1* downstream sequence using primers MRC1-T32-Fusion-F and MRC1-345-downstream-R (Table-2-7). The forward primer overlaps with the reverse primer of reaction A and also incorporated the base change (A to G). The products of reactions A and B were gel extracted using a Nucleospin clean up kit (Macherey Nagel, 740609.10). They were then subjected to fusion PCR as described above and the product gel extracted. This fragment was transformed into a *mrc1Δ::ura4* strain (JMM1405) and the integration was selected for using 5-FOA plates.

2.5 S. pombe Genetic and Cell Biology Techniques

2.5.1 Growth Curves

Cells were grown in YE overnight to ~0.5x10^7 cells/ml. They were then grown for 8-9 hours in YE at the indicated temperature, whilst being kept in exponential phase by dilution. Cell density was calculated every hour using a spectrophotometer (Ultraspec 3000, Pharmacia Biotech) and adapted for the dilution factor.

2.5.2 Spot Tests

Mid-logrithmically growing cells were subjected to 10-fold serial dilutions from 1x10^7 cells/ml to 1x10^3 cells/ml in dH_2O. 5 µl of each of the 5 dilutions was then spotted onto YEA plates. The YEA plates either contained no genotoxic agents (control) or the indicated doses of Hydroxy Urea (HU) (Sigma, H8627), Methyl Methanesulfonate (MMS) (Sigma, 129925) or Camptothecin (CPT) (Acros Organics, 27672). For UV irradiation, the YEA plates with dried spots were subjected to the indicated dose of UV in a Stratalinker 2400 (Stratagene). For ionising radiation (IR) the cells were first exposed to the gamma source (^{137}Cs, Gamma Cell 1000) at 1x10^7 cells/ml, before being serial diluted. The plates were then incubated at 30˚C (unless otherwise stated) for 3-4 days.

2.5.3 Lactose Gradient Synchronisation

Exponentially growing cells were grown in YE to a total of 75 OD^{595} in 150 ml. Cells were pelleted at 3000 rpm for 2 minutes and re-suspended in 1ml of YE. The cells were placed on a lactose gradient consisting of 1 ml of 30%, 28%, 24%, 21%, 18.5%, 15%, 13%, 10%, 7% lactose. This was spun at 1000rpm for 8 minutes. The top fraction containing the G2 cells was removed, resuspended in YE and exposed to either the indicate dose of UV or IR. The cells were then grown at 30˚C whilst being rotated in a Eppendorf Thermomixer hot block.

2.5.4 cdc10-M17 Synchronisation and Irradiation

cdc10-M17 cells were grown at 25˚C (permissive temperature) to 0.25 OD^{595}/ml, then shifted to 36˚C (non-permissive temperature) for 3.5 hours. Cells were either irradiated with the indicated dose of gamma irradiation at 36˚C and released at 25˚C, or directly released to at 25˚C, and irradiated at the indicated time points after release

2.5.5 Elutriation

Cells were grown in YEP to early log phase, giving a total of $10x10^{10}$ cells. These cells were then subjected to elutriation in a Beckman J6-MC elutriator, sorting them by size. The G2 fraction was taken, pelleted, resuspended in YE at a concentration of 0.5 OD^{595}/ml and grown at 30˚C. Cells were subjected to the indicate doses of UV or IR at the indicated times points.

2.5.6 Septation Index/ Mitotic Index

30 µl of synchronous cells from the lactose gradient or elutriation were collected in 70 µl of ice cold absolute ethanol. The cells were pelleted for 1 minute at 3000 rpm. 5 µl of cells from the pellet were dropped onto a slide and allowed to dry. 5 µl of mounting media (50% glycerol, 50% PBS, 1 µg/ml DAPI, 50 µg/ml Calcoflour) was added and the cells visualised on a Leitz Dialux 20 microscope. The number of cells with and without septum, or past mitosis was counted. At least 100 cells were counted per time point.

2.5.7 FACS analysis

500 µl of mid logarithmically growing cells were collected into 1 ml ice cold absolute ethanol. The cells were washed in, and resuspended in, 500 µl of 50 mM tri-sodium citrate containing 50 µl of 10 mg/ml RibonucleaseA (RNase). The tubes were incubated at 37˚C for 2-3 hours. 10 µl of 500 µg/ml propidium iodide (PI) (Sigma) was added to 1 ml of 50 mM tri-sodium citrate (pH7) buffer per sample. 1 ml of the PI sodium citrate mix was added to each of the FACS tubes, and 200 µl of the RNase digested cells added. The cells were then sonicated for 10 seconds at 20 % power (Ultra sonic Processor sonicator). Samples were analysed on FacsCanto machine using the FL-A setting..

2.5.8 Live Cell Imaging of *rad52-GFP* Cells

rad52-GFP cells were grown to $1x10^7$ in YE and exposed to 40 Gy gamma irradiation. 5µl of culture was mounted onto a 2.5% agar patch [Microworks] at the indicated time points after IR. Images were taken on a Deltavsion Microscope and the percentage of cells containing GFP foci calculated.

2.5.9 Imaging of *rad11-GFP* Cells

rad11-GFP cells were grown to $1x10^7$ cells/ml in YE and exposed to 100 Gy gamma radiation. Cells were immediately fixed in ice cold methanol and mounted on to a slide. Images were taken on a Deltavsion Microscope and the number of GFP foci per nucleus calculated.

2.6 Biochemical Techniques

2.6.1 Whole Cell Protein Extracts - TCA extracts

5 OD_{595} of cells were collected and resuspended in 200 µl of 20% w/v trichloro acetic acid (TCA). Glass beads (Sigma) were added up to the level of the TCA. The cells were lysed in a cell disrupter (FastPrep, MP) for 8x 30 seconds at 6.5 m/s. The tube was then punctured using a hot needle and the sample transferred into a fresh Eppendorf tube by centrifugation at 4000 rpm for two minutes. The samples were then spun for 5 minutes at 13000 rpm and the supernatant removed. The extracts were resuspended

in 1X TCA sample buffer (see below) and boiled for 5 minutes. Extracts were spun for 1 minute at 13000 rpm before use.

1x TCA Sample Buffer:

1 volume	4x SDS sample buffer
1 volume	1 M Tris, pH 8
2 volume	dH_2O
2.5%	β-mercaptoethanol

4x SDS Sample Buffer

250 mM	Tris-base, pH6.8
20%	Glycerol
0.004 g/ml (w/v)	Bromphenol blue
0.08 g/ml (w/v)	SDS

2.6.2 SDS PAGE and Immunostaining of Proteins (Western Blot)

Whole cell protein extracts were separated by sodium dodecyl sulphate-polyacrylamide gel electrophoresis (SDS-PAGE). For assaying Chk1-HA phosphorylation an 8% resolving "Magic Gel" was used. For γH2A and Tubulin a 12% separating gel was used (Table 2-2). Gels were run in a BIORAD Mini-POTEAN TetraCell or a C.B.S Double or Triple-wide electrophorsis system in 1x SDS running buffer (0.025 M Tris Base, 0.25 M Glycine, 0.1% SDS) at 80 volts constant through the stacking gel (Table 2-3) and 100-120 volts through the separating gel. A Prestained Protein Marker (NEB, P7708) was run alongside the samples.

Table 2-2

Resolving gel	**8%**	**12%**
H_2O	4.6 ml	3.3 ml
Acrylamide:Bis (30% Acrylamide: 0,8% Bis, Protogel, National Diagnostics)	2.7 ml	4.0 ml
1 M Tris (pH 8.8)	2.5 ml	2.5 ml
10% SDS	0.1 ml	0.1 ml
10% Ammonium persulfate (APS)	0.1 ml	0.1 ml
Temed	0.006 ml	0.004 ml

Table 2-2, SDS-PAGE resolving gel recipe.
For "Magic Gel" mix the Protogel Arcylamide:Bis (30%:0.8%) was replaced with a mix of 19% Acrylamide:Bis (30%:0.8%, Protgel) and 81% Acrylamide (30%) no Bis (Acrylagel, National Diagostics)

Table 2-3

Stacking gel	
H_2O	3.4 ml
Acrylamide:Bis (30% Acrylamide: 0,8% Bis, Protogel, National Diagnostics)	0.83 ml
1 M Tris (pH 6.8)	0.63 ml
10% SDS	0.05 ml
10% Ammonium persulfate (APS)	0.05 ml
Temed	0.005 ml

Table 2-3, SDS-PAGE stacking gel recipe.
For "Magic Gel" mix the Protogel Arcylamide:Bis (30%:0.8%) was replaced with a mix of 19% Acrylamide:Bis (30%:0.8%, Protgel) and 81% Acrylamide (30%) no Bis (Acrylagel, National Diagostics)

Proteins were then transferred from the gel to a Nitrocelulose membrane (GE Healthcare, Nitrocelulose, Hybond, RPN3032D) via wet transfer for 2 hrs at room temperature at 300 mA constant, or overnight at 4˚C at 10 V constant, in 1x transfer buffer (20 mM Tris base, 750 mM Glycine, 20% (v/v) Methanol, 0.025 % (v /v) SDS). The membrane was stained with Ponceau-S solution (0.2% (w/v) Ponceau S, 3% (w/v) TCA) to confirm protein transfer and allow accurate cutting of the membrane. The

membrane was blocked with 3% milk PBST (Marvel dried skimmed milk in phosphate buffered saline (PBS), 0.1% Tween (Sigma P7949)) for 1 hr at room temperature. The primary antibody was added (Table 2-4) to 3% milk PBST and incubated with the membrane for 1 hr at room temperature or 4˚C over night whilst being gently shaken. The primary antibody was then washed off by 3x 10 minute washes in PBST. It was then incubated with the appropriate secondary antibody (Table 2-4) in 3% milk PBST for 1 hr at room temperature whilst being gently shaken. The secondary antibody was washed off via 3x 10 minute washes and 1x 20 minute wash in PBST. The bound antibody was then detected by chemiluminescence (ECL Plus Western Lightning, Perkinelmer, NEL104001EA) and exposed to GE Healthcare Hyperfilm ECL (GZ28906837). The film was developed with a Xograph Imaging Systems Compact X4. Alternatively, for quantification of the western blot, the ECL reaction was imaged on a Image Quant LAS 4000 (GE healthcare) and analysed using Image Quant TC software (GE Health Care)

Table 2-4

Antibody	**Type**	**Supplier**	**Dilution**
Anti-HA	Mouse monoclonal	Santa Cruz, F-7 sc-7392	1:2500
Anti-pS129 (γH2A)	Rabbit polyclonal	Abcam, ab17353	1:2500
Anti-Tubulin	Mouse monoclonal	Sigma, T5168	1:25000
Rabbit anti-Mouse HRP	Rabbit polyclonal	DakoCytomation, P0260	1:2500
Swine anti-Rabbit HRP	Rabbit polyclonal	DakoCytomation, P0217	1:2500

Table 2-4, Antibodies used in this study.

2.6.3 Cell lysates for GST pull down.

20 OD_{595} of mid-logarithmically growing *S. pombe* cell were grown over night and washed in Lysis buffer (see below). The cells were resuspended in 200 µl lysis buffer and lysed using glass beads and a cell disrupter (Fast Prep 24, MP) for 8x 30 seconds at 6,500 m/s. The cell extract was separated from the glass beads by puncturing the tube with a hot needle and spinning into a fresh Eppendorf tube at 4000 rpm for two minutes. The extracts were clarified by centrifugation at 14,000 rpm at 4°C for 10 minutes, and transferring the supernatant into a fresh tube. An additional 400µl of

lysis buffer was added to the cell extracts giving an approximate final protein concentration of 0.5 µg/µl

Lysis buffer

50mM	Tris-HCL, pH8.0
150mM	NaCl
5mM	EDTA
10%	Glycerol
0.1%	NP-40
1mM	Dithiothritol (DTT) (Sigma) (added just before use)
1mM	AEBSF (Sigma) (added just before use)
1mM	Pepstatin (Sigma) (added just before use)

1x complete EDTA Free protease inhibitor (Roche) per 50ml (added just before use)

1x Phostop (Roche) per 10ml (added just before use)

2.6.4 GST Pull Down of Rad4-Crb2

Experiment performed in collaboration with Tony Oliver (Pearl Lab)

Experiments were performed using either GST or GST-Rad4-BRCT3,4 as bait. Each purified protein was immobilised on Amintra Glutathione Resin (Expedeon) at a sufficient concentration to fully saturate all available binding sites, then washed with several applications of lysis buffer to remove any residual, unbound protein.

For the pull-down experiments, 100 µl of immobilised bait-resin was incubated with 300 µl of cell extract (prey) for a period of 2 hours, with rolling/agitation, at 4°C. The resin was then washed with successive applications of lysis buffer, to remove unbound material – typically 3 applications of 1 ml. SDS-PAGE loading buffer was then added to the resin, and samples analysed by western blot (see above) using an anti-HA antibody (Table 2-4).

2.7 LacO-LacI System Experiments

2.7.1 Overview

The LacO-LacI tethering system used in Chapter 3 allows localisation of proteins on the chromatin by using components of the bacterial lactose inducible transcription pathway. In bacteria, in the absence of lactose, the Lac repressor (LacI) protein is bound to a specific DNA sequence, known as the Lac operator (LacO), preventing the transcription of genes required for the metabolism of lactose. By inserting repeats of the LacO sequence in the genome and tagging proteins of interest with the LacI protein, it is possible to tether proteins to a specific genomic locus. This has previously been done for checkpoint proteins in mammalian cells and budding yeast cells (Bonilla et al., 2008, Soutoglou and Misteli, 2008). As described in Chapter 3 the LacO-LacI system was set up in *S. pombe* by Takashi Morishita and Su-Jiun Lin. 256 LacO repeats were inserted into the *ura4* locus and the main checkpoint proteins were cloned into pRep41 and tagged with LacI, GFP and a nuclear localisation signal (NLS) (GFP/LN). This allows expression of the construct upon removal of thiamine.

2.7.2 LiAc Transformation of Cryopreserved *S. pombe*

Due to the instability of the 256 LacO repeats in the genome, it was very important to ensure the cells were not growing for long periods of time, as this would increase the likelihood of losing some of the repeats. Therefore, the LacI plasmids were transformed into the LacO *S. pombe* strains using a rapid transformation protocol (Bicknell et al., 2011). In this protocol, *S. pombe* cells are first made competent and cryopreserved, allowing rapid transformation upon thawing. This was carried out by growing cells to $1x10^7$ at 30°C overnight. The culture was then placed on ice for 15 minutes and washed 3 times in ice-cold dH_2O by spinning at 1600xg for 5 minutes. The pellet was resuspended in ice-cold 30% glycerol, 0.1 M LiAc (pH 4.9) at $1x10^9$ cells/ml. 50 µl aliquots of the cell suspension were then placed into Eppendorf tubes and incubated on ice for 30 minutes, before being placed directly into the -80°C freezer. To transform the cryopreserved competent cells they were quickly thawed in a 37°C water bath for 2 minutes. The cells were mixed with 5 µl carrier DNA (10 mg/ml), 3 µl

of plasmid DNA (~500 µg/ml) and 145 µl of 50% PEG-4000. This was immediately heat shocked at 42°C for 15 minutes. The cells were gently spun down at 3000 rpm for 1 minute and resupended in 200 µl TE. A range of volumes (10 µl to 100 µl) of the cells were plated on to YNBA plates supplemented with the required amino acids and containing thiamine at a 15 µM concentration. Colonies were left to grow for 4 days at 30°C.

2.7.3 Expression of LacI Tagged Proteins

Following transformation of cryopreserved competent S. pombe, one large transformant colony was inoculated into 10 ml of YNB supplemented with the appropriate amino acids and containing thiamine at 15 µM (YNB+T). Cells were grown over night at 30°C. The cells were then diluted into 50 ml of YNB+T and grown to 0.5 OD^{595}/ml (1x10^7 cells/ml), a no expression control sample (T0) of 5 OD^{595} was taken for TCA extract and southern blot. The cultures were then washed 2x in dH_2O and resuspended in 50 ml YNB-no thiamine, at a concentration to give a cell density of 0.5 OD^{595}/ml by the following day. 5 OD^{595} of cells were taken at the in indicated time points after resuspension in YNB containing no thiamine. During this time cells were kept in exponential phase by dilution.

2.7.4 Southern Blot Analysis of LacO

Genomic DNA was extracted using a standard phenol-chloroform extraction process as described above. Concentration of DNA was measured using a Nanodrop and approximately 2 µg of DNA was digested using HindIII (NEB) in a final volume of 200 µl at 36°C. Digested DNA was isoproponol precipitated and resuspended in 20 µl of loading buffer (30% glycerol, 0.25% (w/v) bromophenol blue, 0.25% (w/v) Xylene cyanol FF). All 20 µl of sample was loaded onto a 1% TE agarose gel containing 0.2 µg/ml ethidium bromide and run at 30-80 volts for 24 hours. The run gel was washed for 10 minutes in depurination solution (0.25 M HCL), 45 minutes in Denaturing solution (1.5 M NaCl, 0.5 M NaOH) and 30 minutes in Neutralising solution (1 M Tis, pH 7.5, 1.5 M NaCl).The DNA was then blotted onto Gene Screen membrane [Perkin

Elmer] via capillary blotting in 10x SSC (300 mM sodium citrate, pH 7.0, 1 M sodium chloride) and UV cross linked [UV Stratalinker 2400 Stratagene].

LacO repeat DNA was radiolabelled and used to probe the southern blot. To do this 10 ng lacO gene sequence was boiled for 5 minutes and immediately placed on ice. It was then radio- labelled using a High Prime [Roche] priming kit with deoxycytine 5' triphosphate $\alpha^{32}P$ (dCTP$\alpha^{32}P$) according to manufactures guidelines.

The membrane was placed into a hybridisation tube along with Hybridisation buffer (6x SSC, 5x Denhardts (Ficoll 400, Polyvinylpyrrolidone , Bovine serum albumin) , 0.5% SDS) pre-heated to 65°C was added to a volume of approximately 0.17 ml/cm^2 of membrane. The tube was placed in a hybridisation oven (Jencons-PLS) pre-heated to 65°C for 15 minutes. 5-10 ng of labelled probe DNA per ml of buffer was added, and the membrane incubated in the hybridisation oven at 65°C overnight. The membrane was washed 3x 20 minutes at 65°C in 0.1% SDS 0.1x SSC, exposed to a phospho screen (Amersham) and visualised using a Storm 840 phospho imager (Molecular dynamics).

2.8 Strain, Plasmid and Oligonucleotide Lists

Table 2-5

Strain	Genotype
CPW6	*ade-704,ura4-D18, leu1-32, loxP-rad4-Y559R-loxM3*
CPW8	*ade-704,ura4-D18, leu1-32, loxP-rad4-Y559R-loxM3*
CPW9	*ade-704,ura4-D18, leu1-32, ura4::lacO:natMX6, chk1-HA, crb2-K617E*
CPW10	*ade-704,ura-D18, leu1-32, ura4::lacO:natMX6, chk1-HA, crb2-K617E*
CPW11	*ade-704,ura4-D18, leu1-32, ura4::lacO:natMX6, chk1-HA, crb2-K619E*
CPW12	*ade-704,ura4-D18, leu1-32, ura4::lacO:natMX6, chk1-HA, cb2-K619E*
CPW13	*ade-704,ura4-D18, leu1-32, ura4::lacO:natMX6, chk1-HA, rad9Δ::ura4*
CPW14	*ade-704,ura4-D18, leu1-32, ura4::lacO:natMX6, chk1-HA, rad9Δ::ura4*
CPW22	*ade-704,ura4-D18, leu1-32, chk1-HA, cdc10-m17*
CPW23	*ade-704,ura4-D18, leu1-32, chk1-HA, cdc10-m17*
CPW24	*ade-704,ura4-D18, leu1-32, loxP-rad4-Y559R-loxM3, chk1-HA, cdc10-m17*

CPW25	*ade-704,ura4-D18, leu1-32, loxP-rad4-Y559R-loxM3, chk1-HA, cdc10-m17*
CPW35	*ade-704,ura4-D18, leu1-32,brc1Δ::ura4, chk1-HA, ura4::lacO::natMX6*
CPW36	*ade-704,ura4-D18, leu1-32, brc1Δ::ura4, chk1-HA, ura4::lacO::natMX6*
CPW40	*ade-704, leu1-32, ura4-D18, his-D1, loxP-rad4wt-ura4-loxM3, rad52-GFP::kanMX6*
CPW44	*ade-704,ura4-D18, leu1-32, crb2 T215A, chk1-HA, ura4::lacO::natMX6*
CPW45	*ade-704,ura4-D18, leu1-32, crb2 T215A, chk1-HA, ura4::lacO::natMX6*
CPW53	*ura-D18, leu1-32, cpt1Δ::kanMX6*
CPW56	*ade-704, ura4-D18, leu1-32, ura4::lacO::natMX6, chk1-HA, rad1Δ::ura4*
CPW57	*ade-704, ura4-D18, leu1-32, ura4::lacO::natMX6, chk1-HA, rad1Δ::ura4*
CPW58	*ura-D18 ,leu1-32, cpt1Δ::kanMX6*
CPW70	*ade-704, leu1-32, ura4-D18, exo1Δ::ura4, loxP-rad4-Y599R-loxM3, chk1-HA*
CPW71	*ade-704, leu1-32, ura4-D18, exo1Δ::ura4, loxP-rad4-Y599R-loxM3, chk1-HA*
CPW72	*ade-704, leu1-32, ura4-D18, exo1Δ::ura4, chk1-HA*
CPW73	*ade-704, leu1-32, ura4-D18, exo1Δ::ura4, chk1-HA*
CPW74	*ade-704, leu1-32, ura4-D18, rad52-GFP::kanMX6, loxP-rad4-Y599R-loxM3, chk1-HA*
CPW76	*ade-704, leu1-32, ura4-D18, rad3Δ::ura4*
CPW88	*ade-704, leu1-32, ura4-D18, tel1Δ::kanMX6, chk1-HA, loxP-rad4-Y599R-loxM3, exo1Δ::ura4*
CPW107	*ade-704, leu1-32, ura4-D18, tel1Δ::kanMX6, chk1-HA, loxP-rad4-Y599R-loxM3, exo1Δ::ura4*
CPW108	*ade-704, leu1-32, ura4-D18, tel1Δ::kanMX6, chk1-HA, exo1Δ::ura4*
CPW117	*ade-704,ura4-D18, leu1-32, ura4::lacO::natMX6, chk1-HA, rad17-K118E*
CPW118	*ade-704,ura4-D18, leu1-32, ura4::lacO::natMX6, chk1-HA, rad17-K118E*
CPW121	*ade-704,ura4-D18, leu1-32, rhp18Δ::kanMX6, loxP-rad4-Y599R-loxM3*
CPW122	*ade-704,ura4-D18, leu1-32, rhp18Δ::kanMX6, loxP-rad4-Y599R-loxM3*
CPW134	*ade-704, leu1-32, ura4-D18, tel1Δ::ura4, chk1-HA*
CPW135	*ade-704, leu1-32, ura4-D18, tel1Δ::ura4, chk1-HA*
CPW143	*ade-704, leu1-32, ura4-D18, tel1Δ::kanMX6, exo1Δ::ura4, chk1-HA*
CPW169	*ade-704, leu1-32, ura4-D18, ctp1Δ::kanMX6, chk1-HA*
CPW170	*ade-704, leu1-32, ura4-D18, ctp1Δ::kanMX6, chk1-HA*
CPW171	*ade-704, leu1-32, ura4-D18, ctp1Δ::kanMX6, loxP-rad4-Y599R-loxM3, chk1-HA*
CPW172	*ade-704, leu1-32, ura4-D18, ctp1Δ::kanMX6, loxP-rad4-Y599R-loxM3, chk1-HA*
CPW173	*ade-704, leu1-32, ura4-D18, loxP-rad4Δ::ura4-loxM3* (RMCE base strain)
CPW176	*ade-704, leu1-32, ura4-D18, loxP-rad4wt-loxM3*
CPW177	*ade-704, leu1-32, ura4-D18, loxP-rad4wt-loxM3*
CPW182	*ade-704, leu1-32, ura4-D18, loxP-rad4-K56A-loxM3*
CPW183	*ade-704, leu1-32, ura4-D19, loxP-rad4-K56A-loxM3*
CPW184	*ade-704, leu1-32, ura4-D18, loxP-rad4-K56E-loxM3*
CPW185	*ade-704, leu1-32, ura4-D18, loxP-rad4-K56E-loxM3*
CPW186	*ade-704, leu1-32, ura4-D18, loxP-rad4-T15V-loxM3*
CPW187	*ade-704, leu1-32, ura4-D18, loxP-rad4-T15V-loxM3*
CPW188	*ade-704, leu1-32, ura4-D18, loxP-rad4-R22E-loxM3*
CPW189	*ade-704, leu1-32, ura4-D18, loxP-rad4-R22E-loxM3*
CPW190	*ura4-D18, leu1-32, crb2Δ::ura4, chk1-9myc2HA6His-ura4*
CPW191	*ura4-D18, leu1-32, crb2Δ::ura4 chk1-9myc2HA6His-ura4, leu1-32::2xYFP-crb2 (1-778)*

CPW192	*ura4-D18, leu1-32, crb2Δ::ura4, chk1-9myc2HA6His-ura4, leu1-32::2xYFP-crb2 (1-778) T187A*
CPW193	*ura4-D18, leu1-32, crb2Δ::ura4, chk1-9myc2HA6His-ura4, leu1-32::2xYFP-crb2 (1-778) T215A*
CPW194	*ura4-D18, leu1-32, crb2Δ::ura4, chk1-9myc2HA6His-ura4, leu1-32::2xYFP-crb2 (1-778) T235A*
CPW205	*ade-704, leu1-32, ura4-D18, loxP-rad4-T15V-loxM3, chk1-HA*
CPW206	*ade-704, leu1-32, ura4-D18, loxP-rad4-T15V-loxM3, chk1-HA*
CPW207	*ade-704, leu1-32, ura4-D18, loxP-rad4-R22E-loxM3, chk1-HA*
CPW208	*ade-704, leu1-32, ura4-D18, loxP-rad4-R22E-loxM3, chk1-HA*
CPW209	*ade-704, leu1-32, ura4-D18, loxP-rad4-K56A-loxM3, chk1-HA*
CPW210	*ade-704, leu1-32, ura4-D18, loxP-rad4-K56A-loxM3, chk1-HA*
CPW211	*ade-704, leu1-32, ura4-D18, loxP-rad4-K56E-loxM3,chk1-HA*
CPW212	*ade-704, leu1-32, ura4-D18, loxP-rad4-K56E-loxM3,chk1-HA*
CPW218	*ade-704, leu1-32, ura4-D18, loxP-rad4-ura4-loxM3, chk1-HA*
CPW219	*ade-704, leu1-32, ura4-D18, loxP-rad4-ura4-loxM33, chk1-HA*
CPW220	*ade-704, leu1-32, ura4-D18, loxP-rad4-T15V-K56E-loxM3*
CPW221	*ade-704, leu1-32, ura4-D18, loxP-rad4-T15V-K56E-loxM3*
CPW222	*ade-704, leu1-32, ura4-D18, loxP-rad4-T110V-loxM3*
CPW223	*ade-704, leu1-32, ura4-D18, loxP-rad4-T110V-loxM3*
CPW224	*ade-704, leu1-32, ura4-D18, loxP-rad4-R117E-loxM3*
CPW225	*ade-704, leu1-32, ura4-D18, loxP-rad4-R117E-loxM3*
CPW226	*ade-704, leu1-32, ura4-D18, loxP-rad4-K151A-loxM3*
CPW227	*ade-704, leu1-32, ura4-D18, loxP-rad4-K151A-loxM3*
CPW228	*ade-704, leu1-32, ura4-D18, loxP-rad4-K151E-loxM3*
CPW229	*ade-704, leu1-32, ura4-D18, loxP-rad4-K151E-loxM3*
CPW230	*ade-704, leu1-32, ura4-D18, loxP-rad4-T110V-loxM3, chk1-HA*
CPW231	*ade-704, leu1-32, ura4-D18, loxP-rad4-T110V-loxM3, chk1-HA*
CPW232	*ade-704, leu1-32, ura4-D18, loxP-rad4-R117E-loxM3, chk1-HA*
CPW233	*ade-704, leu1-32, ura4-D18, loxP-rad4-R117E-loxM3, chk1-HA*
CPW234	*ade-704, leu1-32, ura4-D18, loxP-rad4-K151A-loxM3, chk1-HA*
CPW235	*ade-704, leu1-32, ura4-D18, loxP-rad4-K151A-loxM3, chk1-HA*
CPW236	*ade-704, leu1-32, ura4-D18, loxP-rad4-K151E-loxM3, chk1-HA*
CPW237	*ade-704, leu1-32, ura4-D18, loxP-rad4-K151E-loxM3, chk1-HA*
CPW238	*ade-704, leu1-32, ura4-D18, loxP-rad9Δ::ura4-loxM3* (RMCE base strain)
CPW239	*ade-704, leu1-32, ura4-D18, loxP-rad9Δ::ura4-loxM3* (RMCE base strain)
CPW240	*ade-704, leu1-32, ura4-D18, loxP-rad9Δ::ura4-loxM3, chk1-HA*
CPW241	*ade-704, leu1-32, ura4-D18, loxP-rad9Δ::ura4-loxM3, chk1-HA*
CPW242	*ade-704, leu1-32, ura4-D18, loxP-rad9Δ::ura4-loxM3, chk1-HA loxP-rad4-Y599R-loxM3*
CPW243	*ade-704, leu1-32, ura4-D18, loxP-rad9Δ::ura4-loxM3, chk1-HA loxP-rad4-Y599R-loxM3*
CPW244	*ade-704, leu1-32, ura4-D18, loxP-rad9wt-loxM3*
CPW245	*ade-704, leu1-32, ura4-D18, loxP-rad9wt-loxM3*
CPW246	*ade-704, leu1-32, ura4-D18, loxP-rad9wt-loxM3, chk1-HA*
CPW247	*ade-704, leu1-32, ura4-D18, loxP-rad9wt-loxM3, chk1-HA*

CPW248	*ade-704, leu1-32, ura4-D18, loxP-rad9wt-loxM3, chk1-HA, loxP-rad4-Y599R-loxM3*
CPW249	*ade-704, leu1-32, ura4-D18, loxP-rad9wt-loxM3, chk1-HA, loxP-rad4-Y599R-loxM3*
CPW250	*ade-704, leu1-32, ura4-D18, loxP-rad9-Y271A-loxM3*
CPW251	*ade-704, leu1-32, ura4-D18, loxP-rad9-Y271A-loxM3*
CPW252	*ade-704, leu1-32, ura4-D18, loxP-rad9-Y271A-loxM3, chk1-HA*
CPW253	*ade-704, leu1-32, ura4-D18, loxP-rad9-Y271A-loxM3, chk1-HA*
CPW254	*ade-704, leu1-32, ura4-D18, loxP-rad9-Y271A-loxM3, chk1-HA, loxP-rad4-Y599R-loxM3*
CPW255	*ade-704, leu1-32, ura4-D18, loxP-rad9-Y271A-loxM3, chk1-HA, loxP-rad4-Y599R-loxM3*
CPW258	*ade-704, leu1-32, ura4-D18, loxP-rad9-W348A-loxM3, chk1-HA*
CPW259	*ade-704, leu1-32, ura4-D18, loxP-rad9-W348A-loxM3, chk1-HA*
CPW260	*ade-704, leu1-32, ura4-D18, loxP-rad9-W348A-loxM3, chk1-HA, loxP-rad4-Y599R-loxM3*
CPW261	*ade-704, leu1-32, ura4-D18, loxP-rad9-W348A-loxM3, chk1-HA, loxP-rad4-Y599R-loxM3*
CPW262	*ade-704, leu1-32, ura4-D18, loxP-rad9-Y271A W348A-loxM3*
CPW263	*ade-704, leu1-32, ura4-D18, loxP-rad9-Y271A W348A-loxM3*
CPW264	*ade-704, leu1-32, ura4-D18, loxP-rad9-Y271A W348A-loxM3, chk1-HA*
CPW265	*ade-704, leu1-32, ura4-D18, loxP-rad9-Y271A W348A-loxM3, chk1-HA*
CPW266	*ade-704, leu1-32, ura4-D18, loxP-rad9-Y271A W348A-loxM3, chk1-HA, loxP-rad4-Y599R-loxM3*
CPW267	*ade-704, leu1-32, ura4-D18, loxP-rad9-Y271A W348A-loxM3, chk1-HA, loxP-rad4-Y599R-loxM3*
CPW270	*ade-704, leu1-32, ura4-D18, loxP-rad9-W348A-loxM3*
CPW271	*ade-704, leu1-32, ura4-D18, loxP-rad9-W348A-loxM3*
CPW272	*ade-704, leu1-32, ura4-D18, loxP-rad9-Y271A W348A-loxM3, chk1-HA, cdc10-M17*
CPW273	*ade-704, leu1-32, ura4-D18, loxP-rad9-Y271A W348A-loxM3, chk1-HA, cdc10-M17*
CPW274	*ade-704, leu1-32, ura4-D18, loxP-rad9-Y271A W348A-loxM3, chk1-HA, loxP-rad4-Y599R-loxM3, cdc10-M17*
CPW275	*ade-704, leu1-32, ura4-D18, loxP-rad9-Y271A-W348A-loxM3, chk1-HA, loxP-rad4-Y599R-loxM3, cdc10-M17*
CPW276	*ade-704, leu1-32, ura4-D18, loxP-rad9-Y271A-W348A (2A)-loxM3, chk1Δ:kanMX6*
CPW277	*ade-704, leu1-32, ura4-D18, loxP-rad9-Y271A-W348A (2A)-loxM3, chk1Δ:kanMX6*
CPW280	*ade-704, leu1-32, ura4-D18, rad11-GFP::kanMX6*
CPW281	*ade-704, leu1-32, ura4-D18, rad11-GFP::kanMX6*
CPW282	*ade-704, leu1-32, ura4-D18, rad9Δ::kanMX6, ura4::lacO::natMX6, chk1-HA* (remade)
CPW283	*ade-704, leu1-32, ura4-D18, rad9Δ::kanMX6, ura4::lacO::natMX6, chk1-HA* (remade)
CPW284	*ade-704, leu1-32, ura4-D18, exo1Δ::ura4, rad11-GFP::kanMX6*
CPW285	*ade-704, leu1-32, ura4-D18, exo1Δ::ura4, rad11-GFP::kanMX6*
CPW288	*ade-704, leu1-32, ura4-D18, loxP-crb2Δ::ura4-loxM3* (RMCE base strain)
CPW289	*ade-704, leu1-32, ura4-D18, loxP-crb2Δ::ura4-loxM3* (RMCE base strain)
CPW291	*ade-704, leu1-32, ura4-D18, loxP-crb2wt-loxM3*
CPW292	*ade-704, leu1-32, ura4-D18, loxP-crb2wt-loxM3*
CPW293	*ade-704, leu1-32, ura4-D18, loxP-crb2-T187A-loxM3*
CPW294	*ade-704, leu1-32, ura4-D18, loxP-crb2-T187A-loxM3*

CPW295	*ade-704, leu1-32, ura4-D18, loxP-crb2-T215A-loxM3*
CPW296	*ade-704, leu1-32, ura4-D18, loxP-crb2-T215A-loxM3*
CPW297	*ade-704, leu1-32, ura4-D18, loxP-crb2-T235A-loxM3*
CPW298	*ade-704, leu1-32, ura4-D18, loxP-crb2-T235A-loxM3*
CPW299	*ade-704, leu1-32, ura4-D18, loxP-crb2-T215A-T235A-loxM3*
CPW300	*ade-704, leu1-32, ura4-D18, loxP-crb2-T215A-T235A-loxM3*
CPW301	*ade-704, leu1-32, ura4-D18, loxP-crb2-V188P-loxM3*
CPW302	*ade-704, leu1-32, ura4-D18, loxP-crb2-V188P-loxM3*
CPW303	*ade-704, leu1-32, ura4-D18, loxP-crb2-T215A-T235A-V188P-loxM3*
CPW304	*ade-704, leu1-32, ura4-D18, loxP-crb2-T215A-T235A-V188P-loxM3*
CPW305	*ade-704, leu1-32, ura4-D18, loxP-crb2-V184K-loxM3*
CPW306	*ade-704, leu1-32, ura4-D18, loxP-crb2-V184K-loxM3*
CPW307	*ade-704, leu1-32, ura4-D18, loxP-crb2-V212K-loxM3*
CPW308	*ade-704, leu1-32, ura4-D18, loxP-crb2-V212K-loxM3*
CPW309	*ade-704, leu1-32, ura4-D18, loxP-crb2-V232K-loxM3*
CPW310	*ade-704, leu1-32, ura4-D18, loxP-crb2-V232K-loxM3*
CPW311	*ade-704, leu1-32, ura4-D18, loxP-crb2-T187A-loxM3, chk1-HA*
CPW312	*ade-704, leu1-32, ura4-D18, loxP-crb2-T235A-loxM3, chk1-HA*
CPW313	*ade-704, leu1-32, ura4-D18, loxP-crb2-T215A-T235A-loxM3, chk1-HA*
CPW314	*ade-704, leu1-32, ura4-D18, loxP-crb2-V188P-loxM3, chk1-HA*
CPW315	*ade-704, leu1-32, ura4-D18, loxP-crb2-V188P-loxM3, chk1-HA*
CPW316	*ade-704, leu1-32, ura4-D18, loxP-crb2-V184K-loxM3, chk1-HA*
CPW317	*ade-704, leu1-32, ura4-D18, loxP-crb2-V184K-loxM3, chk1-HA*
CPW318	*ade-704, leu1-32, ura4-D18, loxP-crb2-V212K-loxM3, chk1-HA*
CPW319	*ade-704, leu1-32, ura4-D18, loxP-crb2-V232K-loxM3, chk1-HA*
CPW320	*ade-704, leu1-32, ura4-D18, loxP-crb2-V232K-loxM3, chk1-HA*
CPW321	*ade-704, leu1-32, ura4-D18, spbc713.09Δ::kanMX6, chk1-HA*
CPW322	*ade-704, leu1-32, ura4-D18, spbc713.09Δ::kanMX6, chk1-HA*
CPW323	*ade-704, leu1-32, ura4-D18, slx4Δ::kanMX6, chk1-HA*
CPW324	*ade-704, leu1-32, ura4-D18, slx4Δ::kanMX6, chk1-HA*
CPW325	*ade-?, leu1-32, ura4-D18, spbc713.09Δ::kanMX6, mrc1Δ::ura4*
CPW326	*ade-?, leu1-32, ura4-D18, spbc713.09Δ::kanMX6, mrc1Δ::ura4*
CPW327	*ade-?, leu1-32, ura4-D18, slx4Δ::kanMX6, mrc1Δ::ura4*
CPW328	*ade-?, leu1-32, ura4-D18, slx4Δ::kanMX6, mrc1Δ::ura4*
CPW329	*ade-?, leu1-32, ura4-D18, slx1Δ::kanMX6, mrc1Δ::ura4*
CPW330	*ade-?, leu1-32, ura4-D18, slx1Δ::kanMX6, mrc1Δ::ura4*
CPW331	*ade-704, leu1-32, ura4-D18, loxP-crb2-T215A-loxM3, chk1-HA*
CPW332	*ade-704, leu1-32, ura4-D18, loxP-crb2-T215A-loxM3, chk1-HA*
CPW333	*ade-704, leu1-32, ura4-D18, loxP-crb2-T215A-T235A-V188P-loxM3, chk1-HA*
CPW334	*ade-704, leu1-32, ura4-D18, loxP-crb2-T215A-T235A-V188P-loxM3, chk1-HA*
CPW335	*his2, leu-1, ura-D18, cdc13-HA::ura4*
CPW337	*ade-704, leu1-32, ura4-D18, loxP-crb2wt-loxM3, chk1-HA*
CPW338	*ade-704, leu1-32, ura4-D18, loxP-crb2wt-loxM3, chk1-HA*
CPW359	*ade-704, leu1-32, ura4-D18, loxP-crb2-V212K-V232K-loxM3*
CPW360	*ade-704, leu1-32, ura4-D18, loxP-crb2-V212K-V232K-loxM3*

CPW363	*ade-704, leu1-32, ura4-D18, loxP-crb2-V212K-V232K-loxM3, chk1-HA*
CPW364	*ade-704, leu1-32, ura4-D18, spbc713.09Δ::kanMX6, mrc1Δ::ura4, chk1-HA*
CPW365	*ade-704, leu1-32, ura4-D18, spbc713.09Δ::kanMX6, mrc1Δ::ura4, chk1-HA*
CPW366	*ade-704, leu1-32, ura4-D18, slx4Δ::kanMX6, mrc1Δ::ura4, chk1-HA*
CPW367	*ade-704, leu1-32, ura4-D18, slx4Δ::kanMX6, mrc1Δ::ura4, chk1-HA*
CPW369	*ade-704, leu1-32, ura4-D18, mrc1-T32*
CPW370	*ade-704, leu1-32, ura4-D18, mrc1-T32*
CPW371	*ade-704, leu1-32, ura4-D18, mrc1-T32*
AMC501	*ade-704, leu1-32, ura4-D18*
AMC502	*ade-704, leu1-32, ura4-D18*
SJ48	*ade-704, leu1-32, ura4-D18, chk1-HA*
SJ56	*ade-704, leu1-32, ura4-D18, chk1-HA*
SJ62	*loxP-rad4-Y599R-loxM3, chk1:HA, ade6-704, ura4D-18, leu1-32*
SJ63	*loxP-rad4-Y599R-loxM3, chk1:HA, ade6-704, ura4D-18, leu1-32*
SJ64	*loxP-rad4wt-ura4-loxM3, chk1:HA, ade6-704, leu1-32, ura4-D18*
SJ65	*loxP-rad4wt-ura4-loxM3, chk1:HA, ade6-704, leu1-32, ura4-D18*
SJ195	*ura4::lacO::natMX6, chk1-HA, ura4-D18, leu1-32, ade6-704*
SJ196	*ura4::lacO::natMX6, chk1-HA, ura4-D18, leu1-32, ade6-704*
SJ254	*loxP-rad4-Y599R-loxM3, chk1:HA, ura4::lacO::natMX6, ura4-D18, leu1-32*
SJ330	*rad17Δ::ura4, ura4::lacO::natMX6, chk1:HA, leu1-32*
SJ331	*rad17Δ::ura4, ura4::lacO::natMX6, chk1:HA, leu1-32*
SJ332	*crb2Δ::kanMX6, ura4::lacO::natMX6, chk1:HA, leu1-32, ura4-D18*
SJ333	*crb2Δ::kanMX6, ura4::lacO::natMX6, chk1:HA, leu1-32, ura4-D18*
EST2	*rad3Δ::kanMX6, ura4-D18, leu1-32, ade6-704*
KAF1175	*rhp18Δ::kanMX6, ura4-D18, leu1-32, ade6-704*
EST12	*chk1Δ::kanMX6, ura4-D18, leu1-32, ade6-704*
JMM1405	*mrc1Δ::ura4, ura4-D18, leu1-32, ade6-704*
IM279	*spbc713.09Δ, ura4-D18, leu1-32, ade6-704*
IM282	*slx4Δ::kanMX6, ura4-D18, leu1-32, ade6-704*
Bioneer	*slx1Δ::kanMX6, ade6-M210, ura4-D18, leu1-32*
Bioneer	*slx4Δ::kanMX6, ade6-M210, ura4-D18, leu1-32*
Bioneer	*spbc713.09Δ::kanMX6, ade6-M210, ura4-D18, leu1-32*

Table 2-5. List of strains used in this study. Strains from the following peoples collections were used in this study. CPW; Christoper Wardlaw. AMC; Antony Carr. SJ; Su-Jiun. KAF; Kanji Furuya. EST; Ellen Tsang. JMM; Jo Murray. IM; Izumi Miyabe. Bioneer; Bioneer knockout Library. ade? Refers to the strain either being ade-704 or ade-M210

Table 2-6

Plasmid Number	Gene	Description	Additional Information
pCPW 1	*rad9*	pAW8+*rad9*	Cloned using *Spe1/ Sph1* sites
pCPW 2	*rad4*	pAW8+*rad4-K56E*	Mutated pSJ25
pCPW 3	*rad4*	pAW8+*rad4-K56A*	Mutated pSJ25
pCPW 4	*rad4*	pAW8+*rad4-T15V*	Mutated pSJ25
pCPW 5	*rad4*	pAW8+*rad4-R22E*	Mutated pSJ25
pCPW 6	*rad9*	pAW8+*rad9-Y271A*	Mutated pCPW1
pCPW 7	*rad9*	pAW8+*rad9-W348A*	Mutated pCPW1
pCPW 8	*rad9*	pAW8+ *rad9-Y271A,W348A*	Mutated pCPW1
pCPW 9	*rad4*	pAW8+*rad4-T15V, K56E*	Mutated pSJ25
pCPW 10	*rad4*	pAW8+*rad4-T110V*	Mutated pSJ25
pCPW 11	*rad4*	pAW8+*rad4-R117E*	Mutated pSJ25
pCPW 12	*rad4*	pAW8+*rad4-K151A*	Mutated pSJ25
pCPW 13	*rad4*	pAW8+*rad4-K151E*	Mutated pSJ25
pCPW 14	*crb2*	pAW8+*crb2*	Cloned using Spe1 Sph1 sites
pCPW 15	*crb2*	pAW8+*crb2-T187A*	Mutated pCPW14
pCPW 16	*crb2*	pAW8+*crb2-T215A*	Mutated pCPW14
pCPW 17	*crb2*	pAW8+*crb2-T235A*	Mutated pCPW14
pCPW 18	*crb2*	pAW8+*crb2-T215A-T235A*	Mutated pCPW14
pCPW 23	*crb2*	pAW8+*crb2-V188P*	Mutated pCPW14
pCPW 24	*crb2*	pAW8+*crb2-T215A-T235A-V188P*	Mutated pCPW14
pAW1	N/A	For *rad9* and *crb2* base strain construction	
pAW8	N/A	Cre expression plasmid containing lox sites	
pRep41	N/A	*nmt41* thiamine repressible promoter plasmid	*leu+*
pRep42	N/A	*nmt41* thiamine repressible promoter plasmid	*ura+*
pSJ25	*rad4*	pAW8+*rad4*	Cloned using *Sac1 Spe1* sites
pSJ52	*rad3*	pRep41+*rad3-GFP/LN*	
pSJ58	*rad4*	pRep42+*rad4-GFP/LN*	
pSJ59	*rad9*	pRep42+*rad9-GFP/LN*	

Table 2.6, List of plasmids used in this study. Including information on how they were constructed (right hand columns). pCPW are from my plasmid collection, pAW plasmids from Adam Watson, pSJ from Su-Jiun Lin and pRep from the main Carr laboratory collection.

Table 2-7

Number	gene	Name	Use	Sequence
1	*crb2*	*crb2* F-650	loxP check	CAACCATAGTACTAACGAGGC
2	*crb2*	*crb2* R+128	loxP check	ATCATTACTCCTAGGAGGGG
3	*crb2*	*crb2* F+1635	loxM3 check	CATGAGGATGCCTATGACCG
4	*crb2*	*Crb2*+2950	loxM3 check	GAAACCTGCTACGCAAGCC
7	*chk1*	*chk1*-F	*chk1-HA* check	AATCCATGTGAAAGAACGTTGTCAG
8	*chk1*	*chk1*-R	*chk1-HA* check	GGGAATAGGATTATTAACGCTTTGT
14	*rad9*	*rad9*-loxP-reverse	loxP check	TCAACAGGACGGAATCCGGC
15	*rad9*	*rad9*-loxP-Forward	loxP check	TGCCGGATCCCCGGGATTAA
18	*rad9*	*rad9*-loxM-reverse	loxM check	GATGAGGGGAATTCGAGCTCGTTTAAAC
19	*rad9*	*rad9*-loxM-forward	loxM check	GCAACAACTCATTGACTGCTGTAGC
26	*rad9*	*rad9*-S6	cloning *rad9* (Caspari)	CTCGTCCAACTAGTGTAACGTATCGTATGATGAGGG
27	*rad9*	*rad9*-S5.1	cloning *rad9* (Caspari)	CGATAGTGGCATGCTAGGCATGCTAGAAAACACCACATTATAGATTTACC
28	*rad4*	*rad4*-upstream- 2	loxP check	TCCATTTGTCAATCTTCGCAC
29	*rad4*	*rad4*-lox-reverse-2	loxP check	TGATCTATAGGCAGCACCAAG
34	*rad9*	Y271A-F	Mutagenesis	GCTCGATTTGTGCAGCTTACGGTGTCCCAG
35	*rad9*	Y271A-R	Mutagenesis	CTGGGACACCGTAAGCTGCACAAATCGAGC
36	*rad9*	W348A-F	Mutagenesis	TGGATCTATTGGAGCGCAAACTGATCAAAGT
37	*rad9*	W348A-R	Mutagenesis	ACTTTGATCAGTTTGCGCTCCAATAGATCCA
38	*rad9*	W348-F-2	Mutagenesis	CTGGATCTATTGGAGCGCAAACTGATCAAAGT
39	*rad9*	W348-R-2	Mutagenesis	ACTTTGATCAGTTTGCGCTCCAATAGATCCAG
55	*rad4*	K56A-F	BRCT1 mutagenesis	GATACTCCAGCATACAAGGTATGTCGTAAAATCTTACA
56	*rad4*	K56A-R	BRCT1 mutagenesis	TACCTTGTATGCTGGAGTATCAAAATCGCCGGCTATAAG
57	*rad4*	K56E-R	BRCT1 mutagenesis	ATACCTTGTATTCTGGAGTATCAAAATCGCCGGCTATAAG
58	*rad4*	K56E-F	BRCT1 mutagenesis	TGATACTCCAGAATACAAGGTATGTCGTAAAATCTTACA
61	*rad4*	T15V-full-overlap-F	BRCT1 mutagenesis	CTTCGTGATATGTTGTGTCAGTATCGATTTAAAGCAA
62	*rad4*	T15V-full-overlap-R	BRCT1 mutagenesis	TTGCTTTAAATCGATACTGACACAACATATCACGAAG
63	*rad4*	R22E-Fulloverlap-F	BRCT1 mutagenesis	ATCGATTTAAAGCAAAGAGTAAGATTTTTGCACGAC
64	*rad4*	R22E-full-overlap-R	BRCT1 mutagenesis	GTCGTGCAAAAATCTTACTCTTTGCTTTAAATCGAT
65	*rad4*	T110V-F	BRCT2 mutagenesis	GTTTGTCTTGTCAACATTGGCCAACCAGAGAGATCT
66	*rad4*	T110V-R	BRCT2 mutagenesis	AGATCTCTCTGGTTGGCCAATGTTGACAAGACAAAC
67	*rad4*	R117E-F	BRCT2 mutagenesis	CAACATTGGCCAACCAGAGGAATCTCGTATTGAAAATTAT
68	*rad4*	R117E-R	BRCT2 mutagenesis	ATAATTTTCAATACGAGATTCCTCTGGTTGGCCAATGTTG

69	*rad4*	K151A-F	BRCT2 mutagenesis	CACCTCATCGGGTCGCGCATATGAATATGCATTA
70	*rad4*	K151A-R	BRCT2 mutagenesis	TAATGCATATTCATATGCGCGACCCGATGAGGTG
71	*rad4*	K151E-F	BRCT2 mutagenesis	CACCTCATCGGGTCGCGAATATGAATATGCATTA
72	*rad4*	K151E-R	BRCT2 mutagenesis	TAATGCATATTCATATTCGCGACCCGATGAGGTG
73	*rad9*	*rad9-S1-F*	Base strain construction (Caspari)	CGATTGATGTTGGCCATTACACTTTCGTACAAATTTCGGCGCGCGTGTCTATACTAATATAAGTGCGTTAAAGCAGGTGCCGGATCCCCGGGTTAATTAA
74	*rad9*	*rad9-S1-R*	Base strain construction (Caspari)	GAATTTAATTAATTGGGTTACATTATTCACTATCTTATTGATTTATTAGAACTACTATGTAACGTATCGTATGATGAGGGGAATTCGAGCTCGTTTAAAC
83	*crb2*	*crb2*-T187A-F	Mutagenesis	AAACCGTTGGAGAAGTCCTTGTACCTGAAGCCGTAGCT
84	*crb2*	*crb2*-T187A-R	Mutagenesis	ATCGTAAAACTTTGTCCTATGTTGAGCTACGGCTTCAGGT
85	*crb2*	*crb2*-T215A-F	Mutagenesis	AAATGAGACAGAAAGCGGTCAAGTAGAGACTGCACCTACT
86	*crb2*	*crb2*-T215A-R	Mutagenesis	TAGAGAAGTCGCCAGTCGAGTAGGTGTAGTCTCT
87	*crb2*	*crb2*-T235A-F	Mutagenesis	TTCTTTATGGTCGAGTAGAGTCCGCTCCTCCTG
88	*crb2*	*crb2*-T235A-R	Mutagenesis	TTCGGATGTCTCTGGTAAAAAAGCAGGAGGAGCGGACTC
91	*crb2*	*crb2*-clone-F	clone *crb2* into pAW8	AAAAGCATGCTGTAGTTTGTACATCAGGTCA
92	*crb2*	*crb2*-Clone-R	clone *crb2* into pAW8	AAAAACTAGTACTAAGTAGAAATATCAGACTGACTAATAAGACATTCG
95	*crb2*	*crb2*-V188P-F	Mutagenesis	ACCGTTGGAGAAGTCCTTGTACCTGAAACCCCAGCTCA
96	*crb2*	*crb2*-V188P-R	Mutagenesis	TGTAATCGTAAAACTTTGTCCTATGTTGAGCTGGGGTTTCAG
97	*crb2*	*crb2*-lox-Ura-loxF	Make base strain	TTTAAAATTACTTCTTCAACATTACTGATTCTAACAACATAAATCTCCTATCG AACGTATTAATAAAAGTGGAAACATGCCGGATCCCCGGGTTAATTAA
98	*crb2*	*crb2*-lox-Ura-loxR	Make base strain	CTAAAATTAATAAAAAGCTAAATTAATGAGGTGAAACTCAGGGGGAGTTAGTAAAAATAACTATATCAAAAAACCAAAGAATTCGAGCTCGTTTAAAC
108	*crb2*	*crb2*-homology-F	Increase homology of fragment made by 97 and 98	ATTAAACAAGCAAAATCTATTTTCTATGATTGTTTCAAAAAGTCAAGATGAAAAGTTCAAAACTCAAATTTAAAATTACTTCTTCAACATTACTGATTCT
109	*crb2*	*crb2*-homolgy-R	Increase homology of fragment made by 97 and 98	TTTTTGTTTAATATTGAAATTGACACTTTTCGTCAGTATTGCAAATAAATTAATAAACAACAAATATCTAAAATTAATAAAAAGCTAAATTAATGAGAGT
114	*mrc1*	*mrc1*-T32-Fus-F	Create T32A mutation by fusion PCR	TGATCAAGAGGATATTTTAGATGCGCCTCGCACTAGGGTGAGGA
115	*mrc1*	*mrc1-T32-Fus-R*	Create T32A mutation by fusion PCR	TCCTCACCCTAGTGCGAGGCGCATCTAAAATATCCTCTTGATCA

116	*mrc1*	Mrc1-408-up-F	Create T32A mutation by fusion PCR	CAAATTGCTGTATGCTGCTCGA
117	*mrc1*	*mrc1-345-down-R*	Create T32A mutation by fusion PCR	TAACTTTACAGAGCGATATTGATGATAG

Table 2-7. List of Oligonucleotides used in this study. (Caspari refers to oligos obtained from Thomas Caspari's Laboratory)

Chapter 3
The Role of the Rad4 AAD in the *S. pombe* DNA Damage Checkpoint

3.1 Introduction

As described in the "1.6.4 TopBP1 dependent ATR activation" section TopBP1 (the Rad4 homolog) in higher eukaryotes has been shown able to directly activate ATRs kinase activity and is required for checkpoint activation. However, the pathway in which this TopBP1 AAD operates is not fully understood (Kumagai et al., 2006, Delacroix et al., 2007, Mordes et al., 2008a). In budding yeast, at the time this study was initiated, the C-terminus of $Dpb11^{TopBP1}$ had been shown to be involved in the activation of the DNA damage checkpoint, but no AAD had been identified (Mordes et al., 2008b, Navadgi-Patil and Burgers, 2008). It was later seen that Dpb11 did indeed contain an AAD domain. However, this had a relatively minor role in checkpoint ($Mec1^{ATR}$) activation and acts in a semi-redundant pathway with the $Ddc1^{Rad9}$ AAD, after damage in G2 phase of the cell cycle (Navadgi-Patil and Burgers, 2009, Navadgi-Patil et al., 2011, Pfander and Diffley, 2011).

To further understand the role the TopBP1 AAD plays in the activation of the DNA damage checkpoint, and to fully characterise the pathways in which they operate, a comprehensive study to identify and characterise the *S. pombe* $Rad4^{TopBP1}$ AAD and its role in checkpoint activation was initiated. The preliminary experiments in this study were carried out by a previous PhD student and a post doctorate researcher in the Carr laboratory: Su-Jiun Lin and Valerie Garcia, respectively. Initially the data obtained by Su-Jiun Lin is summarised, before going on to describe the findings within this project.

3.2 Summary of Previous Data from the Carr Laboratory

It was previously shown, by Furuya et al. (2004), that the interaction between $Rad4^{TopBP1}$ and $Rad3^{ATR}$ increases after HU-induced replication fork stalling or DNA damage and that this interaction was most likely required for the formation of an active checkpoint complex (Furuya et al., 2004). However, no obvious AAD domain had been identified and the nature of this interaction was not known. A sequence alignment of the Xenopus and human TopBP1 AAD with the yeast homologs, supplied by Charly Chahwan (Carr lab), identified a weakly conserved region within the unstructured C-terminus of Rad4. This aligned with the core of the TopBP1 AAD. The key tryptophan, W1138 in xTopBP1 and W1145 in hTopbp1 AAD, was conserved in all tested yeast homologs as another aromatic residue tyrosine (Figure 3-1A, B). This suggested that this domain within Rad4 could be a putative AAD and that Y599 maybe the corresponding residue to xW1138 and hW1145. It is therefore most likely the key amino acid for any Rad3 activating activity Rad4 may possess.

To test this hypothesis, first it was demonstrated, by GST pull down assays, that the C-terminal region of Rad4 containing the AAD could pull down Rad3 from whole cell extracts and that this was dependent on the Rad4 AAD, and more specifically, Y599. This suggested that the putative Rad4 AAD can bind directly to Rad3. Su-Jiun Lin therefore went on to make *rad4-Y599R* and *rad4-AAD* (deletion of the AAD domain) mutants at the *rad4* endogenous locus using the Recombination Mediated Cassette Exchange method (Materials and Methods; (Watson et al., 2008). The *rad4* mutants showed no growth defects, implying the mutations did not affect Rad4's role in the initiation of DNA replication. However, they did show sensitivity to DNA damaging agents, as seen by spot test analysis. Both the *rad4* mutants showed the same sensitivities to UV, 4NQO (a UV mimetic), HU and MMS (a DNA alkylating agent). This is consistent with the Rad4 AAD having some role in within the checkpoint. Interestingly the Rad4 AAD mutants did not display any significant sensitivity to IR.

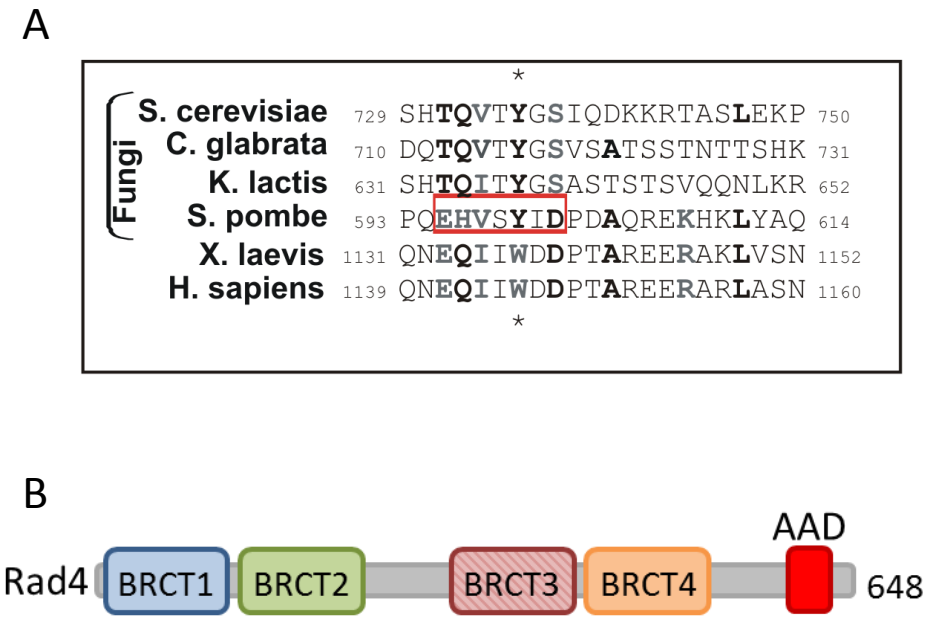

Figure 3-1. Conservation of the TopBP1 AAD in yeasts
A. Alignment of the higher eukaryote TopBP1 AAD with the fungal homologs. The crucial tryptophan is replaced with a tyrosine in all the fungal homologs (marked with an *) B. Cartoon representation of the Rad4 protein showing the position of the potential AAD in the unstructured extreme C-terminus, distinct from the BRCT domains.

rad4-Y599R showed a mild reduction in cell cycle delay after UV radiation in lactose gradient synchronised cells, assessed by septation index and compared to wild type (*rad4+*), suggesting a checkpoint defect. This was further confirmed by a reduction in Cds1 kinase activity and a reduction in Chk1 phosphorylation after UV. Contrary to the checkpoint defect seen after UV damage, no checkpoint defect was seen after IR damage either by septation index or Chk1 phosphorylation. This suggested that the Rad4 AAD was required in S-phase as UV, MMS and 4NQO cause most of their checkpoint activating effect during S-phase. Conversely, IR mainly causes DSB's, as asynchronous *S. pombe* cells are mostly G2 IR elicits most of its damage and response to that damage during G2 phase. To test this theory further, Su-Jiun Lin synchronised cells in G2 using a *cdc25-22* temperature sensitive mutant, released them into a synchronous cell cycle and then treated cells with IR when they reached S-phase. Preliminary results showed the *rad4-Y599R* cells now exhibited a reduction in survival and a mild reduction in Chk1 and H2A phosphorylation after IR. Taken together, this data suggested that the putative Rad4 AAD has a role in Rad3 activation during S-phase.

The aim of the work in this chapter is to confirm the results previously shown by Su-Jiun Lin and to further understand the mechanism, pathway and cell cycle phase in which the Rad4 AAD acts.

3.3 The Rad4 AAD Domain is Most Important for Checkpoint Activation in S-phase.

To confirm that the Rad4 AAD is required after S-phase damage a spot test in *rad4+* (WT) and *rad4-Y599R* cells were subjected to IR and UV was performed (Figure 3-2A). Consistent with the previous data, the *rad4-Y599R* cells showed sensitivity to 100 J/m^2 of UV, but did not show any sensitivity to 50 Gy ionising radiation. To confirm that *rad4-Y599R* is sensitive to S-phase damage, a spot test in the presence of cisplatin, (a DNA cross linking agent known to cause DNA damage that is mainly repaired during replication) was performed (Figure 3-2B).

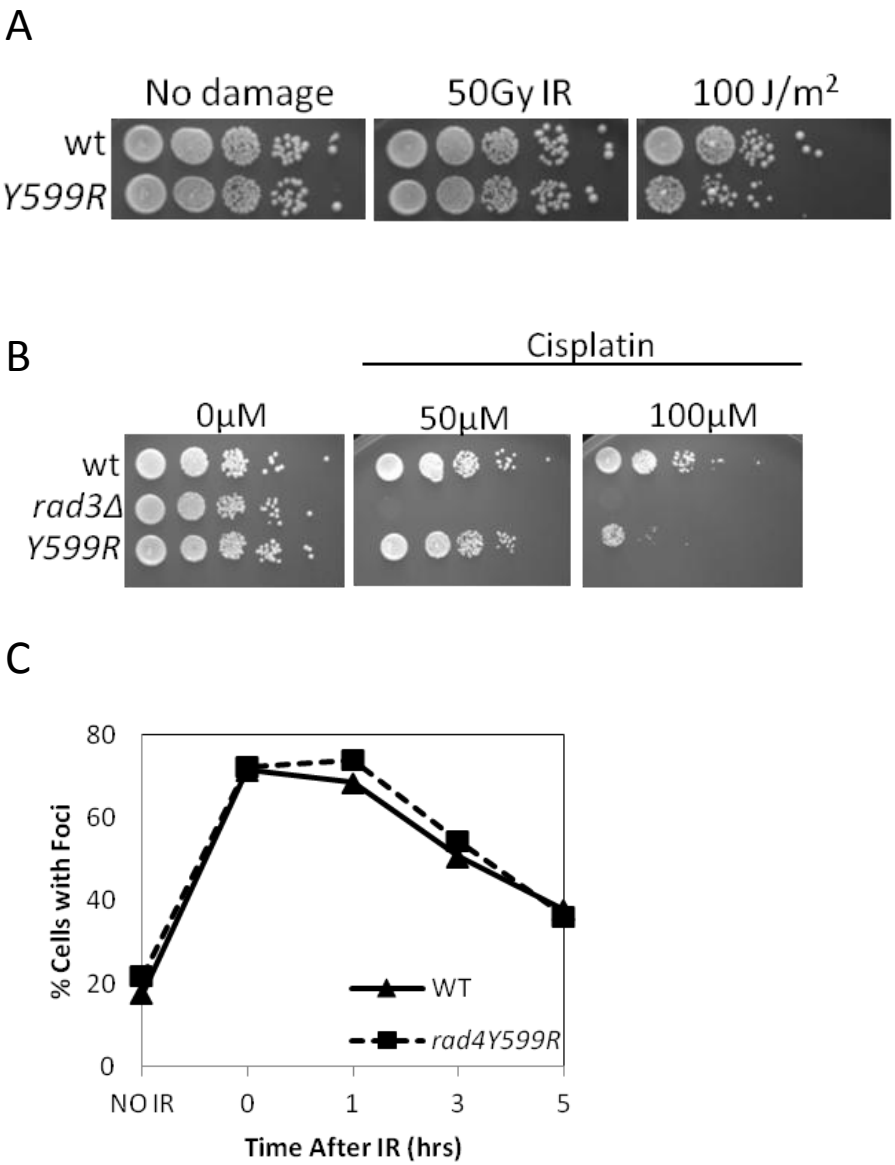

Figure 3-2 *rad4-Y599R* is sensitive to S-phase damage and has no repair defect

A. Spot test analysis of *rad4+* (wt) and *rad4-Y599R* (*Y599R*) cultures exposed to UV or IR damage. 10-fold serial dilutions of $1x10^7$ cells/ml were either exposed to 50 Gy IR and spotted onto YEA plates, or spotted onto YEA plates and exposed to 100 $J/m^{2\ UV}$. The plates were incubated at 30˚C for 3 days. B. spot test analysis of *rad4+* (wt), *rad3Δ* and *rad4-Y599R* (*Y599R*). 10-fold serial dilutions of $1x10^7$ cells/ml were spotted onto YEA plates, containing the indicated concentrations of cisplatin and incubated at 30˚C for 3 days. C. Average of two experiments in which Rad52-GFP foci were visualised before and after 40 Gy IR in *rad4+* (WT) and *rad4-Y599R* cells growing exponentially in YE

The *rad4-Y599R* cells showed sensitivity to 100µM cisplatin, but this sensitivity was not as severe as a *rad3Δ* control, which was completely dead at 50µM. Again this result is consistent with the Rad4 AAD domain most likely acting in Rad3 activation after S-phase damage, but not being essential for Rad3 activation. As described in Chapter 1, Rad4 has been linked to having a role in DNA repair, specifically homologous recombination (Ogiwara et al., 2006, Germann et al., 2011, Hicks et al., 2011). To ensure the *rad4-Y599R* mutant does not have a defect in HR, wild type and *rad4-Y599R* cells harbouring GFP tagged Rad22 (a protein required for the strand invasion step of HR) were subjected to 40 Gy IR. The repair kinetics were followed by % cells with GFP foci at time intervals after damage. It can be seen from Figure 3-2C that the *rad4-Y599R* strain showed almost identical repair kinetics to wild type cells. It is therefore concluded that the Rad4 AAD domain is not important for DNA repair after ionising radiation.

When undertaking cell synchronisation experiments it is important to ensure the results obtained are not an artefact of the synchronisation process. Therefore, to verify that the *rad4*-AAD mutants are indeed partially defective in Rad3 activation in S-phase, cell cycle experiments using alternative synchronisation methods to *cdc25-22* arrest, were carried out. Cdc10 is commonly known as the *S. pombe* START gene and is part of the MBF transcription factor complex. This is required for the transcription of a number of genes required for cells to enter S-phase and undergo DNA replication (Aves et al., 1985, Simanis and Nurse, 1989). A *cdc10-M17* temperature sensitive mutant causes cells to block at the G1-S boundary at the non-permissive temperature 36˚C, therefore allowing cells to be synchronously released into S-phase when shifted back to the permissive temperature of 25˚C (Jeong et al., 2001). *rad4+* and *rad4-Y599R* were therefore crossed to a *cdc10-M17* strain in order to allow G1-S synchronisation and assessment of Rad3 activation after damage in S-phase.

rad4+ cdc10-M17 and *rad4-Y599R cdc10-M17* cells were synchronised at 36˚C for 3.5 hours, exposed to 80 Gy IR and released into S-phase. Chk1-HA phosphorylation was then assayed via western blot, as a measure of Rad3 activation. Importantly, both the *rad4+* and Rad4 mutant cells arrested and released into S-phase with identical kinetics according to FACS analysis (Figure 3-3A).

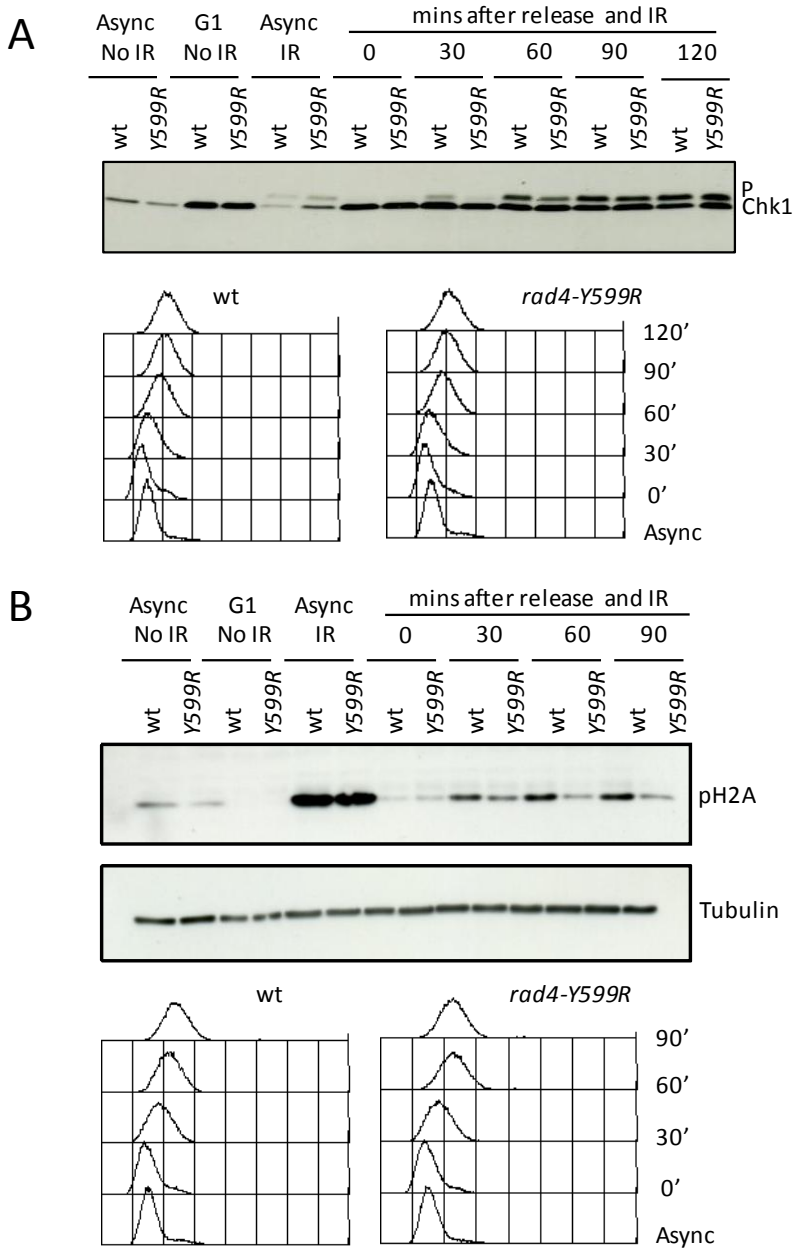

Figure 3-3 *rad4-Y599R* shows a defect in Chk1-HA and H2A phosphorylation after IR in S-phase

A. *rad4+ (wt)* and *rad4-Y599R (Y599R)* cells were synchronised at G1/S using a *cdc10-M17* arrest of 3.5 hours at 36˚C. Cells were irradiated with 80Gy IR and immediately released into S-phase at 25˚C. Top panel; Chk1-HA phosphorylation was monitored by SDS PAGE using α-HA antibody. Bottom panel; DNA content of the cells in the top panel was monitored by FACs analysis, cells progress from 1C to2C DNA content. B. As A, but cells were irradiated with 200Gy and H2A phosphorylation was monitored by SDS PAGE using α-pS129 (Top panel), α-Tubulin was used as a loading control (Middle panel). Bottom panel shows the DNA content of the cells in the experiments shown in the top and middle panels. Cells progress from a 1C to 2C DNA content.

This can be seen by the majority of cells displaying a 1C peak at T0. A 1C peak occurs due to the *cdc10-M17* mutation preventing DNA replication but not cell cycle progression per se, thus uncoupling DNA replication from septation. In this instance septation occurs without DNA replication, giving a 1C DNA content. When cells are released, DNA replication occurs and the FACs profile shifts to the right, giving a 2C peak upon completion of replication (Figure 3-3). The asynchronous cells, although containing a 2C DNA content are not as far right as the synchronised 2C cells due to drift. Drift occurs as the synchronisation process leads to cell elongation (growth) and therefore an increase in mitochondria and its DNA. This DNA is indistinguishable from genomic DNA, thus shifting the Facs peak to the right (Figure 3-3). A reduction in Chk1 phosphorylation can be seen in the *rad4-Y599R* strain at the 30, 60 and possibly 90 minute time points after IR and release, compared to *rad4+*. However, by the 120 minute time point when most cells are in G2 phase, as seen by FACS analysis, the defect in Chk1-HA phosphorylation can no longer be seen in the *rad4-Y599R*. As a control, no apparent reduction in Chk1-HA phosphorylation can be seen in the *rad4* mutant after IR in asynchronous cells. This supports the notion that the Rad4 AAD is most important in S-phase (Figure 3-3A). To confirm this result, a similar experiment was carried out, however in this instance cells were exposed to 200Gy IR and Rad3 kinase activity was assessed by phosphorylation of histone H2A. Consistent with the Chk1-HA phosphorylation data in Figure 3-3A, a defect in H2A phosphorylation can be seen in the *rad4-Y599R* mutant at the 30, 60 and 90 minute time points after IR and release. Again no defect in H2A phosphorylation can be seen after IR in asynchronous cells (Figure 3-3B).

To assess whether this reduction in Chk1-HA phosphorylation after S-phase damage in *cdc10-M17* synchronised cells also leads to a reduction in cell viability, a survival assay was performed. *rad4+* and *rad4-Y599R* cells were once again synchronised at the G1-S boundary (as seen by FACS), the cultures were then split and shifted to permissive temperature and exposed to 50 Gy at 0 minutes after release (early S-phase as seen by FACS), 40 minutes after release (mid S-phase) or 100 minutes after release (late S/G2 phase). Cells were plated onto YEA plates and incubated at 25˚C for 3 days. The relative survival of *rad4-Y599R* compared to *rad4+* was then calculated. A reduction in

relative cell survival of ~25% can be seen in the *rad4-Y599R* cells after IR at T0, this is further increased to a ~50% reduction in survival after IR at T40. However, only a very minor reduction in survival can be seen after IR at T100, when the majority of cells are now in G2 phase (Figure 3-4A). This data is consistent with the previous data from the Carr laboratory which employed cdc25-*22* synchronisation and confirms the role of the Rad4 AAD domain in the S-phase damage checkpoint.

To further ensure there is no role for the Rad4 AAD domain in the G2 checkpoint an elutriation experiment was under taken to synchronise cells in G2. Elutriation is the gold standard in the synchronisation of *S. pombe* cells, as it synchronises cells based on size, rather than requiring a gene mutation and temperature shift. G2 cells in *S. pombe* are a smaller particle than S-phase cells, which remain as two sister cells in S-phase joined together. Therefore, a fraction of a population containing only small cells can be extracted from the elutriator giving a G2 synchronised population. Elutriation synchronised *rad4+* and *rad4-Y599R* cells were followed by septation index for one cell cycle until they reached the following G2 (the point at which the septation index reaches its lowest point). This allows cells to recover from any stress they experienced during the elutriation process (Figure 3-5 A B). Cells were then exposed to either UV or IR damage and samples were taken for western blot. From Figure 3-5C it can be seen that the *rad4-Y599R* strain shows little or no defect in Chk1-HA or H2A phosphorylation after 100Gy or 250Gy IR in G2 (Figure 3-5C). Confirming, beyond doubt, that the Rad4 AAD domain is not required for Rad3 activation in G2 phase.

It can also be seen from Figure 3-5C that both 50 and 100 J/m^2 of UV causes no checkpoint activation in either WT or *rad4-Y599R* (Figure 3-5C). Thus confirming that UV damage causes most of its checkpoint activation in S-phase, validating the results in Figures 3-2A and previous work from the laboratory which shows *rad4-Y599R* is sensitive to UV but not IR damage. It must be noted from Figure 3-5B that the *rad4-Y599R* cells took 140 minutes to reach the next G2 phase whereas WT took 120 minutes. Taking into account the previous data from Su-Jiun Lin and the data in Figures 3-2AB, 3-3AB and Figure3-4A this is almost certainly due to a slight difference in the fraction of cells taken off of the elutriator and not due to a cell cycle progression defect (Figure 3-5B).

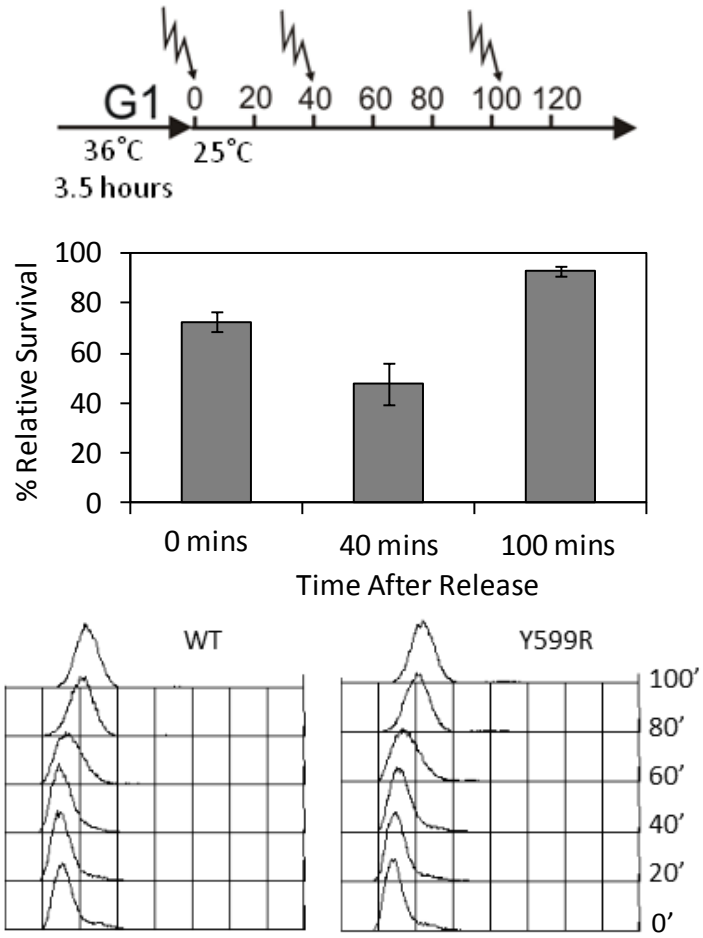

Figure 3-4. *rad4-Y599R* cells show reduced survival after IR in S-phase
cdc10-M17 rad4+ (WT) and *cdc10-M17 rad4-Y599R* cells were synchronised at the G1/S boundary and exposed to 50 Gy IR either 0 minutes (G1/S), 40 minute (S-phase) or 100 minutes (G2) after release. Top panel; schematic of the experimental procedure. Arrows represent timing of IR. Middle panel; Relative % survival of *rad4-Y599R* cells, calculated by % survival of *cdc10-M17 rad4+* (WT) divided by % survival of *cdc10-M17 rad4-Y599R.* % survival was measure by colony formation. Error bars: standard deviation (n=3). Bottom Panel FACs profile of cells used for the survival assay in the middle panel (minutes after release). Cells progress from a 1C to 2C DNA content

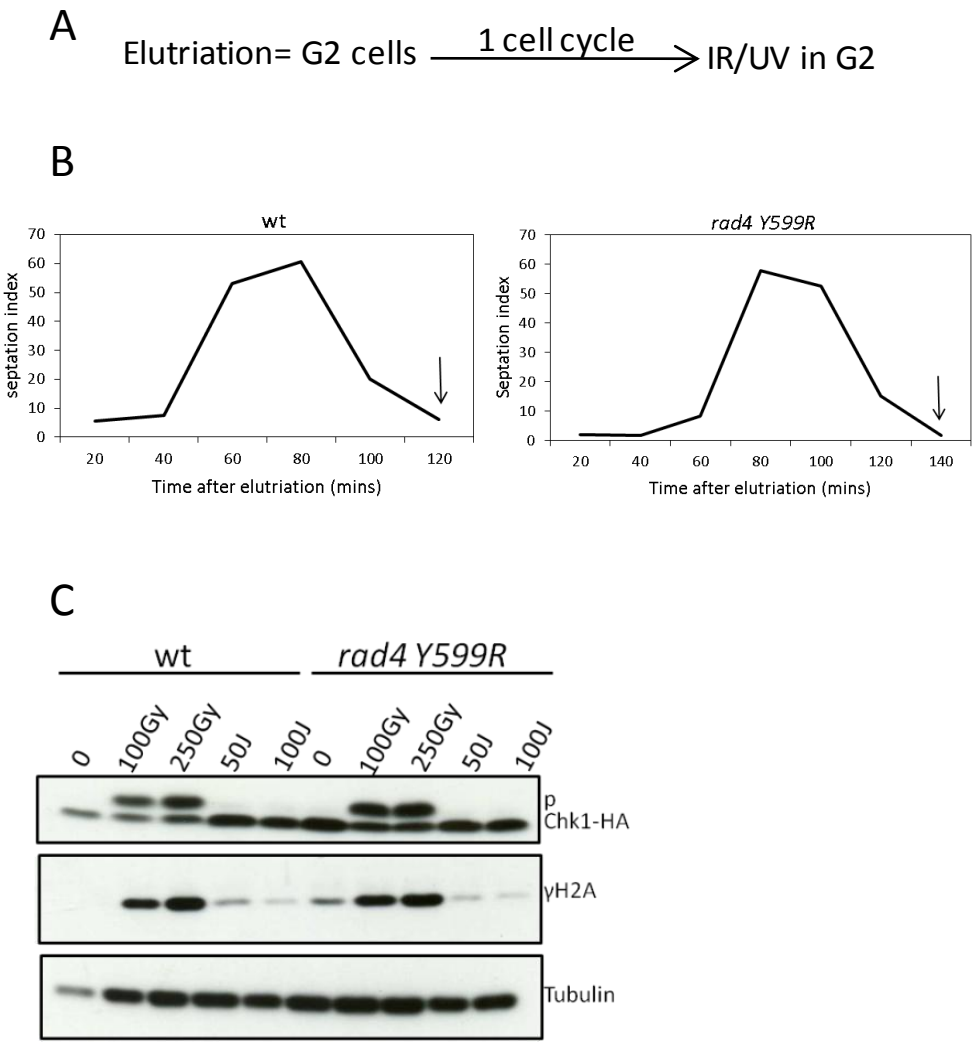

Figure 3-5. *rad4-Y599R* cells show no defect in Rad3 activation after damage in G2 phase

A. Diagram depicting experimental set up. Cells were synchronised in G2 using elutriation and allowed to recover for one cell cycle before being exposed to IR or UV damage in G2. B. Septation index, used to follow cell cycle progression of *rad4+* (wt) and *rad4-Y599R* cells. Arrow indicates when septation index was at its lowest (G2) and cells were exposed to DNA damaging agent. C.SDS PAGE of Chk1 and H2A phosphorylation (α-HA and α-pS129) after IR/UV damage in elutriated G2 *rad4+* (WT) and *rad4-Y599R* (*Y599R*) cells from B. α Tubulin was used as a loading control.

3.4 The Rad4 AAD is Most Important When ssDNA is Limited

Having established that the Rad4 AAD is most important for Rad3 activation in S-phase, the question of "why S-phase" needed to be addressed. To answer this question the differences between the activation of the checkpoint and the metabolism of the damaged DNA between S-phase and G2 were considered. One obvious difference between the checkpoints in S and G2 phases is the presence of the replication checkpoint in S-phase. Although previous data from the Carr laboratory showed *rad4-Y599R* had a twofold reduction in Cds1 kinase activity compared to WT, a reduction in Chk1 phosphorylation after damage in S-phase is also seen. This, therefore, points to a difference in the way in which the damage checkpoint is activated, between the two cell cycle phases. One difference between S-phase and G2 is the lower levels of ssDNA formed after damage in S-phase compared to G2. This lower level of ssDNA in S-phase after damage may be due to a number of reasons. These reasons are explored in the context of the Rad4-AAD.

The first possible reason is that damage, such as that from UV, can be bypassed by the replication fork, leaving small ssDNA lesions behind the fork, these are later repaired by a process known as post replication repair (Daigaku et al., 2010). It may be these small types of S-phase lesions that require the Rad4 AAD for the efficient activation of Rad3. To test this theory, an *rhp18Δ*^{Rad18} mutant was crossed with the *rad4-Y599R* mutant. Rhp18 is an E3 ubiquitin ligase which ubiquitylates PCNA, the replicative sliding clamp, in order to recruit the factors required for post replication repair of the lesion (Verkade et al., 2001). By deleting Rhp18 these small ssDNA lesions should persist for longer, increasing the need for checkpoint activity and therefore the Rad4 AAD. If this is the case *rhp18Δ* should show increased sensitivity to UV in a *rad4-Y599R* background. To this end the *rad4+ rhp18Δ*, *rad4-Y599R* single mutant and the *rhp18Δ rad4-Y599R* double mutant were spot tested and exposed to UV. It can be seen from Figure 3-6 that the *rhp18Δ* is very sensitive to UV, showing sensitivity at doses as low as 10 J/m^2.

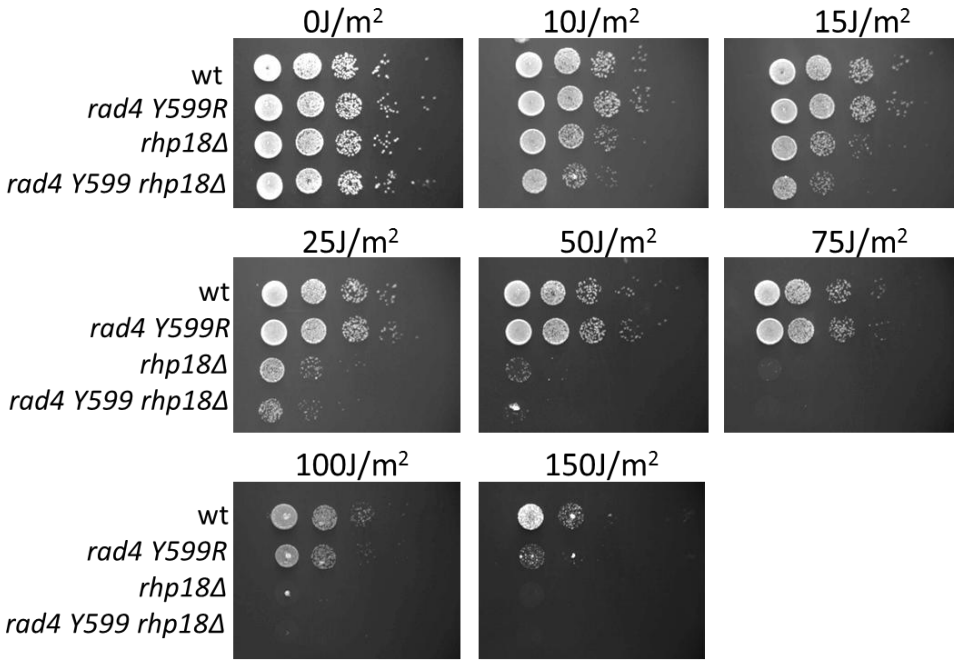

Figure 3-6. *rad4-Y599R* mildly increases the UV sensitivity of *rhp18Δ*
Spot test analysis of *WT, rad4-Y599R, rhp18Δ and rad4-Y599R rhp18Δ* after increasing dosage of UV. Cells were spotted as 10-fold serial dilutions of $1x10^7$ cells/ml on YEA plates, UV irradiated or not and grown for 4 days at 30˚C.

The *rad4-Y599R* mutant shows modest sensitivity to UV damage at 100 J/m^2 consistent with Figure 3-2A. The double *rhp18Δ rad4-Y599R* does exhibit a greater increase in sensitivity than either of the single mutants. This can be seen at 10, 15 and 25 J/m^2 (Figure 3-6).

Whilst consistent with our hypothesis this data can still be interpreted in many ways. The increase in sensitivity was relatively moderate. This may not be consistent with the primary role of the Rad4 AAD in activating Rad3 after formation of these post replication repair lesions. An alternative explanation is, that by stabilising these small lesions in an *rhp18Δ* we may actually be increasing the levels of ssDNA. In an *rhp18Δ* more of the lesions persist for longer, which would reduce the requirement for the Rad4 AAD, if the hypothesis that Rad4 AAD is required when ssDNA is low is correct. From the experiment shown in Figure 3-6, it is impossible to distinguish between these two possibilities, therefore a different approach was undertaken.

After IR damage in G2 phase the DNA is processed by nucleases leading to the formation of large stretches of RPA coated ssDNA. This processing is dependent on the activity of CDC2-CDC13 (CDK-Cyclin), which is higher in G2 phase than S-phase (see "1.5.2 The Formation of ssDNA" and "1.2.2 Regulation Cell Cycle Progression" sections). Therefore, processing of DNA breaks in S-phase is reduced compared to G2 (Limbo et al., 2007, Huertas et al., 2008, Huertas and Jackson, 2009). This is consistent with the results in Figures 3-3, 3-4, 3-5 which show the *rad4-Y599R* being important for Rad3 activity after IR in S-phase but not G2, even though the type of damage caused is presumably similar. One way to address this experimentally would be to reduce DNA processing after damage in G2, therefore reducing the levels of ssDNA and subsequently increasing the importance of the Rad4 AAD for Rad3 activity in G2. In essence, this is essentially making a G2 cell similar to a S-phase cell with respect to DSB processing.

As described in the "1.5.2 The Formation of ssDNA section" one of the first nucleases required for the initial resection of DSBs is Ctp1^{CTiP}, whose activity and transcription is regulated by Cdc2-Cdc13 activity (Limbo et al., 2007, Huertas et al., 2008, Huertas and Jackson, 2009, Mimitou and Symington, 2009). This made Ctp1 an obvious candidate

for deletion in order to reduce ssDNA formation after damage in G2, therefore mimicking an S-phase like damage processing state. If the Rad4 AAD is required in S-phase due to the reduced levels of ssDNA after damage, we should see a reduction in Chk1 phosphorylation in the *rad4-Y599R ctp1Δ* after damage in G2. To test this, asynchronous cultures of rad4+, *rad4-Y599R*, *ctp1Δ* and *rad4-Y599R ctp1Δ* were exposed to 80 Gy IR and samples were taken either 0 minutes or 60 minutes after damage for western blot (Figure 3-7A). Unfortunately no significant reduction in Chk1-HA phosphorylation can be seen in the *rad4-Y599R ctp1Δ* double compared to the single *ctp1Δ* at either time points. This, however, may be due to the dose of IR not being high enough to cause a significant level of damage for a difference in Chk1 phosphorylation to be obvious.

The experiment was therefore repeated with 200 Gy IR (Figure 3-7B). At low exposure, a reduction in Chk1-HA phosphorylation can now be observed in the double *rad4-Y599R ctp1Δ* when compared with the single mutants, at both the 0 minute and 60 minute time points (although it is more obvious at 60 minutes, due to inconsistent loading at the 0 minute time point). Unexpectedly, Chk1-HA phosphorylation can also be seen in *ctp1Δ* and *rad4-Y599R ctp1Δ* without the presence of induced DNA damage, suggesting that *ctp1Δ* cells already form endogenous DNA damage (Figure 3-7A 3-7B high exposure). The presence of endogenous damage that leads to checkpoint activation may lead to changes in the cell cycle which, in turn, may mean that asynchronous *ctp1Δ* cells do not have the same cell cycle profile as WT, thus undermining the experiment. To test for this, FACS analysis was carried out on asynchronous cultures of each of the strains used in Figure 3-7. Indeed, it can be seen in both *ctp1Δ* and *ctp1Δ rad4-Y599R* cultures that the DNA content differs from that of rad4+ and *rad4-Y599R*; these cells seem to be accumulating in S-phase (Figure 3-8A).

To further investigate the differences, growth curves were performed on each of the strains. Exponentially growing cells were diluted to 02. OD_{595}/ml and grown for 8 hours. These cultures were being diluted before reaching stationary phase to keep them growing exponentially. The cell density was measured every hour and adjusted for the dilution factor (Figure 3-8B).

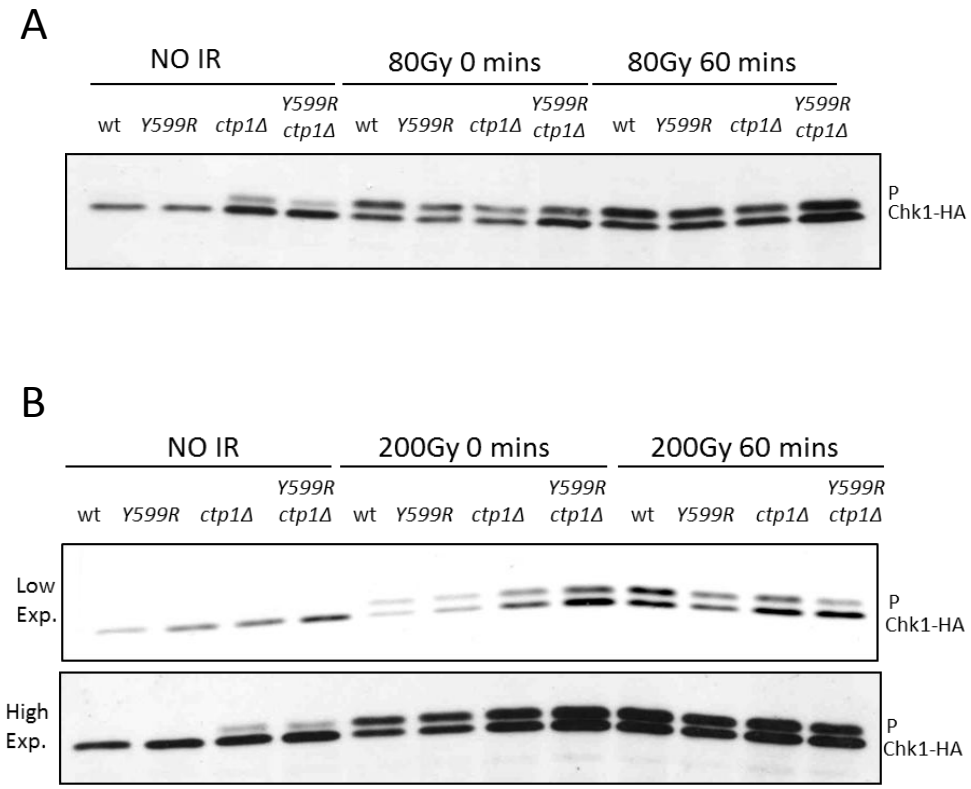

Figure 3-7. Analysis of Chk1 phosphorylation after IR in *rad4-Y599R ctp1Δ cells*

Asynchronously growing *rad4+* (*WT), rad4-Y599R (Y599R), ctp1Δ, rad4-Y599R ctp1Δ* (Y599R ctp1Δ) cells were exposed to 80 Gy IR or not and Chk1-HA phosphorylation was assayed by SDS PAGE using α-HA either 0 minutes or 60 minutes after irradiation. B. As in A except cells were exposed to 200Gy, low exposure (Top panel) and high exposures (Bottom panel) of the same blot are shown.

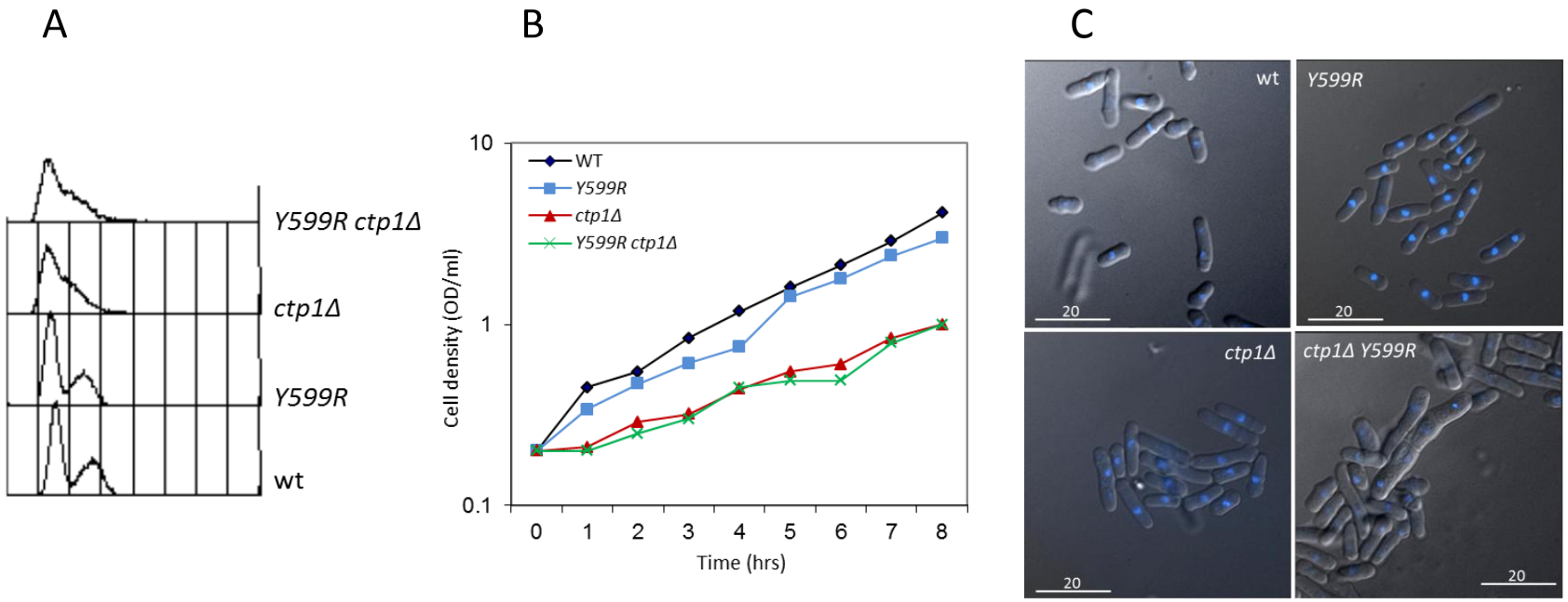

Figure 3-8. *ctp1Δ* and *rad4-Y599R ctp1Δ* cells have cell cycle delay in the absence of damage
A. Facs analysis showing DNA content of asynchronously growing rad4+(*WT), rad4-Y599R, ctp1Δ and rad4-Y599R ctp1Δ* cells B. Growth curve of the same strains used in A. Exponentially growing cells were diluted to 0.2 OD_{595}/ml and grown for 8hrs being diluted down before reaching stationary phase. Cell density was measured using OD_{595}/ml adjusting for the dilution factor every hour. C. Fluorescence microscope images of fixed DAPI stained cells used in B.

Consistent with the FACS and Chk1-HA phosphorylation data, the *ctp1Δ* and *rad4-Y599R ctp1Δ* grew more slowly than the WT or *rad4 Y599R* alone. To see if this was due to activation of the checkpoint, DAPI stained cells were imaged (Figure 3-8C). In *S. pombe,* activation of the DNA damage checkpoint leads to cell elongation as the cells continue to grow without undergoing mitosis (Russell and Nurse, 1986, Furnari et al., 1997). Indeed, *ctp1Δ* cells are slightly elongated compared to WT or *rad4-Y599R* cells, suggesting some checkpoint activation (Figure 3-8C). Taken together the results in Figures 3-8 A, B and C suggest the decrease in Chk1-HA phosphorylation after 200 Gy in the *ctp1Δ rad4-Y599R* could be an artefact (figure 3-7B).

As an alternative approach to testing the theory that the Rad4 AAD is most important in S-phase, due to the lower levels of ssDNA after damage, a similar experiment to that in Figure 3-7 was carried out in a *exo1Δ* rather than *ctp1Δ* background (Figure 3-9B). Exo1, as described in the "1.5.2 The Formation of ssDNA" section, is responsible for creating the large stretches of ssDNA after the initial resection has been carried out by MRN and Ctp1 (Mimitou and Symington, 2008). Exo1 first requires this initial resection by Ctp1 before it can act upon a DSB. Therefore, its activity is also regulated by the cell cycle control of Ctp1 (Symington and Gautier, 2011). In *exo1Δ* cells a small amount of resection can still occur but this extends for only approximately 50-100bp, if samples are taken immediately after damage. Over time, Dna2 can compensate for the lack of Exo1 and resect the DSB, giving large stretches of ssDNA (Huertas, 2010). To ensure that an *exo1Δ* does indeed reduce resection, an *exo1Δ* was crossed with a *rad11-GFP* strain and the number of foci per nucleus was calculated immediately after exposure to 100 Gy (Figure 3-9A). Rad11 is a subunit of RPA so the number of RPA foci per nucleus can act as an indirect read out of the amount of ssDNA present. Indeed, in an *exo1Δ* culture, the number of Rad11-GFP foci per nucleus immediately after 100 Gy IR was reduced by almost half when compared to *exo1+* cells, but was not affected in un-irradiated cells (Figure 3-9B). This shows that the amount of ssDNA after IR damage in asynchronous cells is reduced in an *exo1Δ*.

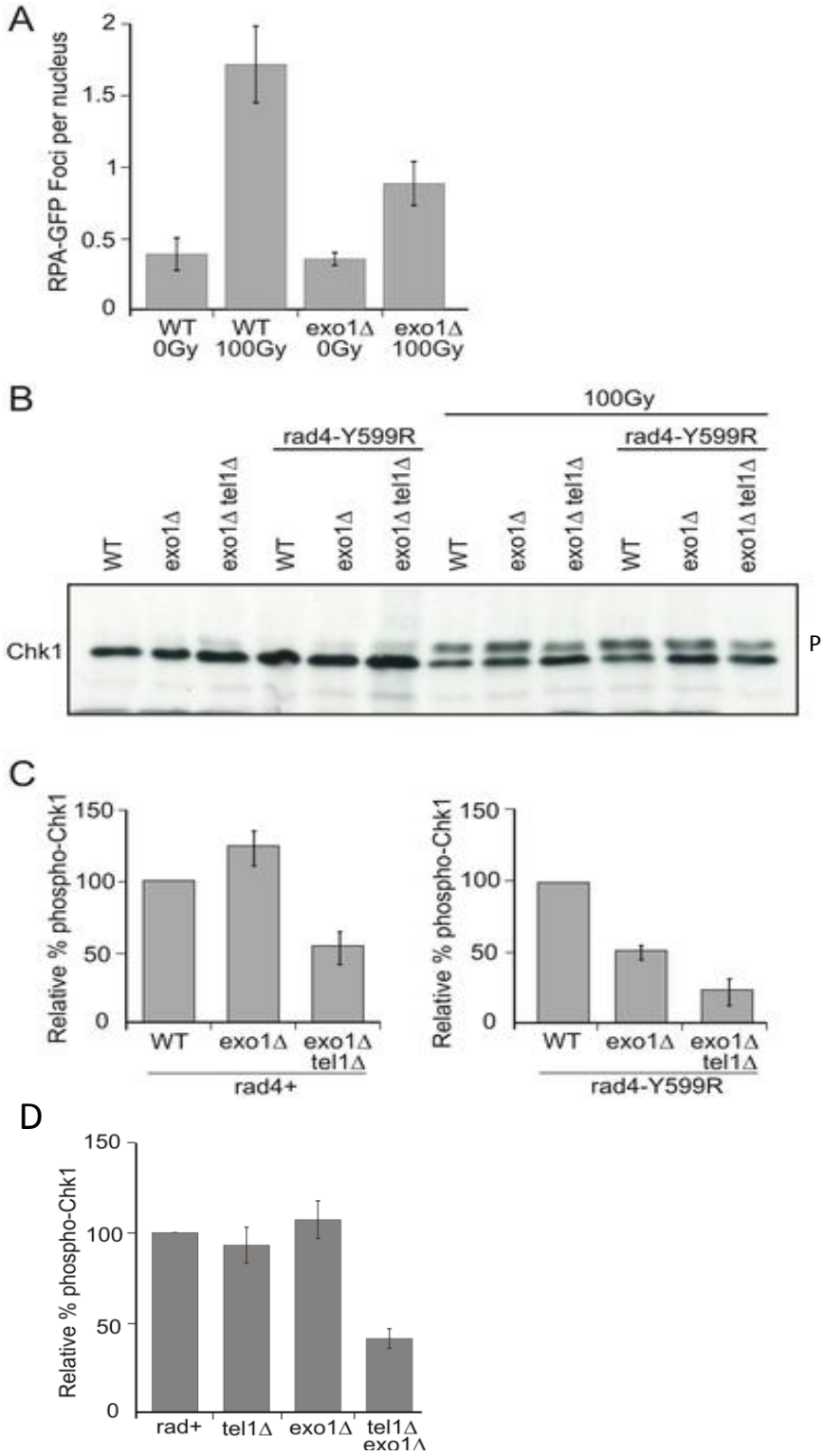
A
RPA-GFP Foci per nucleus
2
1.5
1
0.5
0
WT 0Gy
WT 100Gy
exo1Δ 0Gy
exo1Δ 100Gy
B
100Gy
rad4-Y599R
rad4-Y599R
WT
exo1Δ
exo1Δ tel1Δ
WT
exo1Δ
exo1Δ tel1Δ
WT
exo1Δ
exo1Δ tel1Δ
WT
exo1Δ
exo1Δ tel1Δ
Chk1
P
C
Relative % phospho-Chk1
150
100
50
0
WT
exo1Δ
exo1Δ tel1Δ
rad4+
Relative % phospho-Chk1
150
100
50
0
WT
exo1Δ
exo1Δ tel1Δ
rad4-Y599R
D
Relative % phospho-Chk1
150
100
50
0
rad+
tel1Δ
exo1Δ
tel1Δ exo1Δ

Figure 3-9. *rad4-Y599R* cells have reduced Rad3 activation after IR when resection is reduced

A. Exponentially growing *rad11^{RPA}-GFP* (WT) and *exo1Δ rad11^{RPA}-GFP* (*exo1Δ*) cells were exposed to 0 GY or 100 Gy IR, fixed and assayed for the number of Rad11-GFP foci per nucleus by fluorescence microscopy. Error bars: standard deviation (n=3). B. Asynchronously growing WT, *exo1Δ* and *exo1Δ tel1Δ* strains with or without *rad4-Y599R* mutation were exposed to 0 or 100 Gy and Chk1-HA phosphorylation was monitored immediately afterwards by SDS PADGE using α-HA. C. Quantification of phosphorylated Chk1-HA from B. Phosphorylated bands (P) were quantified relative to unphosphorylated bands and normalised to *rad4+* (Left panel) or *rad4-Y599R* (Right Panel) to understand the effect of limiting resection on checkpoint activation in *rad4* and *rad4-Y599R* backgrounds . Error bars: standard deviation (n=3) D. Quantification of phosphorylated Chk1-HA relative to unphosphorylated Chk1-HA normalised to *rad4+* after 100Gy IR in the indicated strains, as seen by SDS PAGE using α-HA. Error bars: standard deviation (n=3)

Thus, an *exo1Δ* background can be used to access the role the Rad4 AAD is playing when ssDNA is limited. It can be seen from Figure 3-9B and the quantification in Figure 3-9C that, in *rad4+* cells deletion of *exo1* does not lead to a decrease in Chk1-HA phosphorylation compared with *exo1+,* after 100 Gy IR in asynchronous cells. However, when combined with the *rad4-Y599R* mutation, a 50% reduction in Chk1-HA phosphorylation can be seen compared with *rad4-Y599R* alone. This suggests that when resection is limited, such as in S-phase, one of the primary ways to activate Rad3 is via the Rad4 AAD. However, 50% of the Chk1-HA phosphorylation still remains in an *exo1Δ rad4-Y599R* compared with *rad4-Y599R* alone. It may be possible that the $Tel1^{ATM}$-dependent checkpoint, which is known to be involved in checkpoint activation at unresected DNA DSB may be contributing to Chk1-HA phosphorylation (see "1.4.5 Role of the Yeast Homolog, Tel1, in Checkpoint activation" section.).

To test this, *tel1Δ* cells were crossed with the *exo1Δ* and *exo1Δ rad4-Y599R* strains and Chk1-HA phosphorylation after IR was measured. As predicted, in an *exo1Δ* background *tel1Δ* reduced Chk1-HA phosphorylation by 50%, but has no effect in an otherwise WT background (Figure 3-9 C D). This is consistent with the expectation DSBs remain for longer and thus *tel1* is involved in more signalling. In the *exo1Δ rad4-Y599R* background, *tel1Δ* reduced the relative Chk1-HA phosphorylation by another 50% compared with *exo1Δ rad4-Y599R,* leaving only ~25% of the phosphorylation seen in a *rad4-Y599R* alone. This suggests the Rad4 AAD does indeed contribute to a significant amount of the Rad3 activation seen when ssDNA is low and that the defect in *rad4-Y599R* is not associated with the Tel1 pathway (Figure 3-9C).

3.5 The Rad4 AAD Acts in a Chromatin Dependent Pathway

The data in the previous section suggests that the Rad4 AAD domain may be acting in an ssDNA independent manner to activate Rad3. One possibility is that it could be acting in a pathway to amplify or maintain Rad3 activity when activation via the canonical ssDNA dependent pathway is limited. In budding yeast it has been shown that a LacO tethering system, in which the recruitment of two of the main checkpoint

proteins to LacO repeats in the genome via the Lac repressor, bypasses the need for ssDNA in checkpoint activation (Bonilla et al., 2008). It was therefore plausible that a similar system could be used in *S. pombe* to further test the theory that the Rad4 AAD acts independently of ssDNA. To this end, a LacO tethering system similar to that used in budding yeast by Bonilla et al., (2008) was set up in the laboratory by Takashi Morishita and Su-Jiun Lin.

In this system, 256 LacO repeats were inserted into the genome along with a NAT marker at the *ura4* locus on chromosome III. Each of the three main checkpoint proteins; Rad3, Rad9 and Rad4 were tagged with the Lac repressor (LacI), GFP and a nuclear localisation signal (NLS) (GFP/LN) and cloned into pRep41 under the control of the inducible *nmt41* promoter (Figure 3-10A). Su-Jiun Lin showed that expression of the relevant LacI construct upon removal of thiamine rescued the DNA damage sensitivity of *rad3Δ*, *rad9Δ* and a temperature sensitivity of the Rad4 ts mutant *rad4-166*. This shows the addition of the GFP/LN tag did not ablate the function of any of the proteins. Furthermore upon expression of each of the constructs, a single GFP focus could be seen within cells. This indicates that the LacI/LacO interaction was indeed recruiting the checkpoint protein to the chromatin. Su-Jiun Lin was also able to show that expression of any one of the constructs leads to checkpoint activation, as seen by cell elongation and Chk1-HA phosphorylation. This result differed from that seen in Bonilla et al., (2008), where co-expression and recruitment of a least two checkpoint proteins, such as Ddc1 and Ddc2, was necessary for Rad53 phosphorylation in budding yeast.

To confirm Su-Jiun Lin's result, either Rad3-GFP/LN, Rad4-GFP/LN or Rad9-GFP/LN were expressed in +LacO and- LacO cells and Chk1-HA phosphorylation looked for 16-22 hours after induction (*nmt41* expression is known to occur 14-18 hours after the removal of thiamine) (Figure 3-10B). It can be seen that induction of any of the three constructs does indeed lead to Chk1-HA phosphorylation in +LacO cells but not in –LacO cells and that this phosphorylation increases with time after induction (Figure 3-10B). This supports the previous data from the laboratory showing that in *S. pombe*, recruitment of one checkpoint protein to the chromatin is sufficient for checkpoint activation.

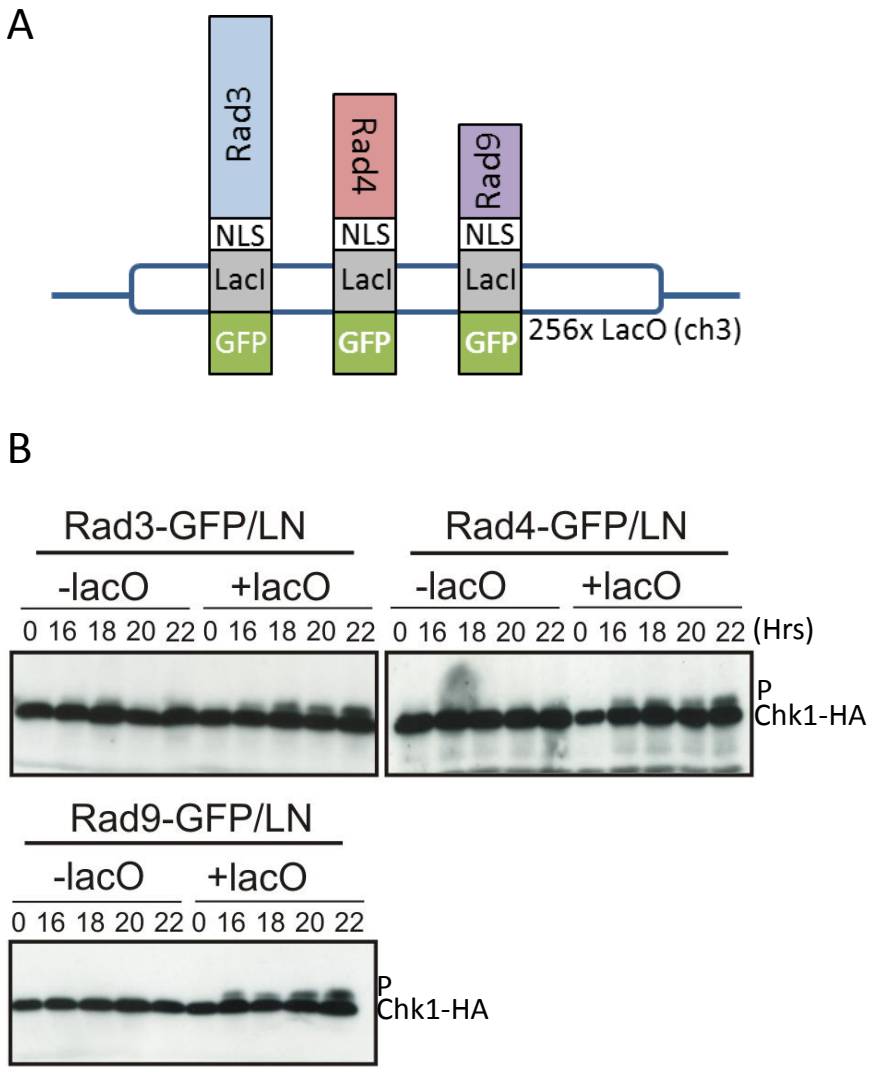

Figure 3-10. Recruitment of checkpoint proteins to the chromatin leads to Rad3 activation

A. Schematic showing the Rad3/Rad4/Rad9-GFP/LN constructs and how they are recruited to the 256 LacO repeats in the chromatin via the LacI-LacO interaction. B. Chk1-HA phosphorylation after expression of Rad3/Rad4/Rad9-GFP/LN in the LacO system. Chk1-HA phosphorylation was assessed by SDS PAGE using α-HA in cells expressing Rad3-GFP/LN, Rad4-GFP/LN or Rad9-GFP/LN from pRep41 (*nmt41* promoter) in strains with or without the genomic LacO array (- LacO, +LacO). Samples were taken at the indicated hours after induction (thiamine removal).

This difference between *S. pombe* and *S. cerevisiae* may be due to differences in how the checkpoint proteins interact and are recruited in the two organisms.

Importantly, previous work from the laboratory showed that recruitment of *Rad4-Y599R*-GFP/LN to the LacO repeats did not lead to Chk1-HA phosphorylation (result is confirmed in Figures 3-11B and 3-12B). Su-Jiun Lin also showed that expression of Rad3-GFP/LN in a *rad4-Y599R* background did not lead to Chk1-HA phosphorylation. This data implies that the Rad4 AAD is essential for checkpoint activation when no ssDNA is present, backing up the hypothesis made from Figure 3-9. It also shows that the LacO system specifically assays the Rad4 AAD-dependent checkpoint pathway, providing an assay system by which the other factors required may be identified. To characterise the requirements for Rad4-AAD activation of Rad3, Rad3-GFP/LN was expressed in a number of different genetic backgrounds where known checkpoint factors had been knocked out or mutated (Figure 3-11A, B, C). It can be seen from Figure 3-11B that an empty vector alone caused no checkpoint activation. This demonstrates that neither having the plasmid present, nor the presence of the genomic LacO caused Chk1 phosphorylation. Also, previous work in the laboratory has shown that expression of LacI alone does not cause Chk1-HA phosphorylation in the LacO background.

Expression of Rad3-GFP/LN caused substantial Chk1-HA phosphorylation after 22hrs induction (Figure 3-11A). This is consistent with Figure 3-10B. Deletion of either Rad9 or Rad1 of the 9-1-1 complex in the LacO system abolished this Rad3 dependent Chk1-HA phosphorylation, suggesting that the complete 9-1-1 complex maybe involved in the Rad4 AAD dependent checkpoint pathway (Figure 3-11A). Furthermore, deletion of the 9-1-1 clamp loader protein *rad17* also prevented Chk1-HA phosphorylation, thus suggesting that Rad17 is also required in this Rad4 AAD pathway. Deletion of the mediator *crb2*^{53BP1} also prevents Chk1-HA phosphorylation after Rad3-GFP/LN expression in the LacO system, therefore implicating Crb2 in the Rad4 AAD pathway. As described in the "1.5.5 The Activation of the ATR Checkpoint Pathway" and the "1.5.7 ATR Checkpoint Maintenance and Amplification" sections Crb2 can be recruited to sites of damage via two independent mechanisms.

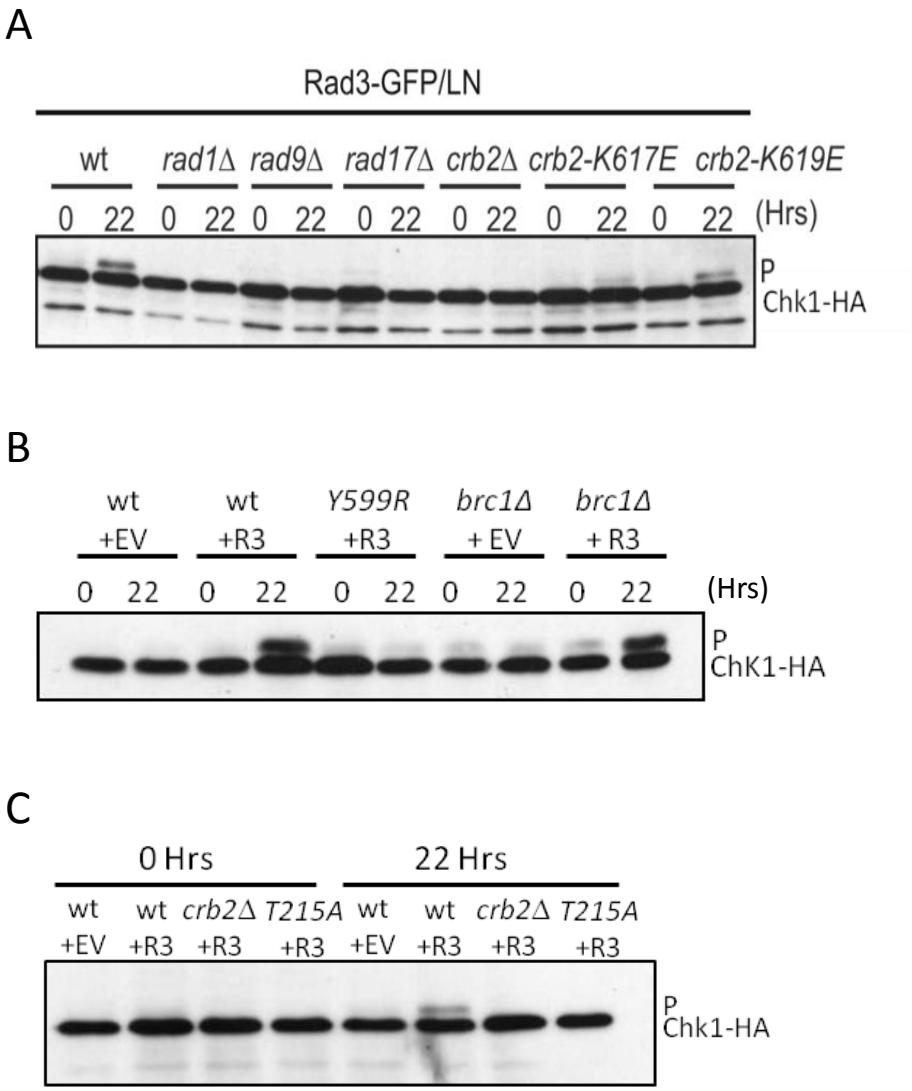

Figure 3-11. Genetic requirements for Rad3 activation in the LacO system
A. Chk-HA phosphorylation was assessed by SDS PAGE using α-HA at 0 or 22hrs after Rad3-GFP/LN induction in the indicated genetic backgrounds. B. As in A. except empty vector was also used as a negative control. +EV indicates cells containing empty vector (pRep41), + R3 indicates cells containing the pRep41-Rad3-GFP/LN vector as used in A. C. As in B, but in the indicated strain backgrounds.

One depends on the histone modifications γH2A and H4K20me and is required for checkpoint amplification and maintenance, the other on an interaction between Rad4 and phosphorylated T215 on Crb2, which is required for the initial checkpoint activation (Du et al., 2003, Du et al., 2006).

As it was predicted that the Rad4 AAD may be required for checkpoint amplification and/or maintenance (and previous data from the laboratory showed that γH2A was required for checkpoint activation in the LacO system), crb2 BRCT domain mutants, K617E and K619E, (that cannot bind γH2A) were tested in the LacO system (Kilkenny et al., 2008)(Figure 3-11A). K617E and K619E mutations reduced Chk1-HA phosphorylation compared with WT, but did not completely abolish it (Figure 3-11A). This may be due to residual Crb2 bound to the chromatin via the H4K20me-Crb2 Tudor domain interaction or to the involvement of a second γH2A binding mediator protein, $Brc1^{PTiP/MDC1}$, which had previously been hypothesised to play a role within the S-phase checkpoint (Williams et al., 2010b). To test this hypothesis, Rad3-GFP/LN was expressed in a +LacO strain harbouring a *brc1* deletion (Figure 3-11B). Surprisingly, no reduction in Chk1-HA phosphorylation after 22hrs of Rad3-GFP/LN expression can be seen, suggesting no role for Brc1 in the Rad4 AAD pathway (Figure 3-11B). To further investigate the role of Crb2 in the Rad4 AAD dependent checkpoint a *crb2-T215A* mutant was crossed into the LacO containing strain. Interestingly upon Rad3-GFP/LN expression, no Chk1-HA phosphorylation can be seen. This implies that the interaction between Rad4 and Crb2 is essential for Rad3 activation in this system (Figure 3-11C). As there is a requirement for both the Crb2 interaction with γH2A and with Rad4, it is possible to predict a model in which Crb2 is recruited to γH2A via its BRCT domain, and where phosphorylation on T215 brings Rad4 to the chromatin, where it can then activate more Rad3 via its AAD.

Although it can be seen from Figure 3-11A that the 9-1-1 complex and Rad17 are required in the Rad4 AAD LacO checkpoint system, the exact role these proteins are playing in the pathway is unclear. It is known that, for the initiation of the DNA damage checkpoint Rad9 phosphorylation recruits Rad4 to the site of damage (Furuya et al., 2004) ("1.5.5 The Activation of the ATR Checkpoint" section). To address this in the Rad4 AAD pathway, Rad3-GFP/LN and Rad4-GFP/LN were co-expressed in the LacO

system in order to see if the requirement of Rad9 could be bypassed. Indeed, the co-recruitment of Rad3 and Rad4-GFP/LN, but not Rad3-GFP-L/N alone, in a *rad9Δ* leads to Chk1-HA phosphorylation (Figure 3-12A). This suggests that Rad9 is playing a role, perhaps with Crb2, in the recruitment or retention of Rad4 in the Rad4 AAD checkpoint pathway. Consistent with this, data from Su-Jiun Lin showed that the phosphorylation of Rad9 on T412 (which rad4 is known to bind to (Furuya et al., 2004)), is also required for ChK1-HA phosphorylation in the LacO system. It is clear that Rad9 is playing an important role in this checkpoint pathway, however the role of the rest of the 9-1-1 complex and its loader is not known in this instance. It is possible that they are merely playing a structural role and are only required for bringing Rad9 to, and/or maintaining Rad9 at, the chromatin. Alternatively, they may be playing a more direct role within the pathway.

To test between these two possibilities, Rad9-GFP/LN was expressed in *rad1Δ* and *rad17Δ* +LacO strains (Figure 3-12B). Similarly to Rad3-GFP/LN expression, rad9-GFP/LN expression in *rad1Δ* or *rad17Δ* +LacO strains did not lead to any Chk1-HA phosphorylation, even though Rad9 is being recruited to the chromatin via the LacI-LacO interaction (Figure 3-12B). This suggests that Rad1 and Rad17 are playing a direct role in the activation of the checkpoint in this system and are not just required to bring or maintain Rad9 at the chromatin. The precise role they are playing is still, however, unclear. Rad17, as described in "1.5.5 The Activation of the ATR Checkpoint Pathway" section, loads the 9-1-1 complex onto the ds-ssDNA junction, a process which is dependent on its ATPase activity (Bermudez et al., 2003, Ellison and Stillman, 2003). To test if Rad17s ATPase activity is the reason rad17 is required a mutant form of Rad17, rad17-A/D (ATPase dead), in which a key residue in the Walker A domain is mutated (K118E) and which thus prevents ATP hydrolysis (Griffiths et al., 1995), was crossed into the LacO background. Upon Rad9-GFP/LN expression, Chk1-HA phosphorylation was seen in the *rad17-A/D* background but not in the *rad17Δ*, although phosphorylation was slightly reduced compared to wt. This suggests that the dependence of Rad17 when Rad9 is recruited is not due to its ATPase activity and therefore its ability to load the 9-1-1 complex.

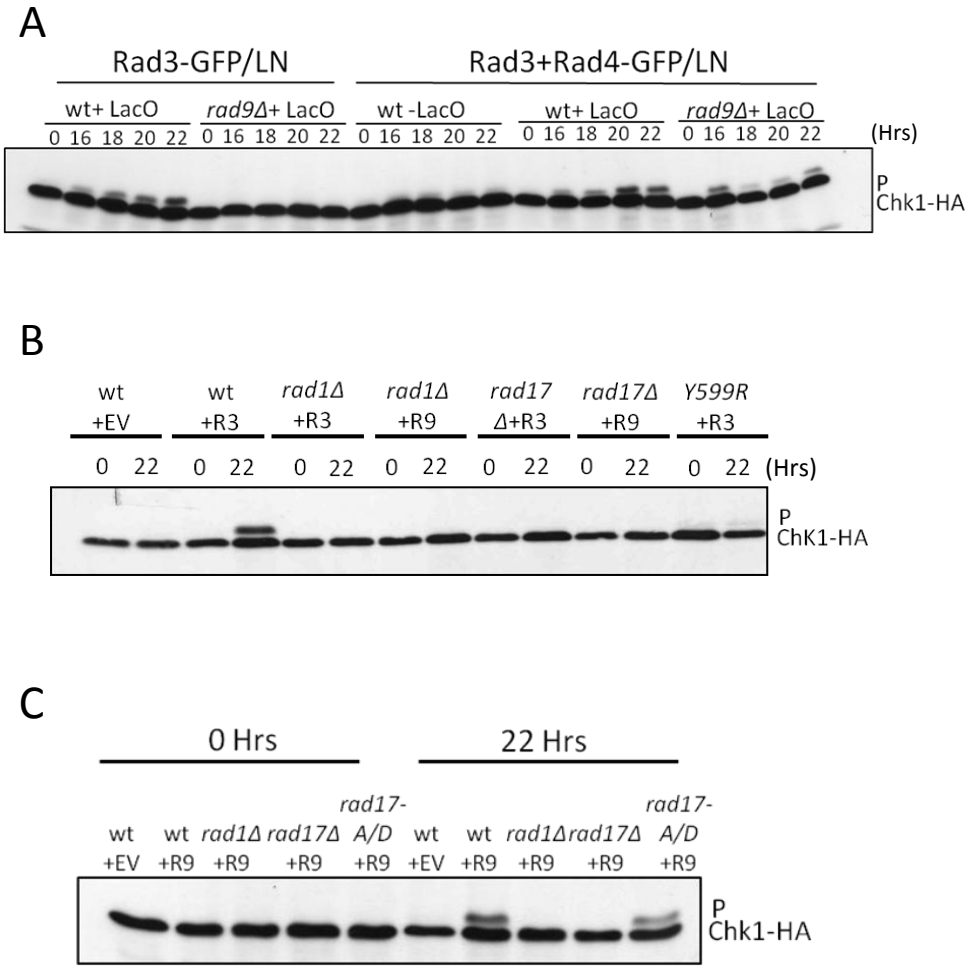

Figure 3-12. Genetic requirements of the 9-1-1 complex and loader in the LacO system

A. Chk1-HA phosphorylation in cells expressing Rad3-GFP/LN or Rad3-GFP/LN +Rad4-GFP/LN for the indicated period of time in *WT +LacO* or *rad9Δ+LacO* strains. Chk1-HA phosphorylation was monitored by SDS PAGE using α-HA. B. Chk1-HA phosphorylation was monitored in +LacO cells by SDS PAGE using α-HA in the indicated genetic backgrounds expressing either Rad3-GFP/LN (+R3), Rad9-GFP/LN (+R9) or empty vector (EV). Samples were taken 0 or 22 hours after induction. As in B. rad17-A/D refers to the *rad17* ATPase dead mutant *K118E*.

The highly repetitive nature of the LacO array can lead to replication problems and recombination between LacO repeats, leading to loss or partial loss of the array (Jacome and Fernandez-Capetillo, 2011). To ensure the results presented in this section are genuine and are not due to any loss of LacO repeats, Southern blot analysis using a probe against the LacO sequence (materials and methods) was carried out on all of the strains used (Figures 3-13 A and B). Samples for southern blot were taken pre-induction at T0 to ensure the LacO repeats were present at the start of the experiment and had not been lost in the strain creation or transformation process. From Figures 3-13A and B it can be seen that the number of LacO repeats between strains varies from the original 10.5 Kb in *rad17Δ* and rad17-A/D, for example, to as little as 3.5 Kb in the initial *rad1Δ* in strain Figure 3-13A. It has been established in budding yeast that the minimal number of LacO repeats required for checkpoint activation is 40 repeats, although 80 repeats (~ 3.2Kb) were required for a full Rad53 phospho shift (Bonilla et al., 2008). With this in mind, to ensure proper comparison between strain backgrounds, the *rad1Δ* +LacO strain in Figure 3-13A which exhibits 3.5 Kb of LacO repeats, was remade (Figure 3-13B) and this new strain with > 8 Kb of repeat sequence was used for all the *rad1Δ* +LacO experiments shown in this chapter. It can therefore be concluded that all the results presented in this section are genuine and are not due to any loss of the LacO repeats.

3.6 Conclusion and Discussion

It has been reported that the AAD domains of the Rad4 homologs are required in different cell cycle stages in different organisms. In budding yeast the $Dpb11^{TopBP1}$ C-terminus is most important in G2 of the cell cycle, however this still acts redundantly with the $Ddc1^{Rad9}$ AAD (Navadgi-Patil and Burgers, 2009, Navadgi-Patil et al., 2011). In higher eukaryotes the TopBP1 AAD has been shown to be essential for checkpoint activation in S-phase especially after replication stress, but it is yet to be seen how important it is in other cell cycle stages (Kumagai et al., 2006, Delacroix et al., 2007, Burrows and Elledge, 2008, Mordes et al., 2008a).

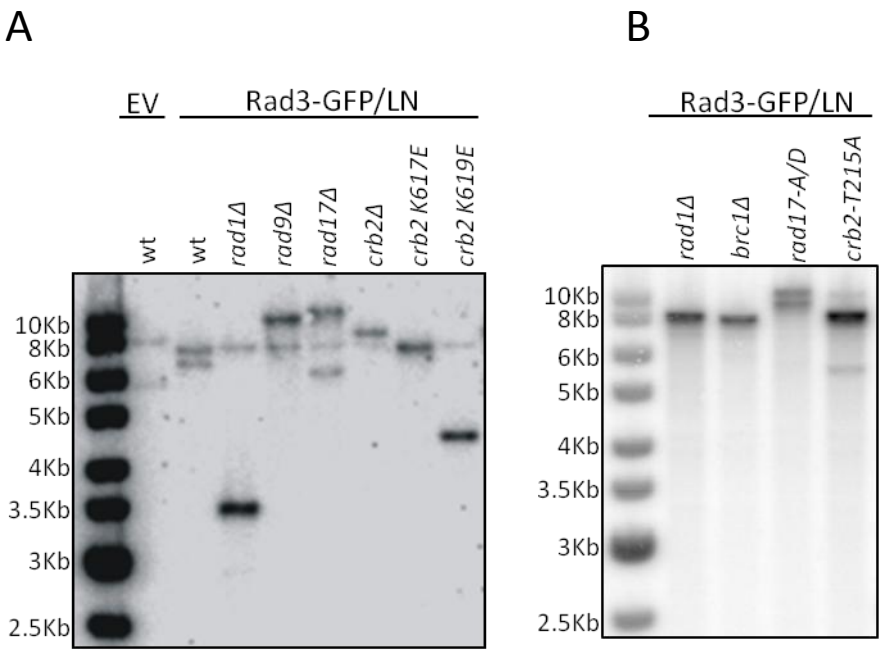

Figure 3-13. LacO strains used in this study have retained the LacO array.
A. Southern blot analysis probing for the LacO sequence in the indicated genetic background pre Rad3-GFP/LN or empty vector (EV) expression. B. As in A.

Here we show that in *S. pombe* the Rad4 AAD is required for checkpoint activation after DNA damage in S-phase and G1/S and, unlike *S.cerevisaie,* not in G2 (Figures 3-3, 3-4, 3-5). A clear reduction in Chk1 and H2A phosphorylation can be seen after gamma irradiation in G1/S and S-phase but not in G2 in the *rad4-Y599R* mutant (Figures 3-3, 3-5). This reduction in Rad3 activation correlates with a reduction in cell survival seen in Figure 3-4A, suggesting that the cells are not able to fully activate the checkpoint. It is also supported by the fact that the *rad4-Y599R* cells are more sensitive to genotoxic agents that have their affect in S-phase (Figure 3-2).

The Rad4 AAD is more important in S-phase due to the reduced level of DNA resection after damage, as seen in Figures 3-7 and 3-9. We propose a model in which a threshold level of active Rad3 is required for a full checkpoint response (Figure 3-14A). In G2 enough Rad3 is activated via a ssDNA dependent, but Rad4 AAD independent, pathway for a full checkpoint response. However, in S-phase where resection is reduced and less ssDNA is present, the Rad4 AAD chromatin dependent (ssDNA independent) pathway is required to amplify the levels of active Rad3 to gain a full checkpoint response (Figure 3-14A). As Tel1 has been reported to be able to bind to unresected DNA ends via an interaction with the MRN complex and phosphorylate Chk1*, tel1* was knocked out in the *exo1Δ* and *Y599R exo1Δ* strains. This *tel1Δ* mutation leads to a reduction in Chk1 phosphorylation in *exo1Δ* and in the *Y599R exo1Δ* strains. This confirms that Tel1 is important for Chk1 phosphorylation when resection is reduced and shows that the Rad4 AAD is not operating in a Tel1 dependent pathway.

The results presented in this chapter suggest there are at least 3 pathways that can contribute to a full DNA damage checkpoint response in *S. pombe*; ssDNA dependent activation of Rad3, Rad4 AAD dependent activation of Rad3 and a Tel1 dependent pathway.

Using a LacO system to identify the components of the Rad4 AAD pathway, it can be seen from Figures 3-11 A, B and C that the Rad4 AAD pathway is dependent on the 9-1-1 complex, Rad17, Crb2 (both its γH2A interacting BRCT domain and Rad4 interacting phosphorylated T215) but not Brc1. Previous data from this laboratory also shows that γH2A and phosphorylation of Rad9 on T412 are also required.

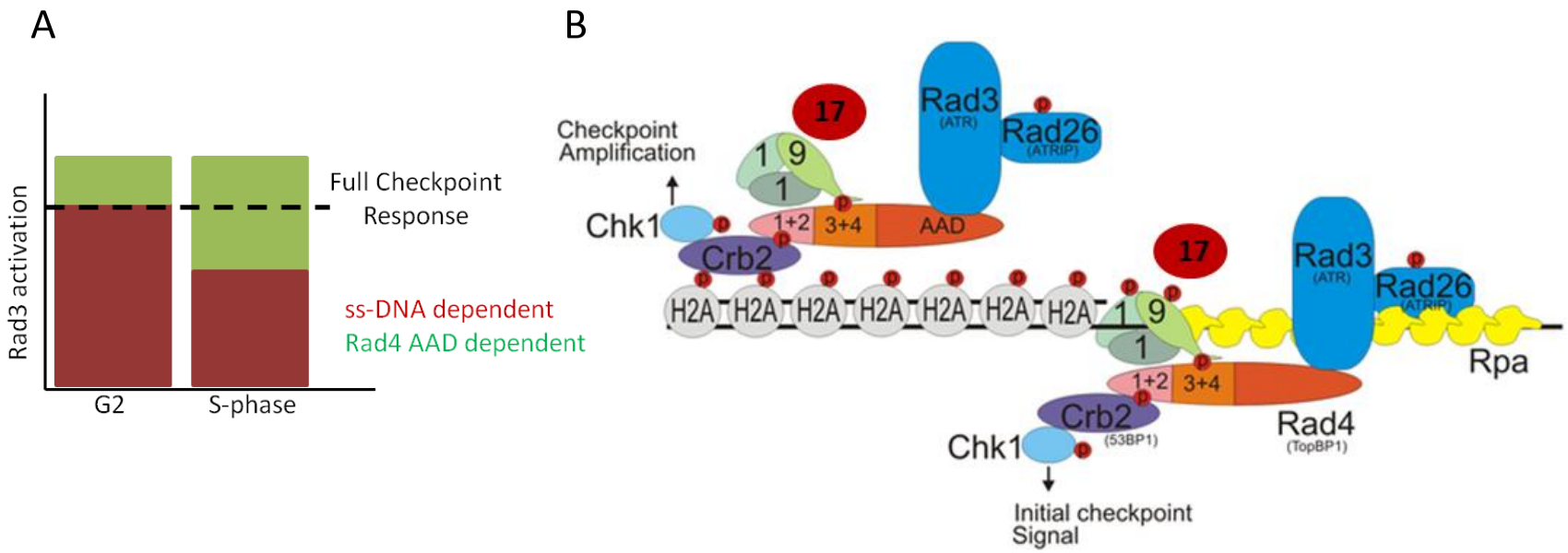

Figure 3-14. Model of checkpoint response in *S.pombe* based on the results in this section

A. Graphical representation depicting a checkpoint threshold model. In G2 phase when large amounts of ssDNA are present after damage enough Rad3 is activated via an ssDNA dependent Rad4 AAD independent pathway for a full checkpoint response. In S-phase when less ssDNA is present after damage the Rad4 AAD, chromatin dependent pathway is required to "boost" the levels of active Rad3 to reach the threshold required for a full checkpoint response. B. Diagram of the two proposed checkpoint pathways to Rad3 activation and a full checkpoint response. Right hand side shows the established ssDNA dependent pathway required for the initial checkpoint response. The left hand side shows the Rad4 AAD pathway required when ssDNA is low to amplify the Rad3 signal to get a full checkpoint response.

The requirement of Rad17 suggested that the 9-1-1 complex needed to be loaded on to DNA. However, the manner in which the 9-1-1 complex is loaded onto the DNA is difficult to envisage. This is because, presumably, there is no 5' ss-ds-DNA junction and no RPA coated ssDNA at the LacO repeats. Also Rad17 is still required when Rad9-GFP/LN is recruited, which should bypass the need for 9-1-1 loading (Figure 3-12B). Indeed the Rad17 ATPase activity is not required when Rad9-GFP/LN is recruited to the chromatin (Figure 3-12C). Therefore an alternative model for the requirement of Rad17 could be proposed. This is that the 9-1-1 complex is not loaded onto the DNA for the LacO dependent checkpoint activation; instead it may just associate with the dsDNA via an alternate mechanism. If this is the case Rad17 may be playing an important role in stabilising the 9-1-1-Rad4 interaction, which is subsequently required for the activation of the recruited Rad3.

It has been shown in Xenopus extracts that Rad17 is able to interact with TopBP1, and this interaction is not required for the recruitment of TopBP1 but is required for its accumulation and retention (Lee and Dunphy, 2010). A similar model could therefore be possible in *S. pombe.* The results in Figure 3-12B also suggest that Rad1 has a role other than forming the complete 9-1-1 complex as it is also required when Rad9-GFP/LN is recruited to the LacO array. One reason for its requirement maybe due to it being implicated as the subunit of the 9-1-1 complex that interacts with Rad17, therefore its requirement may be in retaining Rad17 on the chromatin (Dore et al., 2009). Alternatively it has also been reported that Rad1 may have a role in stabilising Crb2 at the chromatin and this would also explain why Rad1 is required for Rad3 activation in the LacO system even when Rad9-LacI is recruited (Du et al., 2003).

It had previously been shown by the Russell laboratory that Brc1 binds to γH2A via its BRCT domains after DNA damage in S-phase. They went on to hypothesise that one possibility for the sensitivity seen to S-phase damage in a *brc1Δ* was due to a potential Rad4 binding role for the protein (although no evidence was shown for this) (Williams et al., 2010). We therefore predicted that Brc1 may be acting as a mediator protein in the chromatin dependent checkpoint amplification pathway. However, this did not seem to be the case as a *brc1Δ* did not lead to reduced Chk1 phosphorylation in the LacO system. It is therefore likely that Brc1 is playing a role in DNA repair not in

checkpoint activation. Indeed a later study showed that Brc1 may be acting to repair damaged replication forks in parallel with the Rqh1 helicase, however the role of Brc1 is still far from understood (Rozenzhak et al., 2010). This result does show that the LacO specifically assays the checkpoint pathway and not DNA repair pathways. It also further suggests that there is probably no DNA damage at the LacO array, despite its repetitive nature. This means that the LacO system could potentially be used to identify proteins involved in the Rad4 AAD checkpoint pathway without contamination from repair proteins, which may occur in other assays such as the HO break system. This checkpoint protein identification could be done by extracting the DNA from LacO cells expressing Rad3-GFP/LN. The DNA, and any associated proteins, could then be isolated using LacI conjugated beads, which would bind specifically to the LacO DNA. The proteins that were associated with the LacO DNA could then be run on an SDS gel and sent for mass spectrometry. This should identify proteins specifically required for the Rad4 AAD checkpoint pathway, and may identify proteins not previously linked to the checkpoint pathway due, for example, to their role in DNA repair.

Interestingly the Rad4 AAD checkpoint pathway requires both the γH2A binding ability of Crb2 and its phosphorylation on T215, which has a role in binding Rad4 (Figure 3-11A, C). It had previously been reported that the γH2A and Rad4 binding ability of Crb2 act in two distinct pathways for Crb2 recruitment and therefore Chk1 phosphorylation. The evidence presented in Figures 3-11A, C suggests that there may be some overlap between the two pathways for Chk1 phosphorylation. It maybe that ssDNA-Rad9- Rad4 and γH2A act to recruit Crb2 separately as previously reported (Du et al., 2006). However, in recruiting Crb2 to γH2A presumably Rad4 is also recruited, as the two interact in a cell cycle dependent manner via Cdc2 phosphorylation. This interaction between Crb2 and Rad4 in the γH2A dependent recruitment pathway could be important for stably associating Rad4 at the chromatin and thus allowing it to activate Rad3. This would explain why both T215 phosphorylation of Crb2 and its ability to bind γH2A are required for Chk1 phosphorylation in the LacO system.

Overall from the data presented in this chapter and previous data from Su-Jiun Lin we can propose the following model: The checkpoint is first activated via the canonical ssDNA dependent mechanism, as described in the “1.5.5 The Activation of the ATR

checkpoint" section, which is independent of the Rad4 AAD. This leads to phosphorylation of H2A which subsequently recruits Crb2 via its BRCT domain. The $Cdc2^{CDK}$ dependant T215 phosphorylation on Crb2 brings Rad4 to the chromatin. This interaction is stabilised via interactions between Rad4 and Rad9 phosphorylated on T412 by Rad3. The rest of the 9-1-1 complex and Rad17 may also form interactions with these checkpoint proteins and the chromatin forming a stable complex. Rad4, via its AAD, is then able to activate more Rad3 which in turn phosphorylates Crb2 and Chk1, leading to an increase in the checkpoint response. The active Rad3 can also phosphorylate more H2A, leading to more recruitment of the checkpoint proteins and more Rad4 AAD dependent Rad3 activation (Figure 3-14 B). This pathway is more important in S-phase when less ssDNA is present after DNA damage (Figure 3-14 A).

Chapter 4

Identification and Characterisation of the *S. pombe* Rad9 ATR Activation Domain

4.1 Introduction

As the Rad4^{TopBP1} AAD only plays a relatively minor role in Rad3^{ATR} activation, that is mainly to amplify the checkpoint signal in S-phase (Chapter 3), it is possible that other AAD containing proteins are present in *S. pombe*. As described in the "1.5.5 The Activation of the ATR checkpoint Pathway" section, in budding yeast the Rad9 homolog Ddc1 plays a more significant role than the Rad4 homolog, Dpb11, in checkpoint activation (Majka et al., 2006b, Navadgi-Patil and Burgers, 2009).The Ddc1 AAD is the main pathway to Mec1^{ATR} activation in both G1 and G2, with Dpb11 only having a semi redundant role with the Ddc1 AAD in G2 (Navadgi-Patil and Burgers, 2009). It is therefore likely (given the data in Chapter 3) that spRad9 may also have a role in Rad3 activation. It could be hypothesised that the Rad9 AAD may be important for Rad3 activation in G2 in *S. pombe* and may be required to stimulate the activity of Rad3 in the ssDNA dependent pathway (Figure 3-14).

4.2 Identification of a Potential Rad9 AAD in *S. pombe*

To test this hypothesis an alignment between the *S. cerevisiae* Ddc1 AAD and the homologs in a number of fungal species as well as human and Xenopus was performed (Figure 4-1A). The Ddc1 AAD is in the C-terminus of the protein and contains two critical tryptophan residues, W352 and W544. These are in the PCNA-like domain and the unstructured C-terminal tail, respectively (Figure 4-1B).

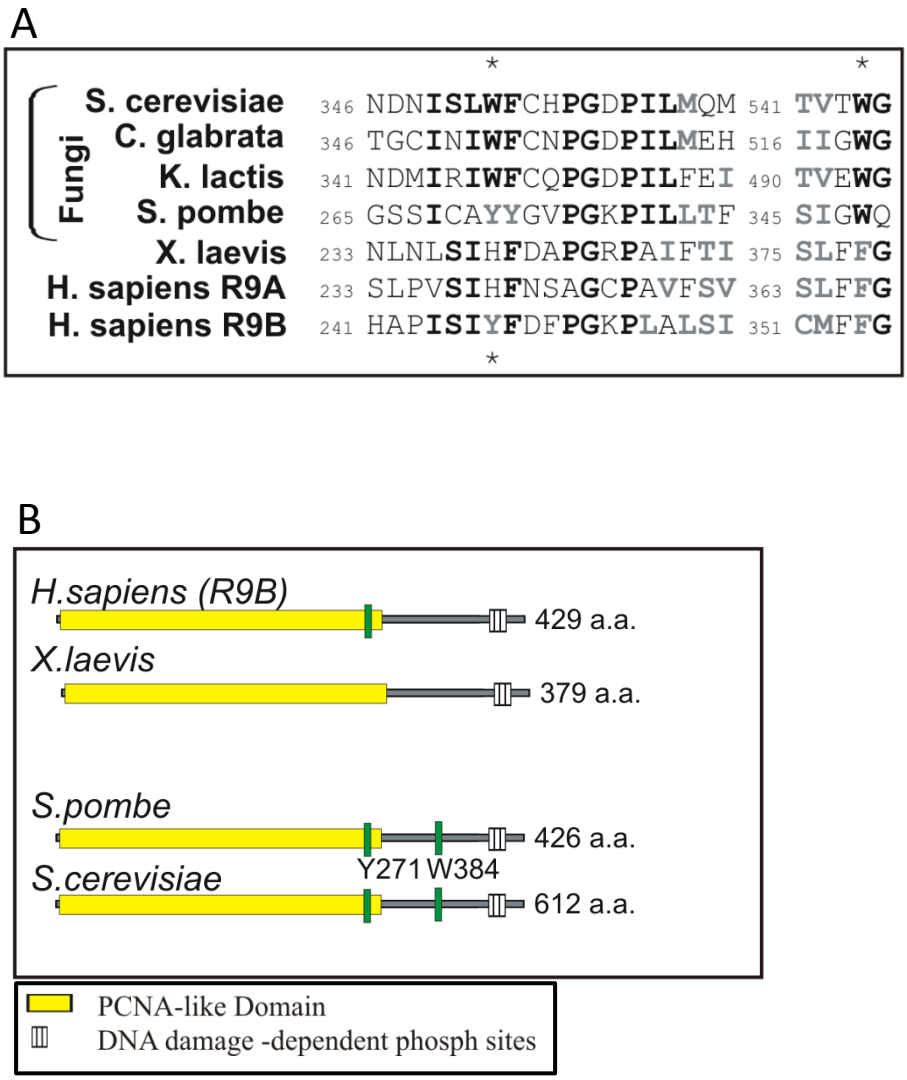

Figure 4-1. Identification of a potential AAD in Rad9
A. Amino acid sequence alignment of the *S.cerevisiae* Ddc1 AAD residues with the *S.pombe*, *C. glabrata, K.lactis*, human and *Xenopus.laevis* homologs. The core aromatic AAD residues are marked with an *B. Schematic of the domain architecture of the Rad9 homologs with the known AAD residues (in the case of scDdc1) or potential AAD residues (human Rad9B and spRad9) annotated. The position of the potential AAD residues in *S.pombe* are noted as Y271 and W384.

Mutation of both of these to alanine is required to fully prevent Ddc1s AAD activity in *vivo* (Navadgi-Patil and Burgers, 2009). Alignment of these regions in Ddc1 shows that the W544 residue is conserved as W348 in *S. pombe* and is also present in the other fungal species (Figure4-1A). W348 is also positioned in the unstructured C-terminal tail, as is the equivalent residue in Ddc1, in a region distinct from the damage induced phosphorylation sites (figure 4-1B).

Perhaps surprisingly, the spW348 (scW544) residue is not conserved in the Xenopus or either of the human homologs. Human and mice are known to contain two Rad9 proteins, Rad9A and Rad9B, with Rad9A carrying out the functions of spRad9 and scDdc1. Rad9B is essential for embryonic development and has a role in resistance to some DNA damaging agents during development (Dufault et al., 2003, Leloup et al., 2010). It can also be seen from Figure 4-1A that Ddc1 W352 in the PCNA-like domain is conserved in *C.glabrata* and *K.Lactis,* but no tryptophan residue is present at this location in the *S. pombe* Rad9 PCNA like domain. However, a tyrosine residue (Y271) is present, which has similar properties to a tryptophan, being a large, polar, hydrophobic, aromatic amino acid. Therefore, it may well be, as with the Rad4 AAD, that this tyrosine is the corresponding residue to the tryptophan and is functioning as an AAD residue.

4.3 rad9 AAD Mutants Have no Growth Defects and Look Like WT

Based on the alignment data, mutations replacing *rad9-Y271* and *W348* with alanine at its endogenous locus were made, using the Recombination Mediated Cassette Exchange (RMCE) method (Materials and Methods, (Watson et al., 2008)). The *Y271A* and *W348A* mutants were crossed with the *rad4-Y599R* mutant, as we hypothesised it may be important to test the double mutants due to redundancy in Rad3 activation being present. The *rad9-Y271A* and *rad9-W348A* mutants showed no growth defects, as seen by growth curves, either on their own or when combined with the *rad4-Y599R* mutant. This suggests that these residues do not play any role in normal cell cycle progression (Figure 4-2A).

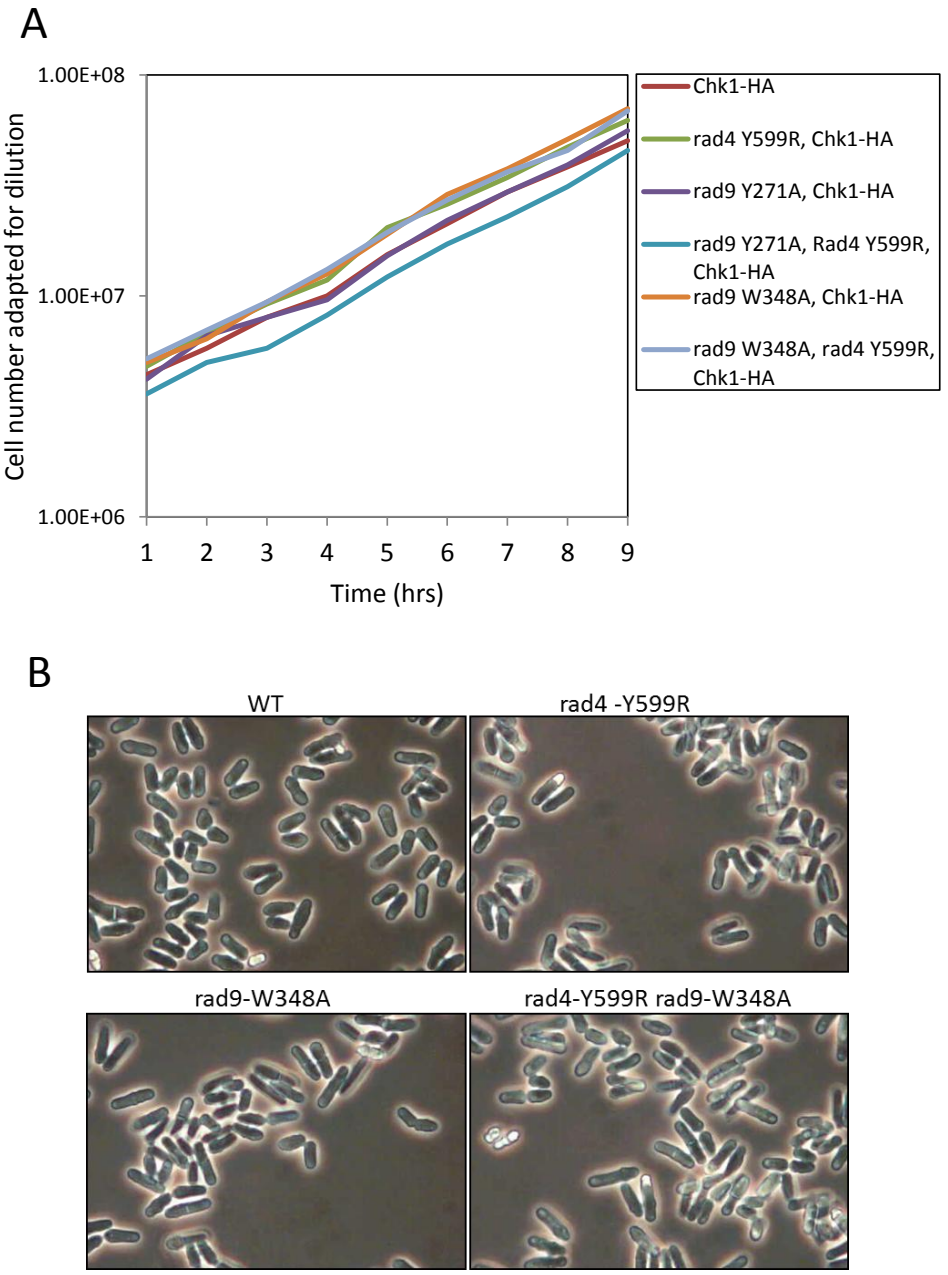

Figure 4-2. *rad9-AAD* mutants grow as WT in the absence of DNA damage
A. Exponentially growing WT (*chk1-HA*) *rad9* AAD and *rad4* AAD mutants as indicated were grown for 9 hours in YE at 30°C whilst being kept in exponential phase by dilution. Cell number was calculated every hour and adapted for the dilution factor. B. Light microscopy pictures of exponentially growing unfixed WT, *rad4-Y599R*, *rad9-W348A* and *rad4-Y599R rad9-W348A* strains.

Microscope images of the mutants were also taken in order to ensure the *rad9* mutant cells were not elongated and therefore did not have any endogenous checkpoint activation, which may be associated with endogenous DNA damage and problems in DNA repair (Figure 4-2B). The microscope pictures of *rad9-W348A* and *rad4-Y599R rad9-W348A* are shown as an example that the *rad9* AAD mutants both alone and with *rad4-Y599R* are not elongated and look like wild type (Figure 4-2B). Taken together the microscope images in Figure 4-2B and the growth curve data in Figure 4-2A confirm there is no cell cycle, replication or endogenous DNA damage problems in the *rad9* mutants (Figure 4-2A, B).

4.4 rad9 AAD Mutants Show Mild Sensitivities to Genotoxic Agents

To test whether the *rad9* AAD mutants were sensitive to genotoxic agents and therefore may be playing a role in the DNA damage and/or replication checkpoint, spot test analysis was carried out in the presence of a number of DNA damaging or replication fork stalling agents (Figure 4-3). In budding yeast the mutation of both of the *ddc1* AAD residues shows a slightly increased sensitivity to UV compared to either mutant alone (Navadgi-Patil and Burgers, 2009). Therefore, to ensure the full role of the potential spRad9 AAD could be seen both the *rad9-Y271A* and *W348A* mutations were combined to give *rad9-2A*, this double mutant was then used for the spot test (Figure 4-3). It can be seen from Figure 4-3 that the *rad9-2A* mutant cells show mild sensitivity to UV at 150J/m^2 when compared to WT cells, but not to the same extent as a *rad3Δ* or even the *rad4-Y599R* mutant strains. *rad9-2A* cells also show moderate sensitivity to the RNR inhibitor HU, this sensitivity is similar to that seen in the *rad4-Y599R* mutant cells but not as severe as in a *rad3Δ* strain. However, *rad9-2A* cells show no sensitivity to CPT, MMS or IR at the doses the tested (Figure 4-3).

To see if the potential Rad9 AAD is acting in a separate pathway to the Rad4 AAD, the *rad9-2A rad4-Y599R* strain was also spotted. Indeed, the double *rad9 rad4 AAD* mutant strain does show increased sensitivity to MMS, HU and UV compared to either of the *rad4* or *rad9* mutants cells alone (Figure 4-3).

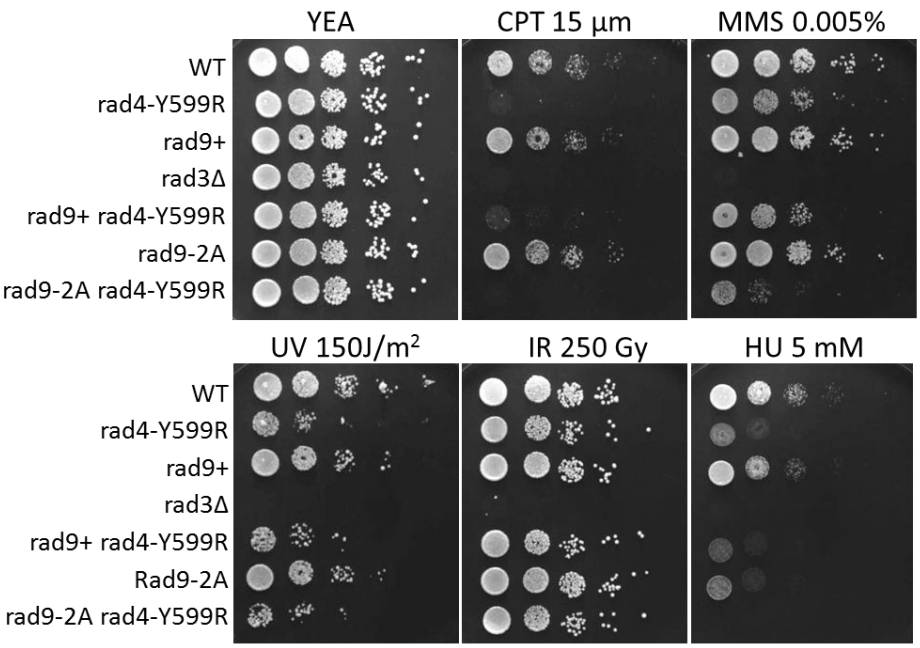

Figure 4-3. *rad9-2A* displays mild sensitivity to genotoxic agents that is additive with *rad4-Y599R*

Spot test analysis of the indicated WT, AAD mutants and *rad3Δ* positive control in the presence of different genotoxic agents. *rad9+* is a WT-like control strain where WT *rad9* has been inserted back into the Lox site containing Rad9 base strain. 10-fold serial dilutions of $1x10^7$ cells/ml were spotted onto YEA plates containing CPT, MMS or HU. Alternatively they were spotted onto YEA containing no genotoxic agents and UV irradiated. For IR cells were γ irradiated, serial diluted and then spotted onto YEA. Plates were incubated at 30°C for 4 days

Therefore, any Rad3 stimulating activity the potential Rad9 AAD may have is operating in a separate pathway to the Rad4 AAD. However, cells which combined the *rad4-Y599R* and *rad9-2A* mutations still did not show any sensitivity to ionising radiation, suggesting that neither of these AAD pathways are required after IR and are probably not required after damage in G2. Unfortunately, from Figure 4-3 it cannot be seen if the *rad9-2A rad4-Y599R* double mutant strain is more sensitive to camptothesin (CPT) than the rad4-Y599R alone, as the rad4-Y599R single mutant is already dead at the dose used. To ensure the presence of the Lox sites up and down stream of the *rad9* open reading frame (Material and Methods) were not responsible for the sensitivities seen, a *rad9+* strain was also spotted in Figure 4-3. *rad9+* is a strain in which WT *rad9* has been placed back into the genome at its endogenous locus using RMCE in the same way the *rad9* AAD mutants were. Figure 4-3 shows that the *rad9+* stain shows the same phenotype as the WT strain, where no Lox sites are present, proving that the sensitivities seen in the *rad9-2A* are due to the point mutations made and not the presence of the Lox sites.

Overall Figure 4-3 shows that the *rad-2A* strain has some mild to moderate sensitivity to HU and UV and is additive with the *rad4-Y599R,* suggesting that they operate in separate pathways in response to these types of agent. Interestingly, the *rad9-2A* mutation also increases the sensitivity of the *rad4-Y599R* mutant to MMS, even though *rad9-2A* alone is not sensitive to MMS. This suggests that the rad4 AAD can fully compensate for the loss of the rad9 AAD in this instant and that the Rad9 AAD pathway is semi redundant with that of the Rad4 AAD. Neither the *rad9-2A* or *rad4-Y599R rad9-2A* cells are sensitive to IR suggesting neither play a role in Rad3 activation after damage in G2.

4.5 The Rad9 AAD Plays a Minor Role in the Intra S-phase DNA Damage Checkpoint

To further understand whether the sensitivity of the putative Rad9 AAD to UV is indeed due to a checkpoint defect, a lactose gradient synchronised septation

index experiment was carried out (Figure 4-4). In this experiment cells are synchronised in G2 using a lactose gradient (Materials and Methods), these cells are then UV irradiated with 10 J/m^2 whilst still in G2. This gives rise to a low level of UV damage, such a thymine dimmers, that does not activate the G2 checkpoint. However, some damage persists into the first S-phase where these types of lesions are bypassed giving rise to ssDNA gaps which then cause checkpoint activation in the following G2 phase. This checkpoint activation can be monitored by septation index; septation occurs in S-phase, following mitosis (Figure 1-1). Therefore activation of the G2/M checkpoint, causing a cell cycle delay, will lead to a subsequent delay in septum formation. If a mutant displays a checkpoint defect after damage, then this checkpoint dependant cell cycle delay is reduced and septation will occur earlier, when compared to WT.

This assay was used to see if the *rad9* AAD mutant further reduced the checkpoint response of *rad4-Y599R* mutant in correspondence with the increased sensitivity seen in Figure 4-3. In a rad9+ strain, a 40 minute delay can be seen in the peak of septation after 10 J/m^2 UV. Septation in the second cell cycle begins at 180 minutes in the absence of UV and peaks at 220 minutes. After UV exposure, septation starts after 220 minutes and peaks at 260 minutes. In comparison, consistent with a mild checkpoint defect, a 20 minute delay in the peak of septation can be seen in the *rad4-Y599R* strain. Septation peaks at 260 minutes in the presence of UV compared with 240 minutes in its absence (Figure 4-4). In the *rad4-Y599R rad9-W348A* strain (unfortunately this experiment was carried out before the creation of the *rad9-2A* strain), after 10 J/m^2 a minimum 20 minute delay to the peak of septation is seen: Septation peaks at, or after, 260 minutes following UV treatment compared to at 240 minutes without (Figure 4-4). This implies that sensitivity seen in the rad9 AAD mutants to UV is not due to a checkpoint defect.

However, it maybe that the *rad9-W348A* mutant does not cause a checkpoint defect, as having one of the putative AAD residues present is enough for the AAD to function. Alternatively a weak checkpoint defect may not be seen in this particular assay, especially as the increase in sensitivity caused by combining *rad9-2A* with *rad4-Y599*R in is weak (Figure 4-3).

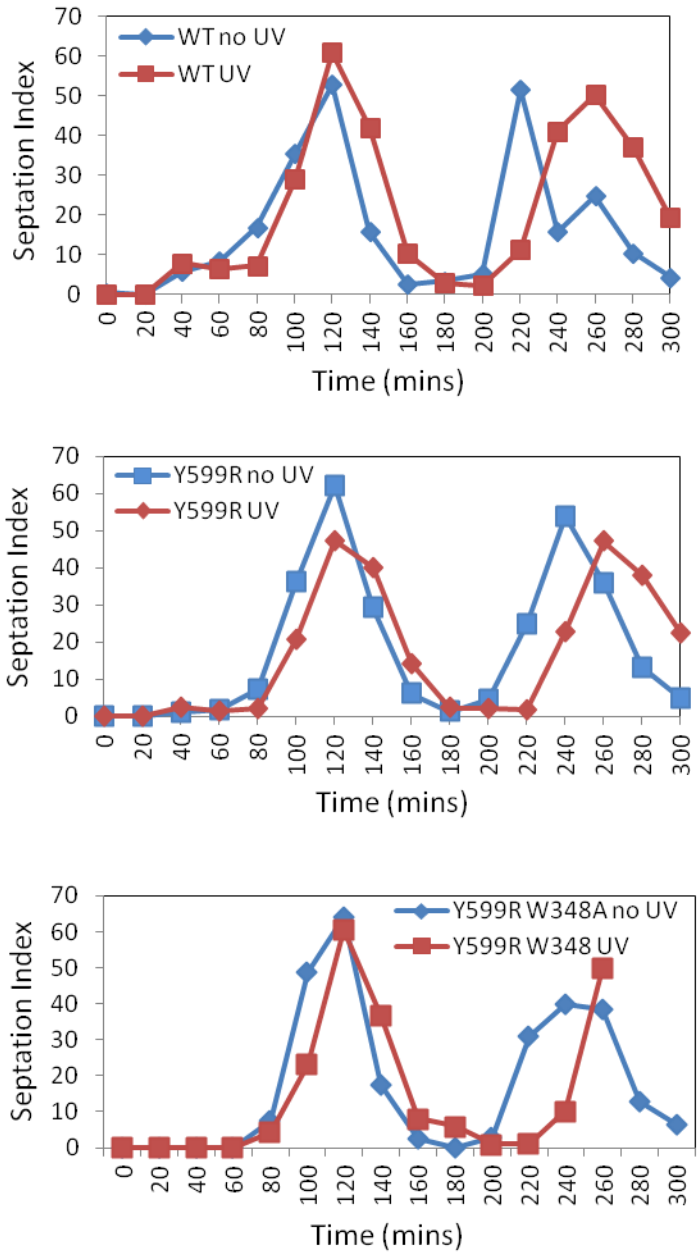

Figure 4-4. *rad9-W348A* does not increase the checkpoint defect of *rad4-Y599R* after low dose UV

WT (top panel), *rad4-Y599R* (middle panel) and *rad4-Y599R rad9-W348A* (bottom panel) were synchronised in G2 by lactose gradient, split, exposed to no UV or 10 J/m^2 and grown in YE at 30°C. Samples were taken every 20 minutes for 300 minutes to assay cell cycle progression by septation index. Septation index (% cells with a septum) was assayed on fixed cells stained with calcofluor and DAPI by fluorescence microscopy.

Therefore to further test the role of the putative Rad9 AAD in Rad3 and checkpoint activation western blot analysis of Chk1 phosphorylation was performed after UV damage in asynchronous cells. It can be seen from Figure 4-5A and the quantification in Figure 4-5B that the *rad4-Y599R* mutation reduced Chk1-HA phosphorylation after UV by ~50% compared to WT (*rad9+*), consistent with the results in Chapter 3. The *rad9-2A* mutant did not cause any reduction in Chk1-HA phosphorylation compared with WT at any of the doses tested. There was even a small increase in Chk1-HA phosphorylation in some of the repeats at higher doses which cannot be explained. However, the *rad9-2A rad4-Y599R* double mutant does decrease the Chk1-HA phosphorylation when compared with the *rad4-Y599R* mutation alone. At 50 J/m^2 the decrease in Chk1 phosphorylation in the double *rad4 rad9* AAD mutant is relatively minor compared to *rad4-Y599R* mutation alone. However, as the dose increases the significance of the rad9 AAD increases, at 150 J/m^2 the Chk1-HA phosphorylation is only ~20% of the *rad9+* and is ~30% less than the *rad4-Y599R* mutant alone. This indicates that the Rad9 AAD is involved in checkpoint/Rad3 activation after UV damage, however, its involvement can only be seen once Rad4s AAD activity has been abolished. Thus, after UV damage the Rad4 AAD is able to fully compensate for the loss of the Rad9 AAD, but not vice versa.

To test if this reduction in Chk1-HA phosphorylation was restricted to UV (S-phase) damage only, a similar experiment to that in Figure 4-5 was performed, however in this instance cells were exposed to IR (Figure 4-6A, B). It can be seen from this experiment that, consistent with the sensitivities in Figure 4-3, the *rad9-2A* mutant does not show a reduction in Chk1-HA phosphorylation after IR (Figure 4-6A, B). Surprisingly, a reduction in Chk1-HA phosphorylation could be seen in the *rad4-Y599R* after low doses of IR but less so at higher doses. While inconsistent with the laboratories previous data that showed no significant effect of the *rad4-Y599R* mutation on IR induced Chk1-HA phosphorylation.

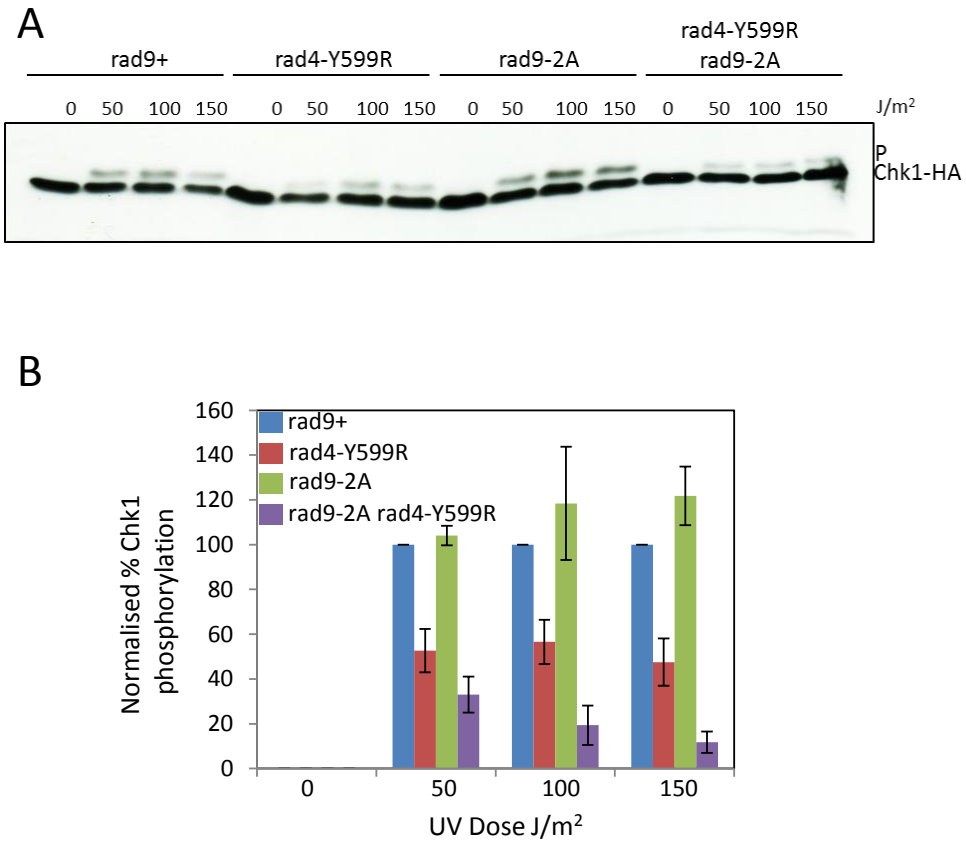

Figure 4-5. The Rad9 AAD is redundant with the Rad4 AAD for Rad3 activation after UV

A. Asynchronous *rad9+, rad4-Y599R, rad92A* and *rad4-Y599R rad9-2A* cells were exposed to UV radiation at the indicated doses. Chk1-HA phosphorylation (P) was assayed by SDS PAGE using α-HA as a readout of Rad3 activation. B. Quantification of A. Phosphorylated Chk1-HA as a % of total Chk1-HA normalised to WT. Error bars: Standard deviation (n=3)

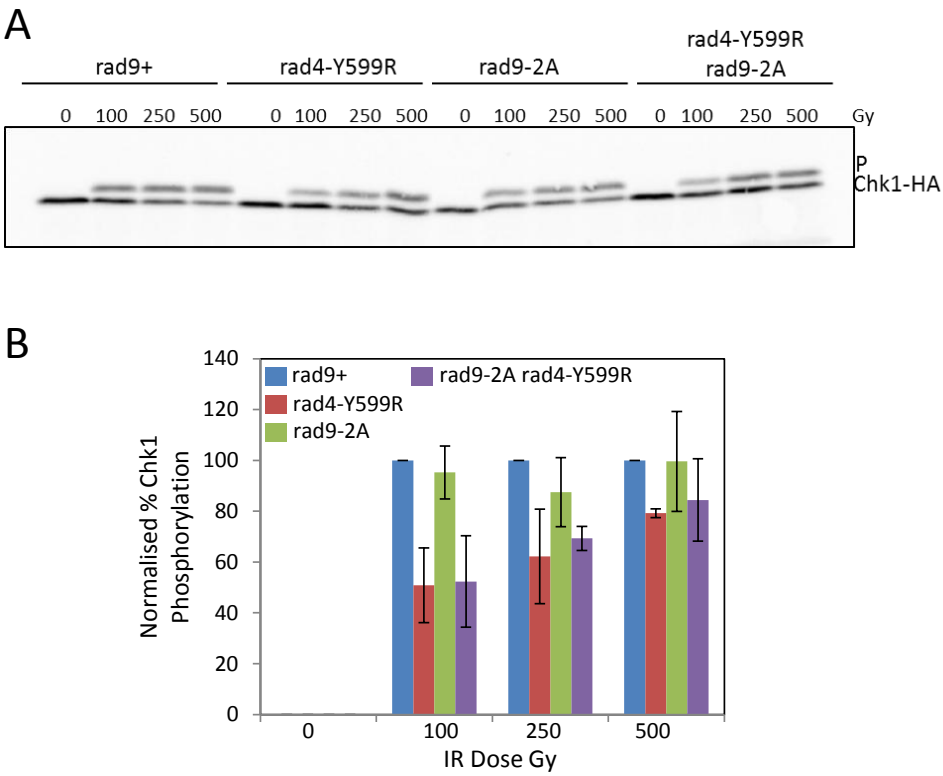

Figure 4-6. The Rad9 AAD has no defect in Rad3 activation after IR in asynchronous cells

A. Asynchronous *rad9+, rad4-Y599R, rad9-2A* and *rad4-Y599R rad9-2A* cells were exposed to γ-radiation at the indicated doses. ChK1-HA phosphorylation (P) was assayed by SDS PAGE using α-HA as a readout of Rad3 activation. B. Quantification of A. Phosphorylated Chk1-HA as a % of total Chk1-HA normalised to WT. Error bars: Standard deviation (n=3)

None the less, the combination of the *rad9-2A* mutant with *rad4-Y599R* does not reduce the Chk1-HA phosphorylation any further, suggesting the Rad9 AAD has no role in the G2 damage checkpoint (Figure 4-6A, B).

To confirm the role of the Rad9 AAD in the intra S damage checkpoint, but not the G2 checkpoint, *rad9+* or *rad9-2A* cells were synchronised at the G1/S boundary using the cdc10-M17 temperature sensitive mutant and were irradiated with 80 Gy ionising radiation. Chk1-HA and H2A phosphorylation were monitored as cells progressed through S-phase into G2 as visualised by FACS analysis (Figure 4-7A, B). Ionising radiation of asynchronous cells, and no IR in *cdc10-M17* synchronised cells were used as controls (Figure 4-7A, B). Consistent with the results in Figure 4-6, no reduction in Chk1-HA or H2A phosphorylation can be seen after IR treatment of asynchronous cells in the *rad9-2A* mutant and no phosphorylation is present in the no IR *cdc10* synchronised control cells (Figure 4-7A). Contrary to this, a reduction in both Chk1-HA and (less obviously) H2A phosphorylation can be seen after IR in G1/S of *rad9-2A* mutant cells compared to *rad9+*. The *rad9-2A* mutant cells show a reduction in Chk1-HA phosphorylation at the 0, 30, 60 and 90 minute time points after IR and release. Importantly no reduction in Chk1-HA phosphorylation can be seen in rad9-2A as cells enter G2-phase at the 120 minute time point (Figure 4-7A, B). A similar pattern of H2A phosphorylation is apparent with a reduction in γH2A being observed at the 0, 30 and 60 minute time points after IR and release in rad9-2A (Figure 4-7A).

These results suggest that the Rad9 AAD is important for Rad3 activation, after damage, in S-phase. It also suggests that the Rad4-AAD cannot completely compensate for the Rad9 AAD after IR in S-phase, as it can after UV damage in asynchronous cells (Figure 4-5A, B, Figure 4-7A, B). Importantly, the reduction in H2A phosphorylation shows that it is probably a reduction in Rad3 activity, not just a problem with recruitment of the proteins required for Chk1 localisation. This is because, unlike Chk1, H2A is always at the chromatin and does not require other checkpoint factors for its localisation. Therefore, we can conclude that the *rad9-2A* mutant is not preventing Rad9 binding to Rad4 or any of its other binding partners, that are required for Chk1 localisation.

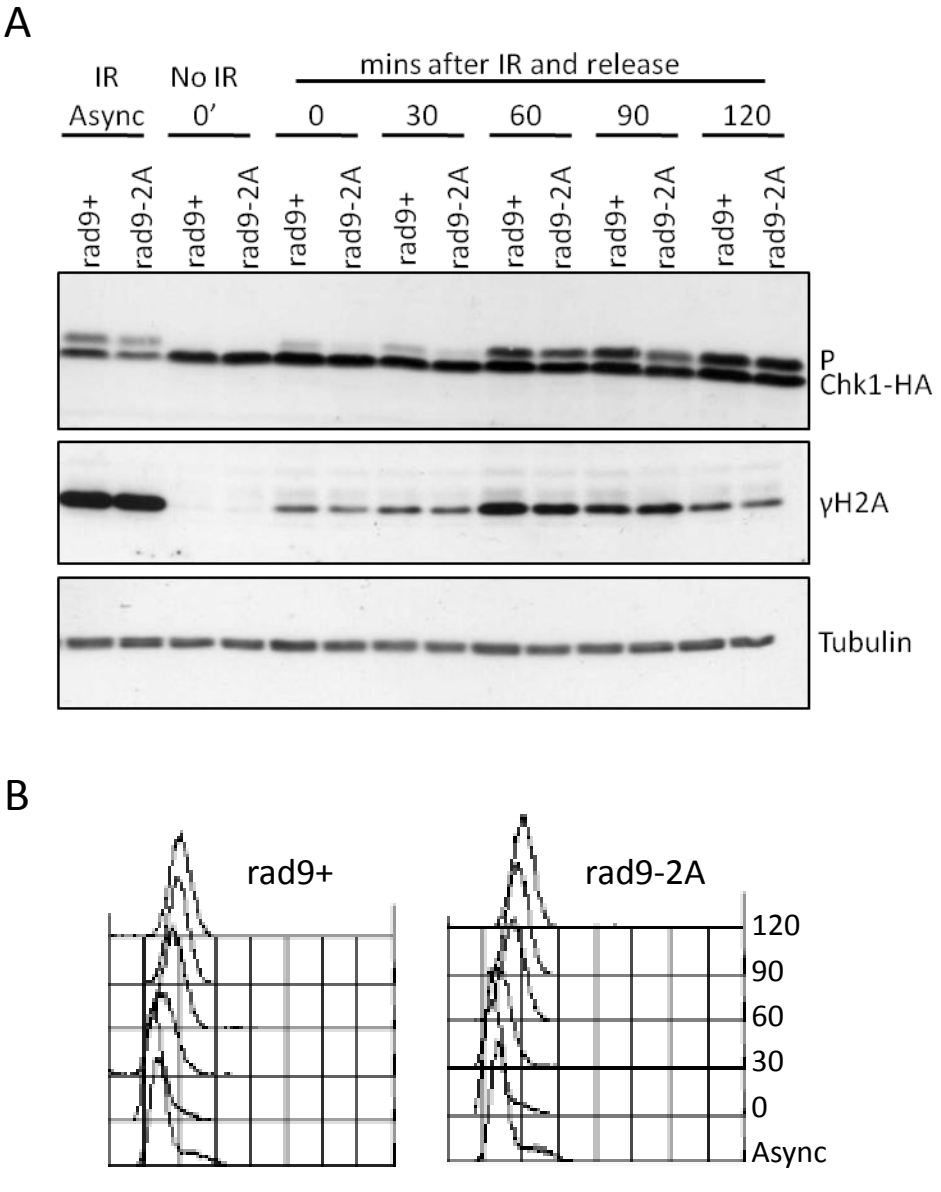

Figure 4-7. *rad9-2A* has a defect in Rad3 activation after IR in S-phase
A*. rad9+* and *rad9-2A* cells were synchronised at G1/S using a *cdc10-M17* arrest of 3.5 hours at 36°C. Cells were irradiated with 80Gy IR and immediately released into S-phase at 25°C. Chk1-HA and H2A phosphorylation was monitored by SDS PAGE using α-HA (top panel) or α-S129 (middle panel) respectively as a readout of Rad3 activation. α-Tubulin was used as a loading control (bottom panel). B. DNA content of cells in A was monitored by FACs analysis as an indicator of cell cycle progression. Cells progress from a 1C DNA content to a 2C content.

4.6 The Rad9 AAD Does Not Play a Major role in the Replication Checkpoint

As the *rad9-2A* mutant cells showed the highest sensitivity to HU when compared with other genotoxic agents, it is possible that the Rad9 AAD is important for activation of Rad3 within the replication checkpoint (as HU causes replication fork stalling) (Figure 4-3). Indeed Rad9 has previously been shown to be required for the replication checkpoint, although the downstream protein Crb2 is not required (Marchetti et al., 2002). Rad9 may therefore be playing a role, after fork stalling, other than its ability to recruit Rad4 and thus Crb2 to the chromatin-its roles after DNA damage. This new role may be the direct activation of Rad3. To test this hypothesis, the *rad9-2A* strain was crossed with a *chk1Δ* mutant and a spot test was performed (Figure 4-8). If the Rad9 AAD is activating Rad3 in the Cds1 dependent replication checkpoint, crossing it with a *chk1Δ* will abrogate both the damage and replication checkpoints. This should increase the sensitivity of the rad9-2A mutant to replication fork stalling, as the damage checkpoint cannot activate if the unstabilised stalled forks collapse.

Although the *rad9-2A chk1Δ* strain is more sensitive to HU than either of the single mutants, the increase in sensitivity is only mild. At 2 mM HU the *rad9-2A* and *chk1Δ* mutants alone do not show any sensitivity to HU, whereas the double mutant shows a slight sensitivity, but not to the extent as a *cds1Δ* or *rad3Δ*. Some UV damage may also lead to replication fork stalling and activation of the replication checkpoint as well as the damage checkpoint. Therefore, the *rad9-2A chk1Δ* strain was also spotted and UV radiated (Figure 4-8). Again the *rad9-2A chk1Δ* cells showed very little increase in sensitivity compared to the *chk1Δ* cells, and this increase can only be seen at the higher doses. Furthermore, the *rad9-2A chk1Δ* strain is not as sensitive as a *rad3Δ* strain to UV, and the *rad9-2A* mutant strain alone is not as sensitive as a *cds1Δ* strain (Figure 4-8).

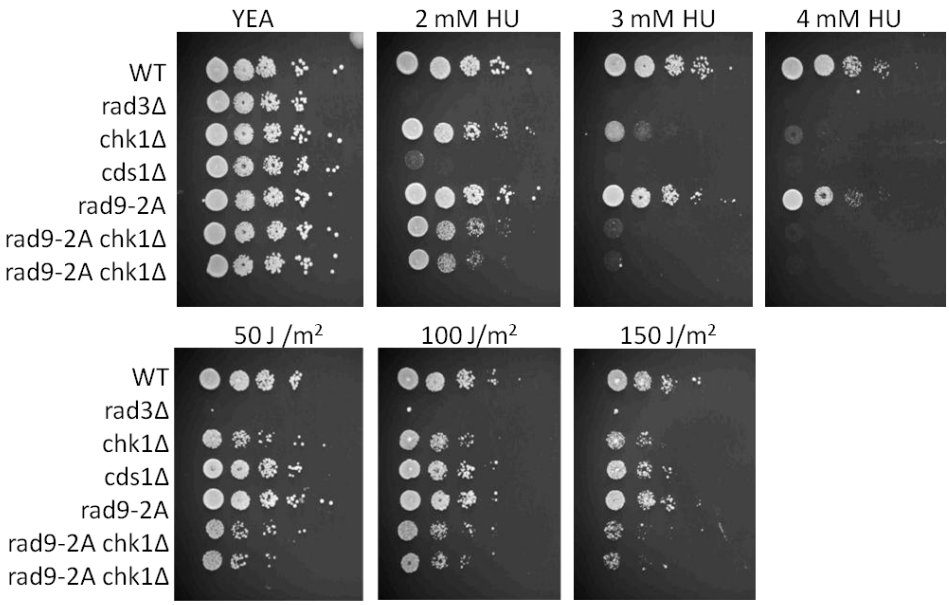

Figure 4-8. The Rad9 AAD plays a minor role in the replication checkpoint
Spot test analysis of *rad9+* (WT), *rad9-2A* and *rad9-2A chk1Δ* in the presence of the indicated doses of HU and UV. *rad3Δ* and *cds1Δ* were used as positive controls. 10-fold serial dilutions of $1x10^7$ cells/ml were spotted onto YEA plates containing HU or alternatively onto YEA containing no genotoxic agents and UV irradiated. Plates were incubated for 4 days at 30°C.

Together the results from Figure 4-8 suggest that the Rad9-AAD does not play a major role in the activation of Rad3 in the replication checkpoint and is therefore most likely only playing a role after damage in S-phase. The sensitivity seen to HU in Figure 4-3 is a relatively high dose of HU, which may therefore result in fork collapse and thus the activation of the damage checkpoint.

4.7 Conclusions and Discussion

In this chapter, data implicating *S. pombe* Rad9 as a Rad3 activator has been presented, the ATR Activation Domain residues have been identified and characterised their role in the DNA damage checkpoint. Mutation of these *rad9* AAD residues, Y271 and W348, has no effect on the unperturbed cell cycle (Figure 4-2A, B), but do show some mild sensitivity to genotoxic agents that have most of their effect in S-phase (Figure4-3A).At least some of this increase in sensitivity is likely to be due to a reduction in Rad3 activation: a moderate reduction in Chk1 and H2A phosphorylation can be seen in G1/S synchronised but not asynchronous cells after IR damage (Figure 4-7A, B; Figure 4-6A, B). Interestingly, increased sensitivity to genotoxic agents can be seen after combination of the *rad9* AAD mutant with the rad4 AAD mutant, rad4-Y599R, (Figure4-3). This is also confirmed by the reduction in Chk1-HA phosphorylation seen in the double *rad9-2A rad4-Y599R* compared with the single mutant cells alone after UV (Figure 4-5A). Indeed the % Chk1-HA phosphorylation at 150 J/m^2 in the double mutant was only ~20% of the *rad9+* or *rad9-2A* mutants alone and ~30% less than that of the *rad4-Y599R* strain (Figure 4-5B). The Rad9 AAD is therefore acting independently of the Rad4 AAD and is playing a semi redundant role in the activation of Rad3 after DNA damage in S-phase.

This role may be most important after large amounts of S-phase damage, such as that caused by IR in S-phase synchronised cells. This is because a reduction in Chk1-HA phosphorylation can be seen in the *rad9-2A* single mutant after IR in S-phase, but not after UV in asynchronous cells even though UV causes most of its damage

in S-phase (Figure 4-7A, B and Figure 4-6A, B). The Rad9 AAD appears not to be involved in the activation of Rad3 in the G2 ssDNA pathway of checkpoint activation, as first hypothesised. It also appears not to play a major role in the activation of Rad3 after replication fork stalling, although it may have a small contribution to this pathway (Figure 4-8).

From the results in Chapter 3 and the results in this chapter, a model for the relative contributions each pathway plays in Rad3 and checkpoint activation can be made (Figure 4-9). After Damage in S-phase the major pathway to Rad3 activation is the ssDNA pathway (Figure 3-14A, B and Figure 4-9). The Rad4 AAD pathway is the next most important in S-phase and is required to amplify the levels of active Rad3 (Figure 3-14A, B and Figure 4-9).The Rad9 AAD pathway is then also required for Rad3 activation in S-phase, but its role can be compensated for by the Rad4 AAD pathway, presumably by the Rad4 AAD pathway further amplifying the active levels of Rad3 to compensate for the loss of the Rad9 AAD. In G2 phase, the ssDNA pathway to Rad3 activation is required for almost all Rad3 activation; however the Rad4 AAD may play a small role depending on ssDNA levels (Figure 4-9).

The conclusions drawn from this chapter for the role of the *S. pombe* Rad9 AAD differ to those previously reported for the budding yeast homolog Ddc1. The Ddc1 AAD plays a much more important role in Mec1 (Rad3) activation than the spRad9 AAD. In budding yeast, as already mentioned, the Dpb11 AAD plays a relatively minor role and is partially redundant with the Ddc1 AAD (Navadgi-Patil and Burgers, 2009). It would therefore seem that during evolution the importance of the Rad9 AAD in *S. pombe* has decreased, and that of the *S. pombe* Rad4 AAD has increased. In the Xenopus and mammalian systems the TopBP1 AAD seems to be very important for ATR activation. Furthermore it appears from Figure 4-1A that the Rad9 AAD residues are not conserved in Xenopus Rad9 or human Rad9A, suggesting that in higher eukaryotes, Rad9 does not have any ATR activating function. However, it has been shown that the residue in human Rad9A corresponding to Y271 in spRad9 and W352 in scDdc1 (H239) is exposed on the surface of the protein when mapped on to the crystal structure and a H239R heterozygous mutant has been found in 16% of patients with lung adenocarcinoma.

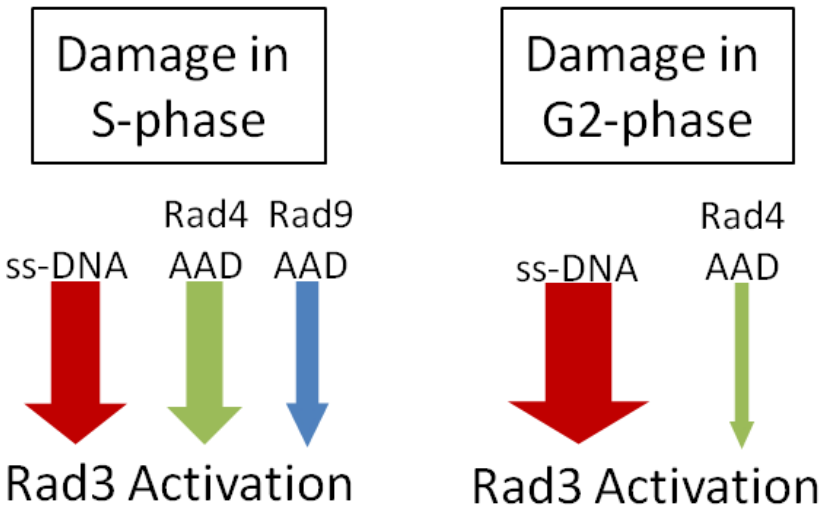

Figure 4-9. Model: The Rad9 AAD plays a minor, semi-redundant, role in Rad3 activation in S-phase

Diagram displaying a model for the relative importance of each of the Rad3 activation pathways in *S.pombe* after damage in S and G2 phases. Thickness of arrow represents the contribution of the Rad4 AAD, Rad9 AAD or ssDNA dependent pathways to Rad3 activation. In S-phase all three pathways play some role in Rad3 activation. However, in G2 most of the Rad3 activation occurs via the ssDNA pathway with the Rad4 AAD may be playing a minor role if levels of ssDNA are low. The Rad9 AAD pathway plays no role in G2. See main text for further detail.

This does suggest it may have an important role (Maniwa et al., 2006, Navadgi-Patil and Burgers, 2009). It is still to be seen if this is in the stimulation of ATR kinase activity.

The cell cycle dependency of the Rad9 AAD also differs between budding and fission yeast, with the Ddc1 AAD being most important in G1 and G2 phases and not being required in S-phase. This is similar to the Rad4 (Dpb11) AAD, which also has distinct cell cycle role between the two organisms. The recent characterisation of DNA2 as the S-phase activator of Mec1 in *S. cerevisiae* suggests that at least one other Rad3 activator maybe be present in *S. pombe* and it is likely this may have a role in Rad3 activation during G2 (Kumar and Burgers, 2013).

Chapter 5

Sequential Phosphorylation of Crb2 by Cdc2 is Required for the Activation of the DNA Damage Checkpoint

5.1 Background

As described in the "1.5.5 The Activation of the ATR Checkpoint Pathway" and "1.6.3 TopBP1 as a scaffold in the DNA Checkpoints" sections, Rad4 acts as a scaffold protein during the activation of the DNA damage checkpoint, by coupling Rad9 (of the 9-1-1 complex) to the mediator protein Crb2 (Garcia et al., 2005). Saka et al., (1997) first identified the interaction between Rad4 and Crb2 by yeast two hybrid and an in *vitro* binding assay (Saka et al., 1997). Crb2 was then shown to be phosphorylated by Cdc2 in a cell cycle and DNA damage dependent manner on T215 (Esashi and Yanagida, 1999). However, a number of reports assigning different functions to the phosphorylation of T215 by Cdc2 have been made. Initially it was reported that the phosphorylation of Crb2-T215 by Cdc2 was required to turn off the DNA damage checkpoint and allow cells to re-enter the cell cycle after damage. It was shown that *crb2-T215A* mutant cells remained arrested with phosphorylated (active) Chk1 even after the DNA had been repaired. However, this study was carried out in *crb2Δ* cells with either *crb2* or *crb2-T215A* highly over expressed from plasmids, the results may therefore be affected by the experimental method used.

A later study showed that Crb2-T215 phosphorylation was required for a late stage of homologous recombination-dependent DNA repair in G2, therefore implicating this Cdc2 dependent phosphorylation in a process other than the damage checkpoint (Caspari et al., 2002). The T215 phosphorylation was then shown to be important for a

full DNA damage checkpoint response. It was shown that a *crb2-T215A* mutant was able to initiate but not sustain Chk1 phosphorylation after DNA damage. In the absence of T215 phosphorylation the interaction between Crb2 and γH2A became essential for checkpoint activation. Furthermore, in a strain where Cdc2 is inactivated and the H2A phosphorylation sites mutated, Chk1 phosphorylation is greatly impaired (Nakamura et al., 2005). This data pointed to the phosphorylation of Crb2-T215 being important for a second pathway of Crb2 recruitment to damage sites that is independent of histone modification. Indeed it was shown, by yeast two hybrid, that the interaction originally seen between Crb2 and Rad4 was dependent on Crb2 -T215 phosphorylation and the BRCT1 and 2 domain containing N-terminus of Rad4. Furthermore, fluorescence microscopy at a HO induced double strand break showed that Crb2 foci can still be seen in a *H2A-AQ* mutant or a *crb2-T215A* mutant, but not in a strain where both mutations were present. This therefore proved that Crb2-T215 phosphorylation by Cdc2 was important for Crb2 recruitment to damage sites and for the DNA damage checkpoint, in a pathway distinct from the chromatin dependent pathway (Du et al., 2006). However, a *crb2-T215A* mutant is only mildly sensitive to DNA damage as it only shows a very modest reduction in viability after IR (Nakamura et al., 2005). Also *a crb2-T215A* mutant combined with a set9Δ (the methylase required for H4-K20Me and therefore crb2's interaction with the chromatin) is not as sensitive as a *crb2Δ* (Du et al., 2006).

This therefore points to other additional requirements for Crb2 recruitment to damage sites and the subsequent recruitment and activation of Chk1. In budding yeast, a number of Cdk1 phosphorylation sites have been identified on the Crb2 homolog Rad9. Initially Granata et al., (2010) showed, by yeast two hybrid and IP, that $Rad9^{Crb2}$S11 was required for the Rad9 interaction with $Dpb11^{Rad4}$. This, as with Crb2-T215, was required for checkpoint activation in a separate pathway to histone modification (Granata et al., 2010). Subsequently (as described in the "1.6.3 TopBP1 as a scaffold in the DNA Checkpoints" section) two more Cdk1 dependent phosphorylation sites were identified on $Rad9^{Crb2}$, S462 and T474, and these were shown to be sufficient for the interaction between Rad9 and the Dpb11 N-terminus.

These sites are cell cycle regulated and required for checkpoint activation in G2, especially when the *set9* homolog *dot1* is deleted (Pfander and Diffley, 2011).

5.2 Identification of Two Additional Cdc2 Sites on Crb2, Du Laboratory Data

The conflicting data with regard to the function of Crb2-T215 phosphorylation, the relatively high viability seen in a *crb2-T215A* mutant, the sensitivity of *crb2-T215A set9Δ* being lower than a *crb2Δ* and the existence of multiple Cdk1 phosphorylation sites on budding yeast $Rad9^{Crb2}$, prompted our collaborator Li Lin Du to search for additional Cdc2 sites on Crb2 that maybe playing a role in checkpoint activation. Using sequence alignments and truncation experiments, the Du laboratory were able to identify two additional potential phosphorylation sites, T187 and T235, on the N-terminus of Crb2, one on either side of the T215 site (Figure 5-1A). T235 is a canonical Cdk (Cdc2) TP site, where as T187 is a TV site which is not a canonical phosphorylation site for any known kinase (Figure 5-1B). Using a HO DSB assay, they showed that mutation of T187, T215 or T235 to alanine in a reporter construct in which Crb2 has been truncated to remove the Tudor and BRCT domains (preventing interaction with the chromatin), and which had a Leucine zipper, to still allow dimerisation (*crb2 (67-353)-LZ*), prevented foci formation. i.e. T187, T215 and T235 are all required for Crb2 localisation to a DSB, as seen by foci formation when crb2 cannot bind the chromatin, suggesting they may be required for checkpoint activation.

The Du laboratory then went on show that, in this reporter construct, all three of the T to A mutants were sensitive to IR and UV. To see if the newly identified sites T187 and T235 were indeed phosphorylated, the Du laboratory had phospho-antibodies generated against the two sites. They showed that both sites were indeed phosphorylated in *nda3-KM311* (G2/M) arrested cells when Cdc2 activity is highest, but were not phosphorylated in the alanine mutants. This also implies that no DNA damage is required for these phosphorylations.

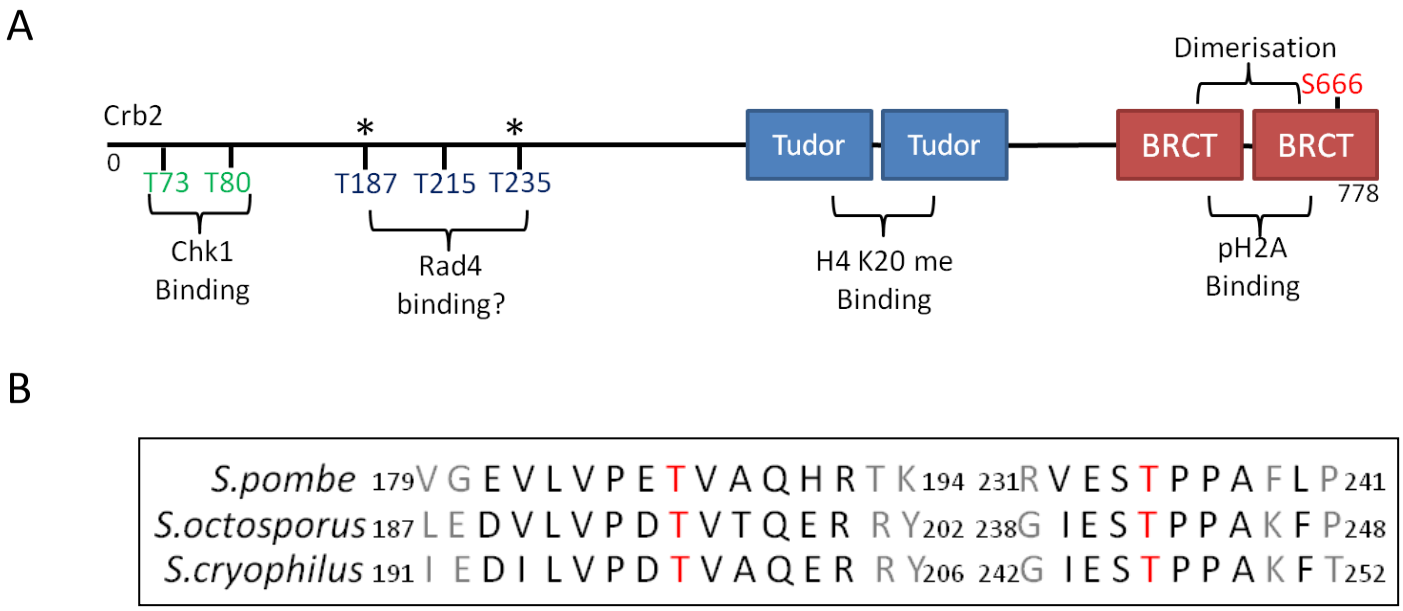

Figure 5-1. Position of potential phosphorylation sites on Crb2 required for Rad4 binding

A. Schematic of Crb2 domain architecture showing; the tandem BRCT domains required for γH2A (pH2A) binding and dimerisation (red boxes), the S666 residue required for dimerisation (red text), the H4K20me binding Tudor domain (blue boxes), the Rad3 dependent phosphorylation sites required for Chk1 binding (green text) and the potential phosphorylation sites required for Rad4 binding (blue text). T215 is the previously characterised site, T187 and T235 marked with a * are the ones characterised as part of this study. B. Sequence alignment of *S.pombe* sequence with that of *S.octosporus and S.cryophilus.* Potential phosphorylation sites T187 and T235 are in red.

As T187 is not a consensus site for any known kinase, it was important to identify the kinase that was phosphorylating this site. Using recombinant protein and a Crb2 peptide (1-265) they showed, in *vitro*, that it was indeed Cdc2-Cdc13 that was phosphorylating T187 and not two other possible candidates; Chk1 or Cds1. Interestingly in *vitro* and in *vivo* T187 phosphorylation was dependent on T215 and T235 being available for phosphorylation. Mutation of T215 or T235 to alanine abolished Crb2 (67-358)-LZ T187 phosphorylation in *nda3-KM311* arrested cells. In *vitro* a moderate reduction of T187 phosphorylation could be seen in a peptide harbouring T215A T235A mutations. This suggested that T187 phosphorylation may be regulated in some way by the prior phosphorylation of T215 and T235.

As homodimerisation of Crb2 is essential for its function, it was interesting to see if both molecules within a dimer had to be phosphorylated on T187 for resistance to DNA damage and recruitment to the HO break site. To this end, the Du laboratory constructed a system in which crb2 (67-358) was tagged with either YFP or the GFP binding protein (GBP). These two constructs were co-expressed from plasmids and led to Crb2 foci formation which localised with Rad52 foci (a DNA repair protein) after HO break induction. No Crb2 foci were seen if only one of the constructs was expressed. This therefore showed that the YFP and GBP tags were sufficient for Crb2 dimerisation and thus localisation to DNA damage sites. If T187 was mutated to alanine in both or either one of the constructs, Crb2 foci formation after HO induction was no longer seen. This suggested that T187 phosphorylation was required on both Crb2 molecules of a dimer. Furthermore both T187 sites of the dimer had to be available for phosphorylation for resistance to IR or UV damage. Mutation of both T187 sites led to high sensitivity to DNA damage, whereas mutation of one or the other led to intermediate sensitivity.

5.3 crb2-T187A is More Sensitive to DNA Damage Than *T215A* or *T235A*

To confirm that full length *crb2-T187A*, *T215A* and *T235A* are sensitive to DNA damage, not just the Du laboratories reporter constructs, a Crb2 base strain was

constructed (materials and Methods) and the three mutants made by RMCE ((Watson et al., 2008); Material and Methods). A spot test was then carried out after UV or ionising radiation using *crb2+*, *crb2Δ* (base strain), *T187A*, *T215A* and *T235A* cultures. In this case the *crb2-T187A* mutant showed strong sensitivity to both UV and IR, which was comparable to that of the crb2Δ (Figure 5-2A). The *crb2-T215A* and *T235A* exhibit a mild level of sensitivity to DNA damage which is between that of *crb2+* (WT) and the *T187A* or *crb2Δ*. This suggests that these sites may be less important than the T187 site (Figure 5-2A). Interestingly, if the *T215A* and *T235A* mutants are combined they now show sensitivity to a similar level of severity as the *crb2Δ*, implying that they are additive and maybe able to partially compensate for each other.

5.4 crb2-T187A, *T215A* and *T235A* Exhibit a DNA Damage Checkpoint Defect

To see if the sensitivities of the Crb2 phospho mutants to DNA damaging agents relate to a checkpoint defect, a G2 checkpoint assay was carried out (Figure 5-3). In this assay cells are synchronised in G2 by lactose gradient and exposed to either no damage, 100 Gy or 250 Gy of ionising radiation. The time it takes for cells to progress into mitosis is then measured by mitotic index (% of post mitotic cells). If there is a defect in the G2 DNA damage checkpoint then cells will progress into mitosis faster than WT and will not exhibit a robust DNA damage-dependent checkpoint delay. From Figure 5-3 it can be seen that *crb2+* cells show a checkpoint delay of ~60 minutes after 100 Gy compared to 0 Gy, this is then increased to ~120 minutes after 250 Gy. However, in the *crb2-T187A* mutant only a very modest delay of ~20 minutes can be seen after 100 Gy and this is barely increased after 250 Gy. This suggests, in this assay, that the *crb2-T187A* strain is almost entirely G2 checkpoint defective (Figure 5-3). The *T215A* and *T235A* mutants show an almost identical and intermediate checkpoint delay with a ~50 minute delay after 100 Gy, which is not increased after 250 Gy. This is consistent with previous data from the Russell laboratory for *T215A* (Figure 5-3) (Nakamura et al., 2005).

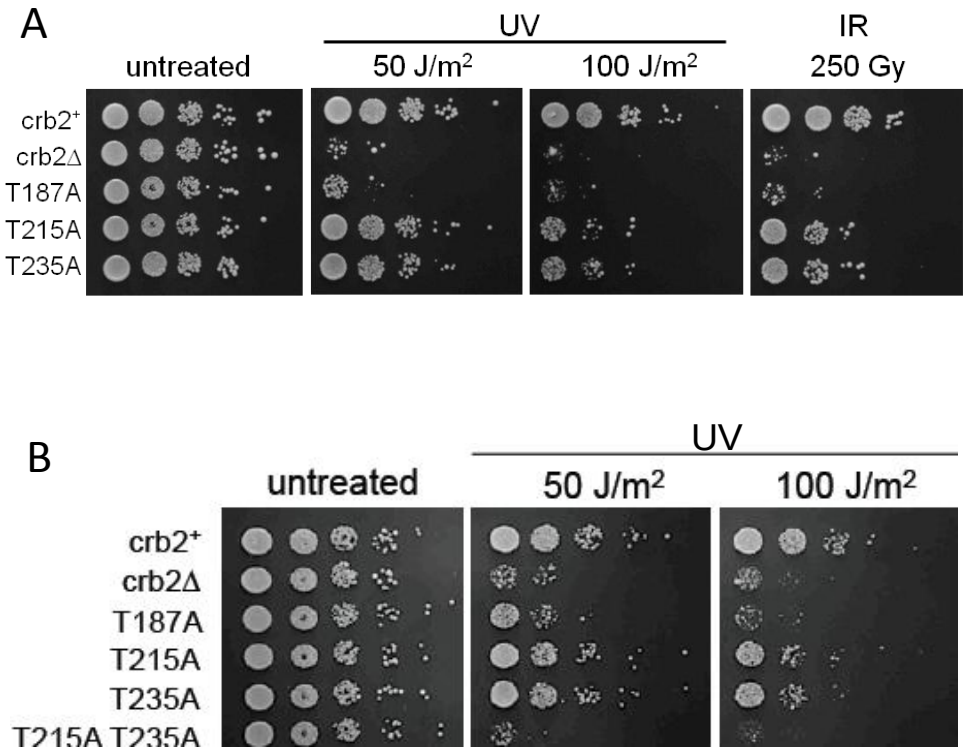

Figure 5-2. *crb2-T187A, T215A* and *T235A* are sensitive to DNA damaging agents

A. Spot test analysis of *crb2+ (WT), crb2Δ, crb2-T187A, crb2-T215A* and *crb2-T235A* after the indicated doses of UV or ionising radiation or after no damage (untreated). 10-fold serial dilutions of $1x10^7$ cells/ml were spotted onto YEA plates and UV irradiated or not. Alternatively for IR cells were γ irradiated, serial diluted and then spotted onto YEA. Plates were incubated at 30°C for 4 days. B. Spot test analysis of *crb2+ (WT), crb2Δ, crb2-T187A, crb2-T215A, crb2-T235A* and *crb2-T215A T235A* double mutant after the indicated doses of UV or no damage, carried out as for UV/no damage in A.

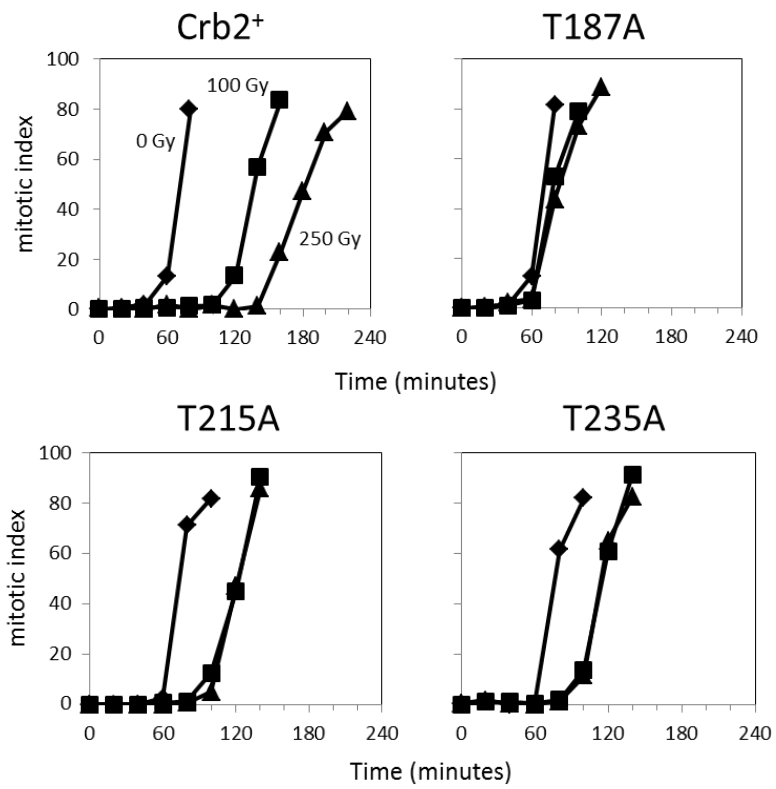

Figure 5-3. *crb2 T187A, T215A, T235A* exhibit a checkpoint defect after ionising radiation

G2 checkpoint assay. The indicated strains were synchronised in G2 via lactose gradient, split and treated with 0 Gy, 100 Gy or 250 Gy. Cells were then grown in YE at 30°C with samples being taken every 20 minutes to measure cell cycle progression. Cell cycle progression was monitored by mitotic index via fluorescence microscopy on DAPI stained fixed cells until ~ 80% of cells had progressed to mitosis. A reduction in time compared to WT indicates a G2 checkpoint defect.

To see if the checkpoint defects seen in the Crb2 phospho mutants are due to a reduction in Chk1 phosphorylation by Rad3, western blot analysis was carried out. Asynchonous *crb2+, T187A, T215A, T235A* and *T215A T235A* cells were exposed to increasing doses of IR, Chk1-HA and H2A phosphorylation was then monitored by western blot (Figure 5-4A). The *T187A* mutant shows no Chk1-HA phosphorylation even at the relatively high 500 Gy dose, which is consistent with the sensitivity and mitotic index data (Figure 5-2A, Figure 5-3, Figure 5-4A). Furthermore, the *T215A* and *T235A* mutants show a very similar intermediate level of Chk1-HA phosphorylation which is less than *crb2+* but not completely abolished (Figure 5-4A). Again this is consistent with the spot test and mitotic index assays. However, slightly inconsistent with the mitotic index data, an increase in Chk1-HA phosphorylation can be seen between 100 Gy and 250 Gy, whereas in Figure 5-3 an increase in cell cycle delay could not (Figure 5-2A, Figure 5-3, Figure5-4A). One reason for this may be that the mitotic index experiment was carried out before the construction of the *crb2* base strain and was therefore done in strains obtained from the Du laboratory. In these strains *crb2* is integrated at the exogenous *leu1* locus and is tagged with 2xYFP. *chk1* is also tagged in these strains with 9myc2HA6His, this may have a mild effect on the phenotypes seen. None the less the *T215A* and *T235A* mutants show a consistent intermediate phenotype.

Interestingly, when combined, the *T215A T235A* double mutant shows an additive reduction in Chk1-HA phosphorylation and exhibits no phosphorylation at any of the IR doses tested. This is similar to that in seen in the *T187A* mutant and consistent with the spot test in Figure 5-2B (Figure 5-4A). Importantly no reduction in phosphorylated H2A (γH2A) can be seen in any of the *crb2* mutants (Figure 5-4A). This implies that Rad3 is still active and can phosphorylate its downstream targets (unlike that seen for the *rad4-Y599R* in Chapter 3). The checkpoint defect seen in the *crb2* phospho mutants is most likely due to a problem in recruiting Crb2 and/or Chk1 to the damage site, not in Rad3 activation per se.

A similar experiment to that in Figure 5-4A was carried out to test if the *crb2* mutants display the same Chk1-HA phosphorylation defect to UV as they do to IR (Figure 5-4B).

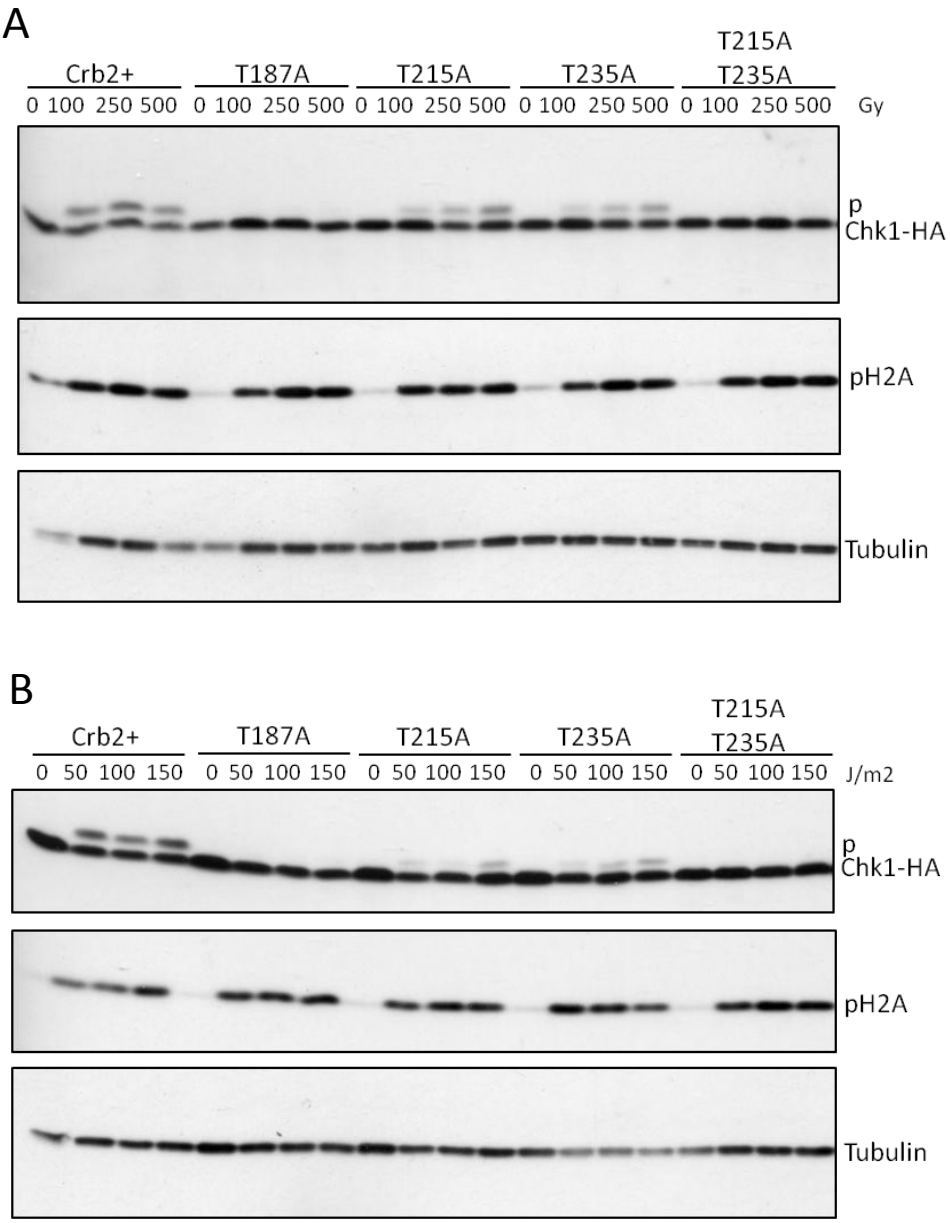

Figure 5-4. The *crb2* phsopho-mutants show reduced Chk1-HA phosphorylation after damage.

A. Checkpoint activation was assayed in the indicated strains after ionising radiation via Chk1-HA and H2A phosphorylation. Asynchronous *crb2+, crb2-T187A (T187A), crb2-T215A (T215A) crb2-T235A (T235A)* and *Crb2-T215A/T235A (T215A T235A)* cells were exposed to γ-radiation at the indicated doses. ChK1-HA phosphorylation (P) was assayed by SDS PAGE using α-HA (top panel) and H2A phosphorylation using α-S129. α-Tubulin was used as a loading control (bottom panel). B. As in A but after UV radiation

An almost identical pattern of both Chk1-HA and H2A phosphorylation can be seen after UV as it can after IR in all the *crb2* phospho mutants. *T187A* and *T215A T235A* show no Chk1-HA phosphorylation at any dose, whereas *T215A* and *T235A* show a moderate reduction in Chk1-HA phosphorylation. This is also consistent with Figure 5-2A and B (Figure 5-4B). No reduction in H2A phosphorylation can be seen in any of the *crb2* phospho mutants after UV, as with IR (Figure 5-4B). This suggests that the phosphorylation of Crb2 is important for checkpoint activation after both ionising radiation and UV damage.

5.5 Conversion of T187 to a Canonical Cdc2 Consensus Site Rescues the *T215A T235A* Checkpoint Defect

As phosphorylation of Crb2 on the non-canonical Cdc2 site (T187) is dependent on the canonical T215 and T235 being available for phosphorylation, a hierarchical mechanism of phosphorylation may be occurring in which the phosphorylation of the canonical sites are required for the phosphorylation of the non-canonical T187 (Du lab data). To test this, V188 on *crb2* was mutated via RMCE to give a canonical Cdc2 TP consensus site at T187 (V188P). The *V188P* mutant did not show any DNA damage sensitivity, suggesting that T187 is still phosphorylated and that converting it to a canonical site has no effect in an otherwise WT back ground (Figure 5-5). However, when the *V188P* mutation is made in a *crb2-T215A T235A* allele, the sensitivity of the *T215A T235A* mutant to DNA damage is partially rescued (Figure 5-5). The triple *V188P T215A T235A* is much less sensitive than the *T215A T235A*, *crb2Δ* and *T187A* and shows an intermediate level of sensitivity (Figure 5-5). This result suggest that there is indeed a hierarchical system of Crb2 phosphorylation and this is at least in part due to T187 being a non-canonical Cdc2 site.

To confirm this result and to see if the *V188P* mutation could restore the Chk1 phosphorylation defect seen in *T215A T235A* in Figure 5-4, Chk1 phosphorylation was assayed by western blot after DNA damage in asynchronous cells (Figure 5-6).

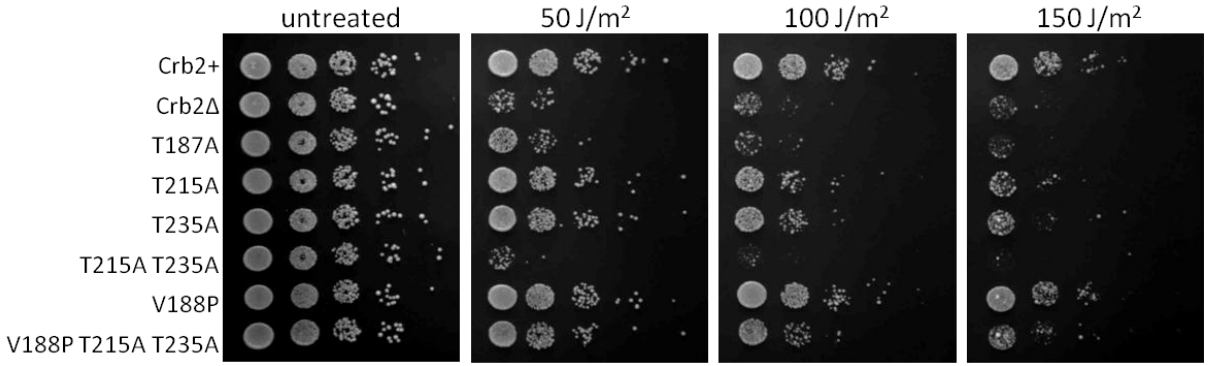

Figure 5-5. Conversion of *crb2-T187* to a canonical Cdc2 site partially rescues *crb2-T215A T235A* sensitivity to UV.

Spot test analysis of *crb2+ (WT), crb2Δ, crb2-T187A (T187A), crb2-T215A (T215A), crb2-T235A (T235A), crb2-T215A/T235A (T215A T235A), crb2-V188P (V188P)* and *crb2-V188P/T215A/T235A (V188P T215A T235A)* after UV radiation at the indicated doses or after no damage (untreated). 10-fold serial dilutions of $1x10^7$ cells/ml were spotted onto YEA plates and UV irradiated or not. Plates were incubated at 30°C for 4 days.

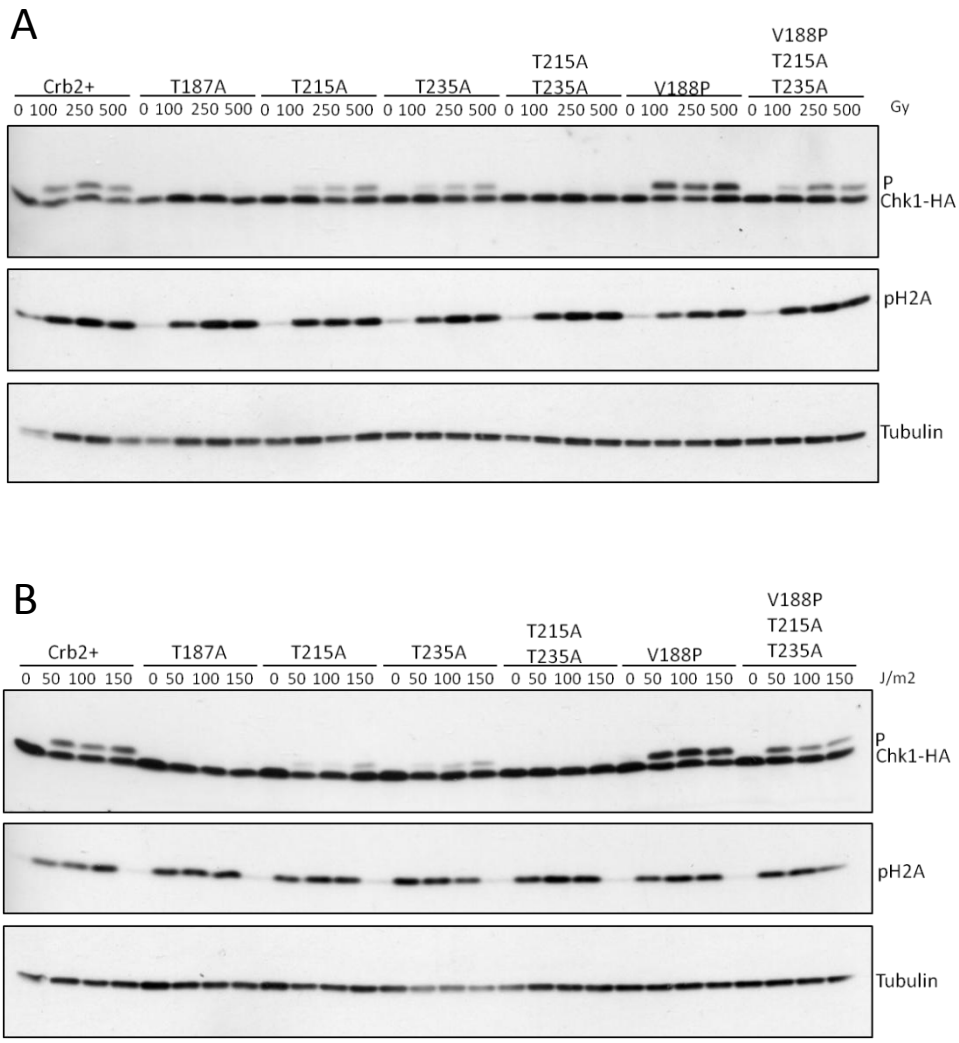

Figure 5-6. Conversion of *crb2-T187* to a canonical Cdc2 site partially rescues *crb2-T215A T235A* Chk1-HA phosphorylation defect after DNA damage.
A. Checkpoint activation was assayed in the indicated strains after ionising radiation via Chk1-HA and H2A phosphorylation. Asynchronous *crb2+* (WT), *crb2Δ*, *crb2-T187A (T187A)*, *crb2-T215A (T215A)*, *crb2-T235A (T235A)*, *crb2-T215A/T235A (T215A T235A)*, *crb2-V188P (V188P)* and *crb2-V188P/T215A/T235A (V188P T215A T235A)* cells were exposed to γ radiation at the indicated doses. ChK1-HA phosphorylation (P) was assayed by SDS PAGE using α-HA (top panel) and H2A phosphorylation using α-S129. α-Tubulin was used as a loading control (bottom panel). B. As in A but after UV radiation. Same blot as in Figure 5-4 except for V188P and V188P/T215/T235 lanes

Indeed, it can be seen, after both IR and UV damage, that the triple *V188P T215A T235A* mutant exhibits a higher level of phosphorylation than *T215A T235A* double (Figure 5-6A, B). This further adds to the notion that converting T187 to a Cdc2 consensus site partially bypasses the need for T215 and T235 phosphorylation in Chk1 activation. Interestingly, the *V188P* mutant showed higher Chk1-HA phosphorylation after both IR and UV damage than *crb2+* (Figure 5-6A, B). This may indicate that converting T187 to a TP site leads to a more robust checkpoint. It could, however, be due to loading inconsistencies between lanes, it is difficult to distinguish between these two possibilities using just the Tubulin loading control. The *V188P* mutation also has no effect on H2A phosphorylation as expected (Figure 5-6A, B).

5.6 Conclusion and Discussion

The data in this chapter, and that from Li Lin Du's laboratory, have identified two new Cdc2 dependent phosphorylation sites on Crb2, one canonical site and one non-canonical, that are phosphorylated in a non-damage dependent manner, both in *vivo* and in *vitro* (Du lab data; Figure 5-1B). These two sites, along with the already identified T215 site, are required for the activation of the DNA damage checkpoint after both ionising radiation and UV. The *T187A* mutant seems to be the most important of the three phosphorylation sites and displays a very strong sensitivity to DNA damage, similar to that seen in a *crb2Δ* (Figure5-2A). This sensitivity relates to a checkpoint defect, as seen by mitotic index and Chk1 phosphorylation (Figure 5-3, 5-4A, B). *crb2-T187A* displays almost no checkpoint arrest after ionising radiation and no visible Chk1-HA phosphorylation can be seen after IR or UV, even at high doses. This suggests that phosphorylation of this residue is critical for checkpoint activation (Figure5-3A, Figure5-4A,B).

As with previous studies, we show that the *T215A* mutation only displays a mild sensitivity to DNA damage and a mild checkpoint defect (Nakamura et al., 2005, Du et al., 2006). This is not consistent with it being the critical residue for Crb2 recruitment, as previously thought. Furthermore, we show that mutation of T235 to alanine displays

a phenotype almost identical to that of *T215A,* suggesting they both have equal importance in checkpoint activation. The combination of *T215A* and *T235A* results in an additive phenotype, implying that these phosphorylations have overlapping function, co-operate in the same process and may partially compensate for the loss of one or the other. The *T215A T235A* mutant displays a similar phenotype to that of *T187A*. This, in conjunction with the fact that T187 phosphorylation is dependent on T215 and T235, indicates a hierarchical system of Crb2 phosphorylation. Converting T187 from a TV to a TP site confirmed this notion, as it partially rescued the sensitivity and checkpoint defect seen in *T215A T235A*. From this data we can therefore build a model in which Cdc2-Cdc13 first phosphorylates Crb2 on both the T215 T235 canonical sites of the Crb2 dimer, independently of DNA damage, possibly in late S-phase (Figure 5-7A). These phosphorylations prime Crb2 for phosphorylation by Cdc2-cdc13 on the non-canonical T187 site, again most likely in a non-damage dependent manner, as phosphorylation can be seen in non-damaged G2/M arrested cells. It is this phosphorylation of T187 that is the most important for checkpoint activation (Figure 5-7B). The role of Cdc2 phosphorylation of Crb2, and its importance in checkpoint activation has therefore been further characterised. However, from the results in this chapter, the molecular mechanism underlying this hierarchical phosphorylation cannot be identified.

From this data, it can be predicted that the T187 phosphorylation is important for the interaction between Crb2 and Rad4 and maybe the critical residue for this interaction, rather than T215. It may be that the previous data showing a reduced interaction between Crb2 and Rad4 in the *T215A* mutant via yeast two hybrid is due to reduced phosphorylation of T187. This hypothesis, along with the mechanism of the hierarchical phosphorylation, will be explored in the next chapter.

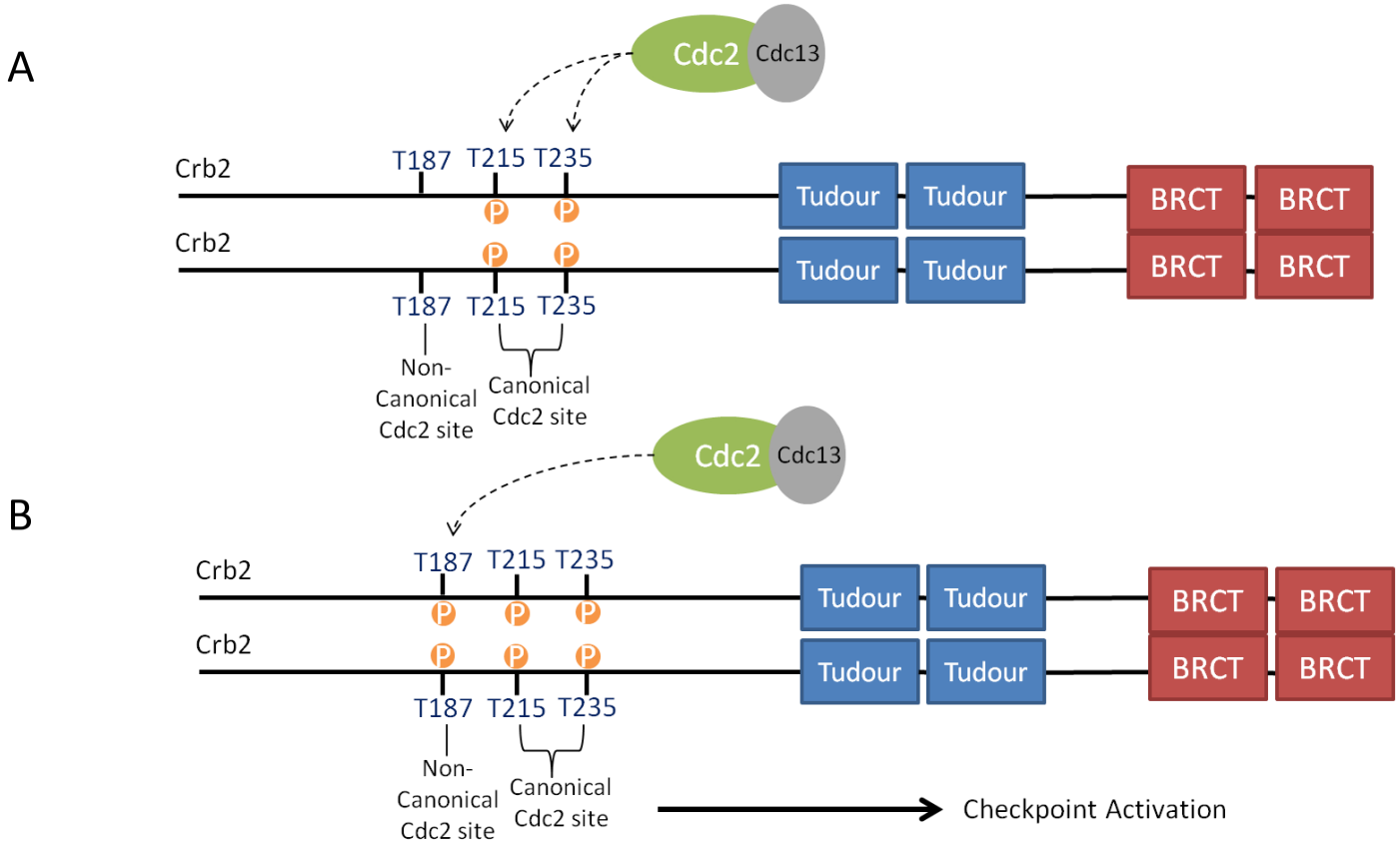

Figure 5-7. Hierarchical model of Crb2 phosphorylation by Cdc2-Cdc13.
A. Cdc2-Cdc13 phosphorylates both the canonical Crb2 T215 and T235 residues in the Crb2 dimer in late S/G2 phase as CDC2 activity increases. B. Once T215 and T235 are phosphorylated Cdc2-Cdc13 can then phosphorylate both the non-canonical T187 residues within the Crb2 dimer. The T187 phosphorylations are required for activation of the DNA damage checkpoint

Chapter 6

Rad4 BRCT Domains 1 and 2 Bind Cdc2 Phosphorylated Crb2

6.1 Background, Pearl and Du Laboratory Data

The data in chapter 5 and that from the Du lab showed that Crb2 is phosphorylated on three sites, T187, T215, T235 by Cdc2-Cdc13, and that this was required for checkpoint activation after DNA damage. Furthermore, phosphorylation of T187 appeared to be the most important for checkpoint activation and its phosphorylation was dependent on phosphorylation of T215 and T235. Mutation of T215 and T235 gave an intermediate phenotype, however when combined, a phenotype similar to that in a T187A mutant was seen.

To further understand the role of these phosphorylations and their hierarchical nature Mathieu Rappas and Tony Oliver of the Pearl laboratory, carried out in *vitro* binding assays and crystallography studies (Summarised in Figure 6-1A, B). The in *vitro* fluorescence polarisation (FP) studies showed that a peptide containing phosphorylated T187 bound to both Rad4 BRCTs 1 and 2 with high affinity, but bound BRCT1 most strongly. A phosphorylated T235 peptide also bound to Rad4 BRCT2, but with a moderate affinity, and did not bind BRCT1. Interestingly, phosphorylated T215, the previously characterised phosphorylation site, did not bind either BRCT1 or BRCT2 of Rad4 with any significant affinity. However, a peptide containing phosphorylation on both T215 and T235 showed a high affinity to a fragment of Rad4 containing functional BRCTs 1 and 2. This affinity was much stronger than either of the phosphorylations alone, suggesting that once pT235 has bound to BRCT2, pT215 can stabilise the interaction by associating with BRCT1 (Figure 6-1A, B). This data is consistent with the phenotypes of the *crb2* phospho-mutants seen in *vivo*. The phospho mutants that give the strongest checkpoint defect are the ones that bind Rad4 with the highest affinity.

A

Crb2 Phosphorylation Site	pT187	pT215	pT235	pT215 pT235
Kinase	Cdc2 (TV)	Cdc2 (TP)	Cdc2 (TP)	Cdc2 (TP TP)
Rad4 BRCT12 binding?	Yes	Weak, Non-specific?	Yes	Yes
BRCT1 Kd (μM)	0.37	> 47	>= 59.2	No Data
BRCT2 Kd (μM)	2.15	> 31	11.7	No Data
BRCT1&2 Kd (μM)	0.5	No binding	9.4	1.97

B

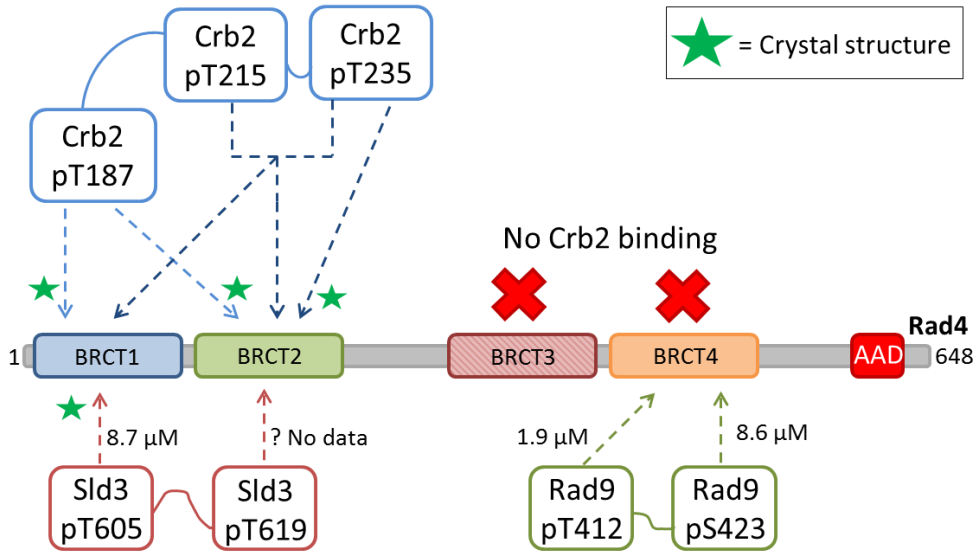

Figure 6-1. Summary of the Pearl laboratories in vitro binding assays and crystallography data.
A. Table summarising in vitro fluorescence polarisation data for Crb2 phospho-peptides and a fragment of recombinant Rad4 containing BRCT domains 1 and 2. To test the interaction with one or the other of the BRCT domains, mutations were made in the phospho binding pocket to prevent binding. B. Schematic diagram of Rad4 showing the position of each of the BRCT domains and which phospho-peptide binds to which BRCT. Interactions that the co-crystal structure has been solved are labelled. Figure A and B are adapted from those of Tony Oliver.

This suggests that the phosphorylations on T187, T215 and T235 are required for the interaction between Crb2 and Rad4. None of the Crb2 peptides tested bound to BRCTs 3 and 4, but peptides based on the previously characterised Rad9 phosphorylated residues, T412 and S423, did bind with relatively high affinity ((Furuya et al., 2004, Furuya et al., 2010)(Figure 6-1B).

To confirm these phospho-dependent interactions and to gain insight into the nature of the interaction between Rad4 and Crb2, Mathieu Rappas and Tony Oliver carried out co-crystallisation studies between Rad4 BRCTs 1 and 2 and the phosphorylated Crb2 peptides (Summarised in Figure 6-1B). Crystals were obtained for pT187 bound to both BRCTs 1 and 2 and for pT235 bound to BRCT2. pT605 of Sld3, which has been shown to be required for initiation of replication, also bound to BRCT1, albeit with lower affinity than T187, and co-crystallised (Fukuura et al., 2011) ("1.6.6 TopBp1 and Initiation of DNA Replication" section) (Figure 6-1B). It can also be predicted that Sld3 pT619 binds BRCT2, but no data was obtained for this.

To understand whether the phospho-interactions between Crb2 and Rad4 seen in *vitro* were also apparent in *vivo*, the Du laboratory carried out pull down assays. In these assays Crb2 peptides containing either pT187, pT215, pT235, pT215 pT235 or no phosphorylation were incubated with *S. pombe* extracts, the peptide was then pulled down and Rad4 was blotted for on a western blot. The non-phosphorylated peptide pulled down no Rad4. Consistent with the in *vitro* data, pT187 pulled down a large quantity of Rad4, pT215 pulled down no Rad4, pT235 pulled down a very small amount and the double pT215/pT235 pulled down almost as much as the pT187. This data therefore confirmed the in *vitro* data from the Pearl laboratory. The phospho sites that interacted most strongly in *vitro*, pT187 and pT215/pT235, interacted most strongly ex-*vivo*. It is also consistent with T187A and the T215A/T235A double having the most severe checkpoint defect (Chapter 5)

6.2 Creation of *rad4* BRCT1 Mutants

From the crystal structures obtained by the Pearl laboratory, the key residues in Rad4 BRCT1 required for binding to phosphorylated residues were identified. To see if Rad4 BRCT1 was indeed required for checkpoint activation, and to confirm that the phospho binding residues were binding phosphorylated Crb2, mutations were made in three residues within the BRCT phospho binding pocket (Figure 6-2A). The mutations made were *T15V, R22E, K56A* and *K56E*. As Rad4 BRCT1 also binds phosphorylated Sld3, and this is its essential function, there was a risk that mutation of the phospho binding pocket could be inviable. For this reason the *K56A* and *K56E* mutants were both constructed. K56E is a charge reversal mutation and should therefore prevent all phospho binding, whereas K56A is a charge neutralisation. K56A should give a milder reduction in binding and is predicted to have a less server phenotype, which is more likely to be viable if full disruption of the phospho-binding pocket is lethal.

The cassette exchange efficiency of the *rad4* mutants can be used as an indicator of the viability of the mutants. If, when inserting a mutant, the loss of the WT allele and associated *ura4* marker at the endogenous locus by RMCE leads to ~< 2% colony growth on 5-FOA (kills ura+ cells), then the mutation is most likely lethal. The remaining ~2% sur*vivo*rs are probably due to gene conversion events between the mutant and WT gene, leading to loss of the ura4 marker but the presence of a *WT rad4* allele (2.4.1 Recombination Mediated Cassette Exchange RMCE and 2.4.2 Creation of *rad4* Mutant Strains by RMCE) (Watson et al., 2008)). From Figure 6-2B it can be seen that all four mutants had a high cassette exchange efficiency and were viable. This suggests that BRCT1 is not essential for Rad4s role in the initiation of replication, even though it does bind to Sld3. Although the Rad4 BRCT1 mutants were viable, the mutations may still be having a significant detrimental effect on the initiation of replication. To ensure that this was not the case FACS analysis to obtain the cell's DNA content was carried out on exponentially growing *rad4+* (*WT*), *T15V, R22E, K56A* and *K56E* cells, at 30°C. It can be seen that all of the mutants have the same profile as the *rad4+* strain. It is, therefore, unlikely that they are significantly affecting the initiation of DNA replication at this temperature.

A

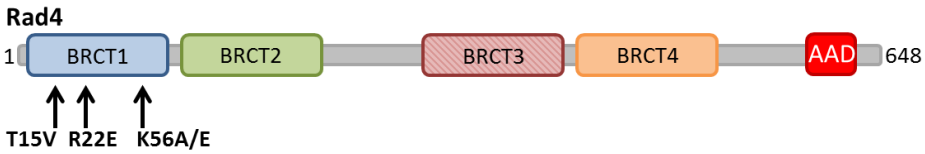

B

Strain	Cassette exchange efficiency	Viable?
WT	42%	Yes
rad4 T15V	16.6%	Yes
rad4 R22E	28%	Yes
rad4 K56A	11.5%	Yes
rad4 K56E	23.1%	Yes

C

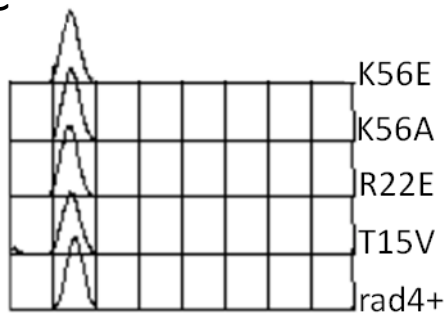

Figure 6-2. *rad4* BRCT1 phospho-binding pocket mutants are viable.
A. Diagram showing the position of the four *rad4* BRCT1 mutants, T15V, R22E, K56A, K56E, within Rad4. B. Table showing the cassette exchange efficiency for inserting WT, *rad4 T15V, R22E, K56A* and *K56E* into the Rad4 base strain. Efficiency is calculated as the number of colonies that grew on 5FOA plates as a percentage of the number of cells plated after cassette exchange. Viability was ensured by sequencing the DNA of the colonies that grew C. FACS profile of asynchronously growing *rad4+, rad4 T15V (T15V), rad4 R22E (R22E), rad4 K56A (K56A) and rad4 K56E (K56E)* strains, displaying a 2C DNA content

6.3 *rad4* BRCT1 Mutants Are Not Temperature Sensitive

As a commonly used temperature sensitive *rad4* mutant, *rad4-116,* used in the laboratory is at *T45* and leads to loss of viability at non permissive temperature, it is possible that the *T15V, R22E* and *K56A/E* mutants may also be temperature sensitive, due to their similar location (Fenech et al., 1991). To ensure that this is not the case, growth curves were carried out in *WT* and each of the mutant strains at 25°C and 36°C. If any of the mutants were temperature sensitive, and therefore had a defect in DNA replication initiation, then a slow growth phenotype would be observed at 36°C but not at 25°C. From Figure 6-3A it can be seen that the *WT* and all of the BRCT1 mutants grow at the same rate at both 25°C and 36°C. To ensure that this is the case, a spot test was also carried out with *rad4+* and the four BRCT1 mutants at 25°C, 30°C and 36°C (Figure 6-3B). Again no growth phenotype can be seen in any of the mutants, at any of the temperatures tested, confirming that the mutations made in rad4 BRCT1 are not temperature sensitive for replication initiation (Figure 6-3B). Furthermore, the cells are not elongated in any of the mutants at 36°C, suggesting no delay in cell cycle progression at this temperature (Figure 6-3C).

6.4 *rad4* BRCT1 Mutants are Sensitive to Genotoxic Agents and Display a Checkpoint Defect

To see if the Rad4 BRCT1 phospho binding mutants are involved in the activation of the DNA damage checkpoint, and, if so, in response to which types of DNA damage, spot tests were performed (Figure 6-4). It can be seen form Figure 6-4 that *T15V, K56A* and *K56E* are sensitive to all the genotoxic agents tested. *T15V* and *K56E* showed the strongest sensitivity, with K56A showing a slightly weaker phenotype (apparent after IR and CPT), as expected. As well as being sensitive to the DNA damaging agents, UV, CPT, IR and MMS *T15V* and *K56A/E* also showed sensitivity to high doses (4mM) of the RNR inhibitor (and therefore replication fork stalling) HU (Figure 6-4). This may imply a role for Rad4 BRCT1 in the replication checkpoint, however, at these doses it maybe that the forks collapse and the DNA damage checkpoint is activated.

A

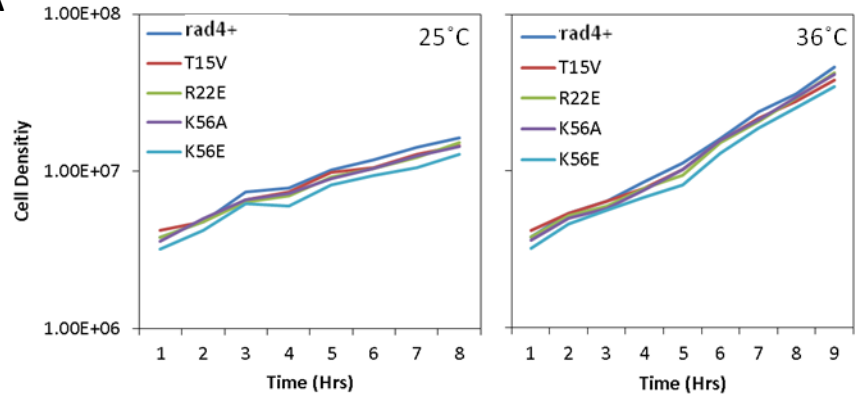
1.00E+08
1.00E+07
1.00E+06
Cell Density
rad4+
T15V
R22E
K56A
K56E
25˚C
36˚C
1 2 3 4 5 6 7 8
1 2 3 4 5 6 7 8 9
Time (Hrs)
Time (Hrs)

B

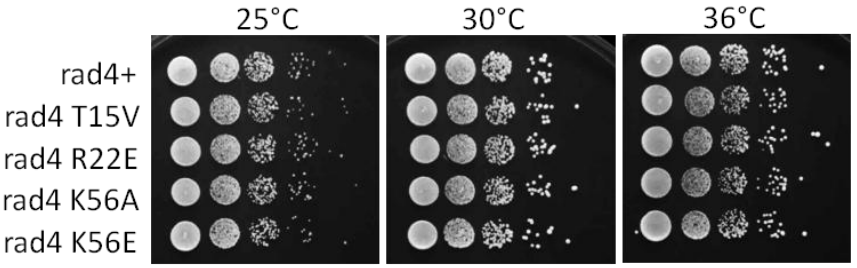
25°C
30°C
36°C
rad4+
rad4 T15V
rad4 R22E
rad4 K56A
rad4 K56E

C

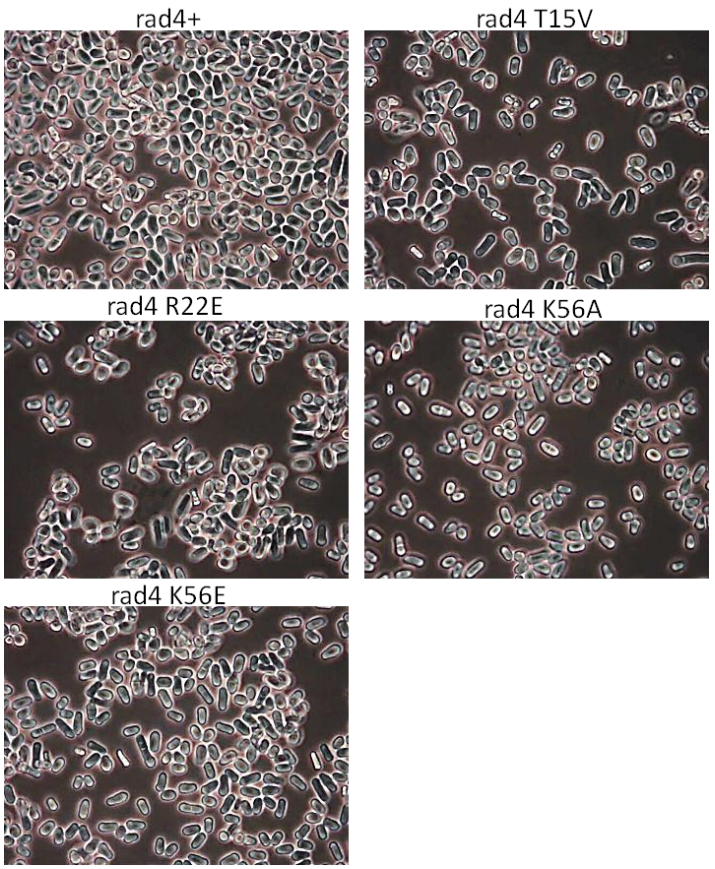
rad4+
rad4 T15V
rad4 R22E
rad4 K56A
rad4 K56E

Figure 6-3. *rad4* BRCT domain 1 mutants have no unperturbed cell cycle defects and are not TS

A. Exponentially growing *rad4+, rad4-T15V (T15V), rad4-R22E (R22E), rad4-K56A (K56A) and rad4-K56E (K56E)* strains were grown for 9 hours in YE at either 25°C or 36°C whilst being kept in exponential phase by dilution. Cell density was calculated every hour and adapted for the dilution factor. B. Spot test analysis of the *rad4* strains in A. 10-fold serial dilutions of $1x10^7$ cells/ml were spotted onto YEA plates and grown for 4 days at either 25°C, 30°C or 36°C. C. Light microscopy pictures of exponentially growing unfixed *rad4* strains from A 36°C.

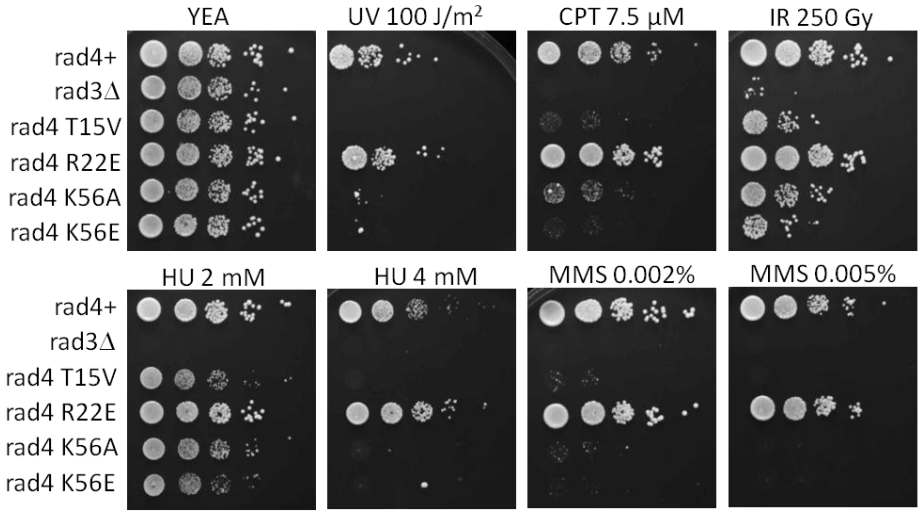

Figure 6-4. *rad4* BRCT domain 1 mutants are sensitive to genotoxic agents.

Spot test analysis of *rad4+, rad4-T15V, rad4-R22E, rad4-K56A, rad4-K56E* and *rad3Δ* positive control in the presence of different genotoxic agents 10-fold serial dilutions of $1x10^7$ cells/ml were spotted onto YEA plates containing CPT, MMS or HU. Alternatively they were spotted onto YEA containing no genotoxic agents and UV irradiated. For IR cells were γ irradiated, serial diluted and then spotted onto YEA. Plates were incubated at 30°C for 4 days

Interestingly *R22E* did not show any sensitivity to any of the DNA damaging or replication fork stalling agents tested, when compared with *rad4+*. In the crystal structures obtained by the Pearl laboratory, R22 was positioned as though it was flipped out of the phospho binding pocket of BRCT1. From looking at previously solved crystal structures of other BRCT domains, it was thought that this positioning of R22 may be a crystallographic artefact, and R22 is actually positioned facing into the phospho binding pocket in *vivo* (Tony Oliver personal communication). However, from the results in Figure 6-4 it would seem that R22 is indeed facing out of the phospho binding pocket and is not involved in the binding of phosphorylated residues.

To understand if the sensitivity of *rad4-T15V* and *K56E* to the genotoxic agents in Figure 6-4 is due to a defect in the DNA damage checkpoint, a G2 checkpoint assay was performed. Cells were synchronised in G2 by lactose gradient and exposed to either 0 Gy, 100 Gy or 250 Gy IR, cell cycle progression was then monitored by mitotic index (Figure 6-5). In *rad4+* (*WT*) cells, a delay of 80 minutes and 120 minutes after 100 Gy and 250 Gy respectively can be seen when compared with 0 Gy, thus showing that the G2 checkpoint is active. In both the *rad4-T15V* and *K56E* mutants, delays of only 20 minutes and 40 minutes after 100 Gy and 250 Gy respectively can be seen, strongly implying a major checkpoint defect in these mutants, as the cells barely arrest after damage (Figure 6-5). To understand if this is due to a reduction in Chk1 phosphorylation by Rad3, western blot analysis was carried out in the four *rad4* BRCT mutants after IR and UV (Figure 6-6 A, C). Consistent with the checkpoint assay in Figure 6-5, *rad4-T15V* and *K56E* show no visible Chk1-HA phosphorylation after ionising radiation even at the relatively high 500 Gy dose. Surprisingly *K56A* also shows no Chk1-HA phosphorylation, even though the sensitivity to IR in Figure 6-4 was not as severe *K56E*. This, however, may be due to a small amount of phosphorylation not being visible on the western blot at this exposure. As expected, *rad4-R22E* shows *WT* like Chk1-HA phosphorylation after IR, consistent with the lack of sensitivity to IR seen in Figure 6-4 (Figure 6-6A). Chk1-HA phosphorylation is also almost abolished in *rad4-T15V, K56A* and *K56E* after UV radiation. However, a small residual level of Chk1-HA phosphorylation can still be seen, particularly in the *K56A* and *K56E* mutants, implying a low level of checkpoint activation (Figure 6-6C).

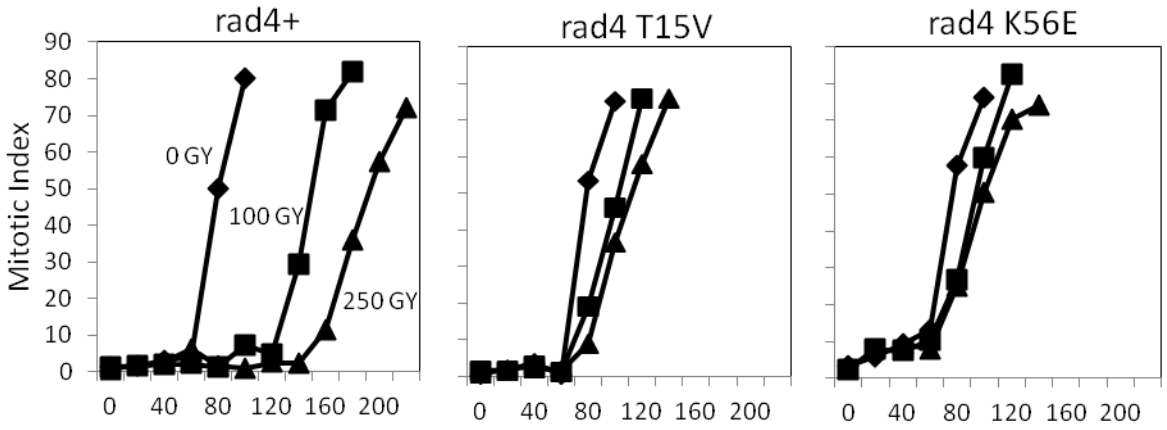

Figure 6-5. *rad4* BRCT domain 1 mutants display a checkpoint defect after IR.
G2 checkpoint assay. *rad4+* (left panel), *rad4-T15V* (middle panel), *rad4-K56E* (right panel) were synchronised in G2 via lactose gradient, split and treated with 0 Gy, 100 Gy or 250 Gy. Cells were then grown in YE at 30°C with samples being taken every 20 minutes to measure cell cycle progression. Cell cycle progression was monitored by mitotic index via fluorescence microscopy on DAPI stained fixed cells until ~ 80% of cells had progressed to mitosis. A reduction in time compared to *rad4+* indicates a G2 checkpoint defect.

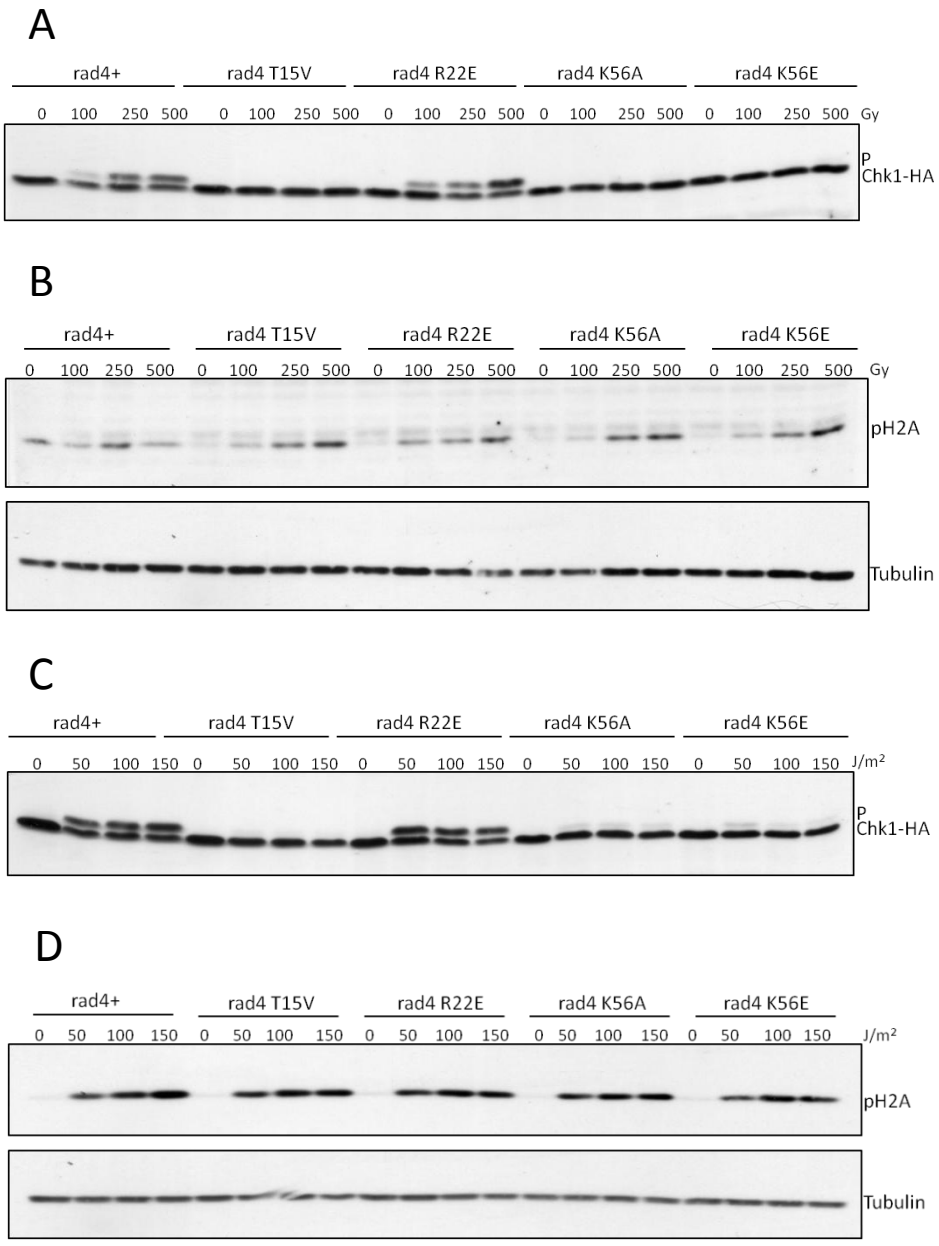

Figure 6-6. *rad4* BRCT domain 1 mutants display reduced Chk1-HA phosphorylation after IR and UV.

A. Checkpoint activation was assayed in the indicated strains after ionising radiation via Chk1-HA phosphorylation. Asynchronous *rad4+, rad4-T15V, rad4-R22E, rad4-K56A and rad4-K56E* cells were exposed to γ-radiation at the indicated doses. Chk1-HA phosphorylation (P) was assayed by SDS PAGE using α-HA. B. As in A except H2A phosphorylation was assayed by SDS PAGE using α-S129 (top panel). α-Tubulin was used as a loading control (bottom panel). C. As in A but after exposure to UV radiation. D. as in B except after exposure to UV radiation

To ensure that the lack of Chk1 phosphorylation in *rad4-T15V K56A/E* is due to a loss of the Rad4-Crb2 interaction and not a loss of Rad3 activity, which could arise due to the mutations made affecting Rad4s AAD activity or recruitment of Rad3 to the site of damage, phospho (γ) H2A was also blotted for after IR and UV. No obvious reduction in γH2A can be seen in any of the *rad4* BRCT mutants after IR or UV. This suggests that loss of Chk1 phosphorylation in these mutants is due to a loss of the Rad4-Crb2 interaction, and therefore Chk1 recruitment to the site of damage, and not to loss of Rad3 activity (Figure 6-6B, D).

6.5 *T15V* and *K56E* Mutations do Abolish all Phospho Binding Ability of Rad4 BRCT1

As the *rad4 K56E* and *T15V* mutants were viable, even though Rad4 BRCT1 has been shown to bind Sld3, there was concern that the mutations were not fully abolishing the function of the Rad4 BRCT1 phospho-binding pocket. Therefore, the *T15V* and *K56E* mutants were combined in the same allele of *rad4* to give a *rad4-T15V K56E* strain (Materials and Methods). The *rad4 T15V K56E* strain was indeed viable even though both residues required for phosphate binding are mutated (Figure 6-7A). Furthermore, this strain showed a normal DNA content by FACS analysis, therefore suggesting there were no major DNA replication initiation problems (Figure 6-7B). Together this data shows that the Rad4 BRCT1 is definitely not essential for initiation of DNA replication in *S. pombe.* To see if the combination of *T15V* and *K56E* caused any further loss of the Rad4-Crb2 interaction when compared with the single mutants, spot test analysis was performed in the presence of a number of genotoxic agents (Figure 6-8). The double *rad4-T15V K56E* shows the same sensitivity as both of the single mutants, to all the genotoxic agents tested. This suggests that the single *T15V* and *K56E* mutations did indeed fully prevent the interaction between Crb2 and Rad4 (Figure 6-8).

A

Strain	Cassette exchange efficiency	Viable?
WT	42%	Yes
rad4 T15V	16.6%	Yes
rad4 R22E	28%	Yes
rad4 K56A	11.5%	Yes
rad4 K56E	23.1%	Yes
rad4 T15V K56E	7.5%	Yes

B

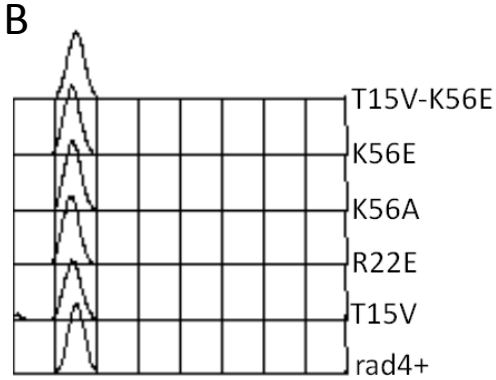

Figure 6-7. *rad4* BRCT1 phospho binding pocket mutants are definitely viable.

A. Table showing the cassette exchange efficiency for inserting WT, *rad4 T15V, R22E, K56A* and *K56E* from Figure 6-2B and *rad4-T15V/K56E* double mutant into the Rad4 base strain. Efficiency is calculated as the number of colonies that grew on 5FOA plates as a percentage of the number of cells plated after cassette exchange. Viability was ensured by sequencing the DNA of the colonies that grew. C. FACS profile of asynchronously growing *rad4+, rad4-T15V (T15V), rad4-R22E (R22E), rad4-K56A (K56A) and rad4-K56E (K56E)* strains from Figure 6-2C and the *rad4-T15V/K56E (T15V-K56E)* strain. All of which display a 2C DNA content

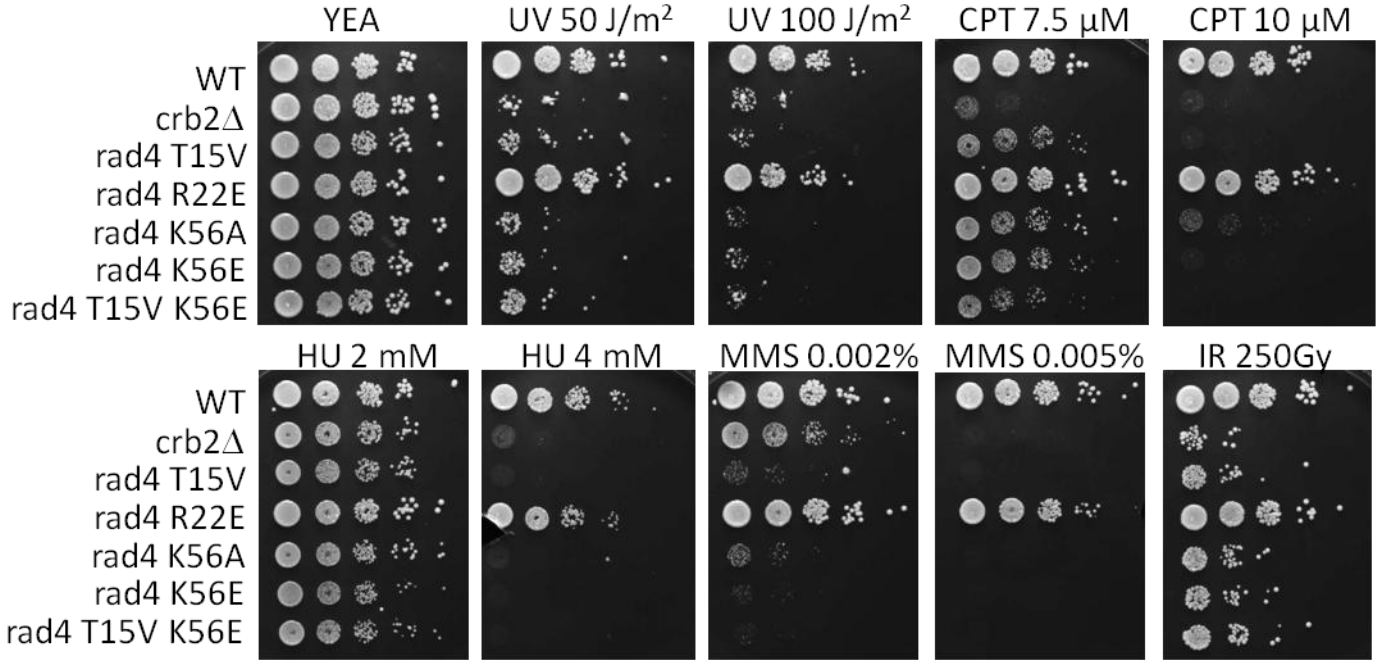

Figure 6-8. *rad4 T15V K56E* is as sensitive to genotoxic agents as either of the single mutants
Spot test analysis of *rad4+ (WT), rad4-T15V, rad4-R22E, rad4-K56A, rad4-K56E, rad4-T15V/K56E crb2Δ* positive control in the presence of different genotoxic agents. 10-fold serial dilutions of $1x10^7$ cells/ml were spotted onto YEA plates containing CPT, MMS or HU. Alternatively they were spotted onto YEA containing no genotoxic agents and UV irradiated. For IR cells were γ-irradiated, serial diluted and then spotted onto YEA. Plates were incubated at 30°C for 4 days

6.6 Creation of *rad4* BRCT2 Mutants

As Crb2 phosphorylated on T187 or T235 can bind to Rad4 BRCT2, and co-crystal structures of this interaction were solved, it was important to see the role of these interactions in *vivo*. This was achieved by making the corresponding mutants to those made in *rad4* BRCT1, in BRCT2, the mutants made were therefore *T110V, R117E, K151A* and *K151E* (Figure 6-9A). As with the BRCT1 mutants, all of the BRCT2 mutants were viable after the cassette exchange step of the RMCE (Figure 6-9B). The cassette exchange efficiencies were slightly low, however, this may just be due to the density to which the cells were grown before plating on 5-FOA (Figure 6-9B). All of the BRCT2 mutants showed a WT DNA content by FACS analysis (Figure 6-10A), suggesting they had no problem in the initiation of DNA replication. They also grew normally at 25˚C, 30˚C and 36˚C, excluding any possibility they were temperature sensitive (Figure 6-10B).

As with the *rad4* BRCT1 mutants, spot test analysis was carried out with the BRCT2 mutants in order to test their sensitivity to genotoxic agents, and therefore any role they may be playing in the checkpoint (Figure 6-11). All four of the BRCT2 mutants show a moderate level of sensitivity to all the genotoxic agents tested (Figure 6-11). This sensitivity is not as strong as that seen for the BRCT1 mutants (Figure 6-4), therefore suggesting that BRCT2 may have a lesser role in the activation of the checkpoint. This coincides with the in *vitro* data from the Pearl laboratory, showing that Crb2 pT187 and pT235 bind at a lower affinity to Rad4 BRCT2, than pT187 dose to Rad4 BRCT1 (Figure 6-1A). Interestingly, unlike *R22E* in BRCT1, the corresponding mutation, *R117E,* in BRCT2 does show sensitivity to genotoxic agents and this sensitivity is similar to that of the T110V and K151A/E mutants. This is consistent with the crystal structure, where, in the case of BRCT2, the arginine residue does face into the phospho binding pocket and make contact with the phosphate on Crb2 (Tony Oliver personal communication). Also, unlike the corresponding BRCT1 mutants, the *K151A* and *K151E* mutants show an almost identical level of sensitivity to all of the genotoxic agents (Figure 6-11).

A

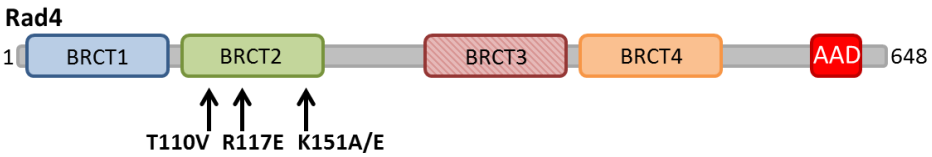

B

Strain	Cassette Exchange efficiency	Viable?
rad4 T110V	4.9%	Yes
rad4 R117E	3.3%	Yes
rad4 K151A	8%	Yes
rad4 K151E	9.25%	Yes

Figure 6-9. *rad4* BRCT2 phospho-binding pocket mutants are viable
A. Diagram showing the position of the four *rad4* BRCT2 mutants, T110V, R117E, K151A, K151E, within Rad4. B. Table showing the cassette exchange efficiency for inserting WT, *rad4-T110V, R117E, K151A* and *K151E* into the Rad4 base strain. Efficiency is calculated as the number of colonies that grew on 5-FOA plates as a percentage of the number of cells plated after cassette exchange. Viability was ensured by sequencing the DNA of the colonies that grew.

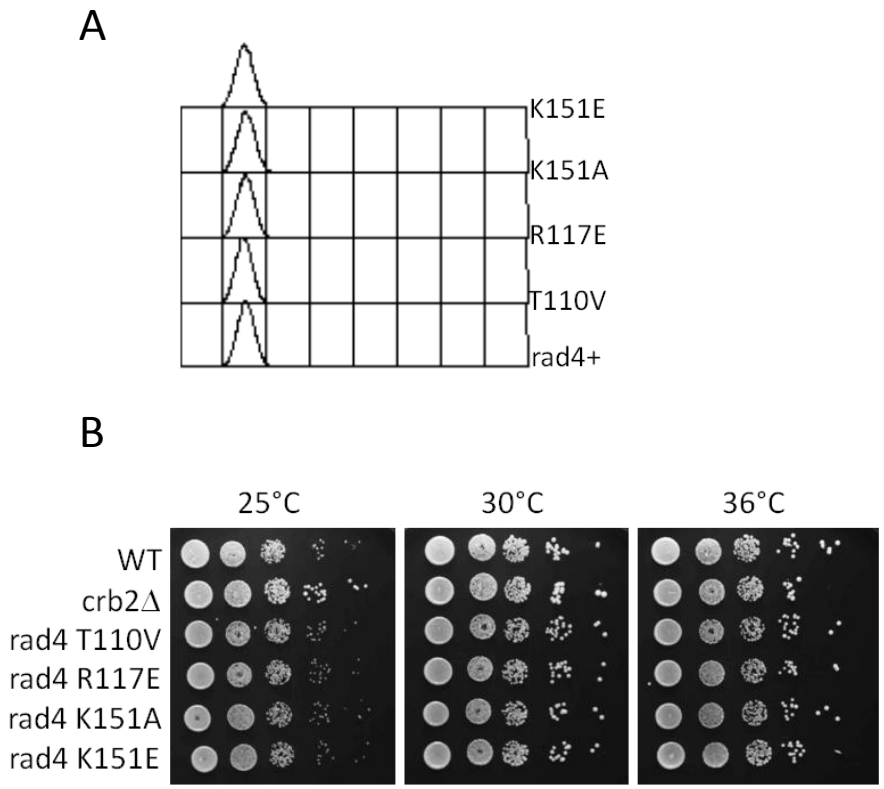

Figure 6-10. *rad4* BRCT domain 2 mutants grow normally and are not TS
FACS profile of asynchronously growing *rad4+, rad4-T110V (T110V), rad4-R117E (R177E), rad4-K151A (K151A) and rad4-K151E (K151E)* strains, displaying a 2C DNA content. B. Spot test analysis of the *rad4* strains in A. 10-fold serial dilutions of $1x10^7$ cells/ml were spotted onto YEA plates and grown for 4 days at either 25°C, 30°C or 36°C.

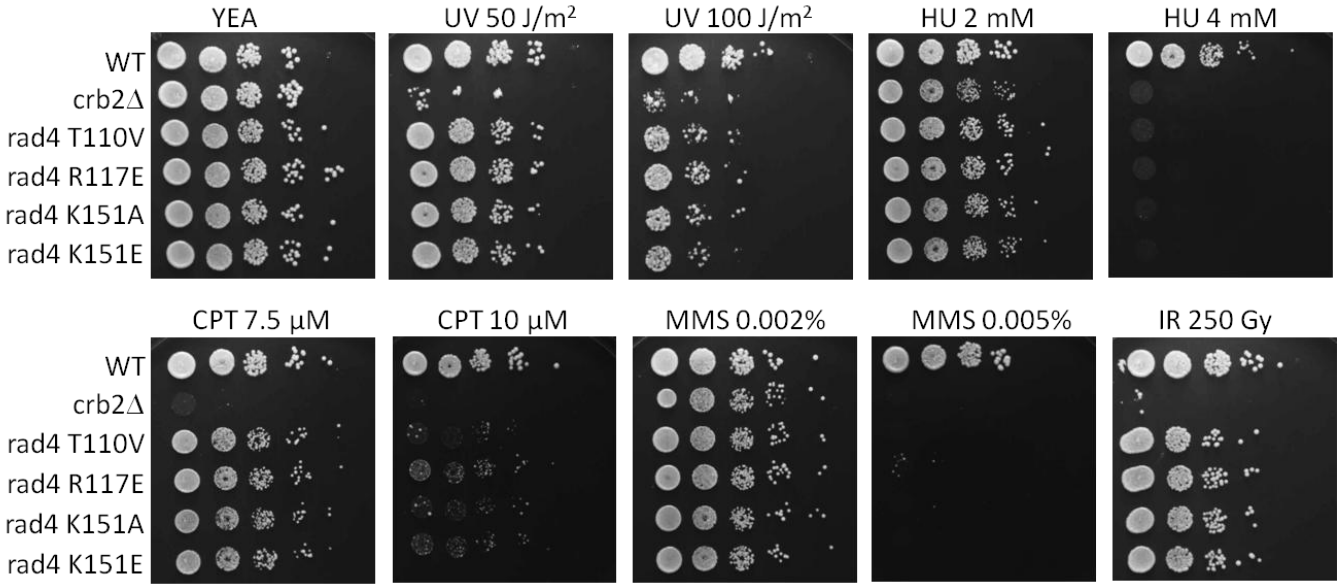

Figure 6-11. rad4 BRCT domain 2 mutants are moderately sensitive to genotoxic agents
Spot test analysis of *rad4+* (WT)*, rad4-T110V, rad4-R117E, rad4-K151A, rad4-K151E* and *crb2Δ* positive control in the presence of different genotoxic agents. 10-fold serial dilutions of $1x10^7$ cells/ml were spotted onto YEA plates containing CPT, MMS or HU. Alternatively they were spotted onto YEA containing no genotoxic agents and UV irradiated. For IR cells were γ-irradiated, serial diluted and then spotted onto YEA. Plates were incubated at 30°C for 4 days

This suggest that it is much easier to disrupt the interaction between Rad4 BRCT2 and phosphorylated Crb2 than it is BRCT1 and Crb2, as K to A is a much less severe mutation than K to E. This is also consistent with the weaker binding affinity of BRCT2 to phopho-Crb2.

6.7 *rad4* BRCT2 Mutants Show a Moderate Checkpoint Defect.

To understand whether the moderate level of sensitivity the Rad4 BRCT2 mutants displayed to genotoxic agents was due to a checkpoint defect, a G2 checkpoint assay, similar to that in Figure 6-5 for the BRCT1 mutants, was performed. *rad4+, T115V, R117E* and *K151E* cells were synchronised in G2 via lactose gradients and exposed to either 0 Gy, 100 Gy or 250 Gy IR. Cell cycle progression was measured via mitotic index (Figure 6-12). Consistent with the moderate sensitivities seen in Figure 6-11 the *rad4* BRCT2 mutants also showed a moderate checkpoint defect (Figure 6-12). The *rad4+* cells showed a 80 minute and 140 minute delay after 100 and 250 Gy respectively, similar to that seen in Figure 6-5. The *K151E* mutant showed the strongest checkpoint defect with delays of 40 and 80 minutes, the next most severe was the *T115V* with 60 and 80 minute delays. The mutant with the least severe checkpoint defect was the *R117E* mutant, which displayed delays of 60 and 100 minutes after 100 Gy and 250 Gy, respectively (Figure 6-12).

Again, to see whether this checkpoint defect relates to a reduction in Chk1 phosphorylation, and therefore most probably the interaction between Rad4 and Crb2, western blots were carried out against phospho Chk1-HA after IR and UV (Figure 6-13 A, C). In line with the checkpoint defect and sensitivity data in Figures 6-12A and 6-11A, a moderate reduction in Chk1-HA phosphorylation can be seen after IR in asynchronous cells (Figure 6-13A). All four of the BRCT2 mutants, *T110V*, *R117E*, *K151A* and *K151E*, show a similar reduction in Chk1-HA phosphorylation compared to *rad4+* cells. It may be that the *R117E* mutant shows slightly more Chk1-HA phosphorylation than the other mutants, which would be consistent with the data in Figure 6-12. However this is very marginal. After UV radiation, the BRCT2 mutants also show a moderate reduction Chk1-HA phosphorylation (Figure 6-13C).

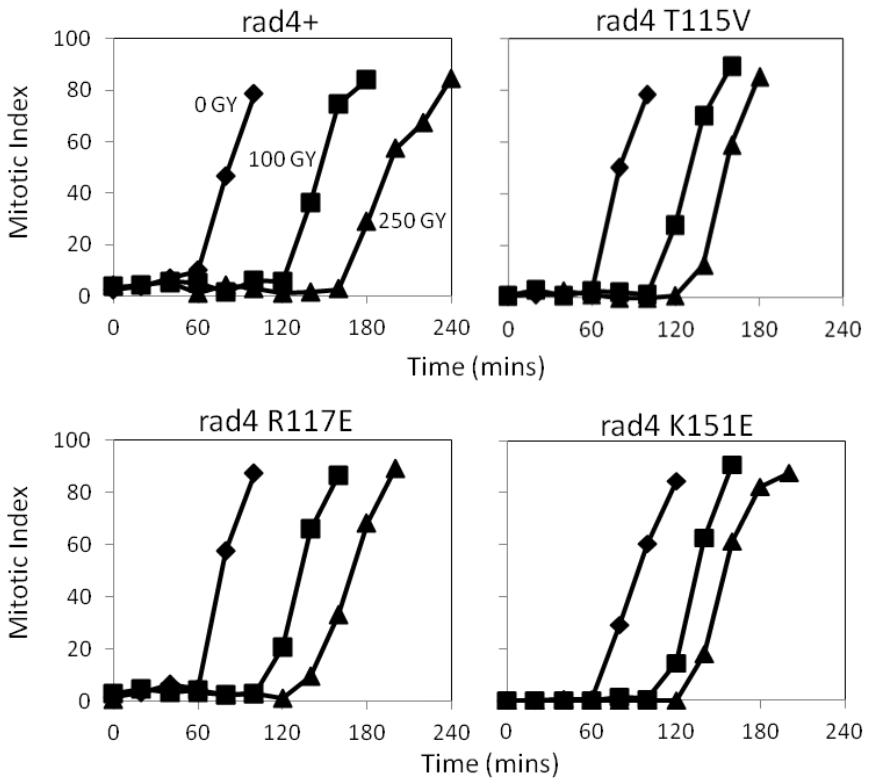

Figure 6-12. *rad4* BRCT domain 2 mutants display a moderate checkpoint defect after IR.

G2 checkpoint assay. *rad4+* (top left panel), *rad4-T115V* (top right panel), *rad4-R117E* (bottom left panel) and *rad4-K151E* (bottom right panel) were synchronised in G2 via lactose gradient, split and treated with 0 Gy, 100 Gy or 250 Gy. Cells were then grown in YE at 30°C with samples being taken every 20 minutes to measure cell cycle progression. Cell cycle progression was monitored by mitotic index via fluorescence microscopy on DAPI stained fixed cells until ~ 80% of cells had progressed to mitosis. A reduction in time compared to *rad4+* indicates a G2 checkpoint defect.

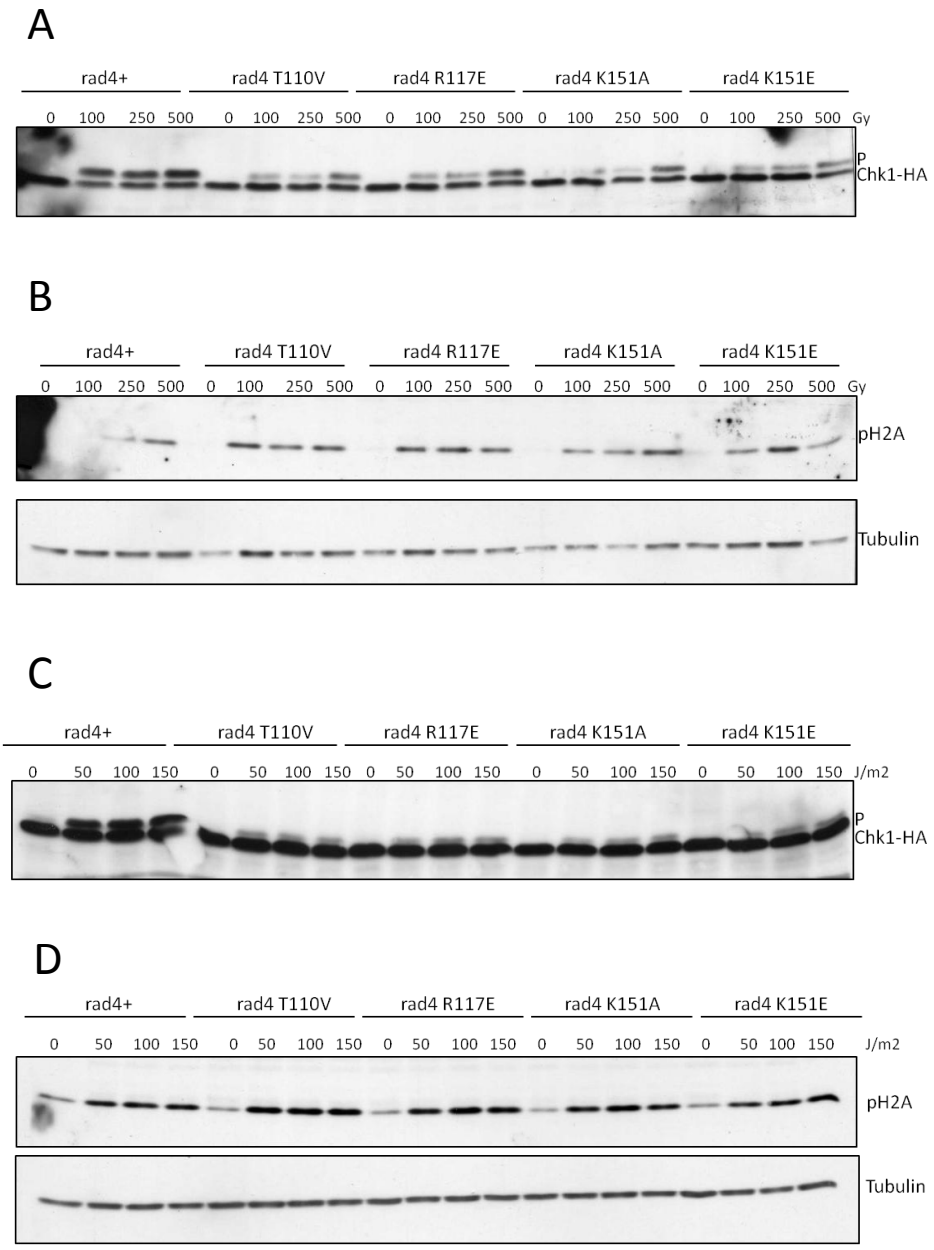

Figure 6-13. *rad4* BRCT domain 2 mutants display reduced Chk1-HA phosphorylation after IR and UV.

A. Checkpoint activation was assayed in the indicated strains after ionising radiation via Chk1-HA phosphorylation. Asynchronous *rad4+, rad4-T110V, rad4-R117E, rad4-K151A and rad4-K151E* cells were exposed to γ radiation at the indicated doses. Chk1-HA phosphorylation (P) was assayed by SDS PAGE using α-HA. B. As in A except H2A phosphorylation was assayed by SDS PAGE using α-S129 (top panel). α-Tubulin was used as a loading control (bottom panel). C. As in A but after exposure to UV radiation. D. as in B except after exposure to UV radiation.

This is less than that seen for the BRCT1 mutants (Figure 6-6C) and consistent with the sensitivities (Figure 6-11). As with the BRCT1 mutants, this reduction in Chk1-HA phosphorylation after IR and UV seen in the BRCT2 mutants is most likely due to a reduction in the interaction of Crb2 and Rad4 and thus reduced Chk1 recruitment. This is because H2A phosphorylation is unaffected in all of the Rad4 BRCT2 mutants after IR and UV, suggesting Rad3 is still active and recruited to the site of DNA damage (Figure 6-13B, D).

6.8 A combination of *rad4* BRCT1 and BRCT2 Mutants is Lethal.

To further understand the roles of the Rad4 BRCTs 1 and 2 in the binding to Crb2 and in the initiation of DNA replication, BRCT1 and BRCT2 mutants were combined in the same *rad4* allele. If both Rad4 BRCTs 1 and 2 are not essential for the initiation of DNA replication the cells will be viable and may have an additive checkpoint defect. However, if BRCT1 and BRCT2 are required for Rad4's essential role in initiation of DNA replication, the cells will be inviable. The mutants made, to ensure no phospho binding remained in BRCTs 1 and 2, were a *K56E K151E* double mutant and a *K56E T15V K151E* triple mutant (Figure 6-14A). It can be seen from figure 6-14B that the *rad4* BRCT1 and BRCT2 combined mutants are inviable. Two cassette exchange reactions, from different transformation isolates, were carried out and plated onto two separate plates for *K56E K151E* and *K56E T15V K151E*. In all cases, the cassette exchange efficiency is very low - between 1.43% and 2.45%. The average exchange efficiency of the two transformation isolates was 1.54% for the *K56E K151E* and 2.10% for the *K56E T15V K151E*, compared with 70.5% for *WT rad4*. This suggested that the BRCT1 and 2 combination mutants were inviable. To confirm this *rad4* was sequenced in the colonies that did grow. All the sequences from both mutant strains came back *WT* (Figure 6-14B). Therefore, the colonies that grow on the 5-FOA were just back ground and the result of gene conversion events. This result therefore indicates that for *rad4'*s essential role in the initiation of replication, either BRCT1 or BRCT2 are required; mutation of one or the other does not lead to inviability, but mutation of both does. Due to this, we cannot see if mutating both BRCT1 and BRCT2 leads to an increased checkpoint defect compared to mutation of one or the other.

A

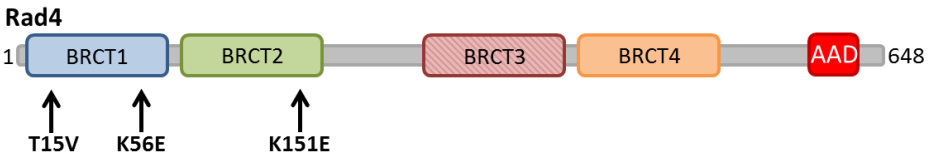

B

Strain	Exchange efficiency (average of 2 plates)	Average of 2 Isolates	N.O. of WT Sequences vs. Mutant
WT	70.50%		4/0
K56E K151E #1	1.65%		4/0
K56E K151E #2	1.43%	1.54%	4/0
K56E T15V K151E #1	2.45%		4/0
K56E T15V K151E #2	1.80%	2.10%	4/0

Figure 6-14. *rad4* harbouring mutations in BRCT domains 1 and 2 are inviable

A. Diagram showing the position of the *rad4* BRCT1 and 2 mutants, T15V, K56E and K151E within Rad4. B. Table showing the cassette exchange efficiency for inserting WT, *rad4-K56E/K151* and *K56E/T15V/K151E* into the Rad4 base strain. Efficiency is calculated as the number of colonies that grew on 5-FOA plates as a percentage of the number of cells plated after cassette exchange. An average of two plates was taken and this was done for two transformation isolates, which was then also averaged (Average of 2 isolates). Inviability was ensured by sequencing the DNA of the colonies that grew.

6.9 Rad4 BRCT Domains Also Bind to Valine Residues in the Minus Three Positions from the Cdc2 Phosphorylation Sites on Crb2

From the Rad4-Crb2 co-crystal structures it could be seen that the Rad4 BRCT1 and 2 domains interacted with a second Crb2 residue in combination with the phosphorylated one. This residue was a valine residing in the minus three position from each of the Cdc2 phosphorylated residues. To test the importance of these Crb2 residues in binding to Rad4 BRCTs 1 and 2, *V184K, V212K, V234K* and *V212K V234K* mutants were made. Spot tests were then carried out in the presence of increasing doses of UV and 250 Gy IR, the sensitivities were compared to *WT* and *crb2Δ* (Figure 6-15) The sensitivities seen for the minus three position valine mutants were very similar to that seen for the associated phosphorylation site mutations (Figure 5-2A, B). *V184K* shows the highest sensitivity out of the single mutants, as did *T187A. V212K* and *V232K* show intermediate levels of sensitivity similar to that of *T215A* and *T235A,* but when combined in a *V212K V232K* double mutant the sensitivity, as with *T215A T235A*, is similar to that of the *V184K* and *crb2Δ* (Figure 6-15, Figure 5-2A, B). This suggests that the minus three valine is just as important as the phosphorylation of Crb2 in relation to its interaction with Rad4 BRCT domains 1 and 2. To confirm that this is the case, western blot analysis was carried out to assay Chk1-HA and H2A phosphorylation (Figure 6-16 A, B). It can be seen from the western blots that crb2 *V184K* almost abolishes all Chk1-HA phosphorylation after both IR and UV, as with the *T187A* mutation. The *V234K* shows a moderate reduction in Chk1-HA phosphorylation after IR and UV, which is consistent with the sensitivities in Figure 6-15 and similar that of *T235A*.

Surprisingly *V212K* shows little or no apparent reduction in Chk1-HA phosphorylation after IR or UV. This is different to the corresponding phosphorylation mutation at *T215A* which shows a moderate reduction in Chk1-HA phosphorylation (Figure 5-4A, B). It may be that the minus three valine is not important in the binding of the T215 site to Rad4. This would be consistent with the data from the Pearl laboratory which shows no significant interaction between T215 and Rad4 BRCT1/2.

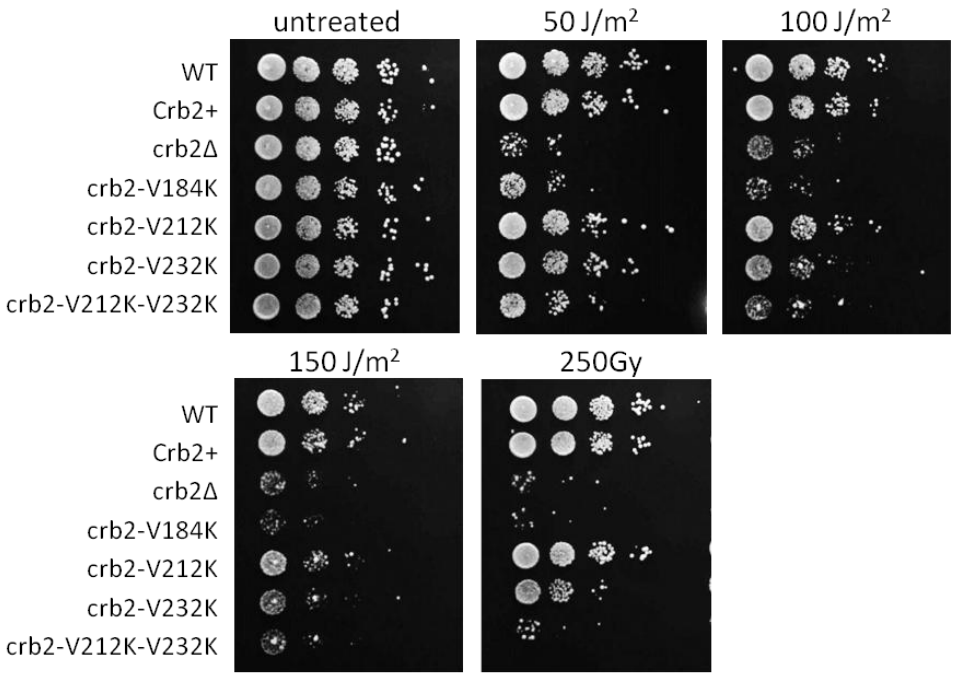

Figure 6-15. *crb2-V184K, V212K, V232K* are sensitive to DNA damage.
Spot test assay with WT, *crb2+, crb2Δ, crb2-V184K, crb2-V212K, crb2-V232K* and *crb2-V212K-V232K* after UV, ionising radiation or no treatment. For UV 10-fold serial dilutions of $1x10^7$ cells/ml were spotted onto YEA and UV irradiated. For IR cells were γ irradiated, 10-fold serial diluted and then spotted onto YEA. Plates were incubated at 30°C for 4 days

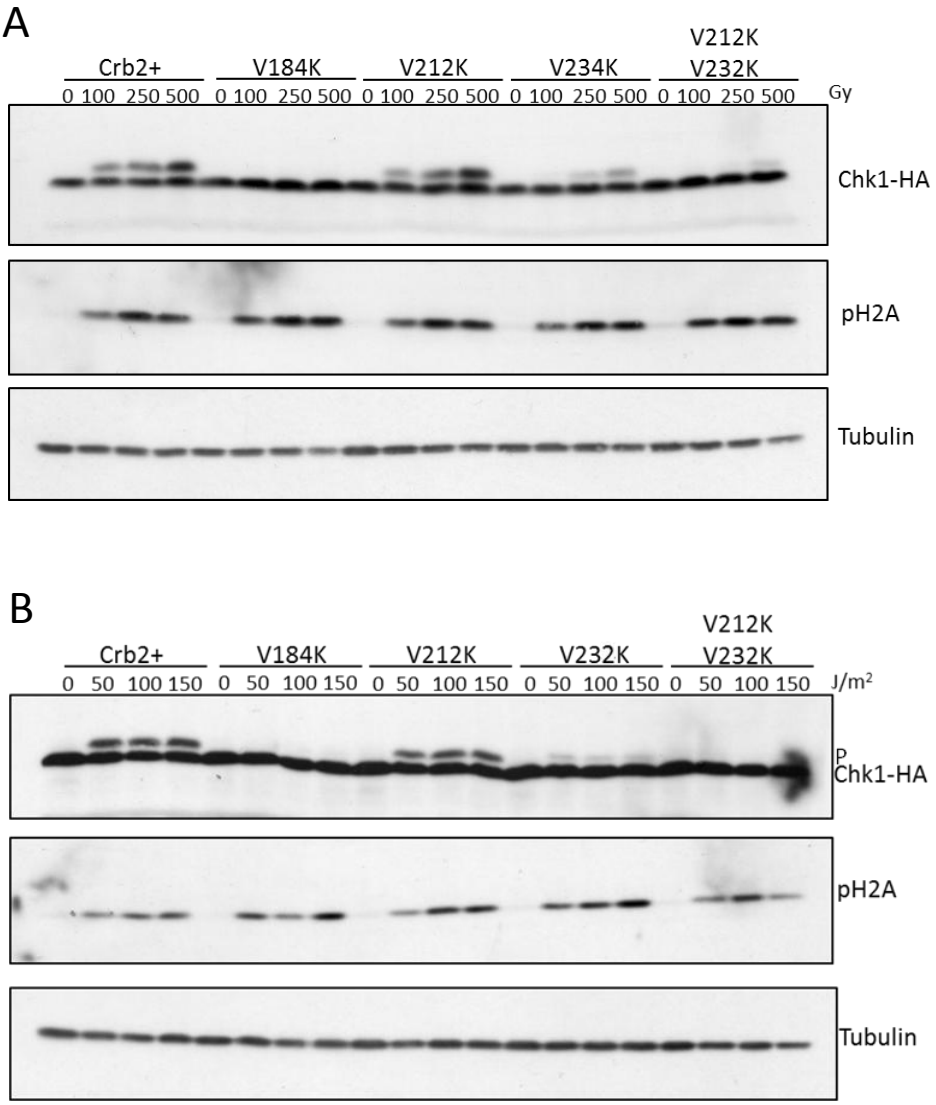

Figure 6-16. *crb2* minus three position mutants show reduced Chk1-HA phosphorylation

A. Checkpoint activation was assayed in *crb2+, crb2-V184K (V184K), crb2-V212K (V212K), crb2-V232K (V232K)* and *crb2-V212K-V232K* (V212K V232K) strains after ionising radiation via Chk1-HA (top panel) and H2A phosphorylation (middle panel) using SDS PAGE and α-HA and α-pS129 antibodies respectively. α-Tubulin (bottom panel) was used in as a loading control. B. As in A but after UV radiation.

However, the *V212K* mutant does exhibit an intermediate sensitivity to both IR and UV in Figure 6-15. It maybe, that the western blot assay is not sensitive enough to see a mild decrease in Chk1-HA phosphorylation. Furthermore, combination of the *V212K* and *V232K* mutants leads to a big decrease in Chk1-HA phosphorylation, almost to the level of the *V184K* mutant and more than either of the single mutants alone, after both IR and UV. This again is consistent with the sensitivity data in Figure 6-15 and the *T215A T235A* western blots in Figure 5-4A, B. As expected, mutating any of the minus three position valines had no effect on H2A phosphorylation after IR or UV (Figure 6-16 A,B). This data shows that the minus three position valine is important for Crb2 binding to Rad4 and that both the valine and the Cdc2 phosphorylation are required. It also implies that it is not just the sequential phosphorylation of Crb2 which is required for the interaction with Rad4, it maybe sequential binding of Rad4 to each of the Crb2 sites.

6.10 Mechanism of Sequential Crb2 Phosphorylation and Rad4 Binding

The data in this chapter, that from the Pearl laboratory, the Du laboratory and from Chapter 5, show that Crb2 is sequentially phosphorylated by Cdc2 on three sites, with T187 being the most important and dependent on the prior phosphorylation of T215 and T235. These phosphorylations bind to Rad4 BRCTs 1 and 2, with BRCT1 being the most important for checkpoint activation. T187 can bind both BRCT1 and 2, T235 binds BRCT2 and this T235 binding affinity is increased by a weak interaction between T215 and BRCT1. This data gives two possible explanations for the sequential phosphorylation of Crb2: The first is that the phosphorylation of T215 and T235 causes a conformational change in Crb2, revealing T187. Rad4 could then make a stable strong interaction between its BRCT1 domain and T187. An interaction between BRCT2 and the second T187 of the Crb2 dimer also occurs, further enhancing the binding. However, this model does not explain why Rad4 BRCT2 binds to pT235 on Crb2 and why this interaction is further enhanced by pT215 and BRCT1. It does not explain why mutation of V188 to proline, thus turning T187 into a canonical cdc2 site, bypasses in part the need for phosphorylation on T215 and T235. Also it does not explain the

requirement for the minus three position valine at T212 and T232. It would therefore seem as if Rad4 first binds to the pT215 and pT235 sites before binding to pT187. This leads to the second hypothesis, in which Crb2 is first phosphorylated on the canonical Cdc2 sites T215 and T235, as they are easier to phosphorylate than the non-canonical T187 site. This recruits Rad4 via the BRCT2 pT235 interaction, this binding is enhanced by pT215 BRCT1. Once recruited, Rad4 T187 is phosphorylated and a strong stable interaction between the two pT187 of the Crb2 dimer and Rad4 BRCTs1 and 2 can occur. However, for this model to work the preliminary binding of Rad4 to pT235 pT215 has to enhance the phosphorylation of T187.

It was shown by Valerie Garcia (Carr lab) that Cdc13, the main *S. pombe* cyclin that binds and activates Cdc2, can interact with the C-terminus of Rad4 in a pull down assay. In collaboration with Tony Oliver from the Pearl laboratory, a similar experiment to further understand this interaction was carried out. A GST Rad4 fragment containing Rad4 BRCTs 3 and 4 (GST-BRCT3, 4) was expressed in *E .coli* cells and bound to a glutathione resin column (Figure 6-17A). Whole cell *S. pombe* extracts from cells containing HA tagged Cdc13 were then made and passed through the column. The protein was then eluted and run on an SDS gel for western blot analysis. It can be seen from Figure 6-17A that Cdc13-HA is indeed pulled down by this BRCT3,4 fragment of Rad4, suggesting that Cdc13 and most likely Cdc2 does bind Rad4. Furthermore, mutation of the BRCT4 phospho binding pocket, *K452E* (BRCT3 does not have a phospho binding pocket) does not affect the interaction between Cdc13 and the Rad4 fragment, suggesting that this is not a phospho specific interaction (Data not shown). This result gives the final mechanistic step to hypothesis two (described above) and leads to the following model.

6.11 Model and Discussion

In late S-phase/ early G2 the Crb2 dimer is phosphorylated on the canonical, easy to phosphorylate, T215 and T235 by the increasingly active Cdc2-Cdc13, in a non-damage dependant manner (Figure 6-18A).

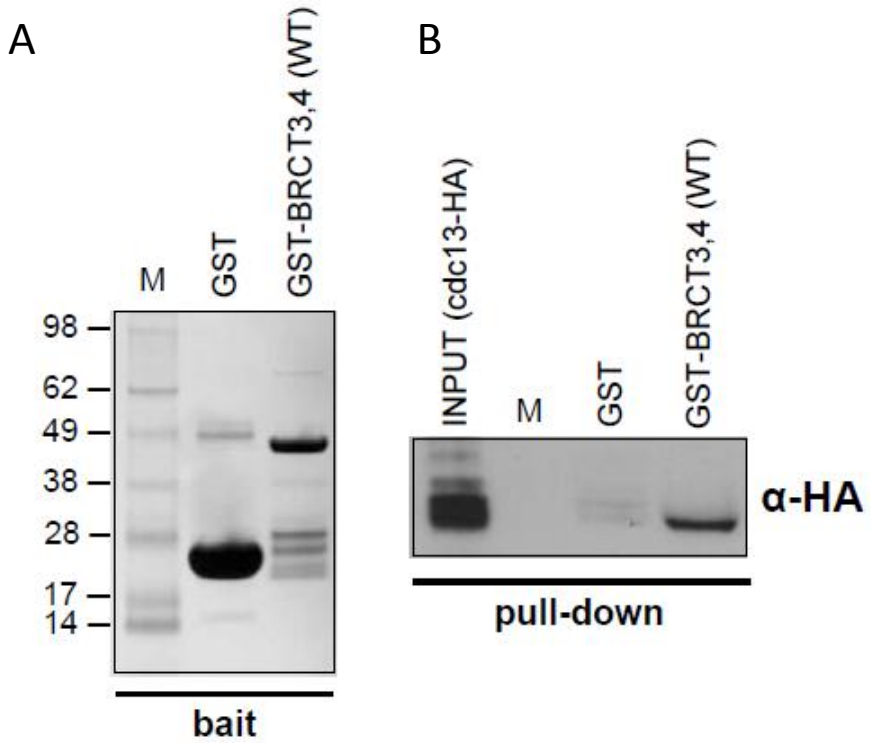

Figure 6-17. Cdc13 binds the C-terminal region of Rad4 containing BRCT domains 3 and 4

A. GST and a purified GST-RAD4 fragment (amino acids 291-495) containing BRCTs 3 and 4 (GST-BRCT4,5 (WT)) used as bait for the Cdc13-HA pull down. B. Pull down assay of Cdc13-HA using either GST or GST-Rad4 BRCT3,4 (GST-BRCT3,4 (WT)). Eluted pulled down protein was subjected to SDS PAGE and Cdc13-HA probed for using α-HA antibodies. Input (cell extracts from *cdc13-HA* cells) can be seen in the left lane. M refers to marker. Experiment carried out in collaboration with Tony Oliver (Pearl Laboratory)

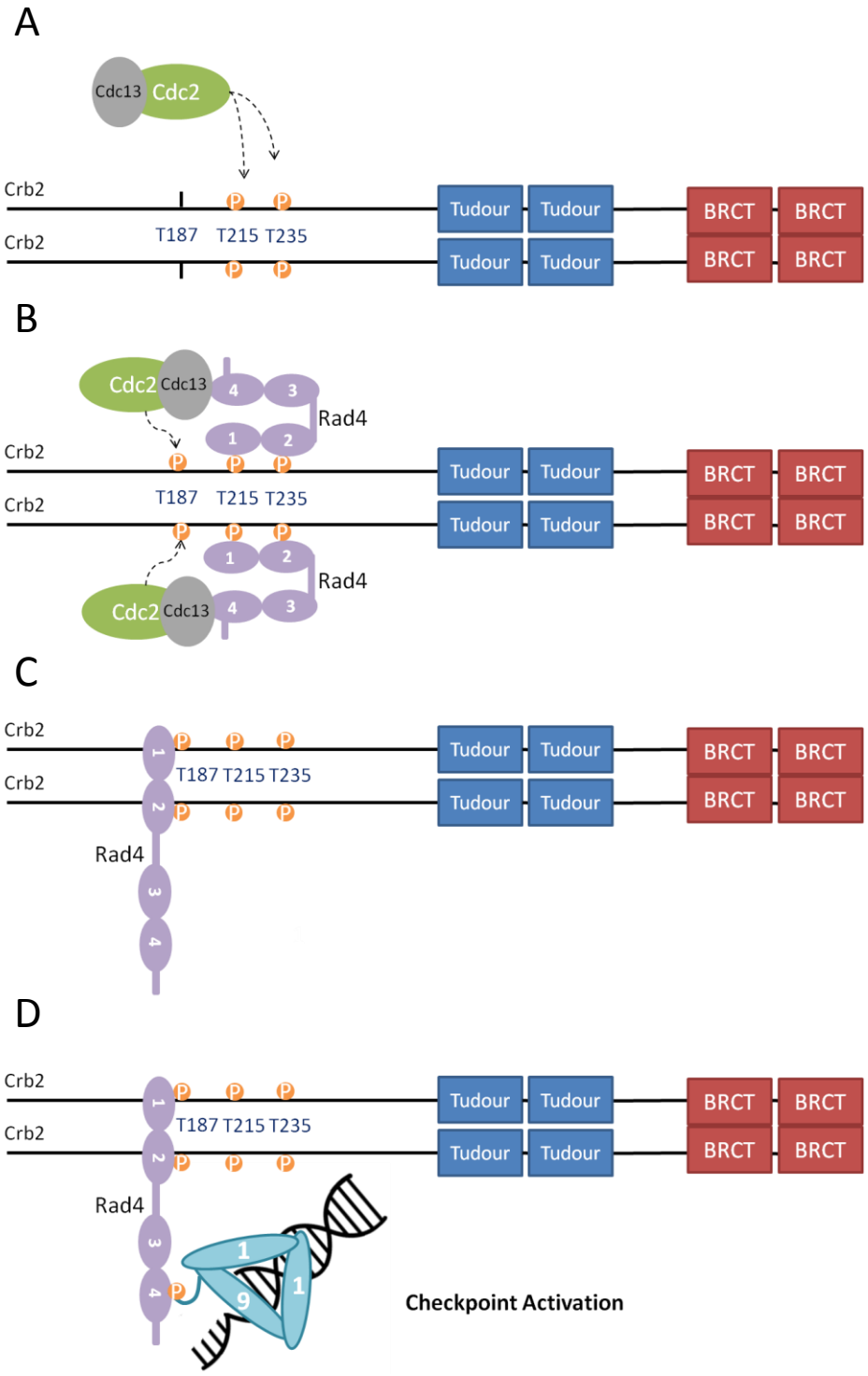
A
Cdc13
Cdc2
Crb2
Crb2
T187
T215
T235
Tudour
Tudour
Tudour
Tudour
BRCT
BRCT
BRCT
BRCT
B
Cdc2
Cdc13
4
3
Rad4
1
2
Crb2
Crb2
T187
T215
T235
Tudour
Tudour
Tudour
Tudour
BRCT
BRCT
BRCT
BRCT
1
2
Rad4
Cdc2
Cdc13
4
3
C
Crb2
Crb2
1
2
T187
T215
T235
Rad4
3
4
Tudour
Tudour
Tudour
Tudour
BRCT
BRCT
BRCT
BRCT
D
Crb2
Crb2
1
2
T187
T215
T235
Rad4
3
4
1
9
1
Checkpoint Activation
Tudour
Tudour
Tudour
Tudour
BRCT
BRCT
BRCT
BRCT

Figure 6-18. Model for Rad4 binding to Crb2 for DNA damage checkpoint activation.

A. Cdc13-Cdc2 phosphorylate the canonical T215 T235 sites on the Crb2 dimer in late S/G2 phase. Rad4 binds to phosphorylated T215 T235 via its BRCT domains 1 and 2 respectively. This brings the associated Cdc13-Cdc2 complex into close proximity of the non-canonical T187 site, facilitating T187 phosphorylation. C. Due to the high affinity Rad4 BRCT1 (and 2) has to pT187 a reorganisation of the Rad4-Crb2 interaction occurs, with Rad4 BRCTs 1 and 2 binding the two pT187 residues of the Crb2 dimer, forming a strong stable interaction. D. Upon DNA damage Rad4 and the associated Crb2 are recruited to the Rad3 phosphorylated Rad9 tail (pT412/pS423) at the site of damage via Rad4 BRCT 4. This then leads to activation of the DNA damage checkpoint.

This leads to the recruitment of Rad4 via an interaction between BRCT2 and pT235, and BRCT1 and pT215. The recruited Rad4 has Cdc13-Cdc2 bound, thus bringing Cdc2-Cdc13 into close proximity of the non-canonical, more difficult to phosphorylate, T187. Now that Cdc2 is in close proximity to Crb2 T187 it can phosphorylate both the T187 sites of the Crb2 dimer (Figure 6-18B). Due to the high affinity Rad4 BRCT1 (and 2) has for T187, a re-organisation of the interaction occurs, Rad4 BRCT1 and 2 now bind across the two pT187 sites of the Crb2 dimer. This gives a stable strong interaction between the two proteins (Figure 6-18C). Upon DNA damage, Rad9 is phosphorylated by Rad3, leading to the recruitment of the Rad4-Crb2 complex to the site of damage via a Rad4 BRCT4-Rad9 pT412 interaction (Furuya et al., 2004) (Figure 6-18D). This model explains all of the data presented in chapters 5 and 6 and that of the collaborators. It incorporates the requirement for the pT215-pT235 BRCT1, 2 interaction for T187 phosphorylation. Why the requirement for T215 and T235 phosphorylation can be bypassed by making T187 a canonical Cdc2 site. The importance of the minus 3 position valine. The requirement for the phosphorylation of both T187 residues of the Crb2 dimer. Why it is important that BRCT1 has higher affinity for T187 than the other two phosphorylations and why BRCT1 and T187 have the strongest phenotype when mutated. However, we cannot completely rule out DDK or other untested kinases for T187 phosphorylation.

The reason for such an elaborate mechanism of Rad4-Crb2 binding is not obvious. It maybe that it allows the cells to selectively activate the Crb2 Chk1 dependent DNA damage checkpoint in G2, rather than the Mrc1 Cds1 dependent replication checkpoint. Having such an elaborate Cdc2 phosphorylation dependent interaction between Crb2 and Rad4 may give cell cycle regulation over which checkpoint is activated. The level of Cdc2 activity required to carry out these phosphorylations may only be high enough as cells move into G2 phase, thus preventing undesirable DNA damage checkpoint activation at a stalled fork. Interestingly, it has previously been shown in budding yeast that Sld2 is also sequentially phosphorylated, initially on canonical CDK sites, which in turn lead to phosphorylation of a non-canonical site, that is required for the interaction with Dpb11 (Rad4). However, in this case the sequential phosphorylation is thought to be required for a conformational change, making the

third phosphorylation site available (Masumoto et al., 2002, Tak et al., 2006). Sequential Cdc2 phosphorylation of Rad4 interacting partners may therefore be a mechanism to ensure that Rad4 interacts with the correct partner at the correct cell cycle phase. The differences in affinity that Rad4 has for these phosphorylation sites may also determine binding partner choice. For example, the higher affinity for Crb2 pT187, than Sld3 pT605, may help prevent cells from firing origins in the presence of DNA damage.

Chapter 7
Replication Checkpoint Dependent Rad4 Interactions

7.1 A Potential Rad4 Interacting Site on Mrc1

As described in the "1.5.6 ATR and the Replication Checkpoint" section *S. pombe* Rad9 and Rad4 are required for the activation of the replication checkpoint as seen by FACS and Rad3 dependent $Cds1^{Chk2}$ activation (Marchetti et al., 2002, Harris et al., 2003, Taylor et al., 2011). However, the mediator protein Crb2 is not required and is dispensable for activation of the replication checkpoint (Tanaka and Russell, 2001, Harris et al., 2003). This therefore poses the question: What is the role of Rad4 within the replication checkpoint? The lack of Crb2 within this pathway means Rad4 cannot be acting, as it does in the damage checkpoint, to scaffold Crb2 to Rad9 on the DNA (Saka et al., 1997, Furuya et al., 2004) (Figure 6-18). One possibility, as described in Chapter 3, is that Rad4 is directly activating Rad3 in the replication checkpoint via its AAD. However, Su-Jiun Lin showed that only a moderate decrease in Cds1 kinase activity, after treatment with HU, is seen in the *rad4-Y599R* strain (Chapter 3, data not shown). This moderate decrease in Cds1 kinase activity after HU in the *rad4-Y599R* strain is not fully consistent with the requirement of Rad4 in the replication checkpoint. This implicates Rad4 in having an additional role in the pathway. One possibility is that Rad4 may be acting as a scaffold, as in the DNA damage checkpoint, but binding to a protein other than Crb2. An obvious candidate is Mrc1, the replication checkpoint specific mediator protein (Tanaka and Russell, 2001).

In this case a model for the role of Rad4 throughout the cell cycle could be envisaged. In early S-phase, Rad4 binds to Sld2/3 for the initiation of DNA replication (Fukuura et al., 2011). In mid S-phase, Rad4 would then bind to Mrc1 for the potential activation of the replication checkpoint. As cells progress to late S-phase/ G2, Rad4 then binds to Crb2 for the activation of the DNA damage checkpoint (Figure 6-18) (Figure 7-1A).

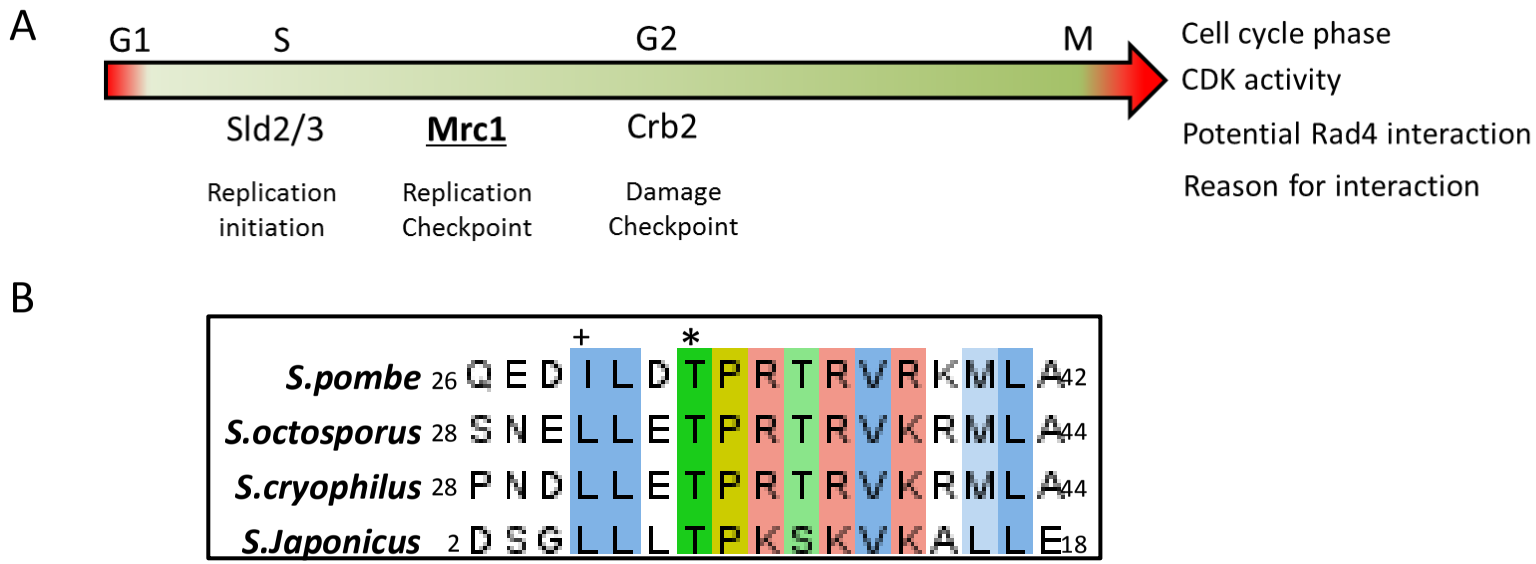

Figure 7-1. Potential Rad4 binding site in Mrc1

A. Diagram showing a model for potential Rad4 interacting proteins throughout the cell cycle. Cdc2 (CDK) activity increases (green arrow increasing intensity, red arrow no/little CDK activity) when cells enter S-phase leading to Sld2/3 phosphorylation and allowing Rad4 to bind for the initiation of the replication checkpoint (Fukuura et al., 2011). As cells progress through S-phase CDK activity increases further, this may allow phosphorylation of Mrc1, allowing Rad4 to bind for the activation of the replication checkpoint upon fork stalling (hypothesis tested in this chapter). As cells enter G2 and CDK activity is at its highest, it can now phosphorylate Crb2, promoting its interaction with Rad4, and thus facilitating the activation of the DNA damage checkpoint upon DNA damage (Chapters 5 and 6). B. Alignment of the potential Rad4 binding sequence within Mrc1 between *S. pombe* and other *Schizosaccharomyces species*. The potential phosphorylation site, T32, is marked with an * and the minus three position residue I29 is marked with a +. Sequence alignment was carried out with the assistance of Sophie George (Carr lab)

The binding partner of Rad4 may be controlled by the level of Cdc2, and possibly phosphatase, activity. Cdc2 may phosphorylate the different targets as its activity increases, with the non-canonical T187 on Crb2 being the most difficult and therefore, last to be phosphorylated (chapter 6) (Figure 7-1A). Also the levels of the target proteins may add another level of control with Mrc1 levels peaking in mid S-phase (Tanaka and Russell, 2001).

For this model to be feasible Mrc1 would need to contain a Rad4 binding site. From the data in Chapter 6 we know that this Rad4 binding site needs to consist of a Cdc2 phosphorylation site which is a SP/TP or, as seen with Crb2 T187, a TV or presumably SV. It also preferentially has a valine at the minus three position from the phosphorylation site. Charly Chawan in the Carr laboratory identified such a Rad4 binding site at T32 within the N-terminus of Mrc1. This site is a canonical Cdc2 TP phosphorylation site and contains an isoleucine at the minus three position (Figure 7-1B). An isoleucine, as with valine, is a non-polar, hyrdrophobic amino acid and would therefore fit into the phsopho-binding pocket of the BRCT domains of Rad4 (personal communication Tony Oliver). Furthermore the TP and surrounding residues are highly conserved amongst *Schizosaccharomyces* species, showing it is evolutionary conserved and may have an important function (Figure 7-B).

To test if Mrc1-T32 is indeed a Rad4 binding site that is required for the activation of the DNA replication checkpoint, an *mrc1-T32A* mutant was constructed usingfusion PCR. This was then inserted over an *mrc1Δ::URA4* at the endogenous *mrc1* locus (section “2.4.5 Creation of *mrc1-T32A* Mutant by Fusion PCR”). Three independent *mrc1-T32A* strains were then tested for their sensitivity to HU and compared to *rad3Δ*, *cds1Δ* and *mrc1Δ* strains by a spot test assay (Figure 7-2). If Rad4 does indeed bind to Mrc1-T32, and this is required for the replication checkpoint, sensitivity to HU should be seen. The sensitivity to HU compared to the control strains used should indicate the importance of any interaction. If the *mrc1-T32A* strain is as sensitive as the *rad3Δ*, *cds1Δ* or *mrc1Δ* then the binding of Rad4 to Mrc1-T32 is essential for the activation of this checkpoint pathway.

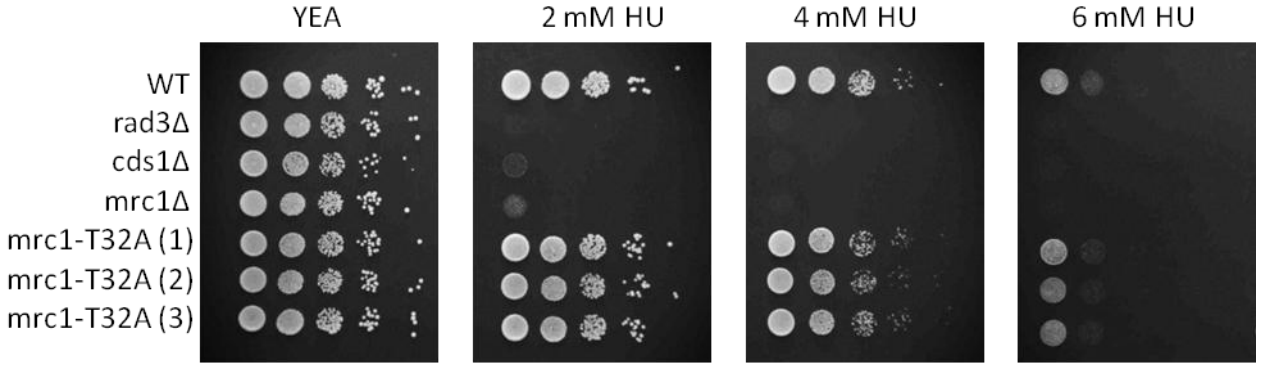

Figure 7-2. mrc1-T32A is not sensitive to hydroxyurea (HU)
Spot test analysis of WT, *rad3Δ, cds1Δ, mrc1Δ* and 3 independent *mrc1-T32A* strains in the presence of HU. 10-fold serial dilutions of $1x10^7$ cells/ml were spotted onto YEA plates containing HU and grown at 30°C for 4 days.

If only a mild level of sensitivity is seen to HU in the *mrc1-T32A* strain, it is likely that any interaction between Rad4 and Mrc1-T32 is not an integral part of the pathway, unlike the interaction between Rad4 and Crb2 in the damage checkpoint. However, from Figure 7-2 it can be seen that none of the three *mrc1-T32A* strains show any sensitivity to HU at any of the doses tested compared to WT. This would therefore suggest that Mrc1-T32 is not required for the activation of the replication checkpoint. Although it cannot be ruled out that Rad4 does bind to T32, it is likely that any interaction is not required for activation of this checkpoint after HU.

7.2 A Slx4-Rad4 Interaction in the Replication Checkpoint?

As it would seem that Rad4 does not interact with Mrc1 for the activation of the replication checkpoint, it maybe that Rad4 binds another protein. As described in "1.6.3 TopBP1 as a scaffold in the DNA Checkpoints" section, the budding yeast homolog (Dpb11) binds to Slx4, an interaction that is also dependent on CDK phosphorylation (Ohouo et al., 2013). The Dpb11-Slx4 interaction is thought to compete with the Dpb11-Rad9^{Crb2} interaction at stalled replication forks, thus reducing the level of Rad53^{Chk1} activation (Ohouo et al., 2013). This reduction in Rad53 activity was reported to be important for allowing Mec1^{Rad3} activity at the stalled fork, without causing a full checkpoint response. This may allow repair of a stalled fork, or replication dependent lesions, without causing cell cycle arrest (Ohouo et al., 2013). However, as budding yeast rely upon Rad53 as the effector kinase for both the DNA damage and replication checkpoint, it maybe that this reduction in Rad53 activity, via an Dpb11-Slx4 interaction, determines the difference between a DNA damage checkpoint response and a replication checkpoint response.

In *S. pombe* it could be hypothesised that an interaction between Rad4 and Slx4 could determine whether the Cds1 dependent replication checkpoint, or the Chk1 dependent DNA damage checkpoint, is activated. It is possible that at a stalled fork Slx4 would bind the BRCT1 and 2 domains of Rad4 with a higher affinity than Crb2. This would prevent Crb2 localisation to the stalled replication fork and thus, in turn, prevent Chk1 recruitment and activation. This would mean that the damage

checkpoint is not active, and that the Rad3 activity is channelled down the Mrc1, Cds1 dependent replication checkpoint pathway. In the presence of DNA damage in late S /G2 Rad4 would be bound to Crb2 via the high affinity Crb2 –pT187 dependent interaction (see Chapters 5 and 6), thus leading to the activation of the DNA damage checkpoint. This model gives an indirect role for Rad4 in the activation of Cds1 by preventing Chk1 activation (Figure 7-3A).

To test this hypothesis, a search was carried out for potential Rad4 interacting sites within *S. pombe* Slx4. In *S. pombe,* two proteins, Spbc713.09 and Slx4, carry out the functions of *S. cerevisiae* Slx4 (Jo Murray personal communication). When aligned with the *S. cerevisiae* Slx4 protein sequence, Spbc713.09 aligns with the N-terminus and Slx4 with the C-terminus (Jo Murray personal communication). It would therefore seem as if, in *S. pombe,* the slx4 locus has undergone an event in evolution leading to it being encoded by two separate genes. Therefore, both the Spbc713.09 and Slx4 proteins were searched for TP/SP or TV/SV sites, which may be Cdc2 phosphorylation sites and Rad4 BRCT binding sites. Two TP/SP sites and nine TV/SV sites were identified within the two proteins (Figure 7-3B). Unfortunately none of these sites were associated with a minus three position valine or isoleucine, meaning that they are not ideal Rad4 binding sites. However, the CDK site on budding yeast Slx4, that Dpb11 interacts with, does not have a valine or isoleucine at the minus three position. Furthermore, none of the sites identified in the *S. pombe* proteins aligned with the known binding site in the *S. cerevisiae* Slx4 (Figure 7-3B). Despite this, a number of the identified sites within Spbc713.09 and Slx4 did look like promising Rad4 binding sites. This is because a number of potential Cdc2 sites are in close proximity to one another, this may promote sequential phosphorylation, as with Crb2 (see Chapter 5).

To see if either of the Slx4 proteins in *S. pombe* were involved in the decision to activate the replication or DNA damage checkpoint, knock out strains were acquired from both the Bioneer Library and Izumi Miyabe (Carr lab). These strains were crossed with an *mrc1Δ* strain and subjected to a spot test in the presence of HU (Figure 7-4). *slx1Δ* (the binding partner of Slx4) cells were also crossed to *mrc1 cells*, as a control, to ensure any phenotype seen was not due to the role of *slx4* in recombination or any other process.

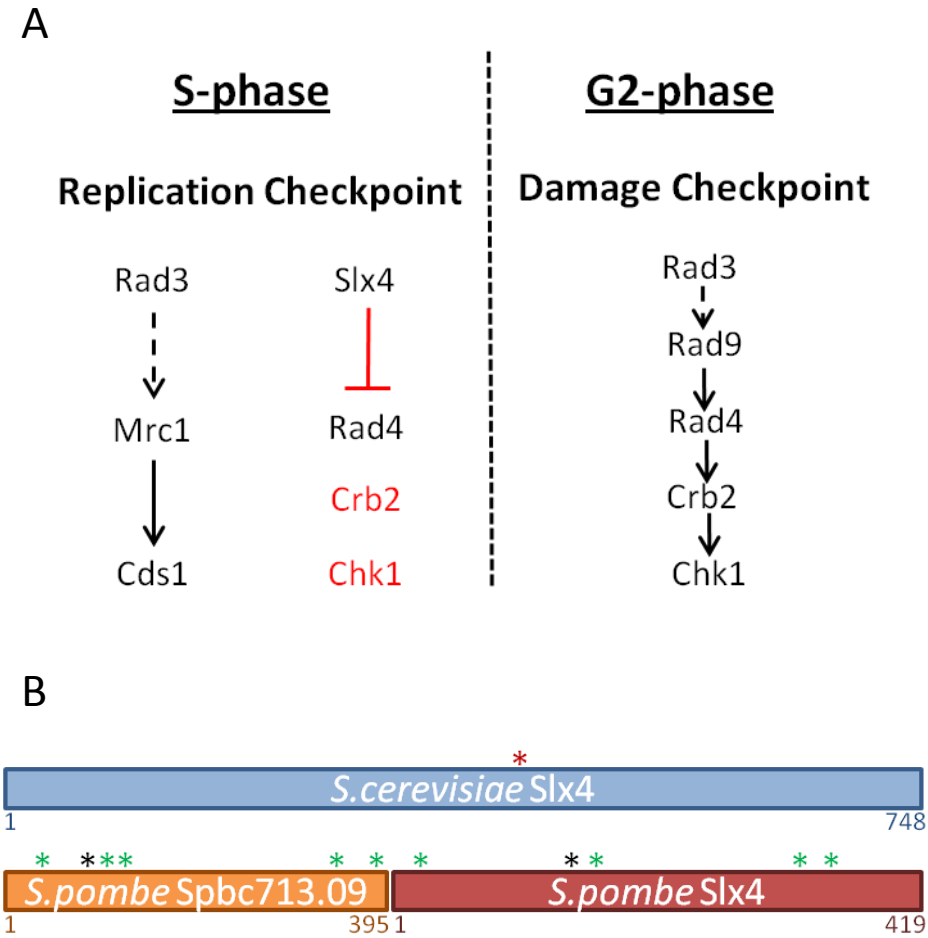

Figure 7-3. Slx4 as a potential Rad4 interacting protein in preventing the activation of the DNA damage checkpoint after replication stress.
A. A potential model for how Rad4 interactions may promote activation of the replication or damage checkpoints under the correct conditions. Left panel: During S-phase replication fork stalling may occur, which requires activation of the Cds1 dependent replication checkpoint but not the Chk1 damage checkpoint. In this case Slx4 may bind to Rad4 preventing its interaction with Crb2, and thus preventing Chk1 recruitment and activation. This would allow activation of only the replication checkpoint. Right panel: In G2 phase the DNA damage checkpoint needs to be activated upon DNA damage. In G2, Slx4 may not bind to Rad4 allowing it to bind to Crb2, which upon damage would allow the recruitment of Chk1 and activation of the damage checkpoint. Red line represents inhibitory binding, red text indicates the protein is not recruited/active. Dotted arrow represents phosphorylation and solid arrow represents binding. Black text represents recruited/active proteins. B. Schematic diagram of *S. cerevisiae* Slx4 and the two corresponding proteins (Spbc713.09 and Slx4) in *S. pombe*. Red * indicates the known Dpb11 interaction site on *S. cerevisiae* Slx4 (Ohouo et al., 2013). Black * represent TP/SP sites on *S. pombe* Spbc713.09 and Slx4. Green * represents TV/SV sites on the *S. pombe* protein.

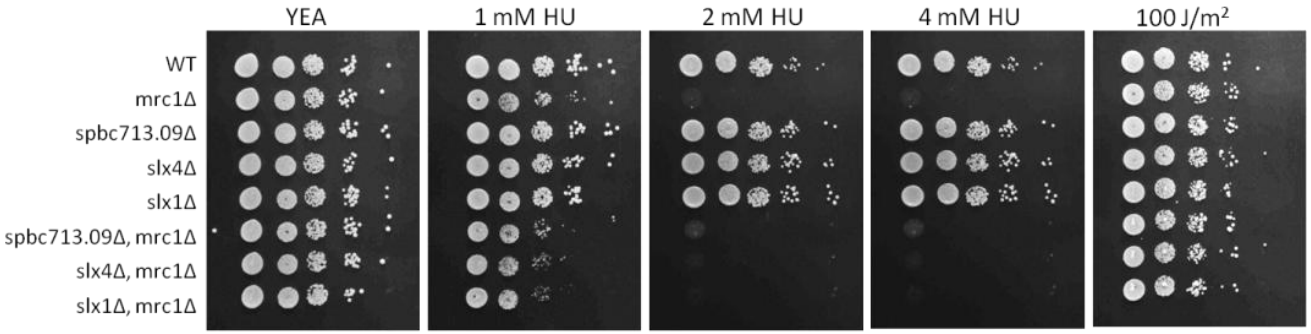

Figure 7-4. *slx4Δ* does not rescue the HU sensitivity of an *mrc1Δ*
Spot test analysis of the indicated WT, *mrc1Δ, spb713.09, slx4Δ, slx1Δ* and combinations thereof in the presence of HU. 10-fold serial dilutions of $1x10^7$ cells/ml were spotted onto YEA plates containing the indicated doses of HU and grown at 30˚C for 4 days

If Slx4 or Spbc713.09 are involved in binding Rad4 to prevent activation of the DNA damage checkpoint, knocking them out should rescue the HU sensitivity of an *mrc1Δ*. This is because *mrc1Δ* cells are sensitive to HU due to the lack of replication checkpoint activation. By deleting the *slx4* genes, Rad4 should now be free to bind to Crb2 and activate the DNA damage checkpoint. This active damage checkpoint should be able to partly compensate for the lack of replication checkpoint activation and rescue some of the *mrc1Δ* phenotype. From Figure 7-4 we can see that this is not the case and that the *slx4Δ mrc1Δ* and *spbc713.09Δ mrc1Δ* strains are just as sensitive, if not slightly more sensitive, than the *mrc1Δ* alone (Figure 7-4). Furthermore, they also show the same phenotype as the *slx1Δ mrc1Δ* mutant, suggesting that neither Slx4 nor Spbc713.09 bind Rad4 to prevent Chk1 activation at stalled replication forks (Figure 7-4).

To confirm the results in Figure 7-4 western blot analysis against Chk1-HA after 4 hrs HU treatment in the *spbc713.09Δ* and *slx4Δ* strains was performed (Figure 7-5A). If these proteins are indeed binding Rad4 to prevent Chk1-HA activation at stalled forks, the knockouts should show increased Chk1 phosphorylation after HU compared with WT. Consistent with the conclusions made from Figure 7-4, no increase in Chk1-HA phosphorylation can be seen in either *slx4Δ* or *spbc713.09Δ* strains after HU compared with WT (Figure 7-5A). Furthermore, only a very minor increase in Chk1-HA phosphorylation can be seen in the *spbc713.09Δ mrc1Δ* strain compared with *mrc1Δ* alone after HU, and no increase is seen in the *slx4Δ mrc1Δ* strain (Figure 7-5B, quantification in 7-5C). As Ohou et al., (2013) showed in budding yeast that an *slx4Δ* strain has increased Rad53 phosphorylation after MMS treatment, the levels of Chk1 phosphorylation after MMS in the *spbc713.09Δ, slx4Δ, spbc713.09Δ mrc1Δ* and *slx4Δ mrc1Δ* strains were tested (Ohouo et al., 2013). It can be seen from Figures 7-5B and C (right hand panel) that the spbc713.09Δ strain has decreased Chk1-HA phosphorylation compared with WT and the *spbc713.09Δ mrc1Δ* has decreased Chk-1HA phosphorylation compared with *mrc1Δ*. This reduction is relatively mild and the opposite of what would be expected if Spbc713.09 was inhibiting Chk1 activation by binding Rad4. This reduction in Chk1 phosphorylation may be due to loss of another function of Spbc713.09, such as reduced DNA processing.

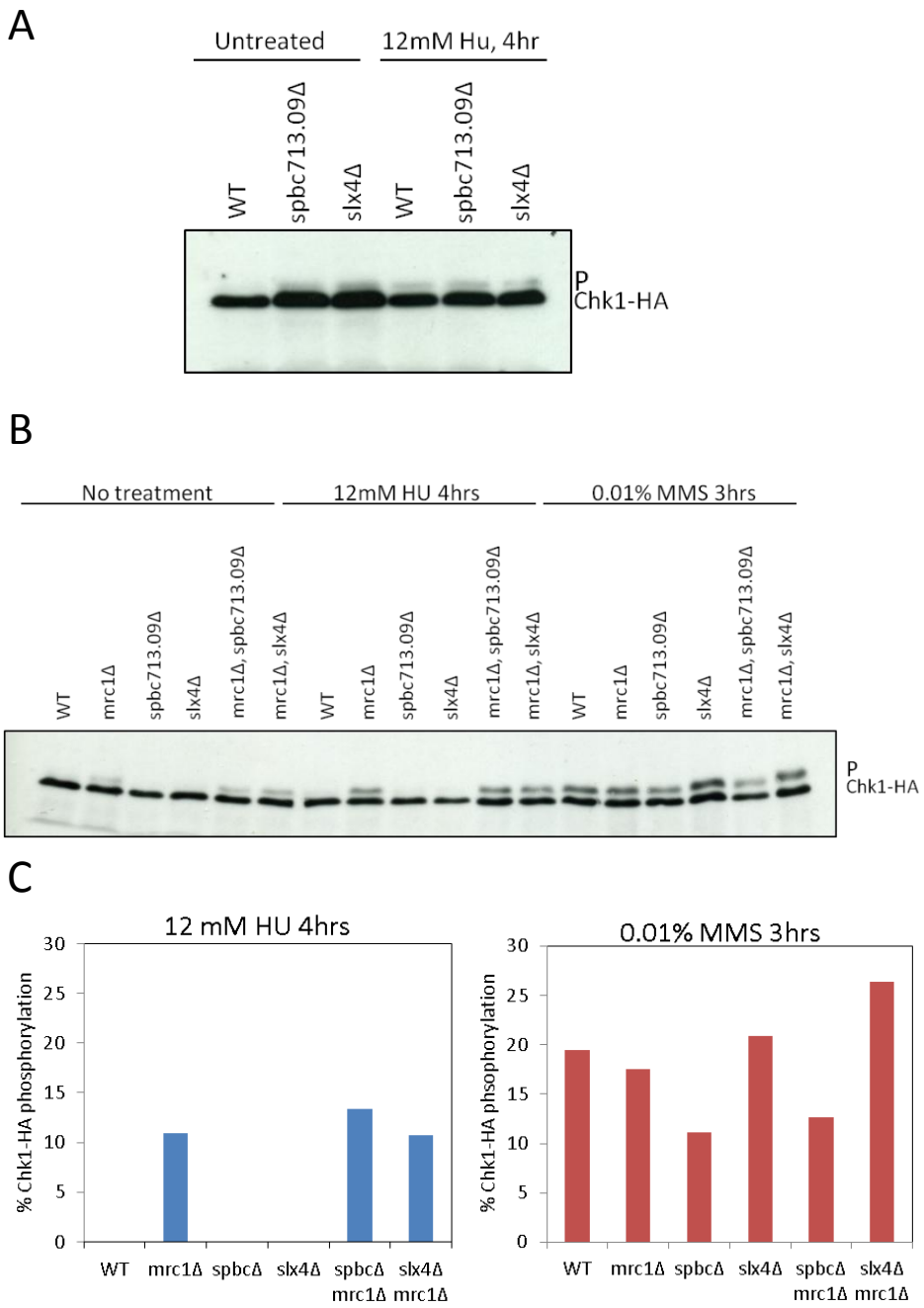

Figure 7-5 *spbc713.09Δ* and *slx4Δ* do not lead to an increase in Chk1 phosphorylation after HU even in an *mrc1Δ* background.

A. Asynchronous WT, *spbc713.09Δ* and *slx4Δ* cells were split and treated with 12mM HU for 4 hours or not treated (untreated). Chk1-HA phosphorylation was then assayed by SDS PAGE and α-HA antibodies. B. Asynchronous WT, *spbc713.09Δ* and *slx4Δ* ,*mrc1Δ, mrc1Δ spbc713.09Δ* and *mrc1Δ slx4 Δ* cells were split and treated with 12mM HU for 4 hours, 0.001% MMS for 3 hrs or not treated (untreated). Chk1-HA phosphorylation was then assayed by SDS PAGE and α-HA antibodies. C. Quantification of B. % chk1-HA phosphorylation was calculated by Chk1-HA phosphorylation (P) as a % of total Chk1-HA minus the % phosphorylation present in untreated cells.

Interestingly, the *slx4Δ* strain exhibits increased Chk1-HA phosphorylation after MMS compared with WT, but this is only a minor (3%) increase. The *slx4Δ mrc1Δ* does also show an increase in Chk1-HA phosphorylation after MMS compared to mrc1Δ, but again this is only a mild (~7%) increase. This is not enough to be consistent with a role for Slx4 in inhibiting the recruitment and activation of Chk1. In both Figures 7-4 and 7-5 a small increase in Chk1-HA phosphorylation can be seen in the *slx4Δ* and *spbc713.09Δ* strains even without genotoxic treatment. This could be due to Rad3 activation in the absence of checkpoint activating DNA structures due to the lack of a Rad4-Slx4/Spc713.09 interaction. Alternatively there may be an increase in spontaneous DNA damage in the *slx* deletes which leads to Rad3 activation. Indeed *slx4* is required for maintenance of the rDNA repeats at the rDNA replication fork barrier (Coulon et al., 2006).

7.3 Conclusions and Discussion

The data in this chapter has failed to shed any further light into the role of Rad4 during the activation of the replication checkpoint. Although Mrc1 contains a conserved potential Rad4 binding site at T32 (Figure 7-1B), mutation of this Cdc2 phosphorylation site, does not lead to an increase in sensitivity to the replication forks stalling agent HU (7-2). From this data we cannot conclude that Rad4 does not bind Mrc1-T32, but it would seem that any interaction that may occur is not essential for activation of the replication checkpoint in an otherwise WT back ground. Further work could be carried out on this mutant to investigate the levels of Cds1 kinase activity or Rad3 dependent Cds1 phosphorylation. This would exclude the possibility that the lack of a sensitivity phenotype is due to activation of the damage checkpoint. Furthermore, Chk1 phosphorylation could also be assayed after HU treatment in the *mrc1-T32A* strain to see if Chk1 phosphorylation has increased due to loss of the replication checkpoint. This, however, is unlikely as both *mrc1Δ* and *cds1Δ* strains show a decrease in survival after HU (Figure 7-2), so if Mrc1-T32 was critical for the activation of the replication checkpoint a similar level of sensitivity should have been apparent.

The results in Figures 7-4 and 7-5 show that the role of budding yeast Slx4 in inhibiting the DNA damage checkpoint via binding Dpb11^{Rad4} and preventing its interaction with Rad9 is most likely not conserved in *S. pombe*. Knocking out either of the *slx4* genes, *spbc713.09* or *slx4*, does not rescue the HU sensitivity of an *mrc1Δ*, or lead to a considerable increase in Chk1-HA phosphorylation after HU or MMS treatment. It maybe that there is a secondary pathway that also inhibits Crb2 recruitment and that knocking out the *slx4* genes is not enough to see a phenotype. In budding yeast Rtt107 (a BRCT domain protein) binds to Slx4 and to H2A, thus by binding γH2A it prevents Rad9 recruitment to the chromatin via its BRCT domain (Ohouo et al., 2013). However, knocking out *RTT107* or *SLX4* leads to a phenotype consistent with increased Rad53 phosphorylation in budding yeast (Ohouo et al., 2013). We should therefore see a phenotype in the *slx4Δ* or *spbc713.09Δ* in *S. pombe,* if the function of *slx4* is indeed conserved, however, this was not the case. In may be worth knocking out the *S. pombe RTT107* homolog, *brc1,* in the *slx4Δ* or *spbc713.09Δ* background, and checking for increased Chk1-HA phosphorylation after HU treatment. It may be that Brc1 is contributing more to the inhibition of the damage checkpoint in *S. pombe* than *S. cerevisiae*. It may also be interesting to test the *slx4Δ spbc713.09Δ* double mutant after HU, as they may be able to compensate for each other. However, the difference in the checkpoint pathways between budding yeast and fission yeast, offers the most likely explanation for the lack of phenotype in Figures 7-4 and 7-5.

Chapter 8

Final Conclusions and Discussion

8.1 Overview

Damage to a cell's DNA, from exogenous or endogenous factors, can lead to the accumulation of mutations and diseases, such as cancer. Organisms have therefore evolved mechanisms to help prevent such mutations occurring. One of the most important mechanisms for preventing mutations is the DNA damage checkpoint. This checkpoint is essential for the recognition of damaged DNA. Upon DNA damage the checkpoint, via signal transduction pathways, prevents cell cycle progression and promotes DNA repair. Here data has been presented, using the model organism *S. pombe,* which helps further understand the early events in the activation of the DNA damage checkpoint. This work makes inroads into understanding how the DNA damage checkpoint is activated in *S. pombe*. It increases our understanding of how the pathways and proteins involved in the checkpoint interact, the importance of these interactions and how they are regulated. It may also give insights into how the checkpoints may be functioning in higher eukaryotes.

8.2 S. pombe ATR Activation Domains

8.2.1 The Rad4 ATR Activation Domain

As described in the "1.6.4 TopBP1 dependent ATR Activation" section TopBP1 and the budding yeast homolog Dpb11 have been shown to have ATR activation activity (Kumagai et al., 2006, Mordes et al., 2008b). In budding yeast, this function of Dpb11 is restricted to G2 phase and is redundant with the $Ddc1^{Rad9}$ AAD (Navadgi-Patil et al., 2011, Pfander and Diffley, 2011). In higher eukaryotes, the pathway in which the TopBP1 AAD operates is less well understood. However, work from the Xenopus system has shown that it is required for ATR activation in S-phase (Kumagai and Dunphy, 2006). To help further understand the role of the TopBP1 AAD, Charly Chawan

(Carr lab) identified, via sequence alignment, a potential AAD in the C-terminus of the *S. pombe* TopBP1 homolog Rad4 (Figure 3-1A). The key residue from the Xenopus TopBP1 AAD, W1138, was conserved as Y599. Data presented here, and that from previous lab members Su-Jiun Lin and Valerie Garcia, shows that the Rad4 AAD can bind to $Rad3^{ATR}$ and is required for a full checkpoint response in G1/S. This cell cycle dependency is most likely to be due to the reduced levels of resection, and therefore ssDNA, after DNA damage in G1/S phase compared to G2. Furthermore, using a LacI-LacO tethering system, it is shown, in Chapter 3, that the Rad4 AAD acts in a chromatin-dependent pathway for checkpoint amplification. This pathway also depends upon γH2A, the Crb2 BRCT domains, Crb2 T215 phosphorylation, the 9-1-1 complex and Rad17 (Figure 3-11A, B, C). Further light has, therefore, been shed on the role and components of the chromatin pathway in Chk1 activation. Previously, the Russell laboratory and others have shown that a pathway requiring γH2A, H4-K20me and Crb2's BRCT and Tudor domains, is important for Chk1 activation (Du et al., 2006, Kilkenny et al., 2008). From the results presented here it is now known that this pathway requires the Rad4 AAD and can operate in G1/S phase to amplify the checkpoint signal initially generated by ssDNA.

Due to the G1/S-phase dependency of this chromatin pathway, we predict a threshold level of Rad3 activation is required for a full checkpoint response. The lower level of nuclease activity, and therefore resection, after damage in G1/S, when compared with G2, leads to reduced ssDNA. This may mean in G1/S-phase that not enough Rad3 is activated via the ssDNA pathway, in order to get a full checkpoint response. Therefore, the chromatin-dependent Rad4 AAD pathway of checkpoint amplification becomes more important for a full checkpoint response (Figure 3-14A, B). An alternative model to the one that has been presented here, is that the threshold for checkpoint activation is higher in S-phase than G2. In this case more Rad3 needs to be activated in S-phase to get a full checkpoint response. In budding yeast such a model has been proposed, with the Gasser laboratory showing that more DNA damage is required in S-phase, than in G2, to activate the checkpoint. They propose the existence of an S-phase threshold which is important to allow the cells to tolerate the ssDNA associated with the replication fork, without activating the checkpoint (Shimada et al., 2002).

However, this is most likely not what we are seeing in *S. pombe,* as the chromatin-dependent amplification pathway should bypass the need for extra ssDNA in S-phase for checkpoint activation.

8.2.2 The Rad9 ATR Activation Domain

Through sequence alignment we have identified that the budding yeast Ddc1 AAD is conserved in the *S. pombe* homolog Rad9 (Figure 4-1A). However, the *S. pombe* Rad9 AAD is less important for Rad3 activation than its budding yeast counterpart, with it only having a redundant role with the Rad4 AAD in the S-phase damage checkpoint (Figure 4-9). More work could be done to further understand the role of the *S. pombe* Rad9 AAD. For example, as it is required in the same cell cycle phases as the Rad4 AAD, it may be interesting to assay the role of the rad9-2A mutant in the LacO system. This would help us to understand whether it is functioning redundantly in the same pathway as the Rad4 AAD, or if it is functioning in a secondary back up pathway. It may also be interesting to see the relative importance of the Rad4 AAD and the Rad9 AAD in stimulating Rad3 kinase activity in *vitro*. This would help us understand if the difference in importance between the two AAD's is due to the recruitment of the proteins to Rad3, or due the Rad4 AAD being a better activator.

An interesting question that arises from the work presented in Chapters 3 and 4 and that from budding yeast is; why have more than one AAD containing protein? In budding yeast three AAD containing proteins, Dpb11, Ddc1 and Dna2, have been identified so far, two of which we have also been identified in *S. pombe* (Navadgi-Patil et al., 2011, Kumar and Burgers, 2013). One reason maybe that the activation of the ATR homologs is such an important process that organisms have evolved to contain more than one activator in case one becomes mutated and dysfunctional. Although this may explain why both Rad4 and Rad9 contain AAD domains, as they are at least in part functionally redundant, it does not explain the requirement for the Dna2 AAD in *S. cerevisiae*. This is because the Dna2 AAD operates in a separate cell cycle phase, and therefore pathway, to the AAD domains of Ddc1 and Dpb11. There may therefore be numerous AADs in *S. cerevisiae* because of the differences in the checkpoint complexes in different cell cycle stages. It maybe that Ddc1 and Dpb11 are not in close

enough proximity to $Mec1^{ATR}$ at stalled fork to activate it, where Dna2 is. At a DSB in G2 it may be the other way around, with Dna2 not being recruited to Mec1 as efficiently as Ddc1 or Dpb11. Indeed, Dna2 is only required for resection of DSBs in a pathway that is redundant with Exo1, therefore Dna2 may not be at all G2 damage sites, where Ddc1 and Dpb11 are (Huertas, 2010). More work needs to be done to understand the proteins that function in the Dna2 and Ddc1/Dpb11 AAD pathways and therefore why the Ddc1 and Dpb11 AADs do not function at stalled forks.

The different cell cycle requirements of the *S. cerevisiae* AAD's does pose the question of whether more proteins in *S. pombe* also contain AADs. One way to search for, and potentially identify AAD containing proteins in *S. pombe* is via the approach Kumar and Burgers (2013) used to Identify the Dna2 AAD in budding yeast. They determined that the AADs already identified in Ddc1 and Dpb11 are in unstructured regions of more than 40 amino acids and contain two aromatic residues. They could then screen proteins with these features for their ability to stimulate Mec1 kinase activity in *vitro* (Kumar and Burgers, 2013). However, this approach requires purification of a number of different proteins, and therefore may be time consuming if the purified proteins are not already available. An initial small scale genetic screen of genes containing the desired features may therefore be an alternative option. One could imagine expressing truncation mutants, where the unstructured domain is deleted, from a plasmid in the corresponding knockout strain and looking for rescue of sensitivity to genotoxic agents. A similar approach could be used to identify AAD containing proteins in human cells. It has been shown, for the TopBP1 AAD, that over expression of the AAD leads to checkpoint activation in the absence of damage (Kumagai et al., 2006). Therefore, the regions of genes corresponding to potential AADs could be over expressed in human cells and checkpoint activation assayed.

It may be possible that only one AAD exists in higher eukaryotes, this is confounded by the fact the TopBP1 AAD mutant is embryonic lethal in mice (Zhou et al., 2013). It maybe that in somatic cells, ATR plays a much less prominent role in the activation of the checkpoint than it does in yeast, due to the increased importance of ATM. Rather than having an ATR activator for each cell cycle phase, as in budding yeast, human cells may only require one. This one activator, TopBP1, may be important in ATR activation

in S-phase, for the replication checkpoint, hence the reason why it is essential in the quickly dividing developmental stages, but possibly not in the rest of the cell cycle, where ATM is more important for checkpoint activation. Indeed there are numerous ATM activators in higher eukaryotes, as described in the “1.4.2 The Activation of ATM” section, which may reflect the checkpoints increased dependency on ATM activation, compared to that in yeast. It would therefore be interesting to see whether numerous Tel1 activators are present in the yeast systems or not. However, very recent preliminary data suggests that NBS1 may also be able to activate ATR in DT40 cells independently of TopBP1 (Kobayashi et al., 2013). Further work needs to be done to validate these results.

8.3 Rad4 BRCT Domain Interactions

For the activation of the *S. pombe* DNA damage checkpoint, the mediator protein Crb2 needs to be bound to Rad4 in order to be recruited to the damage site. This subsequently leads to the recruitment and activation of Chk1, via Rad3 dependent phosphorylation events, and checkpoint activation. For many years the nature of this interaction between Crb2 and Rad4 has been of much debate. The phosphorylation of Crb2-T215 by Cdc2 was thought to be the factor required for this interaction. However, mutation of this site did not give as severe checkpoint defect as might be expected.

Data presented here, and that from the Du and Pearl laboratories, has given thorough mechanistic insight into the nature of the Rad4 Crb2 interaction. We show evidence for a model in which Crb2 is sequentially phosphorylated by Cdc2-Cdc13 (Figure 5-7A B). Initially, Cdc2-Cdc13 phosphorylates Crb2 on two canonical Cdc2 sites, T215 and T235, in a non-damage dependent manner (Figure 6-18A). This leads to association with Rad4, via a BRCT2-pT235 interaction, this is further stabilised by a BRCT1-pT215 interaction. The interaction between Rad4 and Crb2-pT235 pT215 brings Cdc2 into close proximity to the non-canonical Crb2-T187 site, via a non-phospho specific interaction between Cdc13 and Rad4 BRCT3/4. Cdc2 is now able phosphorylate both the T187 residues of the Crb2 homodimer (Figure 6-18B). Due to the strong affinity

Rad4 BRCT1 (and 2) has for pT187, a reorganisation of the Rad4-Crb2 interaction occurs, with Rad4 now binding across the two Crb2 molecules of the dimer, via BRCT1+2-pT187 interactions Figure 6-18C.

The data leading to this model poses a number of interesting questions into how Rad4 interacts with its binding partners and how these interactions are regulated. The first question that arises is; is sequential phosphorylation of Rad4 (or homolog) binding proteins a common theme? As already mentioned in Chapter 6 (section 6.11 Model and Discussion), in budding yeast, Sld2 is sequentially phosphorylated initially on, up to, five canonical $Cdc28^{Cdk}$ sites, with S100 and T214 being of most importance. This then leads to phosphorylation of T84, a non-canonical Cdc28 site. Although T84 is described as a non-canonical Cdc28 site it is still a TP site, the surrounding amino acids make it less favourable for phosphorylation compared with the other sites. It is therefore better described as a weaker Cdc28 consensus site. The authors go on to show, via yeast two hybrid and in *vitro* pull down assays, that only the phosphorylated T84, not the other phosphorylated sites, could bind to BRCT domains 3 and 4 of Dpb11. This rules out the idea that Dpb11 sequentially binds to Sld2, in manner similar to that seen for Rad4 and Crb2. Instead, the authors predict a conformational change model, in which increasing Cdc28 activity leads to phosphorylation of more TP/SP sites. This continues until the phosphorylations cause a large enough conformational change for the T84 site to be exposed, this is then phosphorylated by Cdc28 and Dpb11 binds (Tak et al., 2006). So, although sequential phosphorylation is important in the case of budding yeast Sld2, sequential binding is not.

Furthermore, the budding yeast Crb2 homolog, Rad9, has been shown to be phosphorylated on three different sites by Cdc28 ((Granata et al., 2010, Pfander and Diffley, 2011)Table 8-1). It may be that sequential phosphorylation is also important for its binding to Dpb11. However, not all three of the sites have been characterised in the same study, making it hard to determine if this is the case (Granata et al., 2010, Pfander and Diffley, 2011). Interestingly, the Sld3 proteins in fission yeast, budding yeast and human are also phosphorylated by CDK on numerous sites, which have been shown to be important for their interaction Rad4/ Dpb11/ TopBP1.

Table 8-1

Organism	Binding Protein	Phopho-Site	kinase	Minus 3 Position	BRCT Domain Bound	Reference
S.pombe	Crb2	T187 (TV) T215 (TP) T235 (TP)	Cdc2 Cdc2 Cdc2	Val Val Val	BRCT1+2 BRCT2 BRCT1?	This study
S.cerevisiae	Rad9	S462 (SP) T474 (TP) S11 (SP)	Cdc28 Cdc28 Cdc28	Ile Thr Trp	BRCT1/2 BRCT1/2 N/D	Phander and Diffley 2011; Granata et al., 2010
Human	53BP1	N/D	N/D	N/D	BRCT4/5	Cescutti et al., 2010
Human	MDC1	SDT repeats (pSDpTD) (215-241)	CK2	N/D	BRCT5	Wang et al., 2011; Leung et al., 2013
S.pombe	Sld3	T636 (TP) S673 (SP) T690 (TP)	Cdc2 Cdc2 Cdc2	Val Val Val	BRCT1/2 BRCT1/2 BRCT1/2	Fukuura et al., 2011
S.cerevisiae	Sld3	T600 (TP) S622 (SP)	Cdc28 Cdc28	Val Ile	BRCT1/2 BRCT1/2	Zegerman and Diffley 2007
Human	Treslin	T969 (TP) S1000 (SP)	CDK CDK	Val Val	BRCT0/1/2	Boos et al., 2011
S.pombe	Drc1 /Sld2	T111 (TP)	Cdc2	Leu	BRCT3/4	Fukuura et al., 2011
S.cerevisiae	Sld2	T84 (TP) (5 SP/TPs)	Cdc28	Ile	BRCT3/4	Tak et al., 2006
S.pombe	Rad9	T412 (TQ) S423 (SQ)	Rad3 Rad3	Phe Gly	BRCT4	Furuya et a., 2004
S.cerevisiae	Ddc1	T602 (TQ)	Mec1	Leu	BRCT4	Puddu et al., 2008
Human	Rad9	S387 (SE)	CK2	Ala	BRCT2	Rappas et al., 2010
S.cerevisiae	Slx4	S486 (SP)	Cdc28	Ser	BRCT1/2	Ohou et al., 2012
Human	FancJ/ Bach1	T1133 (TP)	CDK	Ile	BRCT7/8	Gong et al., 2010; Chung et al., 2010
Human	ATR	T1989 (TP)	ATR	Glu	BRCT7/8	Liu et al., 2011
Xenopus	Nbs1	T156 (TI) K158 (KT)	N/D N/P	Ile Val	BRCT1/2	Yoo et al., 2009

Table 8-1. Summary of the interactions made by Rad4 and its homologs. Table shows the Rad4/Dpb11/TopBP1 binding protein, the phosphorylated residue, the kinase that phosphorylates it, the minus three position residue from the phosphorylation site, the Rad4/Dpb11/TopBP1 BRCT domain that binds and the reference from which this information was taken. Homologous or similar interacting proteins are grouped together by colour. Mediator proteins are in red, proteins involved in initiation of DNA replication in blue, 9-1-1 proteins in orange and other interactions in green. N/D refers to no data and N/P means not phosphorylated

S. pombe Sld3 is phosphorylated on three sites by Cdc2, *S. cerevisiae* Sld3 on two sites and human Tresilin on two sites (Zegerman and Diffley, 2007, Boos et al., 2011, Fukuura et al., 2011) (Table 8-1). This could point to the notion that sequential phosphorylation may be important for the interaction between Sld3 and Rad4/Dpb11/TopBP1, but this is yet to be shown. None the less, it would seem that a common theme amongst at least some of the Rad4/Dpb11/TopBP1 binding partners is multiple phosphorylation by CDK. This is especially true for its binding partners involved in initiation of replication and in the yeasts the interaction with Crb2 (Table 8-1).

It would also seem that in yeasts the BRCT domains 1 and 2 of Rad4/Dpb11 always bind to CDK phosphorylated sites. From the currently published data, it may be construed that BRCTs 1 and 2 of Rad4/Dpb11 can only bind CDK sites. BRCT domains 4 is also able to bind CDK phosphorylate sites, and this can be seen for the interaction with Sld2 (Tak et al., 2006, Fukuura et al., 2011). However, it is also able to bind other phosphorylation sites, this is the case for the interaction between Rad4 and Rad9 in fission yeast as well as Dpb11 and Ddc1 in budding yeast (Furuya et al., 2004, Rappas et al., 2011) (Table 8-1). Therefore, it may be that Rad4/Dpb11 BRCT4 has a less specific binding consensus than BRCT1 and 2. This is also the case in human cells, with BRCT2 binding a CK2 site on Rad9 (Rappas et al., 2011).

From the data presented in Chapter 6, the structural data from the Pearl laboratory and previously published data, it is possible to further determine the consensus binding sequence for Rad4, and possibly *S. cerevisiae* Dpb11, BRCT domains 1 and 2. It appears that the minus three position from the phosphorylation site is important for the binding to Rad4, with valine and possibly Isoleucine being the preferred residues (Figure 6-16 A, B). All three of the phosphorylation sites in Crb2 required for the interaction with Rad4 have a valine at the minus three position (Figure 615, 6-16A,B). This is also true for all three of the Cdc2 sites required for Rad4 binding on Sld3 (Fukuura et al., 2011). This may suggest sequential binding between Rad4 and Sld3. Also, the two Cdc28 sites on *S. cerevisiae* Sld3 are preceded at the minus three position by valine and isoleucine. However, only one of the sites on budding yeast Rad9^{Crb2} has an isoleucine at its minus three position. This may imply that Rad4 only binds this one

site and the other two are required for a conformational change, allowing phosphorylation of the binding site, as with Sld2. From this data, it can be predicted that Rad4/Dpb11 BRCTs1 and 2 binds to a V/I-X-X-pT/pS-P/V. This Rad4 binding consensus site could also be expanded to incorporate the binding preferences of the other TopBP1 BRCT domains. It would seem that in all organisms if Rad4/Dpb11/TopBP1 is binding a CDK phosphorylated site it has a valine, Isoleucine or leucine (which has similar properties to valine/isoleucine) at the minus three position, regardless of the BRCT domain binding it. This can be seen for human Treslin, *S. pombe* and *S. cerevisiae* Sld2 and Human FancJ/Bach1 (and possibly Xenopus NBS1, if T156 is phosphorylated and this phosphorylation is by CDK) interactions. The only exception to this is the binding between budding yeast Slx4 and Dpb11, where the Slx4 Cdc28 site has a serine at the minus three position.

This potential Rad4/Dpb11/TopBp1 consensus binding site could, in theory, be used to help identify CDK phosphorylation dependent binding partners. For example, it could be used to identify an interacting partner for Rad4 in the activation of the replication checkpoint. Our attempt to do just this found a consensus binding site in Mrc1. However, mutation of this site did not lead to a checkpoint defect (Figure 7-2). This does not rule out the possibility that Rad4 does indeed bind Mrc1, it may just not be required for checkpoint activation, or that its role is redundant with another pathway. It may be worth searching other proteins known to be at the replication fork, or at stalled forks, for potential Rad4 binding sequences.

Other questions that have arisen from this study are concerned with the Cdc13-Rad4 interaction: what is the nature of the Cdc13-Rad4 interaction? Where does Cdc13 bind on Rad4 BRCT3/4? Is this interaction regulated? Does the binding of Cdc13 to Rad4 determine which target Rad4 binds to? Further work is required to answer all of these questions. It could be interesting to carry out cell cycle studies to see how the binding of Cdc13 to Rad4 changes throughout the cell cycle, and if it simply follows Cdc13 expression. This may also help understand whether the interaction influences which targets are phosphorylated by Cdc2, and bound to by Rad4. It may be that Rad4 is able to localise Cdc2-Cdc13 to specific targets. For example, recruitment of Rad4 to Rad3 phosphorylated Rad9 may target Cdc13-Cdc2 to the site of damage, where it could

phosphorylate repair proteins. To narrow down the Cdc13 binding region on Rad4, pull down assays could be performed with different sized Rad4 BRCT3/4 peptides. The reverse experiment could then be done to find the region of Cdc13 that binds to Rad4. Once these regions have been identified the presence of certain domains, motifs or post translational modification sites may help to shed light on the nature of the interaction and whether or not it is regulated. It may also be interesting to see if cyclins in other organisms are able to bind to the Rad4 homologs.

In human cells it has been shown that TopBP1 is able to bind the Crb2 homolog 53BP1, and that this interaction is required for the DNA damage checkpoint in G1 (Cescutti et al., 2010). However, the nature of this interaction is not understood. Although, TopBP1 BRCTs 4 and 5, which functionally correspond to yeast BRCTs 1 and 2, are required for the interaction, no sites on 53BP1 have been identified (Cescutti et al., 2010) (Table 8.1). It would be interesting to see if the same mechanism of binding that we see for Rad4 and Crb2 is true for the higher eukaryotes. A search of the 53BP1 amino acid sequence shows there are a number of TP/SP sites within the protein, one of which has a valine at the minus three position. There is also an SV site with a minus three position isoleucine and a TV site with a minus three leucine. It is therefore possible that one, or more, of these maybe a TopBP1 binding site. Also, mutants corresponding to those made in the Rad4 BRCT domains 1 and 2 in Figure 6-2 and 6-9 could be made in human TopBP1. This would help to shed light on the role of each of the BRCT domains in humans. It may show which BRCT domains are required for checkpoint activation in each of the cell cycle phases, or after certain types of damage. It may also show the BRCT domain requirement for replication initiation in human cells. It would be interesting to see if either BRCT4 or 5 are required (as with *S. pombe* BRCT1 and 2) or both.

With the increasing level of knowledge about TopBP1 and its homologs, the role of the TopBP1 BRCT domains and their binding partners in disease could also become an important area of research. It would be interesting to see if mutations of any of the BRCT domains are associated with developmental diseases such as Seckel like syndromes. Patients with Seckel syndrome normally have mutations in the checkpoint proteins ATR or ATRIP, or in the DNA replication licensing protein Orc1 (O'Driscoll et

al., 2003, Bicknell et al., 2011, Ogi et al., 2012). As TopBP1 BRCTs 4 and 5 are involved in both the checkpoint and the initiation of DNA replication, it is not unfeasible to hypothesise that a mutation in the phospho-binding pocket of one of these BRCT domains that reduces binding to its targets, could lead to a Seckle like syndrome. However, to date no mutations have been reported in any patients.

Another intriguing possibility is the design of small peptide inhibitors that are able to specifically bind to, and inhibit, TopBP1 BRCT domains. This has already been shown to be possible for the BRCT domains of BRCA1 and computer modelling suggests that it could also be possible for TopBP1 (Yuan et al., 2011). Peptides could be made that resemble the Rad4 BRCT1/2 binding sequence described above. These could then be screened to find peptides that bind with high affinity and would thus prevent TopBP1 from binding its targets. Due to the different binding specificities of BRCT domains of different proteins (for example the BRCT domains of BRCA1 bind pSXXF), or even within a protein, very specific peptides could be generated (Yue et al., 2011). These peptides could be used to help understand the roles of the different BRCT domains of TopBP1 without having to generate cell lines, or have the problem of inviable mutants. If these inhibitors could be made soluble enough, they may make good anti-cancer drugs. Inhibition of TopBP1 BRCT domains may target cancer cells in two ways. Firstly, by inhibiting initiation of DNA replication, they could prevent the rapid cell cycle progression and division seen in cancer cells, therefore preventing their proliferation. Secondly by inhibiting the checkpoint they may sensitise cells to DNA damage through radiation or damage causing drugs. This would be of particular use if the cancer cells already contained mutations in checkpoint or DNA repair pathways, as this would make them more susceptible to the TopBP1 inhibitors than the normal cells of the body.

Overall, from this work important insights into how checkpoints work in *S. Pombe* have been made, similarities and differences between organisms have been exposed and this leads the way for further study in higher eukaryotes.

Bibliography

ABRAHAM, R. T. 2001. Cell cycle checkpoint signaling through the ATM and ATR kinases. *Genes Dev,* 15**,** 2177-96.

ADHIKARY, S. & EILERS, M. 2005. Transcriptional regulation and transformation by Myc proteins. *Nat Rev Mol Cell Biol,* 6**,** 635-45.

ALCASABAS, A. A., OSBORN, A. J., BACHANT, J., HU, F., WERLER, P. J., BOUSSET, K., FURUYA, K., DIFFLEY, J. F., CARR, A. M. & ELLEDGE, S. J. 2001. Mrc1 transduces signals of DNA replication stress to activate Rad53. *Nat Cell Biol,* 3**,** 958-65.

ANDRESON, B. L., GUPTA, A., GEORGIEVA, B. P. & ROTHSTEIN, R. 2010. The ribonucleotide reductase inhibitor, Sml1, is sequentially phosphorylated, ubiquitylated and degraded in response to DNA damage. *Nucleic Acids Res,* 38**,** 6490-501.

ARAKI, H. 2011. Initiation of chromosomal DNA replication in eukaryotic cells; contribution of yeast genetics to the elucidation. *Genes Genet Syst,* 86**,** 141-9.

ARAKI, H., LEEM, S. H., PHONGDARA, A. & SUGINO, A. 1995. Dpb11, which interacts with DNA polymerase II(epsilon) in Saccharomyces cerevisiae, has a dual role in S-phase progression and at a cell cycle checkpoint. *Proc Natl Acad Sci U S A,* 92**,** 11791-5.

AVES, S. J., DURKACZ, B. W., CARR, A. & NURSE, P. 1985. Cloning, sequencing and transcriptional control of the Schizosaccharomyces pombe cdc10 'start' gene. *EMBO J,* 4**,** 457-63.

BAE, S. H. & SEO, Y. S. 2000. Characterization of the enzymatic properties of the yeast dna2 Helicase/endonuclease suggests a new model for Okazaki fragment processing. *J Biol Chem,* 275**,** 38022-31.

BAKKENIST, C. J. & KASTAN, M. B. 2003. DNA damage activates ATM through intermolecular autophosphorylation and dimer dissociation. *Nature,* 421**,** 499-506.

BALL, H. L., EHRHARDT, M. R., MORDES, D. A., GLICK, G. G., CHAZIN, W. J. & CORTEZ, D. 2007. Function of a conserved checkpoint recruitment domain in ATRIP proteins. *Mol Cell Biol,* 27**,** 3367-77.

BALL, H. L., MYERS, J. S. & CORTEZ, D. 2005. ATRIP binding to replication protein A-single-stranded DNA promotes ATR-ATRIP localization but is dispensable for Chk1 phosphorylation. *Mol Biol Cell,* 16**,** 2372-81.

BANIN, S., MOYAL, L., SHIEH, S., TAYA, Y., ANDERSON, C. W., CHESSA, L., SMORODINSKY, N. I., PRIVES, C., REISS, Y., SHILOH, Y. & ZIV, Y. 1998. Enhanced phosphorylation of p53 by ATM in response to DNA damage. *Science,* 281**,** 1674-7.

BARTKOVA, J., HOREJSI, Z., KOED, K., KRAMER, A., TORT, F., ZIEGER, K., GULDBERG, P., SEHESTED, M., NESLAND, J. M., LUKAS, C., ORNTOFT, T., LUKAS, J. & BARTEK, J. 2005. DNA damage response as a candidate anti-cancer barrier in early human tumorigenesis. *Nature,* 434**,** 864-70.

BENTLEY, N. J., HOLTZMAN, D. A., FLAGGS, G., KEEGAN, K. S., DEMAGGIO, A., FORD, J. C., HOEKSTRA, M. & CARR, A. M. 1996. The Schizosaccharomyces pombe rad3 checkpoint gene. *EMBO J,* 15**,** 6641-51.

BERENS, T. J. & TOCZYSKI, D. P. 2012. Colocalization of Mec1 and Mrc1 is sufficient for Rad53 phosphorylation in *vivo*. *Mol Biol Cell,* 23**,** 1058-67.

BERMUDEZ, V. P., LINDSEY-BOLTZ, L. A., CESARE, A. J., MANIWA, Y., GRIFFITH, J. D., HURWITZ, J. & SANCAR, A. 2003. Loading of the human 9-1-1 checkpoint complex

onto DNA by the checkpoint clamp loader hRad17-replication factor C complex in *vitro*. *Proc Natl Acad Sci U S A,* 100**,** 1633-8.

BHATTI, S., KOZLOV, S., FAROOQI, A. A., NAQI, A., LAVIN, M. & KHANNA, K. K. 2011. ATM protein kinase: the linchpin of cellular defenses to stress. *Cell Mol Life Sci,* 68**,** 2977-3006.

BHOUMIK, A., SINGHA, N., O'CONNELL, M. J. & RONAI, Z. A. 2008. Regulation of TIP60 by ATF2 modulates ATM activation. *J Biol Chem,* 283**,** 17605-14.

BHOUMIK, A., TAKAHASHI, S., BREITWEISER, W., SHILOH, Y., JONES, N. & RONAI, Z. 2005. ATM-dependent phosphorylation of ATF2 is required for the DNA damage response. *Mol Cell,* 18**,** 577-87.

BICKNELL, L. S., WALKER, S., KLINGSEISEN, A., STIFF, T., LEITCH, A., KERZENDORFER, C., MARTIN, C. A., YEYATI, P., AL SANNA, N., BOBER, M., JOHNSON, D., WISE, C., JACKSON, A. P., O'DRISCOLL, M. & JEGGO, P. A. 2011. Mutations in ORC1, encoding the largest subunit of the origin recognition complex, cause microcephalic primordial dwarfism resembling Meier-Gorlin syndrome. *Nat Genet,* 43**,** 350-5.

BLAUT, M. A., BOGDANOVA, N. V., BREMER, M., KARSTENS, J. H., HILLEMANNS, P. & DORK, T. 2010. TOPBP1 missense variant Arg309Cys and breast cancer in a German hospital-based case-control study. *J Negat Results Biomed,* 9**,** 9.

BONER, W. & MORGAN, I. M. 2002. Novel cellular interacting partners of the human papillomavirus 16 transcription/replication factor E2. *Virus Res,* 90**,** 113-8.

BONER, W., TAYLOR, E. R., TSIRIMONAKI, E., YAMANE, K., CAMPO, M. S. & MORGAN, I. M. 2002. A Functional interaction between the human papillomavirus 16 transcription/replication factor E2 and the DNA damage response protein TopBP1. *J Biol Chem,* 277**,** 22297-303.

BONILLA, C. Y., MELO, J. A. & TOCZYSKI, D. P. 2008. Colocalization of sensors is sufficient to activate the DNA damage checkpoint in the absence of damage. *Mol Cell,* 30**,** 267-76.

BOOS, D., SANCHEZ-PULIDO, L., RAPPAS, M., PEARL, L. H., OLIVER, A. W., PONTING, C. P. & DIFFLEY, J. F. 2011. Regulation of DNA replication through Sld3-Dpb11 interaction is conserved from yeast to humans. *Curr Biol,* 21**,** 1152-7.

BOSOTTI, R., ISACCHI, A. & SONNHAMMER, E. L. 2000. FAT: a novel domain in PIK-related kinases. *Trends Biochem Sci,* 25**,** 225-7.

BREWERTON, S. C., DORE, A. S., DRAKE, A. C., LEUTHER, K. K. & BLUNDELL, T. L. 2004. Structural analysis of DNA-PKcs: modelling of the repeat units and insights into the detailed molecular architecture. *J Struct Biol,* 145**,** 295-306.

BROWN, E. J. & BALTIMORE, D. 2000. ATR disruption leads to chromosomal fragmentation and early embryonic lethality. *Genes Dev,* 14**,** 397-402.

BROWN, E. J. & BALTIMORE, D. 2003. Essential and dispensable roles of ATR in cell cycle arrest and genome maintenance. *Genes Dev,* 17**,** 615-28.

BRUCK, I., KANTER, D. M. & KAPLAN, D. L. 2011. Enabling association of the GINS protein tetramer with the mini chromosome maintenance (Mcm)2-7 protein complex by phosphorylated Sld2 protein and single-stranded origin DNA. *J Biol Chem,* 286**,** 36414-26.

BRUCK, I. & KAPLAN, D. L. 2011. Origin single-stranded DNA releases Sld3 protein from the Mcm2-7 complex, allowing the GINS tetramer to bind the Mcm2-7 complex. *J Biol Chem,* 286**,** 18602-13.

BURMA, S., CHEN, B. P., MURPHY, M., KURIMASA, A. & CHEN, D. J. 2001. ATM phosphorylates histone H2AX in response to DNA double-strand breaks. *J Biol Chem,* 276**,** 42462-7.

BURROWS, A. E. & ELLEDGE, S. J. 2008. How ATR turns on: TopBP1 goes on ATRIP with ATR. *Genes Dev,* 22**,** 1416-21.

BYUN, T. S., PACEK, M., YEE, M. C., WALTER, J. C. & CIMPRICH, K. A. 2005. Functional uncoupling of MCM helicase and DNA polymerase activities activates the ATR-dependent checkpoint. *Genes Dev,* 19**,** 1040-52.

CAFFERKEY, R., MCLAUGHLIN, M. M., YOUNG, P. R., JOHNSON, R. K. & LIVI, G. P. 1994. Yeast TOR (DRR) proteins: amino-acid sequence alignment and identification of structural motifs. *Gene,* 141**,** 133-6.

CANMAN, C. E., LIM, D. S., CIMPRICH, K. A., TAYA, Y., TAMAI, K., SAKAGUCHI, K., APPELLA, E., KASTAN, M. B. & SILICIANO, J. D. 1998. Activation of the ATM kinase by ionizing radiation and phosphorylation of p53. *Science,* 281**,** 1677-9.

CARNEY, J. P., MASER, R. S., OLIVARES, H., DAVIS, E. M., LE BEAU, M., YATES, J. R., 3RD, HAYS, L., MORGAN, W. F. & PETRINI, J. H. 1998. The hMre11/hRad50 protein complex and Nijmegen breakage syndrome: linkage of double-strand break repair to the cellular DNA damage response. *Cell,* 93**,** 477-86.

CARR, A. M. 2002. DNA structure dependent checkpoints as regulators of DNA repair. *DNA Repair (Amst),* 1**,** 983-94.

CASPARI, T., MURRAY, J. M. & CARR, A. M. 2002. Cdc2-cyclin B kinase activity links Crb2 and Rqh1-topoisomerase III. *Genes Dev,* 16**,** 1195-208.

CELESTE, A., DIFILIPPANTONIO, S., DIFILIPPANTONIO, M. J., FERNANDEZ-CAPETILLO, O., PILCH, D. R., SEDELNIKOVA, O. A., ECKHAUS, M., RIED, T., BONNER, W. M. & NUSSENZWEIG, A. 2003. H2AX haploinsufficiency modifies genomic stability and tumor susceptibility. *Cell,* 114**,** 371-83.

CELESTE, A., PETERSEN, S., ROMANIENKO, P. J., FERNANDEZ-CAPETILLO, O., CHEN, H. T., SEDELNIKOVA, O. A., REINA-SAN-MARTIN, B., COPPOLA, V., MEFFRE, E., DIFILIPPANTONIO, M. J., REDON, C., PILCH, D. R., OLARU, A., ECKHAUS, M., CAMERINI-OTERO, R. D., TESSAROLLO, L., LIVAK, F., MANOVA, K., BONNER, W. M., NUSSENZWEIG, M. C. & NUSSENZWEIG, A. 2002. Genomic instability in mice lacking histone H2AX. *Science,* 296**,** 922-7.

CEROSALETTI, K. & CONCANNON, P. 2004. Independent roles for nibrin and Mre11-Rad50 in the activation and function of Atm. *J Biol Chem,* 279**,** 38813-9.

CESCUTTI, R., NEGRINI, S., KOHZAKI, M. & HALAZONETIS, T. D. 2010. TopBP1 functions with 53BP1 in the G1 DNA damage checkpoint. *EMBO J,* 29**,** 3723-32.

CHAILLEUX, C., TYTECA, S., PAPIN, C., BOUDSOCQ, F., PUGET, N., COURILLEAU, C., GRIGORIEV, M., CANITROT, Y. & TROUCHE, D. 2010. Physical interaction between the histone acetyl transferase Tip60 and the DNA double-strand breaks sensor MRN complex. *Biochem J,* 426**,** 365-71.

CHAPMAN, J. R. & JACKSON, S. P. 2008. Phospho-dependent interactions between NBS1 and MDC1 mediate chromatin retention of the MRN complex at sites of DNA damage. *EMBO Rep,* 9**,** 795-801.

CHEHAB, N. H., MALIKZAY, A., STAVRIDI, E. S. & HALAZONETIS, T. D. 1999. Phosphorylation of Ser-20 mediates stabilization of human p53 in response to DNA damage. *Proceedings of the National Academy of Sciences of the United States of America,* 96**,** 13777-82.

CHEN, Y. & SANCHEZ, Y. 2004. Chk1 in the DNA damage response: conserved roles from yeasts to mammals. *DNA Repair (Amst),* 3**,** 1025-32.

CHOI, J. H., LINDSEY-BOLTZ, L. A., KEMP, M., MASON, A. C., WOLD, M. S. & SANCAR, A. 2010. Reconstitution of RPA-covered single-stranded DNA-activated ATR-Chk1 signaling. *Proc Natl Acad Sci U S A,* 107**,** 13660-5.

CIMPRICH, K. A. & CORTEZ, D. 2008. ATR: an essential regulator of genome integrity. *Nat Rev Mol Cell Biol,* 9**,** 616-27.

CIMPRICH, K. A., SHIN, T. B., KEITH, C. T. & SCHREIBER, S. L. 1996. cDNA cloning and gene mapping of a candidate human cell cycle checkpoint protein. *Proc Natl Acad Sci U S A,* 93**,** 2850-5.

CORREA-BORDES, J. & NURSE, P. 1995. p25rum1 orders S phase and mitosis by acting as an inhibitor of the p34cdc2 mitotic kinase. *Cell,* 83**,** 1001-9.

CORTEZ, D., GUNTUKU, S., QIN, J. & ELLEDGE, S. J. 2001. ATR and ATRIP: partners in checkpoint signaling. *Science,* 294**,** 1713-6.

CORTEZ, D., WANG, Y., QIN, J. & ELLEDGE, S. J. 1999. Requirement of ATM-dependent phosphorylation of brca1 in the DNA damage response to double-strand breaks. *Science,* 286**,** 1162-6.

COTTA-RAMUSINO, C., MCDONALD, E. R., 3RD, HUROV, K., SOWA, M. E., HARPER, J. W. & ELLEDGE, S. J. 2011. A DNA damage response screen identifies RHINO, a 9-1-1 and TopBP1 interacting protein required for ATR signaling. *Science,* 332**,** 1313-7.

COULON, S., NOGUCHI, E., NOGUCHI, C., DU, L. L., NAKAMURA, T. M. & RUSSELL, P. 2006. Rad22Rad52-dependent repair of ribosomal DNA repeats cleaved by Slx1-Slx4 endonuclease. *Mol Biol Cell,* 17**,** 2081-90.

DAIGAKU, Y., DAVIES, A. A. & ULRICH, H. D. 2010. Ubiquitin-dependent DNA damage bypass is separable from genome replication. *Nature,* 465**,** 951-5.

DAUB, H., OLSEN, J. V., BAIRLEIN, M., GNAD, F., OPPERMANN, F. S., KORNER, R., GREFF, Z., KERI, G., STEMMANN, O. & MANN, M. 2008. Kinase-selective enrichment enables quantitative phosphoproteomics of the kinome across the cell cycle. *Mol Cell,* 31**,** 438-48.

DE KLEIN, A., MUIJTJENS, M., VAN OS, R., VERHOEVEN, Y., SMIT, B., CARR, A. M., LEHMANN, A. R. & HOEIJMAKERS, J. H. 2000. Targeted disruption of the cell-cycle checkpoint gene ATR leads to early embryonic lethality in mice. *Curr Biol,* 10**,** 479-82.

DELACROIX, S., WAGNER, J. M., KOBAYASHI, M., YAMAMOTO, K. & KARNITZ, L. M. 2007. The Rad9-Hus1-Rad1 (9-1-1) clamp activates checkpoint signaling via TopBP1. *Genes Dev,* 21**,** 1472-7.

DEPHOURE, N., ZHOU, C., VILLEN, J., BEAUSOLEIL, S. A., BAKALARSKI, C. E., ELLEDGE, S. J. & GYGI, S. P. 2008. A quantitative atlas of mitotic phosphorylation. *Proc Natl Acad Sci U S A,* 105**,** 10762-7.

DERHEIMER, F. A. & KASTAN, M. B. 2010. Multiple roles of ATM in monitoring and maintaining DNA integrity. *FEBS Lett,* 584**,** 3675-81.

DIFFLEY, J. F. 2004. Regulation of early events in chromosome replication. *Curr Biol,* 14**,** R778-86.

DODSON, G. E. & RUSSELL, P. 2011. Enhanced Tel1(ATM) checkpoint signaling at protein-bound double-strand breaks. *Mol Cell Biol,* 31**,** 1936-7.

DOIL, C., MAILAND, N., BEKKER-JENSEN, S., MENARD, P., LARSEN, D. H., PEPPERKOK, R., ELLENBERG, J., PANIER, S., DUROCHER, D., BARTEK, J., LUKAS, J. & LUKAS, C. 2009. RNF168 binds and amplifies ubiquitin conjugates on damaged chromosomes to allow accumulation of repair proteins. *Cell,* 136**,** 435-46.

DORE, A. S., KILKENNY, M. L., RZECHORZEK, N. J. & PEARL, L. H. 2009. Crystal structure of the rad9-rad1-hus1 DNA damage checkpoint complex--implications for clamp loading and regulation. *Mol Cell,* 34**,** 735-45.

DOVEY, C. L. & RUSSELL, P. 2007. Mms22 preserves genomic integrity during DNA replication in Schizosaccharomyces pombe. *Genetics,* 177**,** 47-61.

DU, L. L., NAKAMURA, T. M., MOSER, B. A. & RUSSELL, P. 2003. Retention but not recruitment of Crb2 at double-strand breaks requires Rad1 and Rad3 complexes. *Mol Cell Biol,* 23**,** 6150-8.

DU, L. L., NAKAMURA, T. M. & RUSSELL, P. 2006. Histone modification-dependent and -independent pathways for recruitment of checkpoint protein Crb2 to double-strand breaks. *Genes Dev,* 20**,** 1583-96.

DUFAULT, V. M., OESTREICH, A. J., VROMAN, B. T. & KARNITZ, L. M. 2003. Identification and characterization of RAD9B, a paralog of the RAD9 checkpoint gene. *Genomics,* 82**,** 644-51.

DUURSMA, A. M., DRISCOLL, R., ELIAS, J. E. & CIMPRICH, K. A. 2013. A Role for the MRN Complex in ATR Activation via TOPBP1 Recruitment. *Mol Cell,* 50**,** 116-22.

EDWARDS, R. J., BENTLEY, N. J. & CARR, A. M. 1999. A Rad3-Rad26 complex responds to DNA damage independently of other checkpoint proteins. *Nature cell biology,* 1**,** 393-8.

ELLEDGE, S. J., ZHOU, Z. & ALLEN, J. B. 1992. Ribonucleotide reductase: regulation, regulation, regulation. *Trends Biochem Sci,* 17**,** 119-23.

ELLISON, V. & STILLMAN, B. 2003. Biochemical characterization of DNA damage checkpoint complexes: clamp loader and clamp complexes with specificity for 5' recessed DNA. *PLoS Biol,* 1**,** E33.

EMILI, A. 1998. MEC1-dependent phosphorylation of Rad9p in response to DNA damage. *Mol Cell,* 2**,** 183-9.

ERRICO, A., COSTANZO, V. & HUNT, T. 2007. Tipin is required for stalled replication forks to resume DNA replication after removal of aphidicolin in Xenopus egg extracts. *Proc Natl Acad Sci U S A,* 104**,** 14929-34.

ESASHI, F. & YANAGIDA, M. 1999. Cdc2 phosphorylation of Crb2 is required for reestablishing cell cycle progression after the damage checkpoint. *Mol Cell,* 4**,** 167-74.

FALCK, J., COATES, J. & JACKSON, S. P. 2005. Conserved modes of recruitment of ATM, ATR and DNA-PKcs to sites of DNA damage. *Nature,* 434**,** 605-11.

FALCK, J., MAILAND, N., SYLJUASEN, R. G., BARTEK, J. & LUKAS, J. 2001. The ATM-Chk2-Cdc25A checkpoint pathway guards against radioresistant DNA synthesis. *Nature,* 410**,** 842-7.

FANNING, E., KLIMOVICH, V. & NAGER, A. R. 2006. A dynamic model for replication protein A (RPA) function in DNA processing pathways. *Nucleic Acids Res,* 34**,** 4126-37.

FEKAIRI, S., SCAGLIONE, S., CHAHWAN, C., TAYLOR, E. R., TISSIER, A., COULON, S., DONG, M. Q., RUSE, C., YATES, J. R., 3RD, RUSSELL, P., FUCHS, R. P., MCGOWAN, C. H. & GAILLARD, P. H. 2009. Human SLX4 is a Holliday junction resolvase subunit that binds multiple DNA repair/recombination endonucleases. *Cell,* 138**,** 78-89.

FENECH, M., CARR, A. M., MURRAY, J., WATTS, F. Z. & LEHMANN, A. R. 1991. Cloning and characterization of the rad4 gene of Schizosaccharomyces pombe; a gene showing short regions of sequence similarity to the human XRCC1 gene. *Nucleic Acids Res,* 19**,** 6737-41.

FIELD, S. J., TSAI, F. Y., KUO, F., ZUBIAGA, A. M., KAELIN, W. G., JR., LIVINGSTON, D. M., ORKIN, S. H. & GREENBERG, M. E. 1996. E2F-1 functions in mice to promote apoptosis and suppress proliferation. *Cell,* 85**,** 549-61.

FORMA, E., KRZESLAK, A., BERNACIAK, M., ROMANOWICZ-MAKOWSKA, H. & BRYS, M. 2012. Expression of TopBP1 in hereditary breast cancer. *Mol Biol Rep,* 39**,** 7795-804.

FRITZ, E., FRIEDL, A. A., ZWACKA, R. M., ECKARDT-SCHUPP, F. & MEYN, M. S. 2000. The yeast TEL1 gene partially substitutes for human ATM in suppressing hyperrecombination, radiation-induced apoptosis and telomere shortening in A-T cells. *Mol Biol Cell,* 11**,** 2605-16.

FUKUNAGA, K., KWON, Y., SUNG, P. & SUGIMOTO, K. 2011. Activation of protein kinase Tel1 through recognition of protein-bound DNA ends. *Mol Cell Biol,* 31**,** 1959-71.

FUKUURA, M., NAGAO, K., OBUSE, C., TAKAHASHI, T. S., NAKAGAWA, T. & MASUKATA, H. 2011. CDK promotes interactions of Sld3 and Drc1 with Cut5 for initiation of DNA replication in fission yeast. *Mol Biol Cell,* 22**,** 2620-33.

FURNARI, B., RHIND, N. & RUSSELL, P. 1997. Cdc25 mitotic inducer targeted by chk1 DNA damage checkpoint kinase. *Science,* 277**,** 1495-7.

FURUSE, M., NAGASE, Y., TSUBOUCHI, H., MURAKAMI-MUROFUSHI, K., SHIBATA, T. & OHTA, K. 1998. Distinct roles of two separable in *vitro* activities of yeast Mre11 in mitotic and meiotic recombination. *Embo J,* 17**,** 6412-25.

FURUYA, K., MIYABE, I., TSUTSUI, Y., PADERI, F., KAKUSHO, N., MASAI, H., NIKI, H. & CARR, A. M. 2010. DDK phosphorylates checkpoint clamp component Rad9 and promotes its release from damaged chromatin. *Mol Cell,* 40**,** 606-18.

FURUYA, K., POITELEA, M., GUO, L., CASPARI, T. & CARR, A. M. 2004. Chk1 activation requires Rad9 S/TQ-site phosphorylation to promote association with C-terminal BRCT domains of Rad4TOPBP1. *Genes Dev,* 18**,** 1154-64.

GARCIA, V., FURUYA, K. & CARR, A. M. 2005. Identification and functional analysis of TopBP1 and its homologs. *DNA Repair (Amst),* 4**,** 1227-39.

GATEI, M., JAKOB, B., CHEN, P., KIJAS, A. W., BECHEREL, O. J., GUEVEN, N., BIRRELL, G., LEE, J. H., PAULL, T. T., LERENTHAL, Y., FAZRY, S., TAUCHER-SCHOLZ, G., KALB, R., SCHINDLER, D., WALTES, R., DORK, T. & LAVIN, M. F. 2011. ATM protein-dependent phosphorylation of Rad50 protein regulates DNA repair and cell cycle control. *J Biol Chem,* 286**,** 31542-56.

GERMANN, S. M., OESTERGAARD, V. H., HAAS, C., SALIS, P., MOTEGI, A. & LISBY, M. 2011. Dpb11/TopBP1 plays distinct roles in DNA replication, checkpoint response and homologous recombination. *DNA Repair (Amst),* 10**,** 210-24.

GOING, J. J., NIXON, C., DORNAN, E. S., BONER, W., DONALDSON, M. M. & MORGAN, I. M. 2007. Aberrant expression of TopBP1 in breast cancer. *Histopathology,* 50**,** 418-24.

GONG, Z., KIM, J. E., LEUNG, C. C., GLOVER, J. N. & CHEN, J. 2010. BACH1/FANCJ acts with TopBP1 and participates early in DNA replication checkpoint control. *Mol Cell,* 37**,** 438-46.

GOODARZI, A. A., JONNALAGADDA, J. C., DOUGLAS, P., YOUNG, D., YE, R., MOORHEAD, G. B., LEES-MILLER, S. P. & KHANNA, K. K. 2004. Autophosphorylation of ataxia-telangiectasia mutated is regulated by protein phosphatase 2A. *EMBO J,* 23**,** 4451-61.

GOULD, K. L. & NURSE, P. 1989. Tyrosine phosphorylation of the fission yeast cdc2+ protein kinase regulates entry into mitosis. *Nature,* 342**,** 39-45.

GRANATA, M., LAZZARO, F., NOVARINA, D., PANIGADA, D., PUDDU, F., ABREU, C. M., KUMAR, R., GRENON, M., LOWNDES, N. F., PLEVANI, P. & MUZI-FALCONI, M. 2010. Dynamics of Rad9 chromatin binding and checkpoint function are mediated by its dimerization and are cell cycle-regulated by CDK1 activity. *PLoS Genet,* 6.

GREENWELL, P. W., KRONMAL, S. L., PORTER, S. E., GASSENHUBER, J., OBERMAIER, B. & PETES, T. D. 1995. TEL1, a gene involved in controlling telomere length in S. cerevisiae, is homologous to the human ataxia telangiectasia gene. *Cell,* 82**,** 823-9.

GREER, D. A., BESLEY, B. D., KENNEDY, K. B. & DAVEY, S. 2003. hRad9 rapidly binds DNA containing double-strand breaks and is required for damage-dependent topoisomerase II beta binding protein 1 focus formation. *Cancer Res,* 63**,** 4829-35.

GRIFFITHS, D. J., BARBET, N. C., MCCREADY, S., LEHMANN, A. R. & CARR, A. M. 1995. Fission yeast rad17: a homologue of budding yeast RAD24 that shares regions of sequence similarity with DNA polymerase accessory proteins. *EMBO J,* 14**,** 5812-23.

GUO, Z., KUMAGAI, A., WANG, S. X. & DUNPHY, W. G. 2000. Requirement for Atr in phosphorylation of Chk1 and cell cycle regulation in response to DNA replication blocks and UV-damaged DNA in Xenopus egg extracts. *Genes Dev,* 14**,** 2745-56.

HARRIS, S., KEMPLEN, C., CASPARI, T., CHAN, C., LINDSAY, H. D., POITELEA, M., CARR, A. M. & PRICE, C. 2003. Delineating the position of rad4+/cut5+ within the DNA-structure checkpoint pathways in Schizosaccharomyces pombe. *J Cell Sci,* 116**,** 3519-29.

HARRISON, J. C. & HABER, J. E. 2006. Surviving the breakup: the DNA damage checkpoint. *Annu Rev Genet,* 40**,** 209-35.

HASHIMOTO, Y. & TAKISAWA, H. 2003. Xenopus Cut5 is essential for a CDK-dependent process in the initiation of DNA replication. *EMBO J,* 22**,** 2526-35.

HASSAN, B. H., LINDSEY-BOLTZ, L. A., KEMP, M. G. & SANCAR, A. 2013. Direct role for the replication protein Treslin (Ticrr) in the ATR-mediated checkpoint response. *J Biol Chem*.

HE, J., SHI, L. Z., TRUONG, L. N., LU, C. S., RAZAVIAN, N., LI, Y., NEGRETE, A., SHILOACH, J., BERNS, M. W. & WU, X. 2012. Rad50 zinc hook is important for the Mre11 complex to bind chromosomal DNA double-stranded breaks and initiate various DNA damage responses. *J Biol Chem,* 287**,** 31747-56.

HELLER, R. C., KANG, S., LAM, W. M., CHEN, S., CHAN, C. S. & BELL, S. P. 2011. Eukaryotic origin-dependent DNA replication in *vitro* reveals sequential action of DDK and S-CDK kinases. *Cell,* 146**,** 80-91.

HEROLD, S., WANZEL, M., BEUGER, V., FROHME, C., BEUL, D., HILLUKKALA, T., SYVAOJA, J., SALUZ, H. P., HAENEL, F. & EILERS, M. 2002. Negative regulation of the mammalian UV response by Myc through association with Miz-1. *Mol Cell,* 10**,** 509-21.

HICKS, W. M., YAMAGUCHI, M. & HABER, J. E. 2011. Real-time analysis of double-strand DNA break repair by homologous recombination. *Proc Natl Acad Sci U S A,* 108**,** 3108-15.

HIRAI, I. & WANG, H. G. 2002. A role of the C-terminal region of human Rad9 (hRad9) in nuclear transport of the hRad9 checkpoint complex. *J Biol Chem,* 277**,** 25722-7.

HIRANO, T., FUNAHASHI, S., UEMURA, T. & YANAGIDA, M. 1986. Isolation and characterization of Schizosaccharomyces pombe cutmutants that block nuclear division but not cytokinesis. *EMBO J,* 5**,** 2973-9.

HOPKINS, K. M., AUERBACH, W., WANG, X. Y., HANDE, M. P., HANG, H., WOLGEMUTH, D. J., JOYNER, A. L. & LIEBERMAN, H. B. 2004. Deletion of mouse rad9 causes abnormal cellular responses to DNA damage, genomic instability, and embryonic lethality. *Mol Cell Biol,* 24**,** 7235-48.

HU, J., SUN, L., SHEN, F., CHEN, Y., HUA, Y., LIU, Y., ZHANG, M., HU, Y., WANG, Q., XU, W., SUN, F., JI, J., MURRAY, J. M., CARR, A. M. & KONG, D. 2012. The intra-S phase checkpoint targets Dna2 to prevent stalled replication forks from reversing. *Cell,* 149**,** 1221-32.

HUEN, M. S., GRANT, R., MANKE, I., MINN, K., YU, X., YAFFE, M. B. & CHEN, J. 2007. RNF8 transduces the DNA-damage signal via histone ubiquitylation and checkpoint protein assembly. *Cell,* 131**,** 901-14.

HUERTAS, P. 2010. DNA resection in eukaryotes: deciding how to fix the break. *Nat Struct Mol Biol,* 17**,** 11-6.

HUERTAS, P., CORTES-LEDESMA, F., SARTORI, A. A., AGUILERA, A. & JACKSON, S. P. 2008. CDK targets Sae2 to control DNA-end resection and homologous recombination. *Nature,* 455**,** 689-92.

HUERTAS, P. & JACKSON, S. P. 2009. Human CtIP mediates cell cycle control of DNA end resection and double strand break repair. *J Biol Chem,* 284**,** 9558-65.

HUYEN, Y., ZGHEIB, O., DITULLIO, R. A., JR., GORGOULIS, V. G., ZACHARATOS, P., PETTY, T. J., SHESTON, E. A., MELLERT, H. S., STAVRIDI, E. S. & HALAZONETIS, T. D. 2004. Methylated lysine 79 of histone H3 targets 53BP1 to DNA double-strand breaks. *Nature,* 432**,** 406-11.

IIJIMA, K., OHARA, M., SEKI, R. & TAUCHI, H. 2008. Dancing on damaged chromatin: functions of ATM and the RAD50/MRE11/NBS1 complex in cellular responses to DNA damage. *J Radiat Res,* 49**,** 451-64.

IM, J. S., KI, S. H., FARINA, A., JUNG, D. S., HURWITZ, J. & LEE, J. K. 2009. Assembly of the Cdc45-Mcm2-7-GINS complex in human cells requires the Ctf4/And-1, RecQL4, and Mcm10 proteins. *Proc Natl Acad Sci U S A,* 106**,** 15628-32.

ITAKURA, E., UMEDA, K., SEKOGUCHI, E., TAKATA, H., OHSUMI, M. & MATSUURA, A. 2004. ATR-dependent phosphorylation of ATRIP in response to genotoxic stress. *Biochem Biophys Res Commun,* 323**,** 1197-202.

JACOME, A. & FERNANDEZ-CAPETILLO, O. 2011. Lac operator repeats generate a traceable fragile site in mammalian cells. *EMBO Rep,* 12**,** 1032-8.

JEFFREY, P. D., RUSSO, A. A., POLYAK, K., GIBBS, E., HURWITZ, J., MASSAGUE, J. & PAVLETICH, N. P. 1995. Mechanism of CDK activation revealed by the structure of a cyclinA-CDK2 complex. *Nature,* 376**,** 313-20.

JEON, Y., KO, E., LEE, K. Y., KO, M. J., PARK, S. Y., KANG, J., JEON, C. H., LEE, H. & HWANG, D. S. 2011. TopBP1 deficiency causes an early embryonic lethality and induces cellular senescence in primary cells. *J Biol Chem,* 286**,** 5414-22.

JEON, Y., LEE, K. Y., KO, M. J., LEE, Y. S., KANG, S. & HWANG, D. S. 2007. Human TopBP1 participates in cyclin E/CDK2 activation and preinitiation complex assembly during G1/S transition. *J Biol Chem,* 282**,** 14882-90.

JEONG, J. W., KIM, D. H., CHOI, S. Y. & KIM, H. B. 2001. Characterization of the CDC10 product and the timing of events of the budding site of Saccharomyces cerevisiae. *Mol Cells,* 12**,** 77-83.

JIANG, X., SUN, Y., CHEN, S., ROY, K. & PRICE, B. D. 2006. The FATC domains of PIKK proteins are functionally equivalent and participate in the Tip60-dependent activation of DNA-PKcs and ATM. *J Biol Chem,* 281**,** 15741-6.

JIMENEZ, G., YUCEL, J., ROWLEY, R. & SUBRAMANI, S. 1992. The rad3+ gene of Schizosaccharomyces pombe is involved in multiple checkpoint functions and in DNA repair. *Proc Natl Acad Sci U S A,* 89**,** 4952-6.

KAMIMURA, Y., MASUMOTO, H., SUGINO, A. & ARAKI, H. 1998. Sld2, which interacts with Dpb11 in Saccharomyces cerevisiae, is required for chromosomal DNA replication. *Mol Cell Biol,* 18**,** 6102-9.

KAMIMURA, Y., TAK, Y. S., SUGINO, A. & ARAKI, H. 2001. Sld3, which interacts with Cdc45 (Sld4), functions for chromosomal DNA replication in Saccharomyces cerevisiae. *EMBO J,* 20**,** 2097-107.

KARPPINEN, S. M., ERKKO, H., REINI, K., POSPIECH, H., HEIKKINEN, K., RAPAKKO, K., SYVAOJA, J. E. & WINQVIST, R. 2006. Identification of a common polymorphism in the TopBP1 gene associated with hereditary susceptibility to breast and ovarian cancer. *Eur J Cancer,* 42**,** 2647-52.

KATO, R. & OGAWA, H. 1994. An essential gene, ESR1, is required for mitotic cell growth, DNA repair and meiotic recombination in Saccharomyces cerevisiae. *Nucleic Acids Res,* 22**,** 3104-12.

KEMP, M. & SANCAR, A. 2009. DNA distress: just ring 9-1-1. *Curr Biol,* 19**,** R733-4.

KERZENDORFER, C. & O'DRISCOLL, M. 2009. Human DNA damage response and repair deficiency syndromes: linking genomic instability and cell cycle checkpoint proficiency. *DNA Repair (Amst),* 8**,** 1139-52.

KIANG, L., HEICHINGER, C., WATT, S., BAHLER, J. & NURSE, P. 2009. Cyclin-dependent kinase inhibits reinitiation of a normal S-phase program during G2 in fission yeast. *Mol Cell Biol,* 29**,** 4025-32.

KILKENNY, M. L., DORE, A. S., ROE, S. M., NESTORAS, K., HO, J. C., WATTS, F. Z. & PEARL, L. H. 2008. Structural and functional analysis of the Crb2-BRCT2 domain reveals distinct roles in checkpoint signaling and DNA damage repair. *Genes Dev,* 22**,** 2034-47.

KIM, S. T., LIM, D. S., CANMAN, C. E. & KASTAN, M. B. 1999. Substrate specificities and identification of putative substrates of ATM kinase family members. *J Biol Chem,* 274**,** 37538-43.

KOBAYASHI, M., HAYASHI, N., TAKATA, M. & YAMAMOTO, K. 2013. NBS1 directly activates ATR independently of MRE11 and TOPBP1. *Genes Cells,* 18**,** 238-46.

KOLAS, N. K., CHAPMAN, J. R., NAKADA, S., YLANKO, J., CHAHWAN, R., SWEENEY, F. D., PANIER, S., MENDEZ, M., WILDENHAIN, J., THOMSON, T. M., PELLETIER, L., JACKSON, S. P. & DUROCHER, D. 2007. Orchestration of the DNA-damage response by the RNF8 ubiquitin ligase. *Science,* 318**,** 1637-40.

KOZLOV, S. V., GRAHAM, M. E., PENG, C., CHEN, P., ROBINSON, P. J. & LAVIN, M. F. 2006. Involvement of novel autophosphorylation sites in ATM activation. *EMBO J,* 25**,** 3504-14.

KUMAGAI, A. & DUNPHY, W. G. 2000. Claspin, a novel protein required for the activation of Chk1 during a DNA replication checkpoint response in Xenopus egg extracts. *Mol Cell,* 6**,** 839-49.

KUMAGAI, A. & DUNPHY, W. G. 2006. How cells activate ATR. *Cell Cycle,* 5**,** 1265-8.

KUMAGAI, A., KIM, S. M. & DUNPHY, W. G. 2004. Claspin and the activated form of ATR-ATRIP collaborate in the activation of Chk1. *J Biol Chem,* 279**,** 49599-608.

KUMAGAI, A., LEE, J., YOO, H. Y. & DUNPHY, W. G. 2006. TopBP1 activates the ATR-ATRIP complex. *Cell,* 124**,** 943-55.

KUMAGAI, A., SHEVCHENKO, A. & DUNPHY, W. G. 2010. Treslin collaborates with TopBP1 in triggering the initiation of DNA replication. *Cell,* 140**,** 349-59.

KUMAGAI, A., SHEVCHENKO, A., SHEVCHENKO, A. & DUNPHY, W. G. 2011. Direct regulation of Treslin by cyclin-dependent kinase is essential for the onset of DNA replication. *J Cell Biol,* 193**,** 995-1007.

KUMAR, S. & BURGERS, P. M. 2013. Lagging strand maturation factor Dna2 is a component of the replication checkpoint initiation machinery. *Genes Dev,* 27**,** 313-21.

KURAMAE, E. E., ROBERT, V., SNEL, B. & BOEKHOUT, T. 2006. Conflicting phylogenetic position of Schizosaccharomyces pombe. *Genomics,* 88**,** 387-93.

KURZ, E. U. & LEES-MILLER, S. P. 2004. DNA damage-induced activation of ATM and ATM-dependent signaling pathways. *DNA Repair (Amst),* 3**,** 889-900.

LAMBERT, S. & CARR, A. M. 2012. Replication stress and genome rearrangements: lessons from yeast models. *Curr Opin Genet Dev*.

LANDER, E. S., LINTON, L. M., BIRREN, B., NUSBAUM, C., ZODY, M. C., BALDWIN, J., DEVON, K., DEWAR, K., DOYLE, M., FITZHUGH, W., FUNKE, R., GAGE, D., HARRIS, K., HEAFORD, A., HOWLAND, J., KANN, L., LEHOCZKY, J., LEVINE, R., MCEWAN, P., MCKERNAN, K., MELDRIM, J., MESIROV, J. P., MIRANDA, C., MORRIS, W., NAYLOR, J., RAYMOND, C., ROSETTI, M., SANTOS, R., SHERIDAN, A., SOUGNEZ, C., STANGE-THOMANN, N., STOJANOVIC, N., SUBRAMANIAN, A., WYMAN, D., ROGERS, J., SULSTON, J., AINSCOUGH, R., BECK, S., BENTLEY, D., BURTON, J., CLEE, C., CARTER, N., COULSON, A., DEADMAN, R., DELOUKAS, P., DUNHAM, A., DUNHAM, I., DURBIN, R., FRENCH, L., GRAFHAM, D., GREGORY, S., HUBBARD, T., HUMPHRAY, S., HUNT, A., JONES, M., LLOYD, C., MCMURRAY, A., MATTHEWS, L., MERCER, S., MILNE, S., MULLIKIN, J. C., MUNGALL, A., PLUMB, R., ROSS, M., SHOWNKEEN, R., SIMS, S., WATERSTON, R. H., WILSON, R. K., HILLIER, L. W., MCPHERSON, J. D., MARRA, M. A., MARDIS, E. R., FULTON, L. A., CHINWALLA, A. T., PEPIN, K. H., GISH, W. R., CHISSOE, S. L., WENDL, M. C., DELEHAUNTY, K. D., MINER, T. L., DELEHAUNTY, A., KRAMER, J. B., COOK, L. L., FULTON, R. S., JOHNSON, D. L., MINX, P. J., CLIFTON, S. W., HAWKINS,

T., BRANSCOMB, E., PREDKI, P., RICHARDSON, P., WENNING, S., SLEZAK, T., DOGGETT, N., CHENG, J. F., OLSEN, A., LUCAS, S., ELKIN, C., UBERBACHER, E., FRAZIER, M., et al. 2001. Initial sequencing and analysis of the human genome. *Nature,* 409**,** 860-921.

LARNER, J. M., LEE, H., LITTLE, R. D., DIJKWEL, P. A., SCHILDKRAUT, C. L. & HAMLIN, J. L. 1999. Radiation down-regulates replication origin activity throughout the S phase in mammalian cells. *Nucleic Acids Res,* 27**,** 803-9.

LAVIN, M. F. 2008. Ataxia-telangiectasia: from a rare disorder to a paradigm for cell signalling and cancer. *Nat Rev Mol Cell Biol,* 9**,** 759-69.

LEE, J. & DUNPHY, W. G. 2010. Rad17 plays a central role in establishment of the interaction between TopBP1 and the Rad9-Hus1-Rad1 complex at stalled replication forks. *Mol Biol Cell,* 21**,** 926-35.

LEE, J. & DUNPHY, W. G. 2013. The Mre11-Rad50-NBS1 (MRN) complex has a specific role in the activation of Chk1 in response to stalled replication forks. *Mol Biol Cell,* 24**,** 1343-53.

LEE, J., KUMAGAI, A. & DUNPHY, W. G. 2007. The Rad9-Hus1-Rad1 checkpoint clamp regulates interaction of TopBP1 with ATR. *J Biol Chem,* 282**,** 28036-44.

LEE, J. H. & PAULL, T. T. 2005. ATM activation by DNA double-strand breaks through the Mre11-Rad50-NBS1 complex. *Science,* 308**,** 551-4.

LEE, M. S., EDWARDS, R. A., THEDE, G. L. & GLOVER, J. N. 2005. Structure of the BRCT repeat domain of MDC1 and its specificity for the free COOH-terminal end of the gamma-H2AX histone tail. *J Biol Chem,* 280**,** 32053-6.

LEE, S. J., SCHWARTZ, M. F., DUONG, J. K. & STERN, D. F. 2003. Rad53 phosphorylation site clusters are important for Rad53 regulation and signaling. *Mol Cell Biol,* 23**,** 6300-14.

LEES, E. 1995. Cyclin dependent kinase regulation. *Curr Opin Cell Biol,* 7**,** 773-80.

LELOUP, C., HOPKINS, K. M., WANG, X., ZHU, A., WOLGEMUTH, D. J. & LIEBERMAN, H. B. 2010. Mouse Rad9b is essential for embryonic development and promotes resistance to DNA damage. *Dev Dyn,* 239**,** 2837-50.

LEMPIAINEN, H. & HALAZONETIS, T. D. 2009. Emerging common themes in regulation of PIKKs and PI3Ks. *EMBO J,* 28**,** 3067-73.

LENGSFELD, B. M., RATTRAY, A. J., BHASKARA, V., GHIRLANDO, R. & PAULL, T. T. 2007. Sae2 is an endonuclease that processes hairpin DNA cooperatively with the Mre11/Rad50/Xrs2 complex. *Mol Cell,* 28**,** 638-51.

LEUNG, C. C., GONG, Z., CHEN, J. & GLOVER, J. N. 2011. Molecular basis of BACH1/FANCJ recognition by TopBP1 in DNA replication checkpoint control. *J Biol Chem,* 286**,** 4292-301.

LEUNG, C. C., KELLOGG, E., KUHNERT, A., HANEL, F., BAKER, D. & GLOVER, J. N. 2010. Insights from the crystal structure of the sixth BRCT domain of topoisomerase IIbeta binding protein 1. *Protein Sci,* 19**,** 162-7.

LEUNG, C. C., SUN, L., GONG, Z., BURKAT, M., EDWARDS, R., ASSMUS, M., CHEN, J. & GLOVER, J. N. 2013. Structural Insights into Recognition of MDC1 by TopBP1 in DNA Replication Checkpoint Control. *Structure,* 21**,** 1450-9.

LEUTHER, K. K., HAMMARSTEN, O., KORNBERG, R. D. & CHU, G. 1999. Structure of DNA-dependent protein kinase: implications for its regulation by DNA. *EMBO J,* 18**,** 1114-23.

LIMBO, O., CHAHWAN, C., YAMADA, Y., DE BRUIN, R. A., WITTENBERG, C. & RUSSELL, P. 2007. Ctp1 is a cell-cycle-regulated protein that functions with Mre11 complex to control double-strand break repair by homologous recombination. *Mol Cell,* 28**,** 134-46.

LIMBO, O., PORTER-GOFF, M. E., RHIND, N. & RUSSELL, P. 2011. Mre11 nuclease activity and Ctp1 regulate Chk1 activation by Rad3ATR and Tel1ATM checkpoint kinases at double-strand breaks. *Mol Cell Biol,* 31**,** 573-83.

LIN, W. C., LIN, F. T. & NEVINS, J. R. 2001. Selective induction of E2F1 in response to DNA damage, mediated by ATM-dependent phosphorylation. *Genes Dev,* 15**,** 1833-44.

LINDAHL, T. 1993. Instability and decay of the primary structure of DNA. *Nature,* 362**,** 709-15.

LINDSEY-BOLTZ, L. A. & SANCAR, A. 2011. Tethering DNA damage checkpoint mediator proteins topoisomerase IIbeta-binding protein 1 (TopBP1) and Claspin to DNA activates ataxia-telangiectasia mutated and RAD3-related (ATR) phosphorylation of checkpoint kinase 1 (Chk1). *J Biol Chem,* 286**,** 19229-36.

LIU, C., POWELL, K. A., MUNDT, K., WU, L., CARR, A. M. & CASPARI, T. 2003a. Cop9/signalosome subunits and Pcu4 regulate ribonucleotide reductase by both checkpoint-dependent and -independent mechanisms. *Genes Dev,* 17**,** 1130-40.

LIU, K., BELLAM, N., LIN, H. Y., WANG, B., STOCKARD, C. R., GRIZZLE, W. E. & LIN, W. C. 2009. Regulation of p53 by TopBP1: a potential mechanism for p53 inactivation in cancer. *Mol Cell Biol,* 29**,** 2673-93.

LIU, K., LIN, F. T., RUPPERT, J. M. & LIN, W. C. 2003b. Regulation of E2F1 by BRCT domain-containing protein TopBP1. *Mol Cell Biol,* 23**,** 3287-304.

LIU, K., LUO, Y., LIN, F. T. & LIN, W. C. 2004. TopBP1 recruits Brg1/Brm to repress E2F1-induced apoptosis, a novel pRb-independent and E2F1-specific control for cell survival. *Genes Dev,* 18**,** 673-86.

LIU, K., PAIK, J. C., WANG, B., LIN, F. T. & LIN, W. C. 2006. Regulation of TopBP1 oligomerization by Akt/PKB for cell survival. *EMBO J,* 25**,** 4795-807.

LIU, Q., GUNTUKU, S., CUI, X. S., MATSUOKA, S., CORTEZ, D., TAMAI, K., LUO, G., CARATTINI-RIVERA, S., DEMAYO, F., BRADLEY, A., DONEHOWER, L. A. & ELLEDGE, S. J. 2000. Chk1 is an essential kinase that is regulated by Atr and required for the G(2)/M DNA damage checkpoint. *Genes Dev,* 14**,** 1448-59.

LIU, S., HO, C. K., OUYANG, J. & ZOU, L. 2013. Nek1 kinase associates with ATR-ATRIP and primes ATR for efficient DNA damage signaling. *Proc Natl Acad Sci U S A,* 110**,** 2175-80.

LIU, S., SHIOTANI, B., LAHIRI, M., MARECHAL, A., TSE, A., LEUNG, C. C., GLOVER, J. N., YANG, X. H. & ZOU, L. 2011. ATR autophosphorylation as a molecular switch for checkpoint activation. *Mol Cell,* 43**,** 192-202.

LLORCA, O., RIVERA-CALZADA, A., GRANTHAM, J. & WILLISON, K. R. 2003. Electron microscopy and 3D reconstructions reveal that human ATM kinase uses an arm-like domain to clamp around double-stranded DNA. *Oncogene,* 22**,** 3867-74.

LLORENTE, B. & SYMINGTON, L. S. 2004. The Mre11 nuclease is not required for 5' to 3' resection at multiple HO-induced double-strand breaks. *Mol Cell Biol,* 24**,** 9682-94.

LOEB, L. A. 1991. Mutator phenotype may be required for multistage carcinogenesis. *Cancer Res,* 51**,** 3075-9.

LOPEZ-GIRONA, A., TANAKA, K., CHEN, X. B., BABER, B. A., MCGOWAN, C. H. & RUSSELL, P. 2001. Serine-345 is required for Rad3-dependent phosphorylation and function of checkpoint kinase Chk1 in fission yeast. *Proc Natl Acad Sci U S A,* 98**,** 11289-94.

LOPEZ-MOSQUEDA, J., MAAS, N. L., JONSSON, Z. O., DEFAZIO-ELI, L. G., WOHLSCHLEGEL, J. & TOCZYSKI, D. P. 2010. Damage-induced phosphorylation of Sld3 is important to block late origin firing. *Nature,* 467**,** 479-83.

LOU, Z., MINTER-DYKHOUSE, K., FRANCO, S., GOSTISSA, M., RIVERA, M. A., CELESTE, A., MANIS, J. P., VAN DEURSEN, J., NUSSENZWEIG, A., PAULL, T. T., ALT, F. W. & CHEN, J. 2006. MDC1 maintains genomic stability by participating in the amplification of ATM-dependent DNA damage signals. *Mol Cell,* 21**,** 187-200.

LOVEJOY, C. A. & CORTEZ, D. 2009. Common mechanisms of PIKK regulation. *DNA Repair (Amst),* 8**,** 1004-8.

LU, L. X., DOMINGO-SANANES, M. R., HUZARSKA, M., NOVAK, B. & GOULD, K. L. 2012. Multisite phosphoregulation of Cdc25 activity refines the mitotic entrance and exit switches. *Proc Natl Acad Sci U S A,* 109**,** 9899-904.

LUPARDUS, P. J., BYUN, T., YEE, M. C., HEKMAT-NEJAD, M. & CIMPRICH, K. A. 2002. A requirement for replication in activation of the ATR-dependent DNA damage checkpoint. *Genes Dev,* 16**,** 2327-32.

LUSTIG, A. J. & PETES, T. D. 1986. Identification of yeast mutants with altered telomere structure. *Proc Natl Acad Sci U S A,* 83**,** 1398-402.

MACDOUGALL, C. A., BYUN, T. S., VAN, C., YEE, M. C. & CIMPRICH, K. A. 2007. The structural determinants of checkpoint activation. *Genes Dev,* 21**,** 898-903.

MAGA, G. & HUBSCHER, U. 2003. Proliferating cell nuclear antigen (PCNA): a dancer with many partners. *J Cell Sci,* 116**,** 3051-60.

MAILAND, N., BEKKER-JENSEN, S., FAUSTRUP, H., MELANDER, F., BARTEK, J., LUKAS, C. & LUKAS, J. 2007. RNF8 ubiquitylates histones at DNA double-strand breaks and promotes assembly of repair proteins. *Cell,* 131**,** 887-900.

MAJKA, J., BINZ, S. K., WOLD, M. S. & BURGERS, P. M. 2006a. Replication protein A directs loading of the DNA damage checkpoint clamp to 5'-DNA junctions. *J Biol Chem,* 281**,** 27855-61.

MAJKA, J., NIEDZIELA-MAJKA, A. & BURGERS, P. M. 2006b. The checkpoint clamp activates Mec1 kinase during initiation of the DNA damage checkpoint. *Mol Cell,* 24**,** 891-901.

MAKINIEMI, M., HILLUKKALA, T., TUUSA, J., REINI, K., VAARA, M., HUANG, D., POSPIECH, H., MAJURI, I., WESTERLING, T., MAKELA, T. P. & SYVAOJA, J. E. 2001. BRCT domain-containing protein TopBP1 functions in DNA replication and damage response. *J Biol Chem,* 276**,** 30399-406.

MANIWA, Y., YOSHIMURA, M., BERMUDEZ, V. P., OKADA, K., KANOMATA, N., OHBAYASHI, C., NISHIMURA, Y., HAYASHI, Y., HURWITZ, J. & OKITA, Y. 2006. His239Arg SNP of HRAD9 is associated with lung adenocarcinoma. *Cancer,* 106**,** 1117-22.

MARCHETTI, M. A., KUMAR, S., HARTSUIKER, E., MAFTAHI, M., CARR, A. M., FREYER, G. A., BURHANS, W. C. & HUBERMAN, J. A. 2002. A single unbranched S-phase DNA damage and replication fork blockage checkpoint pathway. *Proc Natl Acad Sci U S A,* 99**,** 7472-7.

MASUMOTO, H., MURAMATSU, S., KAMIMURA, Y. & ARAKI, H. 2002. S-Cdk-dependent phosphorylation of Sld2 essential for chromosomal DNA replication in budding yeast. *Nature,* 415**,** 651-5.

MASUMOTO, H., SUGINO, A. & ARAKI, H. 2000. Dpb11 controls the association between DNA polymerases alpha and epsilon and the autonomously replicating sequence region of budding yeast. *Mol Cell Biol,* 20**,** 2809-17.

MATSUNO, K., KUMANO, M., KUBOTA, Y., HASHIMOTO, Y. & TAKISAWA, H. 2006. The N-terminal noncatalytic region of Xenopus RecQ4 is required for chromatin binding of DNA polymerase alpha in the initiation of DNA replication. *Mol Cell Biol,* 26**,** 4843-52.

MATSUOKA, S., HUANG, M. & ELLEDGE, S. J. 1998. Linkage of ATM to cell cycle regulation by the Chk2 protein kinase. *Science,* 282**,** 1893-7.

MATSUOKA, S., ROTMAN, G., OGAWA, A., SHILOH, Y., TAMAI, K. & ELLEDGE, S. J. 2000. Ataxia telangiectasia-mutated phosphorylates Chk2 in *vivo* and in *vitro*. *Proc Natl Acad Sci U S A,* 97**,** 10389-94.

MCKEE, A. H. & KLECKNER, N. 1997. A general method for identifying recessive diploid-specific mutations in Saccharomyces cerevisiae, its application to the isolation of mutants blocked at intermediate stages of meiotic prophase and characterization of a new gene SAE2. *Genetics,* 146**,** 797-816.

MELANDER, F., BEKKER-JENSEN, S., FALCK, J., BARTEK, J., MAILAND, N. & LUKAS, J. 2008. Phosphorylation of SDT repeats in the MDC1 N terminus triggers retention of NBS1 at the DNA damage-modified chromatin. *J Cell Biol,* 181**,** 213-26.

MELO, J. A., COHEN, J. & TOCZYSKI, D. P. 2001. Two checkpoint complexes are independently recruited to sites of DNA damage in *vivo*. *Genes Dev,* 15**,** 2809-21.

MIMITOU, E. P. & SYMINGTON, L. S. 2008. Sae2, Exo1 and Sgs1 collaborate in DNA double-strand break processing. *Nature,* 455**,** 770-4.

MIMITOU, E. P. & SYMINGTON, L. S. 2009. DNA end resection: many nucleases make light work. *DNA Repair (Amst),* 8**,** 983-95.

MITCHISON, J. M. & CREANOR, J. 1971. Further measurements of DNA synthesis and enzyme potential during cell cycle of fission yeast Schizosaccharomyces pombe. *Exp Cell Res,* 69**,** 244-7.

MIYABE, I., MORISHITA, T., SHINAGAWA, H. & CARR, A. M. 2009. Schizosaccharomyces pombe Cds1Chk2 regulates homologous recombination at stalled replication forks through the phosphorylation of recombination protein Rad60. *J Cell Sci,* 122**,** 3638-43.

MOCHIDA, S., ESASHI, F., AONO, N., TAMAI, K., O'CONNELL, M. J. & YANAGIDA, M. 2004. Regulation of checkpoint kinases through dynamic interaction with Crb2. *EMBO J,* 23**,** 418-28.

MORDES, D. A., GLICK, G. G., ZHAO, R. & CORTEZ, D. 2008a. TopBP1 activates ATR through ATRIP and a PIKK regulatory domain. *Genes Dev,* 22**,** 1478-89.

MORDES, D. A., NAM, E. A. & CORTEZ, D. 2008b. Dpb11 activates the Mec1-Ddc2 complex. *Proc Natl Acad Sci U S A,* 105**,** 18730-4.

MORENO, S. & NURSE, P. 1994. Regulation of progression through the G1 phase of the cell cycle by the rum1+ gene. *Nature,* 367**,** 236-42.

MORISHIMA, K., SAKAMOTO, S., KOBAYASHI, J., IZUMI, H., SUDA, T., MATSUMOTO, Y., TAUCHI, H., IDE, H., KOMATSU, K. & MATSUURA, S. 2007. TopBP1 associates with NBS1 and is involved in homologous recombination repair. *Biochem Biophys Res Commun,* 362**,** 872-9.

MORITA, T., YAMASHITA, A., KASHIMA, I., OGATA, K., ISHIURA, S. & OHNO, S. 2007. Distant N- and C-terminal domains are required for intrinsic kinase activity of SMG-1, a critical component of nonsense-mediated mRNA decay. *J Biol Chem,* 282**,** 7799-808.

MORROW, D. M., TAGLE, D. A., SHILOH, Y., COLLINS, F. S. & HIETER, P. 1995. TEL1, an S. cerevisiae homolog of the human gene mutated in ataxia telangiectasia, is functionally related to the yeast checkpoint gene MEC1. *Cell,* 82**,** 831-40.

MOYER, S. E., LEWIS, P. W. & BOTCHAN, M. R. 2006. Isolation of the Cdc45/Mcm2-7/GINS (CMG) complex, a candidate for the eukaryotic DNA replication fork helicase. *Proc Natl Acad Sci U S A,* 103**,** 10236-41.

MURR, R., LOIZOU, J. I., YANG, Y. G., CUENIN, C., LI, H., WANG, Z. Q. & HERCEG, Z. 2006. Histone acetylation by Trrap-Tip60 modulates loading of repair proteins and repair of DNA double-strand breaks. *Nat Cell Biol,* 8**,** 91-9.

MURRAY, J. M., CARR, A. M., LEHMANN, A. R. & WATTS, F. Z. 1991. Cloning and characterisation of the rad9 DNA repair gene from Schizosaccharomyces pombe. *Nucleic Acids Res,* 19**,** 3525-31.

NAITO, T., MATSUURA, A. & ISHIKAWA, F. 1998. Circular chromosome formation in a fission yeast mutant defective in two ATM homologues. *Nat Genet,* 20**,** 203-6.

NAKADA, D., HIRANO, Y. & SUGIMOTO, K. 2004. Requirement of the Mre11 complex and exonuclease 1 for activation of the Mec1 signaling pathway. *Mol Cell Biol,* 24**,** 10016-25.

NAKADA, D., HIRANO, Y., TANAKA, Y. & SUGIMOTO, K. 2005. Role of the C terminus of Mec1 checkpoint kinase in its localization to sites of DNA damage. *Mol Biol Cell,* 16**,** 5227-35.

NAKADA, D., MATSUMOTO, K. & SUGIMOTO, K. 2003. ATM-related Tel1 associates with double-strand breaks through an Xrs2-dependent mechanism. *Genes Dev,* 17**,** 1957-62.

NAKAMURA, T. M., DU, L. L., REDON, C. & RUSSELL, P. 2004. Histone H2A phosphorylation controls Crb2 recruitment at DNA breaks, maintains checkpoint arrest, and influences DNA repair in fission yeast. *Mol Cell Biol,* 24**,** 6215-30.

NAKAMURA, T. M., MOSER, B. A., DU, L. L. & RUSSELL, P. 2005. Cooperative control of Crb2 by ATM family and Cdc2 kinases is essential for the DNA damage checkpoint in fission yeast. *Molecular and cellular biology,* 25**,** 10721-30.

NAVADGI-PATIL, V. M. & BURGERS, P. M. 2008. Yeast DNA replication protein Dpb11 activates the Mec1/ATR checkpoint kinase. *J Biol Chem,* 283**,** 35853-9.

NAVADGI-PATIL, V. M. & BURGERS, P. M. 2009. The unstructured C-terminal tail of the 9-1-1 clamp subunit Ddc1 activates Mec1/ATR via two distinct mechanisms. *Mol Cell,* 36**,** 743-53.

NAVADGI-PATIL, V. M., KUMAR, S. & BURGERS, P. M. 2011. The unstructured C-terminal tail of yeast Dpb11 (human TopBP1) protein is dispensable for DNA replication and the S phase checkpoint but required for the G2/M checkpoint. *J Biol Chem,* 286**,** 40999-1007.

NEALE, M. J., PAN, J. & KEENEY, S. 2005. Endonucleolytic processing of covalent protein-linked DNA double-strand breaks. *Nature,* 436**,** 1053-7.

NURSE, P. 1997. Regulation of the eukaryotic cell cycle. *Eur J Cancer,* 33**,** 1002-4.

NURSE, P. M. 2002. Nobel Lecture. Cyclin dependent kinases and cell cycle control. *Biosci Rep,* 22**,** 487-99.

NYBERG, K. A., MICHELSON, R. J., PUTNAM, C. W. & WEINERT, T. A. 2002. Toward maintaining the genome: DNA damage and replication checkpoints. *Annu Rev Genet,* 36**,** 617-56.

O'DRISCOLL, M. & JEGGO, P. A. 2003. Clinical impact of ATR checkpoint signalling failure in humans. *Cell Cycle,* 2**,** 194-5.

O'DRISCOLL, M., RUIZ-PEREZ, V. L., WOODS, C. G., JEGGO, P. A. & GOODSHIP, J. A. 2003. A splicing mutation affecting expression of ataxia-telangiectasia and Rad3-related protein (ATR) results in Seckel syndrome. *Nat Genet,* 33**,** 497-501.

O'NEILL, T., DWYER, A. J., ZIV, Y., CHAN, D. W., LEES-MILLER, S. P., ABRAHAM, R. H., LAI, J. H., HILL, D., SHILOH, Y., CANTLEY, L. C. & RATHBUN, G. A. 2000. Utilization of oriented peptide libraries to identify substrate motifs selected by ATM. *J Biol Chem,* 275**,** 22719-27.

OGI, T., WALKER, S., STIFF, T., HOBSON, E., LIMSIRICHAIKUL, S., CARPENTER, G., PRESCOTT, K., SURI, M., BYRD, P. J., MATSUSE, M., MITSUTAKE, N., NAKAZAWA, Y., VASUDEVAN, P., BARROW, M., STEWART, G. S., TAYLOR, A. M., O'DRISCOLL, M. & JEGGO, P. A. 2012. Identification of the first ATRIP-deficient patient and novel mutations in ATR define a clinical spectrum for ATR-ATRIP Seckel Syndrome. *PLoS genetics,* 8**,** e1002945.

OGIWARA, H., UI, A., ONODA, F., TADA, S., ENOMOTO, T. & SEKI, M. 2006. Dpb11, the budding yeast homolog of TopBP1, functions with the checkpoint clamp in recombination repair. *Nucleic Acids Res,* 34**,** 3389-98.

OHOUO, P. Y., BASTOS DE OLIVEIRA, F. M., ALMEIDA, B. S. & SMOLKA, M. B. 2010. DNA damage signaling recruits the Rtt107-Slx4 scaffolds via Dpb11 to mediate replication stress response. *Mol Cell,* 39**,** 300-6.

OHOUO, P. Y., BASTOS DE OLIVEIRA, F. M., LIU, Y., MA, C. J. & SMOLKA, M. B. 2013. DNA-repair scaffolds dampen checkpoint signalling by counteracting the adaptor Rad9. *Nature,* 493**,** 120-4.

OKITA, N., MINATO, S., OHMI, E., TANUMA, S. & HIGAMI, Y. 2012. DNA damage-induced CHK1 autophosphorylation at Ser296 is regulated by an intramolecular mechanism. *FEBS Lett,* 586**,** 3974-9.

PACIOTTI, V., CLERICI, M., LUCCHINI, G. & LONGHESE, M. P. 2000. The checkpoint protein Ddc2, functionally related to S. pombe Rad26, interacts with Mec1 and is regulated by Mec1-dependent phosphorylation in budding yeast. *Genes Dev,* 14**,** 2046-59.

PAINTER, R. B. & YOUNG, B. R. 1980. Radiosensitivity in ataxia-telangiectasia: a new explanation. *Proc Natl Acad Sci U S A,* 77**,** 7315-7.

PARRILLA-CASTELLAR, E. R., ARLANDER, S. J. & KARNITZ, L. 2004. Dial 9-1-1 for DNA damage: the Rad9-Hus1-Rad1 (9-1-1) clamp complex. *DNA Repair (Amst),* 3**,** 1009-14.

PAULL, T. T. & GELLERT, M. 1998. The 3' to 5' exonuclease activity of Mre 11 facilitates repair of DNA double-strand breaks. *Mol Cell,* 1**,** 969-79.

PELLEGRINI, M., CELESTE, A., DIFILIPPANTONIO, S., GUO, R., WANG, W., FEIGENBAUM, L. & NUSSENZWEIG, A. 2006. Autophosphorylation at serine 1987 is dispensable for murine Atm activation in *vivo*. *Nature,* 443**,** 222-5.

PERRY, J. & KLECKNER, N. 2003. The ATRs, ATMs, and TORs are giant HEAT repeat proteins. *Cell,* 112**,** 151-5.

PFANDER, B. & DIFFLEY, J. F. 2011. Dpb11 coordinates Mec1 kinase activation with cell cycle-regulated Rad9 recruitment. *EMBO J,* 30**,** 4897-907.

PINES, J. 1994. Protein kinases and cell cycle control. *Semin Cell Biol,* 5**,** 399-408.

PUDDU, F., GRANATA, M., DI NOLA, L., BALESTRINI, A., PIERGIOVANNI, G., LAZZARO, F., GIANNATTASIO, M., PLEVANI, P. & MUZI-FALCONI, M. 2008. Phosphorylation of the budding yeast 9-1-1 complex is required for Dpb11 function in the full activation of the UV-induced DNA damage checkpoint. *Mol Cell Biol,* 28**,** 4782-93.

QIN, X. Q., LIVINGSTON, D. M., KAELIN, W. G., JR. & ADAMS, P. D. 1994. Deregulated transcription factor E2F-1 expression leads to S-phase entry and p53-mediated apoptosis. *Proc Natl Acad Sci U S A,* 91**,** 10918-22.

QU, M., YANG, B., TAO, L., YATES, J. R., 3RD, RUSSELL, P., DONG, M. Q. & DU, L. L. 2012. Phosphorylation-dependent interactions between Crb2 and Chk1 are essential for DNA damage checkpoint. *PLoS Genet,* 8**,** e1002817.

RAMIREZ-LUGO, J. S., YOO, H. Y., YOON, S. J. & DUNPHY, W. G. 2011. CtIP interacts with TopBP1 and NBS1 in the response to double-stranded DNA breaks (DSBs) in Xenopus egg extracts. *Cell Cycle,* 10**,** 469-80.

RAPPAS, M., OLIVER, A. W. & PEARL, L. H. 2011. Structure and function of the Rad9-binding region of the DNA-damage checkpoint adaptor TopBP1. *Nucleic Acids Res,* 39**,** 313-24.

REBBECK, T. R., MITRA, N., DOMCHEK, S. M., WAN, F., CHUAI, S., FRIEBEL, T. M., PANOSSIAN, S., SPURDLE, A., CHENEVIX-TRENCH, G., KCONFAB, SINGER, C. F., PFEILER, G., NEUHAUSEN, S. L., LYNCH, H. T., GARBER, J. E., WEITZEL, J. N., ISAACS, C., COUCH, F., NAROD, S. A., RUBINSTEIN, W. S., TOMLINSON, G. E., GANZ, P. A., OLOPADE, O. I., TUNG, N., BLUM, J. L., GREENBERG, R., NATHANSON, K. L. & DALY, M. B. 2009. Modification of ovarian cancer risk by BRCA1/2-interacting genes in a multicenter cohort of BRCA1/2 mutation carriers. *Cancer Res,* 69**,** 5801-10.

REDON, C., PILCH, D. R., ROGAKOU, E. P., ORR, A. H., LOWNDES, N. F. & BONNER, W. M. 2003. Yeast histone 2A serine 129 is essential for the efficient repair of checkpoint-blind DNA damage. *EMBO Rep,* 4**,** 678-84.

RHIND, N. & RUSSELL, P. 2000. Chk1 and Cds1: linchpins of the DNA damage and replication checkpoint pathways. *J Cell Sci,* 113 (Pt 22)**,** 3889-96.

ROGAKOU, E. P., BOON, C., REDON, C. & BONNER, W. M. 1999. Megabase chromatin domains involved in DNA double-strand breaks in *vivo*. *J Cell Biol,* 146**,** 905-16.

ROOS-MATTJUS, P., HOPKINS, K. M., OESTREICH, A. J., VROMAN, B. T., JOHNSON, K. L., NAYLOR, S., LIEBERMAN, H. B. & KARNITZ, L. M. 2003. Phosphorylation of human Rad9 is required for genotoxin-activated checkpoint signaling. *J Biol Chem,* 278**,** 24428-37.

ROZENZHAK, S., MEJIA-RAMIREZ, E., WILLIAMS, J. S., SCHAFFER, L., HAMMOND, J. A., HEAD, S. R. & RUSSELL, P. 2010. Rad3 decorates critical chromosomal domains with gammaH2A to protect genome integrity during S-Phase in fission yeast. *PLoS Genet,* 6**,** e1001032.

RUSSELL, P. & NURSE, P. 1986. cdc25+ functions as an inducer in the mitotic control of fission yeast. *Cell,* 45**,** 145-53.

RUSSELL, P. & NURSE, P. 1987a. The mitotic inducer nim1+ functions in a regulatory network of protein kinase homologs controlling the initiation of mitosis. *Cell,* 49**,** 569-76.

RUSSELL, P. & NURSE, P. 1987b. Negative regulation of mitosis by wee1+, a gene encoding a protein kinase homolog. *Cell,* 49**,** 559-67.

SAKA, Y., ESASHI, F., MATSUSAKA, T., MOCHIDA, S. & YANAGIDA, M. 1997. Damage and replication checkpoint control in fission yeast is ensured by interactions of Crb2, a protein with BRCT motif, with Cut5 and Chk1. *Genes Dev,* 11**,** 3387-400.

SAKA, Y. & YANAGIDA, M. 1993. Fission yeast cut5+, required for S phase onset and M phase restraint, is identical to the radiation-damage repair gene rad4+. *Cell,* 74**,** 383-93.

SANSAM, C. L., CRUZ, N. M., DANIELIAN, P. S., AMSTERDAM, A., LAU, M. L., HOPKINS, N. & LEES, J. A. 2010. A vertebrate gene, ticrr, is an essential checkpoint and replication regulator. *Genes Dev,* 24**,** 183-94.

SANTOCANALE, C. & DIFFLEY, J. F. 1998. A Mec1- and Rad53-dependent checkpoint controls late-firing origins of DNA replication. *Nature,* 395**,** 615-8.

SAVIC, V., YIN, B., MAAS, N. L., BREDEMEYER, A. L., CARPENTER, A. C., HELMINK, B. A., YANG-IOTT, K. S., SLECKMAN, B. P. & BASSING, C. H. 2009. Formation of dynamic gamma-H2AX domains along broken DNA strands is distinctly regulated by ATM and MDC1 and dependent upon H2AX densities in chromatin. *Mol Cell,* 34**,** 298-310.

SAVITSKY, K., BAR-SHIRA, A., GILAD, S., ROTMAN, G., ZIV, Y., VANAGAITE, L., TAGLE, D. A., SMITH, S., UZIEL, T., SFEZ, S., ASHKENAZI, M., PECKER, I., FRYDMAN, M., HARNIK, R., PATANJALI, S. R., SIMMONS, A., CLINES, G. A., SARTIEL, A., GATTI, R. A., CHESSA, L., SANAL, O., LAVIN, M. F., JASPERS, N. G., TAYLOR, A. M., ARLETT, C. F., MIKI, T., WEISSMAN, S. M., LOVETT, M., COLLINS, F. S. & SHILOH, Y. 1995. A single ataxia telangiectasia gene with a product similar to PI-3 kinase. *Science,* 268**,** 1749-53.

SCHMIDT, U., WOLLMANN, Y., FRANKE, C., GROSSE, F., SALUZ, H. P. & HANEL, F. 2008. Characterization of the interaction between the human DNA topoisomerase IIbeta-binding protein 1 (TopBP1) and the cell division cycle 45 (Cdc45) protein. *Biochem J,* 409**,** 169-77.

SCHUPBACH, M. 1971. The isolation and genetic classification of UV-sensitive mutants of Schizosaccharomyces pombe. *Mutat Res,* 11**,** 361-71.

SCHWARTZ, M. F., DUONG, J. K., SUN, Z., MORROW, J. S., PRADHAN, D. & STERN, D. F. 2002. Rad9 phosphorylation sites couple Rad53 to the Saccharomyces cerevisiae DNA damage checkpoint. *Mol Cell,* 9**,** 1055-65.

SEOL, H. J., YOO, H. Y., JIN, J., JOO, K. M., KIM, H. S., YOON, S. J., CHOI, S. H., KIM, Y., PYO, H. R., LIM, D. H., KIM, W., UM, H. D., KIM, J. H., LEE, J. I. & NAM, D. H. 2011a. The expression of DNA damage checkpoint proteins and prognostic implication in metastatic brain tumors. *Oncol Res,* 19**,** 381-90.

SEOL, H. J., YOO, H. Y., JIN, J., JOO, K. M., KONG, D. S., YOON, S. J., YANG, H., KANG, W., LIM, D. H., PARK, K., KIM, J. H., LEE, J. I. & NAM, D. H. 2011b. Prognostic implications of the DNA damage response pathway in glioblastoma. *Oncol Rep,* 26**,** 423-30.

SHEEDY, D. M., DIMITROVA, D., RANKIN, J. K., BASS, K. L., LEE, K. M., TAPIA-ALVEAL, C., HARVEY, S. H., MURRAY, J. M. & O'CONNELL, M. J. 2005. Brc1-mediated DNA repair and damage tolerance. *Genetics,* 171**,** 457-68.

SHILOH, Y. 2003. ATM and related protein kinases: safeguarding genome integrity. *Nat Rev Cancer,* 3**,** 155-68.

SHIMADA, K., PASERO, P. & GASSER, S. M. 2002. ORC and the intra-S-phase checkpoint: a threshold regulates Rad53p activation in S phase. *Genes Dev,* 16**,** 3236-52.

SHIOTANI, B. & ZOU, L. 2009. Single-stranded DNA orchestrates an ATM-to-ATR switch at DNA breaks. *Mol Cell,* 33**,** 547-58.

SHIRAHIGE, K., HORI, Y., SHIRAISHI, K., YAMASHITA, M., TAKAHASHI, K., OBUSE, C., TSURIMOTO, T. & YOSHIKAWA, H. 1998. Regulation of DNA-replication origins during cell-cycle progression. *Nature,* 395**,** 618-21.

SHROFF, R., ARBEL-EDEN, A., PILCH, D., IRA, G., BONNER, W. M., PETRINI, J. H., HABER, J. E. & LICHTEN, M. 2004. Distribution and dynamics of chromatin modification induced by a defined DNA double-strand break. *Curr Biol,* 14**,** 1703-11.

SIBANDA, B. L., CHIRGADZE, D. Y. & BLUNDELL, T. L. 2010. Crystal structure of DNA-PKcs reveals a large open-ring cradle comprised of HEAT repeats. *Nature,* 463**,** 118-21.

SIMANIS, V. & NURSE, P. 1989. Characterization of the fission yeast cdc10+ protein that is required for commitment to the cell cycle. *J Cell Sci,* 92 (Pt 1)**,** 51-6.

SIPICZKI, M. 2000. Where does fission yeast sit on the tree of life? *Genome Biol,* 1**,** REVIEWS1011.

SJOTTEM, E., REKDAL, C., SVINENG, G., JOHNSEN, S. S., KLENOW, H., UGLEHUS, R. D. & JOHANSEN, T. 2007. The ePHD protein SPBP interacts with TopBP1 and together they co-operate to stimulate Ets1-mediated transcription. *Nucleic Acids Res,* 35**,** 6648-62.

SMITS, V. A., REAPER, P. M. & JACKSON, S. P. 2006. Rapid PIKK-dependent release of Chk1 from chromatin promotes the DNA-damage checkpoint response. *Curr Biol,* 16**,** 150-9.

SOBHIAN, B., SHAO, G., LILLI, D. R., CULHANE, A. C., MOREAU, L. A., XIA, B., LIVINGSTON, D. M. & GREENBERG, R. A. 2007. RAP80 targets BRCA1 to specific ubiquitin structures at DNA damage sites. *Science,* 316**,** 1198-202.

SOFUEVA, S., DU, L. L., LIMBO, O., WILLIAMS, J. S. & RUSSELL, P. 2010. BRCT domain interactions with phospho-histone H2A target Crb2 to chromatin at double-strand breaks and maintain the DNA damage checkpoint. *Mol Cell Biol,* 30**,** 4732-43.

SOHN, S. Y. & CHO, Y. 2009. Crystal structure of the human rad9-hus1-rad1 clamp. *J Mol Biol,* 390**,** 490-502.

SONODA, E., SASAKI, M. S., BUERSTEDDE, J. M., BEZZUBOVA, O., SHINOHARA, A., OGAWA, H., TAKATA, M., YAMAGUCHI-IWAI, Y. & TAKEDA, S. 1998. Rad51-deficient vertebrate cells accumulate chromosomal breaks prior to cell death. *Embo J,* 17**,** 598-608.

SOUTOGLOU, E. & MISTELI, T. 2008. Activation of the cellular DNA damage response in the absence of DNA lesions. *Science,* 320**,** 1507-10.

SPYCHER, C., MILLER, E. S., TOWNSEND, K., PAVIC, L., MORRICE, N. A., JANSCAK, P., STEWART, G. S. & STUCKI, M. 2008. Constitutive phosphorylation of MDC1 physically links the MRE11-RAD50-NBS1 complex to damaged chromatin. *J Cell Biol,* 181**,** 227-40.

ST ONGE, R. P., BESLEY, B. D., PELLEY, J. L. & DAVEY, S. 2003. A role for the phosphorylation of hRad9 in checkpoint signaling. *J Biol Chem,* 278**,** 26620-8.

STEWART, G. S., MASER, R. S., STANKOVIC, T., BRESSAN, D. A., KAPLAN, M. I., JASPERS, N. G., RAAMS, A., BYRD, P. J., PETRINI, J. H. & TAYLOR, A. M. 1999. The DNA double-strand break repair gene hMRE11 is mutated in individuals with an ataxia-telangiectasia-like disorder. *Cell,* 99**,** 577-87.

STEWART, G. S., WANG, B., BIGNELL, C. R., TAYLOR, A. M. & ELLEDGE, S. J. 2003. MDC1 is a mediator of the mammalian DNA damage checkpoint. *Nature,* 421**,** 961-6.

STUCKI, M., CLAPPERTON, J. A., MOHAMMAD, D., YAFFE, M. B., SMERDON, S. J. & JACKSON, S. P. 2005. MDC1 directly binds phosphorylated histone H2AX to regulate cellular responses to DNA double-strand breaks. *Cell,* 123**,** 1213-26.

STUCKI, M. & JACKSON, S. P. 2004. MDC1/NFBD1: a key regulator of the DNA damage response in higher eukaryotes. *DNA Repair (Amst),* 3**,** 953-7.

STUCKI, M. & JACKSON, S. P. 2006. gammaH2AX and MDC1: anchoring the DNA-damage-response machinery to broken chromosomes. *DNA Repair (Amst),* 5**,** 534-43.

SUN, Y., JIANG, X., CHEN, S., FERNANDES, N. & PRICE, B. D. 2005. A role for the Tip60 histone acetyltransferase in the acetylation and activation of ATM. *Proc Natl Acad Sci U S A,* 102**,** 13182-7.

SUN, Y., JIANG, X. & PRICE, B. D. 2010. Tip60: connecting chromatin to DNA damage signaling. *Cell Cycle,* 9**,** 930-6.

SUN, Y., XU, Y., ROY, K. & PRICE, B. D. 2007. DNA damage-induced acetylation of lysine 3016 of ATM activates ATM kinase activity. *Mol Cell Biol,* 27**,** 8502-9.

SUN, Z., HSIAO, J., FAY, D. S. & STERN, D. F. 1998. Rad53 FHA domain associated with phosphorylated Rad9 in the DNA damage checkpoint. *Science,* 281**,** 272-4.

SVENDSEN, J. M., SMOGORZEWSKA, A., SOWA, M. E., O'CONNELL, B. C., GYGI, S. P., ELLEDGE, S. J. & HARPER, J. W. 2009. Mammalian BTBD12/SLX4 assembles a Holliday junction resolvase and is required for DNA repair. *Cell,* 138**,** 63-77.

SYMINGTON, L. S. & GAUTIER, J. 2011. Double-strand break end resection and repair pathway choice. *Annu Rev Genet,* 45**,** 247-71.

TAK, Y. S., TANAKA, Y., ENDO, S., KAMIMURA, Y. & ARAKI, H. 2006. A CDK-catalysed regulatory phosphorylation for formation of the DNA replication complex Sld2-Dpb11. *EMBO J,* 25**,** 1987-96.

TAKAHASHI, T., HARA, K., INOUE, H., KAWA, Y., TOKUNAGA, C., HIDAYAT, S., YOSHINO, K., KURODA, Y. & YONEZAWA, K. 2000. Carboxyl-terminal region conserved among phosphoinositide-kinase-related kinases is indispensable for mTOR function in *vivo* and in *vitro*. *Genes Cells,* 5**,** 765-75.

TAKEISHI, Y., OHASHI, E., OGAWA, K., MASAI, H., OBUSE, C. & TSURIMOTO, T. 2010. Casein kinase 2-dependent phosphorylation of human Rad9 mediates the interaction between human Rad9-Hus1-Rad1 complex and TopBP1. *Genes Cells,* 15**,** 761-71.

TANAKA, K. & RUSSELL, P. 2001. Mrc1 channels the DNA replication arrest signal to checkpoint kinase Cds1. *Nat Cell Biol,* 3**,** 966-72.

TANAKA, S., KOMEDA, Y., UMEMORI, T., KUBOTA, Y., TAKISAWA, H. & ARAKI, H. 2013. Efficient Initiation of DNA Replication in Eukaryotes Requires Dpb11/TopBP1-GINS Interaction. *Mol Cell Biol,* 33**,** 2614-22.

TANAKA, S., UMEMORI, T., HIRAI, K., MURAMATSU, S., KAMIMURA, Y. & ARAKI, H. 2007. CDK-dependent phosphorylation of Sld2 and Sld3 initiates DNA replication in budding yeast. *Nature,* 445**,** 328-32.

TANAKA, T., YOKOYAMA, M., MATSUMOTO, S., FUKATSU, R., YOU, Z. & MASAI, H. 2010. Fission yeast Swi1-Swi3 complex facilitates DNA binding of Mrc1. *J Biol Chem,* 285**,** 39609-22.

TARICANI, L. & WANG, T. S. 2006. Rad4TopBP1, a scaffold protein, plays separate roles in DNA damage and replication checkpoints and DNA replication. *Mol Biol Cell,* 17**,** 3456-68.

TAYLOR, M., MOORE, K., MURRAY, J., AVES, S. J. & PRICE, C. 2011. Mcm10 interacts with Rad4/Cut5(TopBP1) and its association with origins of DNA replication is dependent on Rad4/Cut5(TopBP1). *DNA Repair (Amst),* 10**,** 1154-63.

TERCERO, J. A., LABIB, K. & DIFFLEY, J. F. 2000. DNA synthesis at individual replication forks requires the essential initiation factor Cdc45p. *EMBO J,* 19**,** 2082-93.

TERCERO, J. A., LONGHESE, M. P. & DIFFLEY, J. F. 2003. A central role for DNA replication forks in checkpoint activation and response. *Mol Cell,* 11**,** 1323-36.

THOMPSON, L. H. 2012. Recognition, signaling, and repair of DNA double-strand breaks produced by ionizing radiation in mammalian cells: the molecular choreography. *Mutat Res,* 751**,** 158-246.

TRUJILLO, K. M., YUAN, S. S., LEE, E. Y. & SUNG, P. 1998. Nuclease activities in a complex of human recombination and DNA repair factors Rad50, Mre11, and p95. *J Biol Chem,* 273**,** 21447-50.

TSAI, E. Y., JAIN, J., PESAVENTO, P. A., RAO, A. & GOLDFELD, A. E. 1996. Tumor necrosis factor alpha gene regulation in activated T cells involves ATF-2/Jun and NFATp. *Mol Cell Biol,* 16**,** 459-67.

UCHIKI, T., DICE, L. T., HETTICH, R. L. & DEALWIS, C. 2004. Identification of phosphorylation sites on the yeast ribonucleotide reductase inhibitor Sml1. *J Biol Chem,* 279**,** 11293-303.

UEDA, S., TAKEISHI, Y., OHASHI, E. & TSURIMOTO, T. 2012. Two serine phosphorylation sites in the C-terminus of Rad9 are critical for 9-1-1 binding to TopBP1 and activation of the DNA damage checkpoint response in HeLa cells. *Genes Cells,* 17**,** 807-16.

UZIEL, T., LERENTHAL, Y., MOYAL, L., ANDEGEKO, Y., MITTELMAN, L. & SHILOH, Y. 2003. Requirement of the MRN complex for ATM activation by DNA damage. *EMBO J,* 22**,** 5612-21.

VENCLOVAS, C. & THELEN, M. P. 2000. Structure-based predictions of Rad1, Rad9, Hus1 and Rad17 participation in sliding clamp and clamp-loading complexes. *Nucleic Acids Res,* 28**,** 2481-93.

VERKADE, H. M., TELI, T., LAURSEN, L. V., MURRAY, J. M. & O'CONNELL, M. J. 2001. A homologue of the Rad18 postreplication repair gene is required for DNA damage responses throughout the fission yeast cell cycle. *Mol Genet Genomics,* 265**,** 993-1003.

VIALARD, J. E., GILBERT, C. S., GREEN, C. M. & LOWNDES, N. F. 1998. The budding yeast Rad9 checkpoint protein is subjected to Mec1/Tel1-dependent hyperphosphorylation and interacts with Rad53 after DNA damage. *EMBO J,* 17**,** 5679-88.

WALTES, R., KALB, R., GATEI, M., KIJAS, A. W., STUMM, M., SOBECK, A., WIELAND, B., VARON, R., LERENTHAL, Y., LAVIN, M. F., SCHINDLER, D. & DORK, T. 2009. Human RAD50 deficiency in a Nijmegen breakage syndrome-like disorder. *Am J Hum Genet,* 84**,** 605-16.

WANG, B., MATSUOKA, S., CARPENTER, P. B. & ELLEDGE, S. J. 2002. 53BP1, a mediator of the DNA damage checkpoint. *Science,* 298**,** 1435-8.

WANG, H. & ELLEDGE, S. J. 1999. DRC1, DNA replication and checkpoint protein 1, functions with DPB11 to control DNA replication and the S-phase checkpoint in Saccharomyces cerevisiae. *Proc Natl Acad Sci U S A,* 96**,** 3824-9.

WANG, H. & ELLEDGE, S. J. 2002. Genetic and physical interactions between DPB11 and DDC1 in the yeast DNA damage response pathway. *Genetics,* 160**,** 1295-304.

WANG, J., GONG, Z. & CHEN, J. 2011. MDC1 collaborates with TopBP1 in DNA replication checkpoint control. *J Cell Biol,* 193**,** 267-73.

WARD, I. M. & CHEN, J. 2001. Histone H2AX is phosphorylated in an ATR-dependent manner in response to replicational stress. *J Biol Chem,* 276**,** 47759-62.

WARD, I. M., MINN, K., JORDA, K. G. & CHEN, J. 2003. Accumulation of checkpoint protein 53BP1 at DNA breaks involves its binding to phosphorylated histone H2AX. *J Biol Chem,* 278**,** 19579-82.

WATSON, A. T., GARCIA, V., BONE, N., CARR, A. M. & ARMSTRONG, J. 2008. Gene tagging and gene replacement using recombinase-mediated cassette exchange in Schizosaccharomyces pombe. *Gene,* 407**,** 63-74.

WATTS, F. Z. & BRISSETT, N. C. 2010. Linking up and interacting with BRCT domains. *DNA Repair (Amst),* 9**,** 103-8.

WEINERT, T. & HARTWELL, L. 1989. Control of G2 delay by the rad9 gene of Saccharomyces cerevisiae. *J Cell Sci Suppl,* 12**,** 145-8.

WEINERT, T. A. 1992. Dual cell cycle checkpoints sensitive to chromosome replication and DNA damage in the budding yeast Saccharomyces cerevisiae. *Radiat Res,* 132**,** 141-3.

WEINERT, T. A. & HARTWELL, L. H. 1988. The RAD9 gene controls the cell cycle response to DNA damage in Saccharomyces cerevisiae. *Science,* 241**,** 317-22.

WEINERT, T. A., KISER, G. L. & HARTWELL, L. H. 1994. Mitotic checkpoint genes in budding yeast and the dependence of mitosis on DNA replication and repair. *Genes Dev,* 8**,** 652-65.

WILLIAMS, G. J., LEES-MILLER, S. P. & TAINER, J. A. 2010a. Mre11-Rad50-NBS1 conformations and the control of sensing, signaling, and effector responses at DNA double-strand breaks. *DNA Repair (Amst),* 9**,** 1299-306.

WILLIAMS, J. S., WILLIAMS, R. S., DOVEY, C. L., GUENTHER, G., TAINER, J. A. & RUSSELL, P. 2010b. gammaH2A binds Brc1 to maintain genome integrity during S-phase. *EMBO J,* 29**,** 1136-48.

WILLIAMS, R. S., MONCALIAN, G., WILLIAMS, J. S., YAMADA, Y., LIMBO, O., SHIN, D. S., GROOCOCK, L. M., CAHILL, D., HITOMI, C., GUENTHER, G., MOIANI, D., CARNEY, J. P., RUSSELL, P. & TAINER, J. A. 2008. Mre11 dimers coordinate DNA end bridging and nuclease processing in double-strand-break repair. *Cell,* 135**,** 97-109.

WILLIS, N. & RHIND, N. 2009. Mus81, Rhp51(Rad51), and Rqh1 form an epistatic pathway required for the S-phase DNA damage checkpoint. *Mol Biol Cell,* 20**,** 819-33.

WILLIS, N. & RHIND, N. 2010. The fission yeast Rad32(Mre11)-Rad50-NBS1 complex acts both upstream and downstream of checkpoint signaling in the S-phase DNA damage checkpoint. *Genetics,* 184**,** 887-97.

WILLSON, J., WILSON, S., WARR, N. & WATTS, F. Z. 1997. Isolation and characterization of the Schizosaccharomyces pombe rhp9 gene: a gene required for the DNA damage checkpoint but not the replication checkpoint. *Nucleic Acids Res,* 25**,** 2138-46.

WOLLMANN, Y., SCHMIDT, U., WIELAND, G. D., ZIPFEL, P. F., SALUZ, H. P. & HANEL, F. 2007. The DNA topoisomerase IIbeta binding protein 1 (TopBP1) interacts with poly (ADP-ribose) polymerase (PARP-1). *J Cell Biochem,* 102**,** 171-82.

WOOD, V., GWILLIAM, R., RAJANDREAM, M. A., LYNE, M., LYNE, R., STEWART, A., SGOUROS, J., PEAT, N., HAYLES, J., BAKER, S., BASHAM, D., BOWMAN, S., BROOKS, K., BROWN, D., BROWN, S., CHILLINGWORTH, T., CHURCHER, C., COLLINS, M., CONNOR, R., CRONIN, A., DAVIS, P., FELTWELL, T., FRASER, A., GENTLES, S., GOBLE, A., HAMLIN, N., HARRIS, D., HIDALGO, J., HODGSON, G., HOLROYD, S., HORNSBY, T., HOWARTH, S., HUCKLE, E. J., HUNT, S., JAGELS, K., JAMES, K., JONES, L., JONES, M., LEATHER, S., MCDONALD, S., MCLEAN, J., MOONEY, P., MOULE, S., MUNGALL, K., MURPHY, L., NIBLETT, D., ODELL, C., OLIVER, K., O'NEIL, S., PEARSON, D., QUAIL, M. A., RABBINOWITSCH, E., RUTHERFORD, K., RUTTER, S., SAUNDERS, D., SEEGER, K., SHARP, S., SKELTON, J., SIMMONDS, M., SQUARES, R., SQUARES, S., STEVENS, K., TAYLOR, K., TAYLOR, R. G., TIVEY, A., WALSH, S., WARREN, T., WHITEHEAD, S., WOODWARD, J., VOLCKAERT, G., AERT, R., ROBBEN, J., GRYMONPREZ, B., WELTJENS, I., VANSTREELS, E., RIEGER, M., SCHAFER, M., MULLER-AUER, S., GABEL, C., FUCHS,

M., DUSTERHOFT, A., FRITZC, C., HOLZER, E., MOESTL, D., HILBERT, H., BORZYM, K., LANGER, I., BECK, A., LEHRACH, H., REINHARDT, R., POHL, T. M., EGER, P., ZIMMERMANN, W., WEDLER, H., WAMBUTT, R., PURNELLE, B., GOFFEAU, A., CADIEU, E., DREANO, S., GLOUX, S., et al. 2002. The genome sequence of Schizosaccharomyces pombe. *Nature,* 415**,** 871-80.

WRIGHT, R. H., DORNAN, E. S., DONALDSON, M. M. & MORGAN, I. M. 2006. TopBP1 contains a transcriptional activation domain suppressed by two adjacent BRCT domains. *Biochem J,* 400**,** 573-82.

WU, X. & LEVINE, A. J. 1994. p53 and E2F-1 cooperate to mediate apoptosis. *Proc Natl Acad Sci U S A,* 91**,** 3602-6.

XIA, Z., MORALES, J. C., DUNPHY, W. G. & CARPENTER, P. B. 2001. Negative cell cycle regulation and DNA damage-inducible phosphorylation of the BRCT protein 53BP1. *J Biol Chem,* 276**,** 2708-18.

XU, M., BAI, L., GONG, Y., XIE, W., HANG, H. & JIANG, T. 2009. Structure and functional implications of the human rad9-hus1-rad1 cell cycle checkpoint complex. *J Biol Chem,* 284**,** 20457-61.

XU, Y., ASHLEY, T., BRAINERD, E. E., BRONSON, R. T., MEYN, M. S. & BALTIMORE, D. 1996. Targeted disruption of ATM leads to growth retardation, chromosomal fragmentation during meiosis, immune defects, and thymic lymphoma. *Genes Dev,* 10**,** 2411-22.

XU, Y. J., DAVENPORT, M. & KELLY, T. J. 2006. Two-stage mechanism for activation of the DNA replication checkpoint kinase Cds1 in fission yeast. *Genes Dev,* 20**,** 990-1003.

XU, Y. J. & KELLY, T. J. 2009. Autoinhibition and autoactivation of the DNA replication checkpoint kinase Cds1. *J Biol Chem,* 284**,** 16016-27.

YABUUCHI, H., YAMADA, Y., UCHIDA, T., SUNATHVANICHKUL, T., NAKAGAWA, T. & MASUKATA, H. 2006. Ordered assembly of Sld3, GINS and Cdc45 is distinctly regulated by DDK and CDK for activation of replication origins. *EMBO J,* 25**,** 4663-74.

YAMAMOTO, R. R., AXTON, J. M., YAMAMOTO, Y., SAUNDERS, R. D., GLOVER, D. M. & HENDERSON, D. S. 2000. The Drosophila mus101 gene, which links DNA repair, replication and condensation of heterochromatin in mitosis, encodes a protein with seven BRCA1 C-terminus domains. *Genetics,* 156**,** 711-21.

YAMANE, K., WU, X. & CHEN, J. 2002. A DNA damage-regulated BRCT-containing protein, TopBP1, is required for cell survival. *Mol Cell Biol,* 22**,** 555-66.

YAN, S., LINDSAY, H. D. & MICHAEL, W. M. 2006. Direct requirement for Xmus101 in ATR-mediated phosphorylation of Claspin bound Chk1 during checkpoint signaling. *J Cell Biol,* 173**,** 181-6.

YAN, S. & WILLIS, J. 2013. WD40-repeat protein WDR18 collaborates with TopBP1 to facilitate DNA damage checkpoint signaling. *Biochem Biophys Res Commun,* 431**,** 466-71.

YOO, H. Y., KUMAGAI, A., SHEVCHENKO, A., SHEVCHENKO, A. & DUNPHY, W. G. 2007. Ataxia-telangiectasia mutated (ATM)-dependent activation of ATR occurs through phosphorylation of TopBP1 by ATM. *J Biol Chem,* 282**,** 17501-6.

YOO, H. Y., KUMAGAI, A., SHEVCHENKO, A., SHEVCHENKO, A. & DUNPHY, W. G. 2009. The Mre11-Rad50-NBS1 complex mediates activation of TopBP1 by ATM. *Mol Biol Cell,* 20**,** 2351-60.

YOSHIOKA, S., KATO, K., NAKAI, K., OKAYAMA, H. & NOJIMA, H. 1997. Identification of open reading frames in Schizosaccharomyces pombe cDNAs. *DNA Res,* 4**,** 363-9.

YOU, Z., CHAHWAN, C., BAILIS, J., HUNTER, T. & RUSSELL, P. 2005. ATM activation and its recruitment to damaged DNA require binding to the C terminus of NBS1. *Mol Cell Biol,* 25**,** 5363-79.

YU, X., CHINI, C. C., HE, M., MER, G. & CHEN, J. 2003. The BRCT domain is a phospho-protein binding domain. *Science,* 302**,** 639-42.

YUAN, Z., KUMAR, E. A., CAMPBELL, S. J., PALERMO, N. Y., KIZHAKE, S., MARK GLOVER, J. N. & NATARAJAN, A. 2011. Exploiting the P-1 pocket of BRCT domains toward a structure guided inhibitor design. *ACS Med Chem Lett,* 2**,** 764-767.

YUE, M., SINGH, A., WANG, Z. & XU, Y. J. 2011. The phosphorylation network for efficient activation of the DNA replication checkpoint in fission yeast. *J Biol Chem,* 286**,** 22864-74.

ZEGERMAN, P. & DIFFLEY, J. F. 2007. Phosphorylation of Sld2 and Sld3 by cyclin-dependent kinases promotes DNA replication in budding yeast. *Nature,* 445**,** 281-5.

ZEGERMAN, P. & DIFFLEY, J. F. 2010. Checkpoint-dependent inhibition of DNA replication initiation by Sld3 and Dbf4 phosphorylation. *Nature,* 467**,** 474-8.

ZENG, Y., FORBES, K. C., WU, Z., MORENO, S., PIWNICA-WORMS, H. & ENOCH, T. 1998. Replication checkpoint requires phosphorylation of the phosphatase Cdc25 by Cds1 or Chk1. *Nature,* 395**,** 507-10.

ZHAO, H., TANAKA, K., NOGOCHI, E., NOGOCHI, C. & RUSSELL, P. 2003. Replication checkpoint protein Mrc1 is regulated by Rad3 and Tel1 in fission yeast. *Mol Cell Biol,* 23**,** 8395-403.

ZHAO, X., CHABES, A., DOMKIN, V., THELANDER, L. & ROTHSTEIN, R. 2001. The ribonucleotide reductase inhibitor Sml1 is a new target of the Mec1/Rad53 kinase cascade during growth and in response to DNA damage. *Embo J,* 20**,** 3544-53.

ZHAO, X., MULLER, E. G. & ROTHSTEIN, R. 1998. A suppressor of two essential checkpoint genes identifies a novel protein that negatively affects dNTP pools. *Mol Cell,* 2**,** 329-40.

ZHAO, X. & ROTHSTEIN, R. 2002. The Dun1 checkpoint kinase phosphorylates and regulates the ribonucleotide reductase inhibitor Sml1. *Proc Natl Acad Sci U S A,* 99**,** 3746-51.

ZHOU, Z. W., LIU, C., LI, T. L., BRUHN, C., KRUEGER, A., MIN, W., WANG, Z. Q. & CARR, A. M. 2013. An Essential Function for the ATR-Activation-Domain (AAD) of TopBP1 in Mouse Development and Cellular Senescence. *PLoS Genet,* 9**,** e1003702.

ZOU, L. 2007. Single- and double-stranded DNA: building a trigger of ATR-mediated DNA damage response. *Genes Dev,* 21**,** 879-85.

ZOU, L. & ELLEDGE, S. J. 2003. Sensing DNA damage through ATRIP recognition of RPA-ssDNA complexes. *Science,* 300**,** 1542-8.

ZOU, L., LIU, D. & ELLEDGE, S. J. 2003. Replication protein A-mediated recruitment and activation of Rad17 complexes. *Proc Natl Acad Sci U S A,* 100**,** 13827-32.